Lars Sørum

Environmental Aspects of Municipal Solid Waste Combustion

NTNU Trondheim
Norges teknisk-naturvitenskapelige universitet

Doktor ingeniøravhandling 2000:93
Institutt for Termisk energi og vannkraft

ITEV rapport 2000:07

NTNU

Norges Teknisk-Naturvitenskapelige Universitet
The Norwegian University of Science and Technology

Report no:
NTNU 2000:93
ITEV 2000:07

Classification
Open

POSTADRESSE
NTNU
INSTITUTT FOR TERMISK ENERGI OG VANNKRAFT
Kolbjørn Hejes vei 1A
N-7491 Trondheim - NTNU

TELEFONER
Sentralbord NTNU: 73 59 40 00
Instituttkontor: 73 59 27 00
Vannkraftlaboratoriet: 73 59 38 57

TELEFAX
Instituttkontor: 73 59 83 90
Vannkraftlaboratoriet: 73 59 38 54

Title of report	**Date**
ENVIRONMENTAL ASPECTS OF MUNICIPAL SOLID WASTE COMBUSTION	November 2000
	No. of pages/appendixes 178/41
Author Lars Sørum	**Project manager (sign.)** Johan E. Hustad
Division Faculty of Mechanical Engineering Institute of Thermal Energy and Hydropower	**Project no.**
ISBN no. 82-79841202	**Price group**

Abstract
The overall objective of this thesis is concerned with environmental aspects of MSW combustion. The thesis is divided into three parts, which have been investigated in detail:

1. *Pyrolysis Characteristics and Kinetics of Municipal Solid Wastes*
2. *Formation of NO From Combustion of Volatiles From Municipal Solid Wastes*
3. *The Fate of Heavy Metals in Municipal Solid Waste Combustion*

In the first part of this thesis the pyrolysis characteristics and kinetics of 11 different components, representing the dry cellulosic fraction and plastics of MSW, was investigated. The thermograms of the different components revealed different weight loss characteristics, which can be attributed to their different chemical composition. In the kinetic analysis, the plastics PS, PP, LDPE and HDPE were all modelled as a single reaction describing the degradation of the hydrocarbon polymer. For the cellulosic fraction and PVC, a model of three independent parallel reactions was successfully used to describe the thermal degradation.

The second part investigates the formation of NO from combustion of volatiles from MSW. Experiments on single components and their mixtures were conducted in a small-scale fixed bed reactor and numerical simulations using the opposed flow diffusion flame program OPPDIF were performed. The experiments and simulations on the combustion of volatiles from paper/cardboard showed that NO is mainly formed from fuel-nitrogen. For the plastics LDPE and PVC, however, the experiments show that NO mainly originates from the thermal and possibly the prompt NO mechanisms.

The third part investigates the fate of the heavy metals As, Cd, Cr, Cu, Hg, Ni, Pb and Zn in MSW combustion. Heavy metal partitioning and chemistry of heavy metals in MSW combustion were studied experimentally in a real combustion plant and theoretically by using equilibrium calculations. The experimental study showed that the major part of Cd, Cr, Pb and Zn remained in the bottom ash, while the major part of Hg was captured in the flue gas cleaning system. The influence of varying MSW composition and operation parameters such as temperature, Cl/metal- and S/metal ratios, fly ash content and fuel/air ratio on the heavy metal partitioning and chemistry was investigated. The results showed that the heavy metals responded differently with regards to volatilisation and re-condensation when changing the MSW composition and operational paramcters.

	Indexing terms: English	**Indexing Terms: Norwegian**
Group 1	Heat Engineering	Varmeteknikk
Group 2 Selected by author	Solid Fuels	Faste brensler
	Waste	Avfall
	Combustion	Forbrenning
	Emissions	Utslipp

ENVIRONMENTAL ASPECTS OF MUNICIPAL SOLID WASTE COMBUSTION

by

Lars Sørum

A thesis submitted to

The Norwegian University of Science and Technology

for the degree of

Doktor Ingeniør

November 2000
The Norwegian University of Science and Technology
Faculty of Mechanical Engineering
Institute of Thermal Energy and Hydropower

"An expert is a man
who has made all the mistakes
which can be made
in a very narrow field"

Niels Bohr (1885–1962),
Danish physicist.

Preface

I want to thank my academic advisor, Prof. Johan E. Hustad, for encouraging me to take on this Ph.D. study. I also want to thank Prof. Hustad for his guidance and for introducing me to leading authorities within the different fields of this thesis. It has been very interesting working within the field of MSW combustion, and I feel that I have gained knowledge in a field where there is a large potential for R&D.

This work has mainly been financed through a 3-year scholarship from the Nordic Council of Ministers' Energy Research Programme on Solid Fuels. However, The Norwegian Foreign Department, SINTEF Energy Research, Department of Thermal Energy and Trondheim Energy Board, Department of District Heating have also contributed financially, enabling me to finish my Ph.D. study. A sincerely *thank you* to all of my financial contributors.

Being a Nordic scholar enabled me to spend time at the Technical University of Denmark (DTU) in Lyngby. A co-operation with the CHEC group (Combustion and Harmful Emission Control) at DTU led to altogether 4 stays (2-3 months each) over a period of 3 years. These stays at CHEC were to me very fruitful. It was exiting and inspiring to be a part of a new working environment. A great *thank you* to the staff at the CHEC group at DTU for organising and helping me out during my 4 stays.

In order to be able to produce scientific papers of high quality within three different topics, it has been necessary for me to work with leading authorities within these topics. Maybe they have learned something new as well, since none of my co-authors on the presented papers have worked much with waste as a fuel, but rather biomass or coal. I want to thank all my

co-authors; Morten G. Grønli (SINTEF), Morten Fossum (SINTEF), Øyvind Skreiberg (NTNU), Johan E. Hustad (NTNU), Egil Evensen (Trondheim Energy Board), Peter Glarborg (DTU), Anker Jensen (DTU), Flemming Frandsen (DTU), Kim Dam-Johansen (DTU) and Janusz Nowakowski (Technical University of Szczecin, Poland) for their contribution.

There is not only an academic/technical aspect with a lot of challenges to overcome but also a human aspect to a Ph.D. study. A lot of my spare time has been used during this Ph.D. study. Encouragement to continue the work at times when things may look dark is therefore important. In this context I would like to thank Øyvind Skreiberg for being patient, encouraging, listening and for discussing parts of my work not directly related to his field of expertise. I also want to thank my family (brother, sisters and mother) and my in-laws for helping out, making it possible for me to work more in my spare time than I could have done without their help. Last, but definitively not least I want to thank my wife Trine and my daughter Hanne. Trine has encouraged me and helped me with her love, patience and understanding throughout this study. She has also given up a lot, giving me the opportunity to do this study. To my daughter Hanne: your curious nature and everlasting ability to ask questions about anything and everything will make you a research scientist sometime. To our expected child: (:-))

Lars Sørum

Trondheim 22.10.00

Contents

Thesis objectives

The overall objective of this thesis is to study some of the most important environmental aspects connected to the nature of MSW as a fuel in combustion systems. The design and operation of MSW combustion plants, in order to meet present and future emission requirements, is a challenge due to the large variation in composition and the inhomogeneous nature of MSW. MSW is in fact a set of different fuels, with different elemental composition, physical properties, and chemical structure. Detailed knowledge of combustion related characteristics of single components and their mixtures and influence of compositional effects is therefore important. The overall objective of this thesis is therefore to contribute with such knowledge through experimental and theoretical studies in the field of MSW combustion. The thesis is divided into three parts, which has been investigated in detail:

1. *Pyrolysis Characteristics and Kinetics of Municipal Solid Wastes*

2. *Formation of NO From Combustion of Volatiles From Municipal Solid Wastes*

3. *The Fate of Heavy Metals in Municipal Solid Waste Combustion*

The first part, which investigates the pyrolytic degradation behaviour of MSW components and mixtures thereof, deals with the initial step of the combustion process. The lack of comparable data and detailed knowledge on the pyrolytic degradation behaviour and kinetic data of components and mixtures of MSW motivated this work. Fundamental knowledge on the initial degradation behaviour is of importance in modelling, design and operation of combustion plants for MSW in order to be able to control the

combustion process and consequently the emissions of pollutant species. Hence, the objective of this study is to obtain detailed information on the pyrolysis characteristics and chemical kinetic data of the most important components in MSW.

The second part, which investigates the formation of NO from volatiles of MSW components and mixtures thereof, deals directly with formation of pollutant species. Knowledge in this field is especially important in the evaluation and development of primary reduction techniques for NO_x. The objective of this study is to investigate the formation of NO in detail for different components of MSW such as paper, cardboard and plastics and their mixtures. The focus was on determining typical conversion levels and trends for NO formation from different MSW components in a small-scale laboratory furnace and not on absolute emission levels for MSW combustion plants.

The third part focus on the fate of heavy metals in MSW combustion. From an environmental point of view, heavy metals are important since they may be emitted to the environment by air (flue gas), water (from flue gas cleaning system) and soil (ash disposal). The lack of knowledge on the fate of As, Cd, Cr, Cu, Hg, Ni, Pb and Zn at typical conditions for MSW combustion motivated this work. As opposed to some similar studies in this field, ash species were included in order to investigate possible interactions with the heavy metals. Knowledge in the field of heavy metal partitioning and chemistry is needed when assessing the environmental consequences for all outgoing mass flows of an MSW incinerator. The objective of this study is therefore to investigate the fate of heavy metals in MSW combustion through experimental and theoretical studies. In the theoretical study the influence of varying operational parameters and MSW compositions on the equilibrium distribution of these heavy metals at typical combustion

conditions in a grate furnace are investigated. Whereas the experimental study determined the fate of some selected heavy metals in a grate fired combustion plant for MSW at typical operating conditions.

Overall summary

MSW consists of several different fractions such as paper/cardboard, plastics, wet organic wastes, glass, metals, etc. The complexity of MSW in terms of composition, together with the increasing awareness of the environmental hazards of waste disposal and lack of landfill sites, have in the last decades promoted an increased number of alternative waste treatment systems. Material recovery and re-use, combustion with energy recovery, composting and landfilling are the most common parts of today's waste management system. Factors influencing the choice of MSW management systems are waste amounts and composition, environmental and economical aspects and infrastructure (i.e. type of housing, access to landfill sites, possible energy buyers, etc.). The choice of waste management system will influence the composition of MSW subjected to energy recovery. The increased separation of components from the waste stream and complex waste management systems gives new possibilities for classification of waste as a fuel with a certain quality and composition. Knowing the composition and combustion characteristics of the respective components will make it easier for operators and manufacturers of combustion plant to assess the consequences of burning different wastes. Some of the most important environmental aspects of MSW combustion have been investigated in detail in this thesis, with emphasis on two important parameters:

- Changes in composition (related to waste management)

- Fuel complexity (i.e. many different components with different combustion properties)

Summary and conclusions of papers

A brief summary and main conclusions of the three different parts in this thesis are given below.

Part I (Paper I)

Pyrolysis Characteristics and Kinetics of Municipal Solid Wastes

Pyrolysis characteristics and kinetics of 11 different components, representing the dry cellulosic fraction and plastics of MSW, has been investigated. The aim of this study was to obtain detailed information on the pyrolytic degradation characteristics and chemical kinetics of the most important components in MSW, which can be useful in the modelling, design, and operation of thermal conversion processes for MSW (i.e. pyrolysis, gasification and combustion systems). The pyrolytic degradation characteristics of these components have been studied by thermogravimetry (TGA). In addition, proximate- and ultimate analysis and determination of the higher heating value (HHV) are included. The variations in fuel properties of the paper/cardboard and plastic components were relatively large. The ash content for the different paper/cardboard components, varied from 1-28 wt%, with corresponding HHV values of 19.3-10.4 MJ/kg and fixed carbon content of 10.5-4.7 wt%. The plastics PS, PP, LDPE and HDPE were 100% volatile and HHV were between 42-47 MJ/kg. PVC, on the other hand, has a similar content of hydrocarbons and consequently a similar HHV as the cellulosic fraction (22.8 MJ/kg). The major difference between PVC and the cellulosic fraction with regards to the ultimate composition was that PVC had a chlorine content of 48 wt% and only 6 wt% of oxygen. Paper and cardboard have a similar pyrolytic degradation behaviour as wood, occurring at 200-500°C. The DTG temperature peak was located at approximately 360°C. The degradation of PS, PP, LDPE and

HDPE occurred at 350-500°C, while PVC had a completely different degradation behaviour, volatilising between 200°C and 525°C in two major steps. The cellulosic fraction of MSW was modelled as a set of three reactions describing the degradation of hemicellulose, cellulose and lignin, with average activation energies of 111, 244 and 43 kJ/mole, respectively. PS, PP, LDPE and HDPE were all modelled as a single reaction describing the thermal degradation of the hydrocarbon polymer with activation energies of 312, 337, 341 and 445 kJ/mole, respectively. The degradation of PVC was modelled with three reactions describing the release of benzene during dehydrochlorination, dehydrochlorination and degradation of remaining hydrocarbons with activation energies of 388, 110 and 150 kJ/mole, respectively. Possible interactions between different paper and plastic components in mixtures were also investigated. The only significant interaction between the different components was between the cellulosic fraction and PVC. In a mixture, the dehydrochlorination of PVC increases the reactivity of cellulosic matter.

Part II (Paper II)

Formation of NO from Combustion of Volatiles from Municipal Solid Wastes

An experimental and theoretical study on the formation of NO from combustion of volatiles from municipal solid wastes has been performed. Experiments on single components and their mixtures were conducted in a small-scale fixed bed reactor. In addition, numerical simulations using the opposed flow diffusion flame program OPPDIF were performed to obtain a further understanding of the experimental results. Conversion factors for fuel-N to NO were determined for single components of newspaper, cardboard, glossy paper, low-density polyethylene (LDPE) and

poly(vinylchloride) (PVC) and their mixtures, using gases with oxygen concentrations of 12, 21 and 40 vol.%. For single components experiments at 100 vol.% oxygen were also performed. The conversion factors for paper and cardboard varied from 0.26 to 0.99. The experiments and simulations both show that NO was mainly formed from the fuel-nitrogen for the paper and cardboard. The conversion factor for LDPE and PVC varied from 0.71 to 10.09 and 0.04 to 0.37, respectively. Conversion factors higher than 1.0 in the case of LDPE clearly show that NO was formed by thermal and/or prompt mechanisms. For the plastics LDPE and PVC the experiments show that NO mainly originates from the thermal and possibly the prompt NO mechanisms. Increased formation of NO was observed for newspaper, cardboard, glossy paper, PVC and LDPE, when increasing the oxygen concentration in the oxidiser from 12 to 40 vol.%. Increasing the temperature of the oxidiser from 973 to 1123 K led to more NO from newspaper and LDPE. Simulations with OPPDIF confirmed these trends.

For mixtures, a comparison between calculated conversion factors (based on a weighted sum of the conversion factors for single components) and the experimentally determined conversion factor for pellets of the mixture were performed. For mixtures of paper and cardboard a significant difference in conversion factor for the sum of single components and mixture experiments could only be found at 40 vol.% of oxygen. For mixtures of paper/cardboard and plastics, however, significant differences in the conversion factor were observed at all oxygen concentrations when comparing experiments on a mixture of paper and plastics with the weighted sum of the single components. The explanation was found in the different combustion properties for paper/cardboard and plastic, which in this case make the formation of thermal NO from LDPE more favourable for the single component than in mixtures with other components. The simulations with OPPDIF confirmed the trends observed in the experimental study and

allowed an assessment of the contribution of the different mechanisms of NO formation.

Part III (Paper III and IV)

The Fate of Heavy Metals in Municipal Solid Waste Combustion

Heavy metal partitioning and chemistry of heavy metals in MSW combustion were studied experimentally in a real combustion plant and theoretically by using equilibrium calculations.

Experimental study (Paper III). An experimental investigation of the outgoing mass flows from Trondheim Energy Board's (TEV) MSW incinerator has been carried out. Concentrations of heavy metals in the bottom ash, filter ash and residues from flue gas cleaning system was determined. Using this information it was possible to establish a heavy metal balance for the incineration plant. It was found that 63wt% of Cd, 86wt% of Zn, 94wt% of Pb, 98wt% of Cr and 100wt% of Fe remains in the bottom ash. The filter ash captured most of the volatile Cd (24wt%), Zn (13wt%), Pb (5wt%) and Cr (2wt%). The wet scrubber captured most of the Hg (87wt%). Generally, the heavy metals in this study are less volatile than observed in other studies, indicating a relatively low temperature on the grate. The water-cooled grates used in this incinerator and/or different conditions for mixing of fuel/air compared to the other incinerators may explain the lower temperature. The calculated concentrations of heavy metal in the MSW was 1.6 mg/kg of Hg, 5 mg/kg of Cd, 1044 mg/kg of Zn, 439 mg/kg of Pb, 21.1 mg/kg of Cr and 8823 mg/kg of Fe.

Theoretical study (Paper IV). In order to supplement the experimental study on heavy metal partitioning and obtain further knowledge on the chemistry of heavy metals in MSW combustion, a theoretical study using

equilibrium calculations was performed. The lack of knowledge on the fate of As, Cd, Cr, Cu, Hg, Ni, Pb and Zn at typical conditions for MSW combustion motivated this work. As opposed to similar studies in this field, ash species were included in order to investigate possible interactions with the heavy metals. The influence of varying MSW composition and operation parameters such as temperature, Cl/metal- and S/metal ratios, fly ash content and fuel/air ratio on the heavy metal partitioning and chemistry were investigated. The conclusions are divided in two separate parts; one considering the conditions on the grate and one considering the conditions in the flue gas as it goes from the furnace to the filter.

On the grate (950-1600 K)

The equilibrium calculations investigating the volatile behaviour on the grate showed that Cd, Hg and Pb were fully volatilised between 950 and 1600 K. Cr, however, was stable in solid phase practically over the entire temperature range. Only a small amount was volatilised at high temperatures. No influence on the volatility of Cr was observed when changing the sulphur or chlorine content. Cd, Hg and Pb showed no response, while Cr became slightly more volatile at higher temperatures with decreasing fuel/air ratio.

The volatile behaviour of As, Cu and Zn were largely altered when shifting from reducing to oxidising conditions. Whereas As and Zn become less volatile when shifting from reducing to oxidising conditions, Cu becomes more volatile. Changing the sulphur content only resulted in a change for Cu, making it less volatile with increasing sulphur content at reducing conditions.

At reducing conditions the volatile behaviour of As and Zn was not influenced by changes in the chlorine content, while Cu become more

volatile when increasing the content of chlorine. At oxidising conditions, Cu (at low chlorine content) and Zn becomes more volatile, while As experienced no change when increasing the chlorine content.

Although the equilibrium distribution changed, Ni experienced no change in the volatile behaviour when varying the sulphur content. Ni did, however, become more volatile when increasing the chlorine content, while varying λ did not significantly alter the volatile behaviour of Ni. These observations apply both for reducing and oxidising conditions.

Furnace to Filter (300-1600 K)

Investigation of the condensing behaviour of the heavy metals as they pass through the boiler and enter the flue gas cleaning system on their way to the stack (500–300 K), revealed that only Hg was present in gas phase.

Increasing the Cl/Cl_{BC} (Cl_{BC} means the chlorine content at base case conditions) ratio from 1.0 to 10, lower the temperature where Cu, Ni and Zn are fully volatilised from 970, 1520 and 1670 K to 670, 1000 and 780 K, respectively. A lower temperature of condensation will increase the possibility of heavy metal species condensing on very small particles or aerosols, which might escape the filter system and consequently be emitted through the stack.

Solid phase interaction between As and Cr with Ca and silicates of Ni and Zn were identified. In the case of As at oxidising conditions, the formation of $Ca_3(AsO_4)_2$ (cr) was dependent on the S/Ca ratio. A high S/Ca ratio, which was obtained by a high sulphur content or low concentration of fly ash in the flue gas, will favour the formation of As_2O_5 (cr) rather than the less volatile $Ca_3(AsO_4)_2$ (cr). A low S/Ca ratio will on the other hand favour the formation of $Ca_3(AsO_4)_2$ (cr). Another important consequence of

increasing the sulphur/chlorine ratio in the flue gas (S/S_{BC} ratios equal or higher than 1.5), was the shift from solid phase metal chlorides to sulphates for Cd, Cr, Cu, Ni, Pb and Zn at lower temperatures. In the case of Pb and Zn, a shift from the highly corrosive species $PbCl_2$ (cr,l) and $ZnCl_2$ (cr,l) to $PbSO_4$ (cr) and $ZnSO_4$ (cr) may reduce corrosion in the boiler sections significantly in a combustion plant for MSW. Increasing the sulphur/chlorine ratio in the flue gas may be obtained by removing waste with high chlorine content such as PVC, or reducing the fly ash content. At high fly ash content the sulphur is bound to the ash as $CaSO_4$ (cr) up to 1300 K. Reducing the fly ash content will increase the amount of available sulphur to form heavy metal sulphates.

1 Introduction

Waste is the remains of our production and consumption, everything we throw away because we do not want it or can not use it anymore. The definition of different types of waste may differ from country to country. Definitions used by Statistics Norway are as follows[1]:

Consumer Waste (CW): Regular waste, also bulky waste such as furniture etc. from households, small shops etc. and offices. The same applies for waste of similar nature and amount from other enterprises.

Production Waste (PW): Waste from commercial and service enterprises, which in nature or amount separates substantially from CW.

Special Waste (SW): Waste which it is not suitable to be handled together with consumer waste because it can result in serious pollution or danger of harming humans or animals.

Household Waste (HW): Waste from private households.

Commercial Waste (ComW): Waste from public and private enterprises and institutions.

Municipal Solid Waste (MSW): All waste, which is managed through municipal sanitation (i.e. practically all household waste and large portions of the commercial waste).

1.1 Waste generation, composition and management

Figure 1.1 shows the amounts of waste generated in Norway in 1996. Almost 75% of a total of 24 mill. ton of waste generated in Norway are masses of soil, gravel, rocks, etc. mostly from the construction industry. This type of waste is also a part of the waste definition, however the management of this category does normally not constitute a pollution problem. The large amount of these masses, however, does constitute a land disposal problem. Waste from the fish industry, which is disposed into the sea from the ocean going fleet is also included in the definition of waste, but does not cause any significant pollution to the environment. Special waste is subjected to special management and treatment outside the "ordinary" waste management system due to its hazardous nature. The special waste in Norway originates mainly from the chemical production industry, chemical products and metal industry.

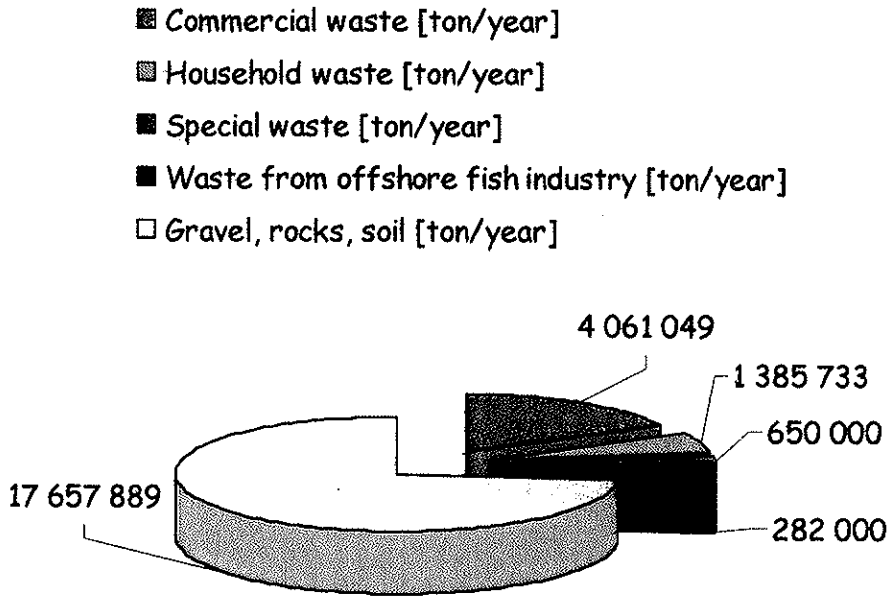

Figure 1.1 Total waste amounts in Norway in 1996 [ton/year][2].

In general, the wastes delivered to thermal conversion plants are MSW or pre-sorted MSW also called refuse derived fuel (RDF). Figure 1.2 shows how the annual generated amounts of MSW (and the corresponding share of HW and ComW) and recycled amount of MSW have increased from 1992 to 1999. The yearly generated amounts of MSW increased with 19% from 1992 to 1999 (i.e. increased from 2.22 to 2.65 mill. ton)[3]. Estimations performed by Statistics Norway states that the amount of MSW will be 3.56 mill. ton in 2010, given the same waste management policy as today[4]. Of the 2.22 mill. ton of MSW generated in 1992, 1.01 mill. ton is HW and 1.21 mill. ton is ComW, while in 1999 the corresponding amounts were 1.40 and 1.25 mill. ton, respectively. In the last decade the amount of MSW subjected to recycling has increased substantially. The fraction of recycled MSW increased from 8 to 30 wt% from 1992 to 1999. Paper, cardboard and cartons together with wet organic waste and yard waste constitute the major fraction of the recycled HW (46 + 15.5 + 11.3wt%), while wood waste, paper, cardboard and cartons together with metals are the major recycled fractions of ComW (28.9 + 19.4 + 17.1 wt%)[1,5].

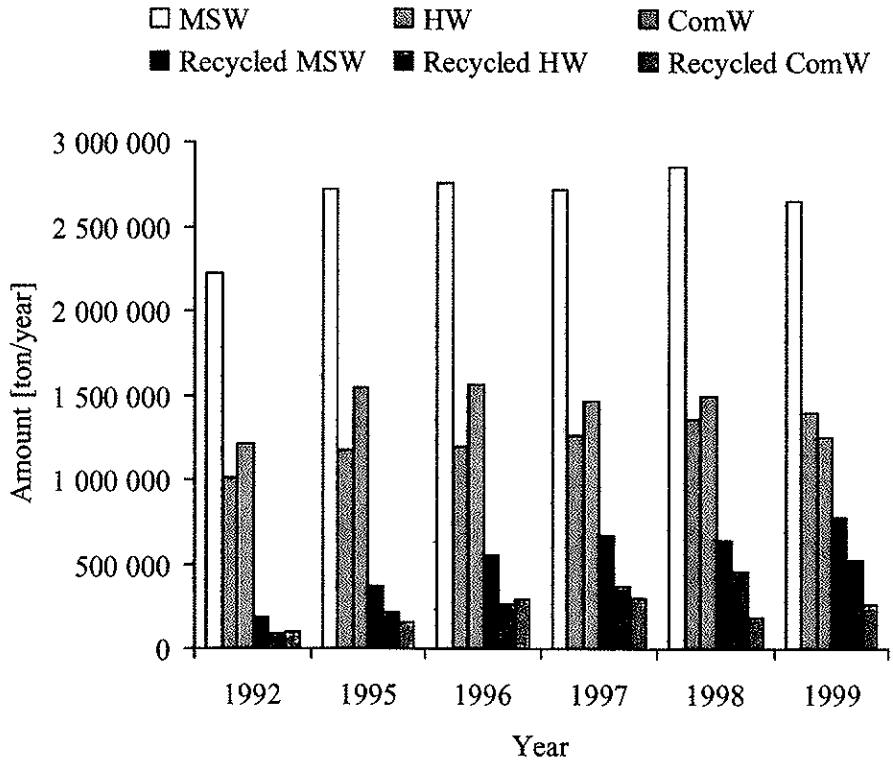

Figure 1.2 Annual generated and recycled amounts of MSW in Norway from 1992 to 1999. The amount of HW and ComW constituting MSW with their respective recycled amounts are also included[3].

Figure 1.3 shows the typical composition of MSW in some selected countries. The compositions of MSW vary relatively much. Poland, compared to the other countries, has less high calorific waste and much wet organic waste, making it less suitable for combustion without any pre-sorting. The yearly per capita generation of MSW for these countries varies also. As examples, Poland has a yearly generation of MSW of 260 kg/capita, whereas the corresponding amounts for Norway and USA are 470 and 800 kg/capita, respectively[6,7].

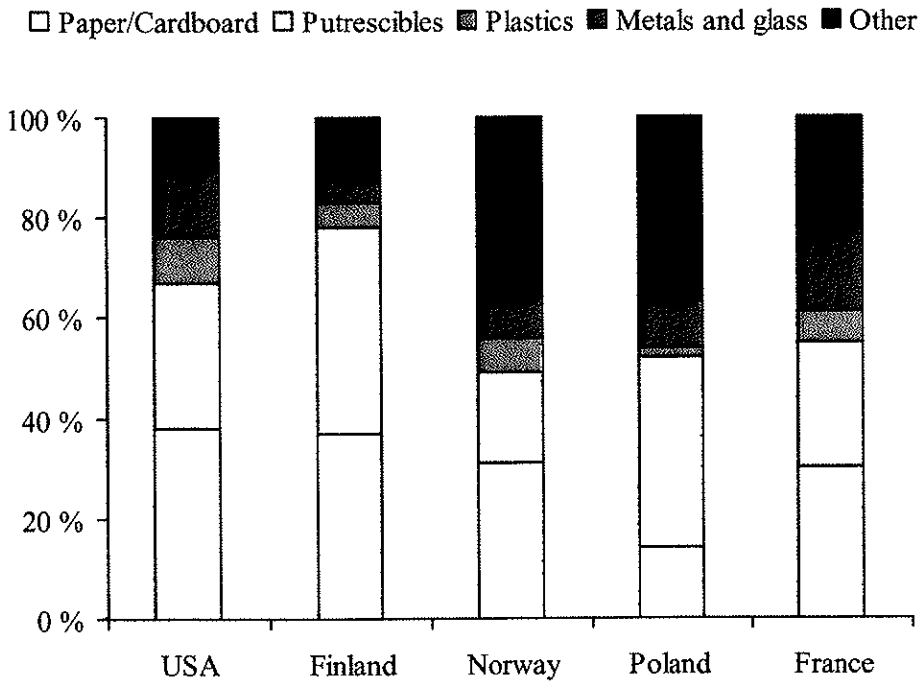

Figure 1.3 Comparison of composition of MSW in some selected countries on weight basis[6,8,9,10].

In recent years, waste management has become increasingly complex. Earlier, Municipal Solid Waste (MSW) was sent to landfill sites, which was considered the most economic way of handling MSW. However, in the last decades the awareness of the environmental hazards and the lack of landfill sites, have promoted an increased number of alternative waste treatment systems. Today MSW management systems are complex and a product of several different factors. Factors influencing the choice of MSW management systems are waste amounts and composition, environmental and economical aspects and infrastructure (i.e. type of housing, access to landfill sites, possible energy buyers, etc.). Material recovery and re-use, combustion with energy recovery, composting and landfilling are the most common parts of today's waste management system. Table 1.1 shows a commonly used waste management hierarchy, which is

implemented in many of the industrialised countries worldwide[11]. Generally, the fraction of MSW being subjected to re-use, recycling or combustion with energy recovery has increased on the expense of landfilling. Figure 1.4 show current disposal practice for a large number of European countries together with Japan, Canada and USA. As observed from this figure, landfilling is still the dominating disposal method in most of these countries. However, this is about to change since many countries have now banned landfilling of putrescibles. It is also interesting to observe that countries with a high population density, such as Japan, Denmark, The Netherlands and Switzerland, have a higher combustion to landfill ratio. The reason for this is probably the need for volume reduction due to the lack of landfill sites. The banning of landfilling of wet organic waste significantly influence the composition of MSW subjected to energy recovery as it normally constitute approximately 20 to 30 wt% of the total MSW composition[8,9]. In addition to this, changing consumer patterns and new products will alter the composition of MSW. The increased separation of components from the waste stream and complex waste management systems gives new possibilities for classification of waste as a fuel with a certain quality and composition. Knowing the composition and combustion characteristics of the respective components will make it easier for operators and manufacturers of combustion plant to assess the consequences of burning different wastes.

Table 1.1 Waste management hierarchy[11].

Priority	Options	Explanation/Benefits
1	Reduction	Reduction of wastes at the source through technological and design improvements (e.g. improved product lifetime) and reduction of use of consumables. Consistent with economic sustainability (Priority to be given to the minimisation of special waste, with some target materials to be eliminated entirely from the waste stream).
2	Re-Use	Putting objects back into use (e.g. bottles, car and machinery components) through designing for re-use for the same function or finding a secondary use (e.g. use of old tyres as boat fenders).
3	Recovery - Recycling	Putting materials back into use (e.g. glass, plastics, paper, cans etc.). Potential for considerable saving in energy consumption and reduced emissions to atmosphere. Economic incentive to recycle will improve following Government policy to make disposal to landfill more expensive.
	- Composting	Processing organic materials to produce soil additives/growing media reducing the demand for artificial fertilisers and for natural resources. Aerobic composting of waste lessens potential emissions of greenhouse gas, methane, from landfill sites.
	- Energy Recovery	Four main approaches are:- • combustion with energy recovery • processing selected waste for use as a fuel • burning methane produced in landfill sites • controlled anaerobic digestion of sewage or municipal waste to produce methane for combustion. Energy recovery is five times more efficient from waste combustion than from collecting and burning landfill gas. Combustion reduces waste volume for final disposal by about 90%. However, there can be toxic emissions and residues, requiring special precautions, and it remains generally more expensive than landfill, despite increasing landfill costs.
4	Disposal	No benefit derived from the materials. Increases in landfill tax will reduce its attractiveness. Disadvantages of landfill include loss of amenity at the site and on the transport routes, the release of methane into the atmosphere and the potential for leaching of harmful substances into ground water supplies. Other disposal options include combustion without energy recovery and chemical destruction or permanent storage of specialised wastes.

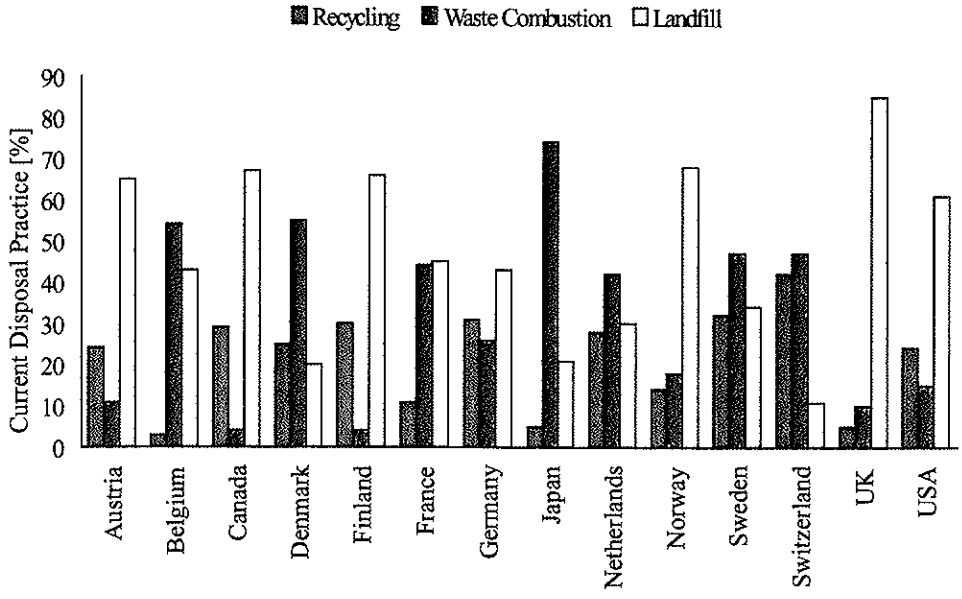

Figure 1.4 Current disposal practice in selected European countries, and USA, Japan and Canada[11].

1.2 Chemical composition and structure of MSW

The combustible fraction of MSW mainly consists of cellulosic matter (i.e. paper, cardboard, wood, grass, etc.) and different plastics. The most common plastic types are the pure hydrocarbon plastics such as high-density polyethylene (HDPE), low-density polyethylene (LDPE), polystyrene (PS) and polypropylene (PP) and the chlorine containing poly(vinylchloride) (PVC). Information on the production, chemical structure and composition of paper and plastics has been collected from a selection of books and reports[12-32]. Table 1.2 shows the elemental composition and heating values of MSW and fractions thereof compared to other fuels such as wood, domestic heating oil, coal and natural gas. MSW has a lower heating value due to the higher ash and moisture content, and lower content of hydrocarbons than the other fuels. However, the variations in elemental composition vary largely between different fractions of MSW.

Table 1.2 Elemental compositions and heating values of MSW, MSW fractions, wood, coal, oil and natural gas[20,21,22,23,24,25].

	Composition [wt%]	C [wt%]	H [wt%]	O [wt%]	N [wt%]	S [wt%]	Cl [wt%]	Ash [wt%]	Moisture [wt%]	HHV [MJ/kg]	H_{eff} [MJ/kg]
MSW	100	37.53	4.98	26.85	0.96	0.24	0.79	28.6	24.8	15.6	10.2
Paper/Cardboard	*33.1*	*43.11*	*5.89*	*40.26*	*0.20*	*0.24*	*0.30*	*10*	*10*	*17.6*	*14.3*
Plastics	*6.5*	*72.89*	*10.11*	*10.63*	*1.10*	*0.39*	*3.88*	*1*	*10*	*36.3*	*28.2*
Metal	*3.7*	*n.a.*	*n.a.*	*n.a.*	*n.a.*	*n.a.*	*n.a.*	*100*	*0*	*0*	*0*
Glass	*6.4*	*n.a.*	*n.a.*	*n.a.*	*n.a.*	*n.a.*	*n.a.*	*100*	*0*	*0*	*0*
Organic waste	*24.4*	*49.00*	*6.33*	*36.41*	*2.4*	*0.23*	*0.63*	*5*	*70*	*20.7*	*3.9*
Other combustibles	*12.6*	*52.14*	*6.57*	*31.34*	*2.0*	*0.66*	*2.29*	*5*	*30*	*22.6*	*13.3*
Rest fraction	*13.3*	*n.a.*	*n.a.*	*n.a.*	*n.a.*	*n.a.*	*n.a.*	*100*	*0*	*0*	*0*
Wood (Pine)		51.8	6.1	41.2	0.3	0.01	n.a.	0.59	10	20.9	17.4
Coal (anthracite)		76.1	1.8	1.8	0.6	0.6	n.a.	19.1	0	27.8	27.4
Oil (domestic)		86.4	13.4	0	0	0.19	n.a.	0.01	0	45.8	42.8
Natural gas (North sea)		74.7	23.7	1.0	0.6	0	n.a.	0	0	52.2	47.0

Table 1.3 Content of heavy metals in MSW and MSW fractions subjected to emission requirements in exisiting combustion plants in Norway. The values are average values from one comprehensive experimental study performed by Rigo & Chandler[26] and a literature review performed by The Norwegian Pollution Control Authority[20].

	Composition [wt%]	As [g/ton]	Cd [g/ton]	Cr [g/ton]	Cu [g/ton]	Hg [g/ton]	Mn [g/ton]	Ni [g/ton]	Pb [g/ton]
MSW	100	18.20	40.88	55.73	462.93	1.13	217.3	28.43	28.6
Paper/Cardboard	*33.1*	*0.89*	*0.201*	*17.61*	*32.72*	*1.23*	*39.2*	*17.50*	*7.98*
Plastics	*6.5*	*9.70*	*15.50*	*81.30*	*95.80*	*0.217*	*45.9*	*15.70*	*247.0*
Metal	*3.7*	*82.10*	*17.70*	*316.10*	*9890.0*	*3.48*	*1736.7*	*100.0*	*672.0*
Glass	*6.4*	*151.00*	*2.72*	*94.40*	*26.10*	*0.22*	*187.9*	*14.4*	*201.0*
Wet organic waste	*24.4*	*3.04*	*2.30*	*40.60*	*238.5*	*1.02*	*227.9*	*17.96*	*67.50*
Other combustibles	*12.6*	*18.60*	*14.10*	*83.30*	*48.50*	*0.50*	-	*14.30*	*132.5*
Rest fraction	*13.3*	*11.20*	*275.50*	*48.70*	*105.00*	*1.88*	*522.5*	*81.30*	*349.2*

MSW also contains trace elements such as heavy metals. Heavy metals are defined by having a density greater than ~5 g/cm^3. Studies have shown that the concentration of heavy metals in MSW compared to other solid fuels such as biomass and coal is relatively high[27,28,29]. It is important to be aware of the large variations in heavy metal concentrations in MSW, also within each fraction of MSW as several studies have shown[20,26,30]. Table 1.3 shows the concentrations of the heavy metals arsenic (As), cadmium (Cd), chromium (Cr), copper (Cu), mercury (Hg), manganese (Mn), nickel (Ni) and lead (Pb) subjected to emission requirements in existing combustion plants for MSW. The data generated in this table are average data from two comprehensive studies. Compared to the other combustibles, paper and cardboard have relatively high concentrations of Hg. Plastics on the other hand, have relatively high concentrations of As, Cd, Cr, Cu and Pb. The concentration of heavy metals in wet organic waste varies largely from study to study. However, on an average basis, wet organic waste has high concentrations of Cu and Mn, while other combustibles (wood, rubber, leather, textiles, etc.) have high concentrations of As, Cd, Cr and Pb.

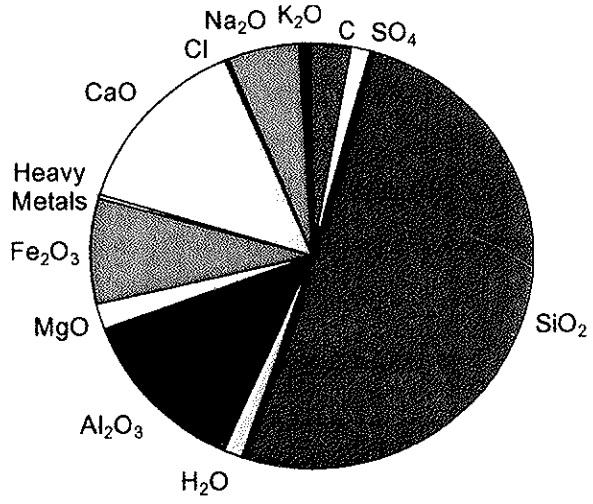

Figure 1.5 Example of major components in bottom ash from a grate fired mass burn plant[11].

Figure 1.5 shows the chemical composition of bottom ash from a grate fired combustion plant for MSW. It is observed that the major fraction of the ash contains oxides of species such as silicon (Si), calcium (Ca), aluminium (Al) and iron (Fe). However, the chemical composition of ashes from MSW combustion might vary depending on fuel composition and combustion process[11].

1.2.1 Cellulosic fraction

The cellulosic fraction in MSW consists of several different types of paper, cardboard, wood and other wet organic wastes. Paper as we know it today is always made of fibrous raw material. The most important source of fibre is wood. The raw material for paper production can be any number of different types of trees, both hardwood and softwood. More than 90% of the world's total fibre production originates from wood. However, in some parts of the world, other cellulosic matter such as bagasse and bamboo are also used for the production of paper.

1.2.1.1 Chemical structure

Paper consists of mostly the same components as wood namely cellulose, hemicellulose and lignin. However, the content of the three components can be quite different depending on type of paper. Fibres from different raw materials have different physical properties such as length, width and thickness. The chemical composition can also be different. Table 1.4 shows the chemical composition of birch (hardwood), spruce and pine (both softwoods) on an extractive-free basis.

Table 1.4 Chemical compositions of Scandinavian birch, spruce and pine on an extractive-free basis[12].

	Birch	**Spruce**	**Pine**
Cellulose [wt%]	40	44	43
Hemicellulose [wt%]	39	27	27
Lignin [wt%]	21	29	30
Extractives [wt%]	3	2	5

In paper production (production of *paper pulp*) mechanical or chemical energy is used to decompose the raw material into fibre and fibre fragments. When producing mechanical pulp the pulp yield as a percentage of the wood used is typically 96-100wt%. When producing chemical pulp, chemicals are used for the removal or softening of the binding substance between fibres so they end up as free single fibres without or with a small amount of mechanical energy (e.g. pumping). Chemical pulp has a typical pulp yield of 30-60wt%. The substances removed when producing chemical pulp is lignin and hemicellulose.

Cellulose. The woods largest single component is cellulose. Cellulose is a clearly definable substance which, in fact, exists in isolation, and in an almost pure form, in the fine hairs attached to the seeds of cotton. Chemically cellulose is a linear polymer of β-D-glucopyranose units linked by 1,4 glycosidic bonds (Figure 1.6). Normally the length consists of 7000 units, but the molecular weight dispersion is very large. It has been shown that cellulose from cotton has a degree of polymerisation (DP) of up to 10000. Because of its fibrous structure and strong hydrogen bonding, cellulose has a high tensile strength and is insoluble in most solvents.

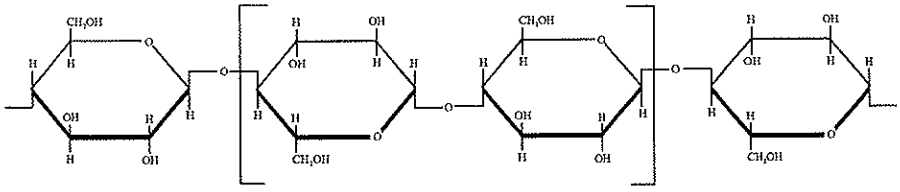

Figure 1.6 Chemical structure of cellulose.

Hemicellulose. Closely associated with cellulose in plant cell walls, particularly those of lignified tissues, is a group of chemically ill defined polysaccharides of low molecular weight to which, almost a century ago, the name *hemicellulose* was given. The loose definition of this group stems from the fact that individual molecules contain more than one kind of sugar residue. These residues are present

in variable proportions. Figure 1.7 show principal sugar residues of wood hemicellulose. Hemicellulose is much more soluble and susceptible to chemical degradation than cellulose. Wood hemicellulose is soluble in water or in aqueous alkali, by which they can be isolated from delignified tissues.

Lignin. Lignin is a complex, systematically polymerised, highly aromatic substance with a three-dimensional, highly branched chain. It never occurs alone in nature, but it is present, as an encrustant, in all woody tissues. The structure of lignin is in large parts determined, but since a quantitatively preparation of lignin has not successfully been separated from the wood, the whole structure is not known. The chemistry of lignin is to a very large extent involved in most pulping reactions, since lignin is the less desirable of the three main wood components. Therefore it has to be removed or bleached to an extent varying with the grade of pulp desired. Figure 1.8 shows a schematic proposal for lignin structure.

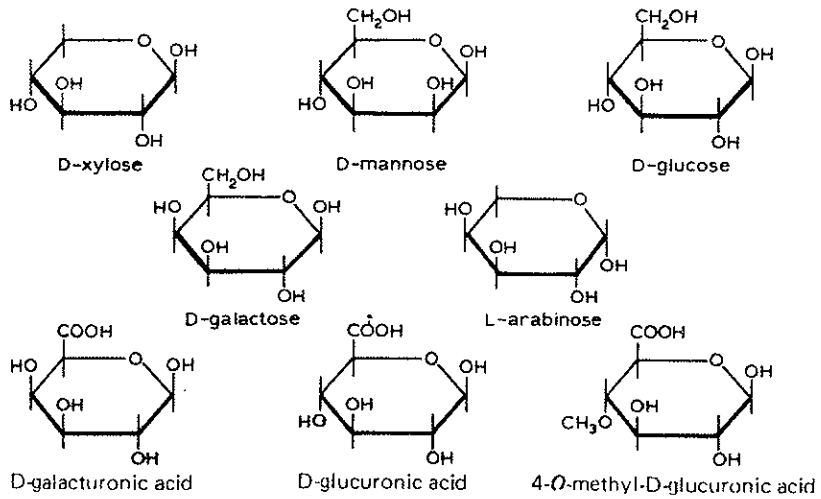

Figure 1.7 Principal sugar residues of wood hemicellulose[12].

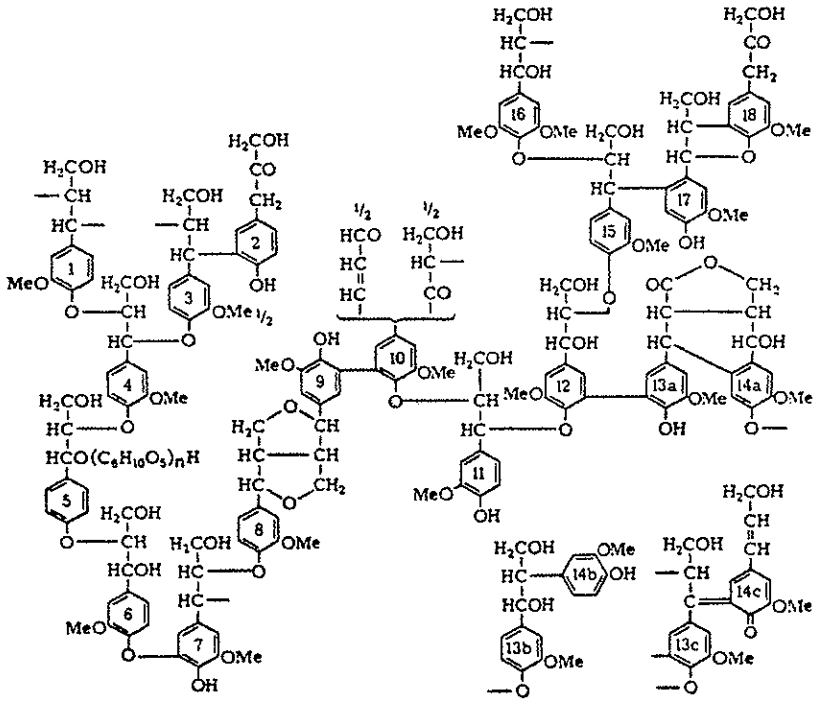

Figure 1.8 Schematic proposal for lignin structure[32].

Extractives. The extraneous components of wood include aliphatic, aromatic and alicyclic compounds, hydrocarbons, alcohols, ketons and various acids, esters, phenolic compounds, resins, terpens to mention some. These components are easily extracted from the wood using organic solvents or water.

Inorganic components. In addition to the cellulose, hemicellulose and lignin there are also additives in paper. The main inorganic additives in paper originate from the coating process and can be divided into three different groups: pigment, binder and chemical additives. The pigments contribute with the largest share in the coating process (80-95%), while binder constitutes 5-20% and chemical additives only 1-2%. Clay is the most used pigment in the coating process. Table 1.5 shows a number of different pigments and their chemical composition.

Table 1.5 Different types and corresponding chemical composition of pigment in paper[15].

Pigment	Chemical composition
Clay (kaolin)	$Al_2O_32SiO_22H_2O$
Calcium carbonate	$CaCO_3$
Titan oxide	TiO_2
Satin white	$3CaOAl_2O_33CaSO_43H_2O$
Barium sulphate	BaSO4
Talc	$3MgO4SiO_2H_2O$
Aluminium hydrate	$Al(OH)_3$

The main function of the binder is, in dry condition, to bind the pigment on the surface of the paper and hold single pigment particles together. There are two different types of binder: natural and synthetic. In the first group, animal glue and gelatins, casein, soyaprotein, carboxylmethylcellulose and several cellulose derivatives are used. The synthetic binders are made out of dispersion of mixed polymers with a variation in degree of polymerisation. To this group, which goes under the name latex, one will find mixed polymers of styrene-butadiene, butadiene-methyl-metacrylat, acrylic acid ester, butadiene-acrylonitrile and polyvinylacetate. In addition, polyvinylalcohol, which is soluble in water, belongs to this group. The purpose of the chemical additives is in general to: improve the dispersion of pigment, change the viscosity of the coating melt, reduce the foam tendency of the coating melt, change colour, harden the coating layer, prevent bacterial attack on the coating melt and serve as a lubricant during the coating process. Chemical additives can both be inorganic and organic.

Wu et. al. studied the chemical kinetics of coated printing and writing paper and in this study an ultimate analysis of this paper was included. The coated printing and writing paper contained 10-15% of calcium carbonate filler and the paper was produced from bleached kraft processed pulp. Table 1.6, shows the ultimate analysis of the coated paper sample.

Table 1.6 Ultimate analysis of coated paper sample[31].

Component	Composition
C [wt%]	30.5
H [wt%]	4.6
O [wt%]	37.7
N [wt%]	2.9
S [wt%]	1.5
Cl [wt%]	1.5
Si [ppmw]	112 800
Ca [ppmw]	72 300
Al [ppmw]	48 200
Mg [ppmw]	6 780
Fe [ppmw]	4 160
Cr [ppmw]	30
Mn [ppmw]	29
Zn [ppmw]	< 10
Cd [ppmw]	< 10
Pb [ppmw]	< 10

1.2.2 Plastics

Petroleum is today the major raw material for plastic production. This is very different from the situation 40-50 years ago, when coal and cellulosic material such as waste oak husks, sugar cane, soya beans and natural rubber were used as raw materials.

1.2.2.1 Chemical structure

All plastic materials, before compounding with additives, consist of a mass of very large molecules. In the case of a few naturally occurring materials, such as bitumen, shellac, and amber, the compositions are heterogeneous and complex but in all other cases the plastic materials belong to a chemical family referred to as high polymers. For most practical purposes, a *polymer* may be defined as a large molecule built up by repetition of small, simple chemical units or *monomers*. Figure 1.9 shows the repeating units or monomers of the different plastics. For both HDPE and LDPE the polymer structure is essentially a long chain of aliphatic

hydrocarbons. For general technological purposes, the difference in density between HDPE and LDPE is due to the chain branching. PP has a slightly different structure than LDPE and HDPE with a methyl group (CH_3) in the repeating unit, but is also an aliphatic hydrocarbon type. PS is made from the styrene monomer and the repeating unit contains a benzene ring. For PVC the methyl group of PP has been substituted with chlorine (Cl). Commercial PVC polymers are largely amorphous, slightly branched molecules with the monomer residues arranged in head-to-tail sequence. The major difference between PVC and the other plastic is the high content of chlorine (approximately 50 wt%).

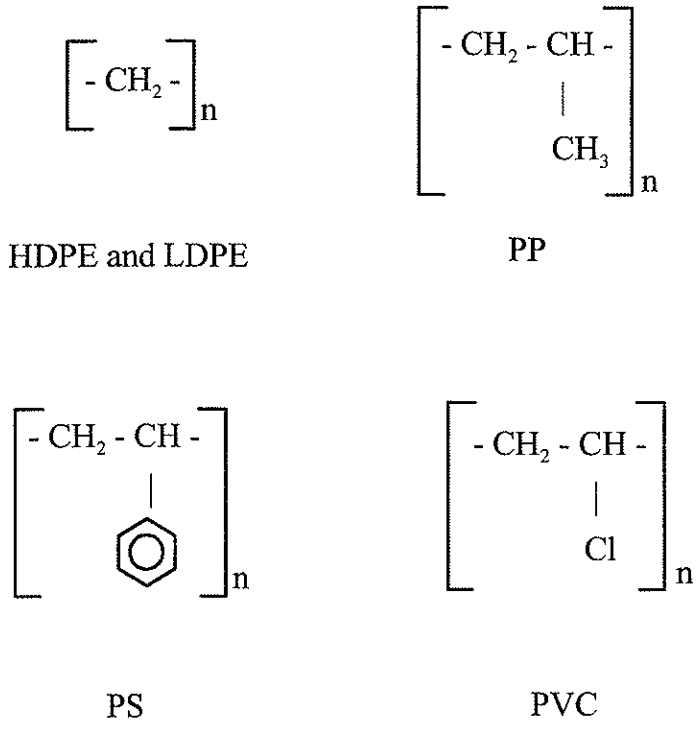

Figure 1.9 Repeating units (monomers) for 5 different plastics[18].

1.2.2.2 Chemical bonds in polymers

Several types of chemical bonds are present between atoms and molecules in polymer materials. The single chain molecule is kept together by strong valence bonds (primary bonds). Much weaker secondary bonds (e.g. dipole force) tie the different molecules together. Dissociation energies for some selected primary bonds are shown in Table 1.7.

Table 1.7 Dissociation energies for some selected primary bonds[18].

Bond	Dissociation energy [kJ/mole]
C-C	347
C=C	611
C-H	414
C-O	360
C=O	749
C-N	306
C≡N	892
C-Cl	339
C-F	431
O-H	465
O-O	147
Si-Si	178
S-S	268

1.3 Thermal conversion technologies for MSW

This section will briefly give an introduction to different thermal conversion technologies for MSW and RDF. A general introduction to different thermal conversion technologies will be given together with a brief process description of different thermal conversion plants.

In general there are three potential thermal conversion technologies for MSW or RDF, namely *pyrolysis*, *gasification* or direct *combustion*. Figure 1.10 shows an overview of the different technologies and their products and potential

end-use. The primary products can be char, tar/oil, fuel gas and/or heat depending on the employed conversion technology. Literature on the different thermal conversion technologies is gathered from several reports and papers[33-44].

Pyrolysis is the thermal degradation (devoltilisation) of the fuel in absence of an oxidising agent at temperatures of typically 400-800°C. This leads to the formation of a mixture of liquid/oil (tar components), gases and char of which the relative proportions depend very much on the process conditions. Temperature, pressure, heating rate and residence time can be used to influence the proportions and characteristics of the main products of this process. The products can be used in a variety of ways. However, when using MSW as a feedstock, the quality of the products is such that the most practical use of the produced char and oil/liquid is as a fuel. The pyrolysis gas can be used for power and heat generation, or synthesised to produce methanol or ammonia.

Gasification, means partial oxidation of the fuel in order to produce a fuel gas. The process is designed to maximise the gaseous product-yield. Some processes also include melting of inorganic components by adding pure oxygen creating a high temperature oxidising environment (temperatures > 2000°C). The vitrified mineral aggregate (slag) can safely be used for instance as gravel in road construction without leaching hazards. The process temperature of gasification is relatively higher than for pyrolysis. Typical temperature range is 800-1100°C, compared to 400-800°C for pyrolysis. The gaseous product typically contains CO, CO_2, H_2, CH_4, H_2O, N_2 and small amounts of higher hydrocarbons. In addition there will also be some contaminants such as small char particles, and small amounts of ashes and tars. The partial oxidation can be carried out by using air, oxygen, steam, carbondioxide or a mixture of these. Air gasification (most used in waste gasification) produces a low heating value (LHV) gas (4-10 MJ/Nm^3, the calorific value of natural gas being 39 MJ/Nm^3), while oxygen gasification produces a medium heating value (MHV) gas (10-15 MJ/Nm^3). The fuel gas can

through synthesis be upgraded to methanol, be burned externally in a boiler for producing hot water or steam, be burned in a gas turbine for electricity production or be burned in internal combustion engines such as diesel and spark ignition engine for the same purpose. Before the fuel gas can be used in gas turbines or internal combustion engines, the contaminants (tar, char particles, ash) have to be removed. The hot gas from the gas turbine can be used to raise steam to be utilised in a steam turbine (Integrated Gasification Combined Cycle)

Combustion means complete oxidation of the fuel. The hot flue gas produced during combustion can be used to heat a boiler and raise steam, which can be used in a combined heat and power (CHP) plant to produce electricity and hot water for district heating, or only one of these two options.

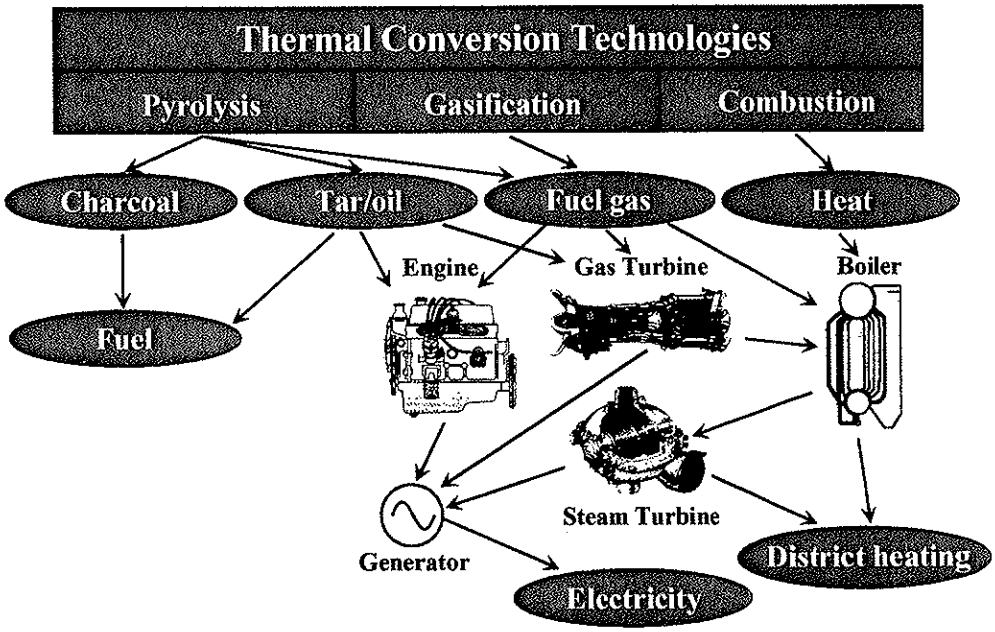

Figure 1.10 Thermal conversion technologies for wastes, their products and potential end-use[34].

Although there are several possibilities for thermal conversion of MSW and RDF, combustion remains the only commercially proven large-scale technology today. There exist some large-scale thermal conversion plants utilising advanced technologies, such as pyrolysis and gasification around the world. They are, however, considered as demonstration plants. However, several large companies are working on improving advanced technologies to meet the requirements in terms of environmental, economic and operational performance. The major share of combustion plants around the world is of the *mass burn* type. A mass burn combustion plant feed the as-received MSW, with the exception of oversized material (appliances and furniture etc.), directly into the furnace where it is burned on a grate without pre-treatment such as size reduction, shredding or material separation prior to burning. Another option is the *fluidised bed* (FB) combustion – type. In a FB combustion plant the as-received MSW is usually shredded to reduce the size and sorted to remove non-combustibles to produce RDF and then burned in a suspension fired furnace.

1.3.1 Grate fired mass burn units

The most widely deployed energy from waste process is mass burn with wet, dry or semi-dry gas cleaning systems. Mass burning technologies were developed in Europe at the turn of the century and have undergone substantial advancement in the past 20 years. By installing advanced combustion control systems, altering the configuration of the furnace and the location of the air injection ports, the combustion performance of these systems has been greatly improved. In addition, some facilities now process waste (e.g. by mixing) before feeding it to a mass burn plant and consider the extra cost to be warranted because the system runs more smoothly. Figure 1.11 shows an example of a mass burn facility. In mass burn facilities, little or non-processed waste is burned on a moving grate in a furnace. The furnace is large and robust in order to withstand large objects in the waste stream. In a mass burn system, the waste, typically from the municipal collecting

system, is dumped in a storage bunker. Possible large bulky items should be sorted out before the waste is fed to the furnace. The waste is mixed in the storage bunker before fed to the furnace where the combustion takes place. The burned out residue falls from the end of the grate into a water quench bath, before it is transported to the storage bunker. Heat from the hot combustion gases is recovered in the boiler, before the flue gas is cleaned to remove fine particles (fly ash), acid gases, heavy metals and organic species. Internationally, there is a diversity of installed air pollution control (APC) equipment in mass burn facilities. Some APC systems remove fine fly ash particles from the hot combustion gases using electrostatic precipitators prior to wet scrubbing by alkaline solvents to remove the acid gas components and flue gas condensation/reaction products. Units that utilise dry or semi-dry scrubbing systems (involving injection of an alkaline powder as a slurry) generally utilise fabric bag filters downstream of the scrubber systems to remove fly ash and other residue fractions (scrubber residues, condensation/reaction products). Additional APC measures, e.g. use of high surface area carbon-based sorbents are seeing increased use for mercury control and reduction of organic emissions. The scrubber residues and bag filter dust are known as the APC residues and are often combined with the fly ash. Both the fly ash and APC residues (scrubber residues, bag filter dust and other sorbent residues) contain potentially harmful material, such as heavy metals and are often combined prior to disposal. New requirements on NO_x emissions have also led to the implementation of NO_x abatement equipment or technology, such as selective reduction by using ammonia (NH_3) injection (selective non-catalytic reduction (SNCR) or selective catalytic reduction (SCR)).

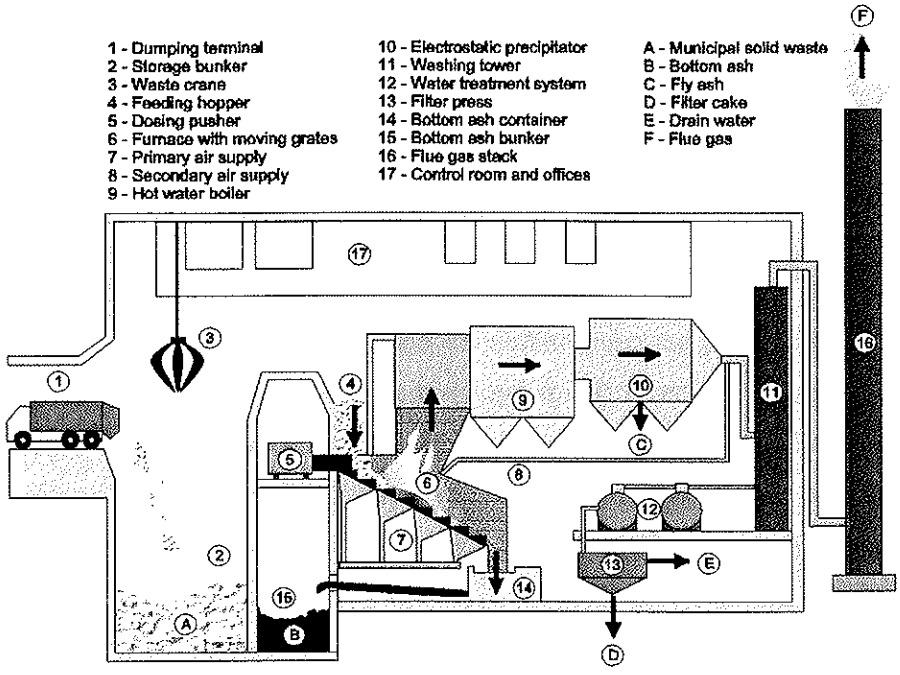

Figure 1. 11 Typical grate fired mass burn facility[42].

1.3.2 Fluidised bed combustion

An alternative approach to mass burn systems is to first sort the MSW to remove recyclable materials (e.g. magnetic separation of the ferrous component) and wet putrescible materials (see Figure 1.12). The combustible material is then shredded and burned as refuse derived fuel (RDF). Further processing can be used to remove glass, grit, sand, certain plastics and aluminium materials if desirable. Air classifiers or rotary drums may also be used to further process the fuel product by removing additional non-combustible materials. During the processing the material is thoroughly mixed, improving its homogeneity.

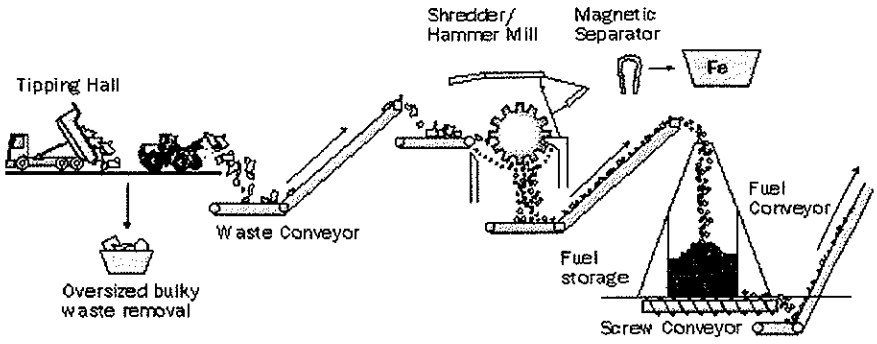

Figure 1.12 Fuel preparation at Dundee Waste-to-Energy plant[41].

Fluidised bed combustion (FBC) technology is suited for the utilisation of RDF. RDF is fed to the FBC reactor and burned in a fine inert material, such as sand, fluidised by air blowing upwards through it. Flue gas cleaning systems typically consists of cyclone separators for the removal of larger particles; limestone injection into the combustion chamber or lime injection into the flue gas for acid gas abatement; injection of activated carbon for removal of mercury and dioxins and bag house filters for removal of the finer particulate materials (see Figure 1.13). The bottom ash removed from the base of the FBC is not quenched and contains a high proportion of sand particles from the fluidised sand bed. It is mixed with boiler dust before leaving the plant. The flue gas cleaning residue streams consist of cyclone dust (fly ash) and APC residues (desulphurisation residues and bag house filter dust). These streams are often combined prior to disposal.

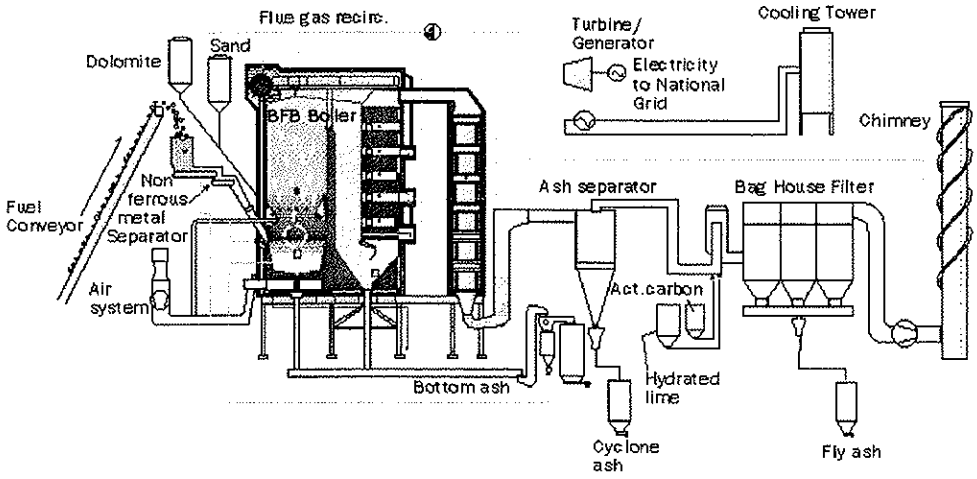

Figure 1. 13 Schematic drawing of process line for Dundee BFBC[41].

1.3.3 Small-scale combustion plants

The UK Strategy for Sustainable Waste Management talks about the "desirability of recovering or disposing of waste close to the place where it is produced". This is called the "proximity principle", which places the responsibility for the waste on the communities producing it, aims to minimise environmental impacts through the transport of waste and aims to result in waste treatment facilities which are more suited to and acceptable to local communities. Another interesting positive aspect promoting the use of smaller combustion plants is the electricity market liberalisation. As electricity markets become more liberalised, increased opportunities are created for smaller generators to sell electricity directly to users. By avoiding the use of national transmission grids and limiting the use of local transmission networks, small-scale generators can avoid the associated costs and therefore realise a higher price for their electricity than would otherwise have been the case. This will in turn help to improve the economics of such projects. These arguments are often used to promote the possibility of using small-scale combustion plants in areas with a relatively small population.

There not many producers of small-scale combustion plants worldwide. Norway, however, are in the fortunate position of having two producers of small-scale combustion or gasification plants for waste and biomass (Organic Power AS and Energos ASA). The definition of the term "small-scale" is not absolute and may vary. Energos and OPAS deliver plants in the range of 6-12 and 0.5-2 MW_{th}, respectively. A schematic overview of the Energos technology is shown in Figure 1.14. A typical Energos combustion plant consists of fuel silo and storage bunker (1,2). Controlled loading of the fuel into the oven is managed by a feeding system before the fuel is combusted on a moving grate system in a primary and secondary combustion chamber (3,4). The bottom as is fed into the ash container. The heat from the hot flue gases from combustion the furnace is recovered in a boiler (5,6). After the boiler, the cooled flue gas enters the flue gas cleaning system consisting of dry lime and activated carbon injection (7) and a baghouse filter (8) before it leaves the stack (9). A sophisticated control and surveillance system (10) makes it possible to control NO_x emissions with primary measures.

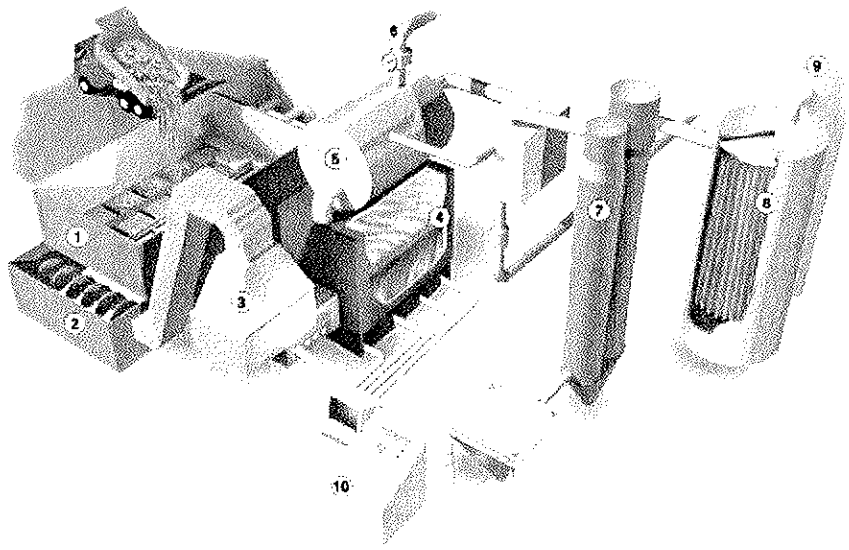

Figure 1.14 Schematic overview of the Energos combustion plant[43].

1.3.4 Gasification

Gasification is not a new technology, although its application to waste feedstock is still being developed. Coal gasification has been used since the early 1800s to produce town gas and the first four-stroke engine was run on producer gas in 1876.

Figure 1.15 shows a schematic overview of the TPS (Termiska Prosesser AB) gasification process. The waste has to be pre-processed into dry RDF pellets before fed to the gasifier. An atmospheric gasifier (circulating fluidised bed) using air as gasifying medium at a temperature of 870°C produces a fuel gas and tar. Larger particles are removed by the use of cyclones before entering the tar cracker. The tar cracker, which also is a circulating fluidised bed reactor, converts the tar into gas. A typical fuel gas consists of 8 vol.% H_2, 11% CO, 7% C_xH_y, 13% CO_2, 49% N_2 and 12% H_2O. Another set of cyclones removes larger particles before the fuel gas is cooled, cleaned from fine particles by a fabric filter and removing acid gases by adding dry lime in a scrubber. The cooled and cleaned fuel gas is then utilised in a combined cycle (gas and steam turbine) to maximise energy efficiency of the process.

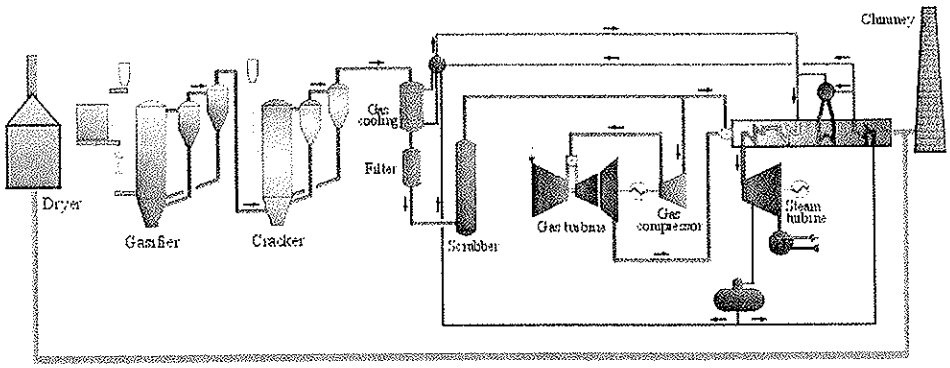

Figure 1.15 Schematic overview of the TPS gasification process.

1.3.5 Pyrolysis

Figure 1.16 shows a schematic process description of the Ticino Canton Pyrolpleq pyrolysis plant in Switzerland. Pre-processing of the waste is necessary in order to remove undesirable objects and for particle size reduction. The pre-processed waste is fed into a rotary pyrolysis kiln. The rotary kiln is externally heated by using a part of the hot flue gas from combustion of the pyrolysis gas. The waste inside the rotary kiln is heated to 450-550°C and pyrolysed in less than an hour. The resulting volatiles from pyrolysis leave the kiln at 550°C. At the end of the pyrolysis drum is a screening section, which divides the solid residue into two fractions. The mainly fine-particle pyrolysis char is discharged with exclusion of air. The screen oversize consists of recyclable metallic residues and coarse inert matter and is discharged wet through a water seal. Hot gas filtration by means of ceramic filter cartridges cleans the pyrolysis gas before entering the combustion chamber, where the pyrolysis gas is burnt at temperatures above 1200°C with a residence time above 2 seconds. The hot gas from the combustion chamber is fed to a steam generator producing steam for a steam turbine. After passing through the steam generator the cooled flue gas is cleaned by means of a dry scrubber (injection of lime and activated carbon) removing acid gases and volatile heavy metals and a fabric filter removing particulate matter.

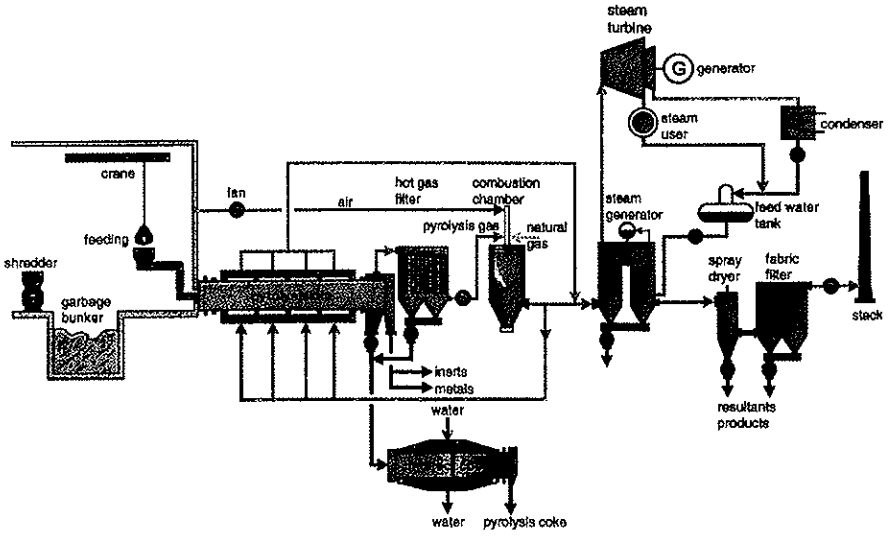

Figure 1.16 Process description of the Ticino Canton Pyrolpleq pyrolysis process in Switzerland[35].

1.4 Emission requirements and abatement

The increasing awareness of the environmental hazards connected to emissions from MSW combustion lead to stricter and stricter emission requirements. MSW contain many elements at relatively high concentrations leading to harmful emissions, such as heavy metals, nitrogen, sulphur, chlorine, etc. This has led to substantial efforts in developing combustion systems, which can operate within given emission requirements. In Table 1.8 the Norwegian emission requirements (similar to the EU requirements) for emissions to air for new combustion plants for MSW larger than 3 ton/day are given. In addition to these emission requirements there are also emission/management requirements connected to the management/effluent of ashes and products from the flue gas cleaning system.

Table 1.8 Norwegian emission requirements (similar to EU requirements) to air for new combustion plants with a capacity larger than 3 ton/day[45].

Component(s)	**Emission requirements [mg/Nm^3@11vol% O_2, dry]**
Particulate matter (PM_{10})	10
Hg	0.05
Cd+Ti	0.05
Pb+Cr+Cu+Mn+Sb+As+Co+Ni+V+Sn	0.5
CO	50
HF	1
HCl	10
TOC	10
NO_x (measured as NO_2)	200
NH_3	10
SO_x (measured as SO_2)	50
Dioxins	0.1[a]

[a] ng/Nm^3 2378 TCDD-equivalents (Nordic standard)

There are several environmental and health hazards connected to the emission of the species in Table 1.8. Particulate matter (PM) is injurious to health at sufficient concentrations in the air that we breathe. They may harm the bronchia, and increase the risk for asthma, and the transport of carcinogenic and other substances injurious to health down to the lungs. PM less than 2.5 μm ($PM_{2.5}$) constitute the major portion of PM emissions from MSW combustion plants and may therefore be of special interest. There are, however, no restrictions to $PM_{2.5}$ due to lack of data on the health effects. Heavy metals are toxic in the environment and accumulate in the food chain. Heavy metals do not break down, but will remain in the environment forever. Some of the heavy metals, especially cadmium, can deposit in the soil and be absorbed by plants. Mercury can be transformed into methyl mercury in sediments and be accumulated in the food chain, especially through fresh water. Exposure to excessive levels of heavy metals can provoke a number of health effects. Excessive amounts of lead and mercury are especially dangerous with regards to damage to the nervous system and fetal life. Lead can also give cardiovascular diseases and anaemia. Excessive amounts of cadmium can damage the kidney after long term exposure and accumulating in the body.

Restrictions on CO emissions are connected to a good operation of the combustion plant rather than possible health effects since the concentrations of CO in the air must be higher than what can be produced by a combustion plant for MSW to cause health effects. HCl contributes to acid rain and is highly corrosive, while HF is hazardous to plants and animals. The health effects of HF to human beings is not considered to be of importance since the exposure level in air caused by MSW combustion plant will be too low. SO_2 oxidise in the atmosphere to sulphuric acid, which is highly corrosive and contributes to acid rain. SO_2 may cause damage to the bronchia in human beings. Emission of NO_x from combustion of MSW represents a considerable environmental and health problem. Exposure to NO_x gives irritation effects and infection like reactions in lungs and reduced lung function[46]. NH_3 may damage vegetation, and cause corrosion and material damage. In addition NH_3 have a negative effect on the human respiratory system. TOC (Total Organic Compounds) also called VOC (Volatile Organic Compounds) are harmful for lungs and people with asthma are especially exposed. Dioxins (also called chlorinated organic compounds) in general are toxic to the environment and to human beings. Reduced immune defence and capacity for reproduction, and development of cancer are health effects caused by excessive dioxin exposure[46].

In order to meet the strict emission regulations, the combustion plant is equipped with an air pollution control system (APC). The APC typically consists of a dry or wet scrubber to remove acid components such as HCl and SO_x. Activated carbon is usually injected into the flue gas to remove dioxins and volatile heavy metals such as mercury, while a filter collects particulate matter. NO_x emissions can be controlled by *primary* or *secondary* measures. Primary measures involve treatment prior to or during the combustion process and are not considered to be part of the air APC system. Generally, there are a wide range of possible primary reduction techniques, such as staged air combustion, reduced excess air (improved mixing), reburning, flue gas recirculation and combustion with pure oxygen. Secondary measures mean injection of a reducing agent for selective NO_x

reduction. The most important reducing agents are ammonia (NH_3), sal ammonia (ammonia aq. max 24%) and urea ($[NH_2]_2CO$). Two methods, which may be used, are selective non-catalytic reduction (SNCR) and selective catalytic reduction (SCR). In an SNCR system the reducing agent needs to be injected in the flue gas in a narrow temperature window (1123-1223 K) for optimum reduction conditions. However, by using a catalyst (SCR) it is possible to shift the optimum temperature window to lower temperatures (~500-700 K)[47].

1.5 References

1 Natural Resources and the Environment, Report from Statistics Norway, 2000. (http://www.ssb.no/emner/01/sa_nrm/nrm2000/).

2 White paper no. 8 (Parliament report) on government environmental policy and state of the environment, Norwegian Department of the environment, 1999.

3 Statistics Norway, Waste statistics on MSW, 2000. (http://www.ssb.no/emner/01/05/avfall_tab_fig/t_kagvts.html)

4 Bruvoll, A. and Ibenholt, K., Projection of Waste Amounts and Environmental Effects in connection to Waste disposal, Report 1999/32 from Statistics Norway, 1999. (http://www.ssb.no/emner/01/05/rapp_9932/).

5 Statistics Norway, Waste statistics on Commercial waste, 2000. (http://www.ssb.no/emner/01/05/avfall_tab_fig/t_nagvma.html)

6 Willigenburg, A. and Malinen, H., *Warmer Bulletin*, 1995, **47**,16-17.

7 Temmink, H., *Biomass and Bioenergy*, 1995, **vol. 9**, 351-363.

8 Norwegian Pollution Control Authority, Our Common Environment - Waste, Report TA 664, 1992 (in Norwegian).

9 US Environmental Protection Agency, *Characterisation of Municipal Solid Waste in the United States – 1997 Update*, Report No. EPA 530-R-98-007,1998.

10 Kulik, A. and Witoszek, A., *WPROST*, 1994, 4, 36-37.

11 Laughlin, K, "The management of residues from thermal processes", Report from the International Energy Agency prepared by CRE Group Ltd., CRE Ref. No. 8056/3, UK, March 2000.

12 Wenzl, H.F.J., *in The Chemical Technology of Wood*, Academic Press Inc., 1970.

13 Rydholm, S. A., *in Pulping Processes*, Interscience Publishers, USA, 1965.

14 Olsson, I., *in Papertypes for different use*, No. X-731, Swedens Forrest Industry Union, Markaryd, Sweden, 1986 (in swedish).

15 Hult, N., *in Coating of paper*, No. Y-308, Swedens Forrest Industry Union, Markaryd, Sweden, 1986 (in swedish).

16 Christensen, P. K., *Wood processing chemistry*, Compendium from Institute of Chemical Engineering, Norwegian University of Science and Technology, 1995 (in norwegian).

17 Rance, H. F., *in Handbook of Paper Science – Vol. 1*, Elsevier, The Netherlands, 1980.

18 Brydson, J.A., *in Plastics Materials*, Butterworth-Heinemann Ltd., Oxford, UK, 1995.

19 Agrawal, R.K., Phd thesis no. 8504302 Clarkson University, USA, 1984.

20 Norwegian Pollution Control Authority, Emissions from MSW management, Report 96:16 (in Norwegian), 1996.

21 Tillman, D. A., *in The Combustion of Solid Fuels & Wastes*, Academic Press, San Diego, USA, 1991.

22 Flagan, R. C. and Seinfeld, J. H., "Fundamentals of air pollution engineering", Prentice-Hall Inc., 1988.

23 Wilen, C., Moilanen, A. and Kurkela, E., "Biomass feedstocks analyses", VTT Publication 282, 1996, Espoo, Finland.

24 Røkke, N., Phd thesis, ITE-rapport 1994:33, Norwegian University of Science & Technology, 1994.

25 Hellsten, G. and Mørtstedt, S., "Energy- and chemical engineering", ISBN 82-585-0243-3, 1985.

26 Rigo, H. G.; Chandler, A. J. (1994), Metals in MSW - Where are they and where do they go in an incinerator?, *Proceedings of the National Waste Processing Conference*, ASME, USA.

27 Heie, Aa; Sørum, L. (1997), Interconsult Report 3924.003.

28 Frandsen, F. J., (1995), Ph.D. Thesis, Technical University of Denmark.

29 Nussbaumer, T. (1994), Emissions from biomass combustion, *Proceedings of IEA Biomass Combustion Conference*, Cambridge.

30 Clarke, M. J., (1991), *Waste Age United States*, **May issue**, 105-118.

31 Wu, C-H., Chang, C-Y., Lin, J-P., and Hwang, J-Y., 1997, *Fuel*, **12**, 1151-1157.

32 Siau, J. F, "Transport Processes in Wood", Springer-Verlag Series in Wood Science, 1984.

33 IEA CADDET Centre for Renewable Energy, Report title: "Advanced Thermal Conversion Technologies for Energy from Solid Waste", ISBN 1 900683 03 2, 1998.

34 Grønli. M.G., Ph.D. thesis NTNU 1996:115, The Norwegian University of Science and Technology, 1996.

35 Bracker, G-P., von Christen, F-E., Stadtmüller, J., Power, March, 1998.

36 "Thermal treatment of household waste – An evaluation of five techniques (The summary of a comparative study)", Report from Novem, The Netherlands, 1995.

37 "Gasification of waste – Evaluation of the waste processing facilities of the Thermoselect and TPS/greve", Novem report 9420, The Netherlands, 1994.

38 Whiting, K., "Thermal Processing of Solid Waste", Warmer Bulletin, 53, March, 1997.

39 Schubert, R. and Stahlberg, R., "Continuous In-Line Gasification/Vitrification Process for Thermal Waste Treatment", Proceedings of "Waste to Energy – The Latest Technical Development", Malmø, Sweden, Sept., 1999.

40 Greil, R. and Stammbach, M. R., "Aplications of The RCP-System Based on RCP-Derivatives: The Von Roll 16 MW Standard Plant", Proceedings of "Waste to Energy – The Latest Technical Development", Malmø, Sweden, Sept., 1999.

41 Thurgood, M., "DERL Energy from Waste Facility Dundee, Scotland", Report from the International Energy Agency, (In Press).

42 Sørum, L.; Fossum, M.; Evensen, E.; Hustad, J. E. (1997), Heavy Metal Partitioning in a Municipal Solid Waste Incinerator, *Proceedings of the Fifth Annual North American Waste-to-Energy Conference*, Apr 22-25, North Carolina, USA.

43 http://www.energos.com

44 http://www.organicpower.com

45 Faximile from The Norwegian Pollution Control Authority, 04.08.00.

46 Benestad, C., Braastad, G., Normann, H. H., Færden, T., Nåmdal, S., Moe, M., Hoel, A., *Combustion Plants - Instructions for Officials in Charge*, Report no. 95:13, The Norwegian Environmental Protection Agency, Oslo, **1995**, p. 86 (in Norwegian).

47 Skreiberg, Ø., Ph.D. thesis NTNU 1997:128, The Norwegian University of Science and Technology, 1997.

2 Pyrolysis characteristics and kinetics of MSW

2.1 Introduction

The aim of this section is to give a short introduction to the use of thermogravimetric analysis (TGA) to determine pyrolysis characteristics of MSW components in connection to the work performed in Paper I. A short description of the TGA equipment and a general description of degradation mechanisms is given.

TGA can be used to find the thermal degradation behaviour and chemical kinetics during pyrolysis. TGA is performed by using a TGA apparatus, which is an highly automated instrument that yields continuous data on the mass loss (TG) and rate of mass loss (DTG) of a sample as a function of either temperature or time as the sample is heated at a programmed heating rate. Figure 2.1 shows a schematic view of the SDT 2960 Simultaneous TGA-DTA from TA Instruments used in this study. The system is based on a dual beam horizontal design in which each ceramic beam (arm) functions as one half of a DTA (Differential Temperature Analysis) thermocouple pair, as well as part of a horizontal null-type balance. One arm accommodates the sample and measures its property changes. The other arm accommodates the reference and is used to generate the DTA (ΔT) measurement, as well as to correct the TGA measurement for temperature effects like beam growth. A taut-band meter movement located at the rear of each of the ceramic arms measures the weight change. An optically activated servo loop maintains the balance arm in the horizontal reference (null) position by regulating the amount of current flowing through the transducer coil. An infrared LED light source and a pair of photosensitive diodes detect movement of the arm. A flag at the end of the balance arm controls the amount of light reaching each photo sensor. As weight is lost or gained, the beam becomes unbalanced, causing unequal light to strike the photodiodes.

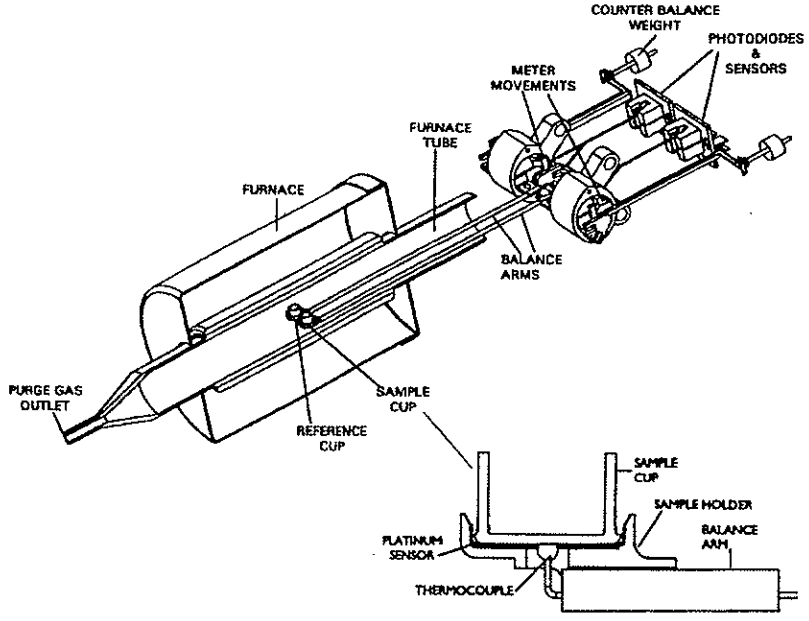

Figure 2.1 Schematic figure of the SDT 2960 Simultaneous TGA-DTA from TA Instruments[1].

A restoring current is generated to eliminate this imbalance and retain the null position. The amount of restoring current is a direct measure of the weight change. The DTA (ΔT) measurement is made by a pair of matched platinum/platinum-rhodium thermocouples, which are contained inside the ceramic arms and welded to platinum sensors located in the bottom of the sample and reference holders. The thermocouple in contact with the sample is also used to monitor the sample temperature. A bifilar-wound furnace provides uniform controlled heating up to 1500°C. The SDT 2960 have a sample capacity up to 200 mg and a balance sensitivity of 0.1μg. The heating rate can be set from 0.1 to 100°C/min for experiments from ambient to 1000°C and 0.1 to 25°C/min for experiments from ambient to 1500°C.

Selecting the proper sample size and heating rate is very important. Too large samples may shift the decomposition from control by chemical kinetics to control by heat and mass transfer. Performing experiments with a too high heating rate may introduce thermal lag, which causes the temperature measurement to be incorrect[2]. Figure 2.2 shows TG and DTG curves for different MSW components derived from the TGA apparatus. The experiments were performed with a heating rate of 10°C/min and a sample mass of 5 mg. As observed, the pyrolysis characteristics of the MSW components are quite different in terms of mass loss and rate of mass loss as a function of temperature. Figure 2.3 show a generalised view of the degradation mechanisms for paper/cardboard and different plastics. During pyrolysis, the different materials will start to decompose at different temperatures depending on their chemical composition. The pyrolytic degradation of cellulosic materials such as paper and cardboard can be described by three independent parallel reactions. The chemical components of the cellulosic fraction, hemicellulose, cellulose and lignin decompose into volatiles and char. The hydrocarbon based plastics, HDPE, LDPE, PP and PS, however decomposes completely into volatiles in a single reaction. PVC separates from the other plastics with its high content of chlorine and degradation behaviour. It is assumed that PVC decomposes into volatiles and char in three independent parallel reactions.

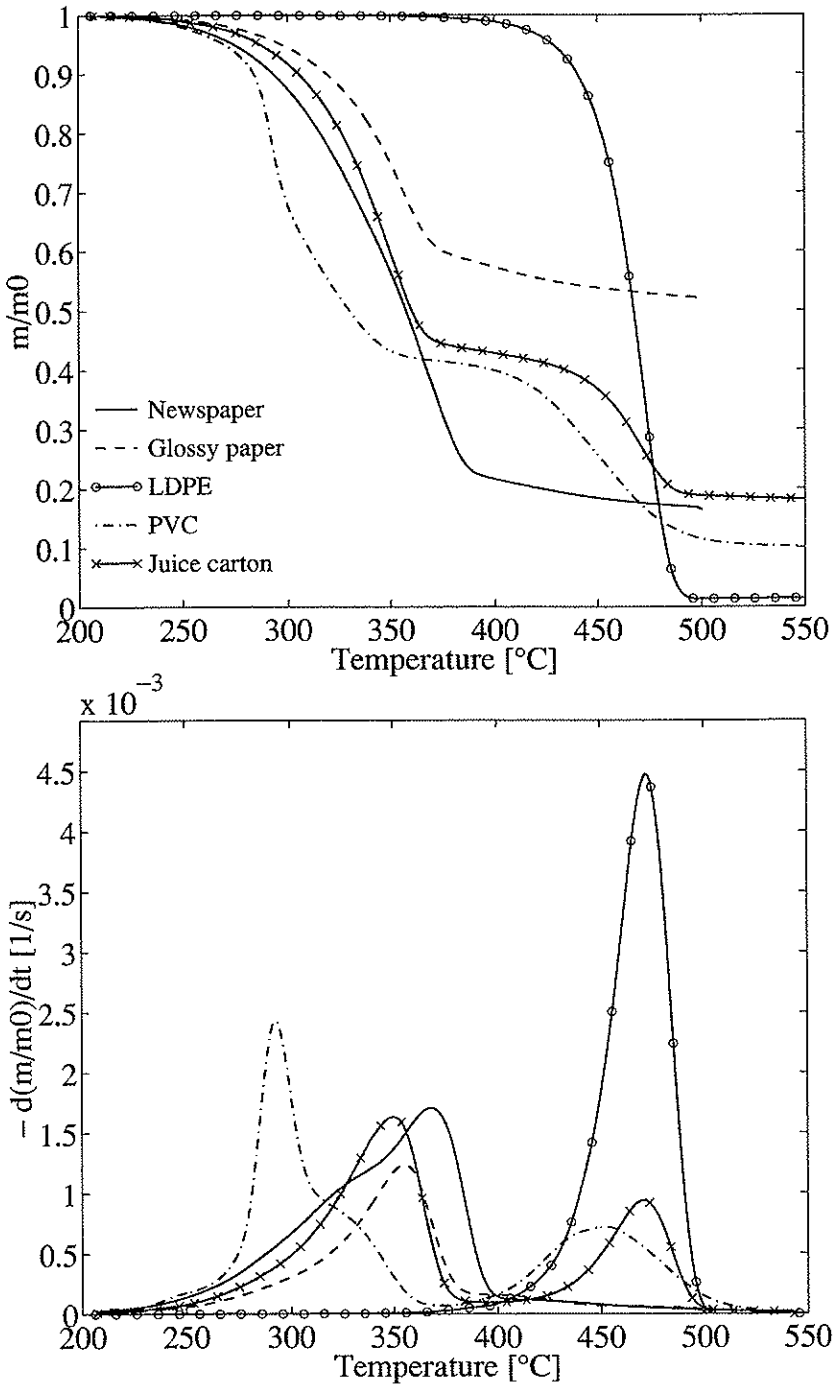

Figure 2.2 TG and DTG curves for different paper and plastic components of MSW.

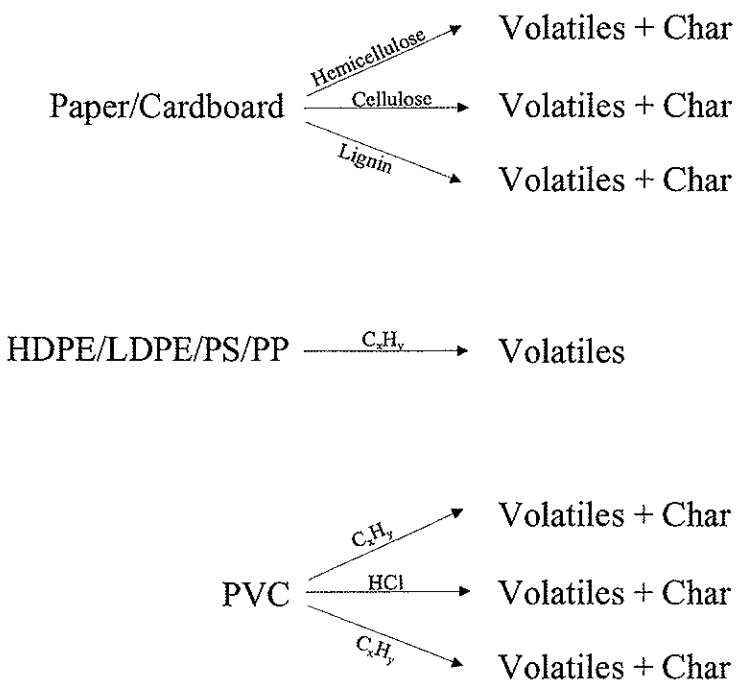

Figure 2.3 Degradation reactions of paper, cardboard, HDPE, LDPE, PP, PS and PVC.

2.2 References

1 Brochure from TA Instruments.

2 Grønli, M. G., Antal, M. J. and Vãrhegyi, G., *Ind. & Eng. Chem. Research*, 38 (6), 1999.

2.3 Paper I

Pyrolysis Characteristics and Kinetics of Municipal Solid Wastes

Authors:

Lars Sørum*, Morten G. Grønli** and Johan E. Hustad*

*Norwegian University of Science & Technology, Institute of Thermal Energy and Hydropower

** SINTEF Energy Research, Department of Thermal Energy

Paper Submitted to the Scientific Journal ***FUEL***

ABSTRACT

The large variety in Municipal Solid Waste (MSW) composition and differences in thermal degradation behaviour of MSW components makes modelling, design and operation of thermal conversion systems a challenge. The pyrolysis characteristics of 11 different components, representing the dry cellulosic fraction and plastics of MSW, have been investigated. The aim of this study is to obtain detailed information on the pyrolysis characteristics and chemical kinetics of the most important components in MSW. A thermogravimetric analysis including determination of kinetic parameters are performed at a constant heating rate of 10°C/min in an inert atmosphere. The cellulosic fraction of MSW was modelled by three independent parallel reactions describing the degradation of hemicellulose, cellulose and lignin. The plastics polystyrene, polypropylene, low-density polyethylene and high-density polyethylene were all modelled as single reactions describing the degradation of hydrocarbon polymers. The degradation of PVC was modelled with three parallel reactions describing the release of benzene during dehydrochlorination, dehydrochlorination reaction and degradation of remaining hydrocarbons. Possible interactions between different paper and plastic components in mixtures were also investigated. It was found that the reactivity of cellulosic matter was increased in a mixture with PVC.

1 INTRODUCTION

The awareness of the environmental consequences connected to waste disposal together with the large amounts and inhomogeneous nature of MSW has led to complex waste management systems. Material reuse/recycling, anaerobic digestion, composting and combustion with energy recovery are some of the methods that are used in addition to landfilling. The lack of landfill sites and assessments of the environmental consequences of landfilling have led many countries to ban landfilling of combustible wastes, including wet organic waste.

There is also an increase in reuse and recycling of MSW fractions such as paper and cardboard, beverage cartons and plastics. Together with the variation in MSW management policy, changing consumer patterns and new products will also alter the composition of MSW subjected to energy recovery. The differences in annual per capita generation, composition and management of MSW in USA, Norway and Poland shown in Table 1, illustrates that the external conditions for selecting a proper energy recovery system may vary largely from country to country.

Table 1. Annual per capita generation, composition and management of MSW in USA, Norway and Poland[1-5].

	Annual per capita generation (kg)	**Paper/ cardboard (wt%)**	**Plastics (wt%)**	**Wet organic waste (wt%)**	**Metals and glass (wt%)**	**Rest fraction (wt%)**
USA	800	38	9	29	14	10
Norway	470	31	7	18	8	36
Poland	260	14	2	38	9	37

	Landfilling (wt%)	**Energy recovery (wt%)**	**Recycling[a] (wt%)**
USA	61	15	24
Norway	68	18	14
Poland	99	0	1

[a] Includes composting

Poland has the lowest annual generation with 260 kg/capita, whereas Norway and USA have 470 and 800 kg/capita, respectively. The composition also shows large variations, especially between USA/Norway and Poland. The Polish waste has less high calorific waste such as paper/cardboard and plastics, whereas the fraction of low calorific wet organic waste is higher. With these relatively large differences in composition, it is important to have knowledge on the properties of MSW as a fuel.

Characterisation of MSW including quantification, composition, and proximate and ultimate analysis has to some extent been reported in previous

work[6-13]. Pyrolysis studies including kinetic modelling of single MSW components and mixtures have revealed large variations in kinetic rate constants (activation energy and frequency factor) [14-22]. This scatter may be attributed to differences in materials, experimental apparatus and conditions, and analytical methods used in the kinetic evaluation. The scatter and lack of data on pyrolysis characteristics and kinetics have motivated this work. In the present work, four paper qualities (newspaper, recycled paper, glossy paper, cardboard), one wood species (spruce), five different plastics (PS = polystyrene, PP = polypropylene, LDPE = low-density polyethylene, HDPE = high-density polyethylene, PVC = poly(vinylchloride)) and one multi-material component (juice carton) have been characterised. This includes proximate- and ultimate analysis and determination of the higher heating value (HHV). The pyrolytic degradation characteristics of these components have been studied by thermogravimetry (TGA). Pyrolysis kinetics has been obtained by using a single reaction model and a model of independent parallel reactions. The aim of this work is to gather data and obtain knowledge, which can be useful in the modelling, design, and operation of thermal conversion processes for MSW (i.e. pyrolysis, gasification and combustion systems).

2 EXPERIMENTAL

2.1 Materials

Components representing the major part of the combustible MSW have been studied. The samples studied represent the cellulosic fraction (paper, cardboard, wood) and plastic and multi-material fraction of MSW.

Cellulosic Fraction: The most important fibre source for paper production is wood. Wood consists of three major components: cellulose (40-45 wt%), the skeletal polysaccharide; hemicellulose (27-39 wt%) which form the matrix; and lignin (21-30 wt%), the encrusting substance that binds the cells together[77].

Additionally, wood contains many low-molecular-weight organic compounds known as extractives (2-5 wt%) and small amount of mineral matter (0-3 wt%) known as ash. Paper pulp can be produced from wood either mechanically or chemically[24-28]. Mechanical energy is used for defibration to fibre and fibre fragments in the production of mechanical pulp. The pulp yield, as a percentage of the wood used, is typically 96-100 wt%. The most commonly used boiling processes to make chemical pulp are the sulphite, soda and sulphate (kraft) processes. Approximately 80% of the world's chemical pulp produced are made by the kraft boiling process, using NaOH and Na_2S as solvents. During the boiling process, hemicellulose and lignin are gradually removed and the proportion of cellulose increases. Chemical and half-chemical pulps have typical yields of 30-60 wt% and 50-85 wt%, respectively. Removal of the coloured substances (mainly lignin) from the pulp is usually done by chlorine and/or alkali treatment. After bleaching, the lignin content in the pulp can be reduced to less than 1.0 wt%. Originating from the coating process, paper or cardboard may also contain inorganic additives (pigment), binder and chemical additives (lubricant, foam reducer of coating melt, etc.).

The samples of newspaper, recycled paper, glossy paper and cardboard were taken before it was dumped in the waste bin. Meaning that the samples were clean, dry and not contaminated with other substances such as wet organic wastes. Spruce, being the most commonly used raw material for paper production in Norway, was cut from forests outside Trondheim. *Scandinavian Spruce* (*Picea abies*) has a typical cellulose, hemicelluloses and lignin content of 43, 27 and 29 wt%, respectively. *Newspaper* and other paper qualities with a relatively short lifetime are usually made from mechanical pulp, but 5-10 wt% of chemical pulp can be added to make the processing easier. Newspaper, with a typical pulp yield of 90 wt%, has a hemicellulose and lignin content of 26 and 28 wt%, respectively. It is very difficult to know the origin of *recycled paper,* since it can be made of any number of different paper qualities. *Glossy paper* (coated paper, magazine paper)

can be produced in many different qualities depending on the blend of sulphate/sulphite and mechanical mass. Glossy paper with a typical pulp yield of 75-80 wt% has a hemicellulose and lignin content of 19% and 26%, respectively. Glossy paper may contain up to 30 wt% clay, which is used in the coating process to get a good finish of the surface. The *cardboard* used in this work is made of two different types of pulp. Unbleached sulphate pulp are typically used in the flat layer of unbleached cardboard, while unbleached half chemical pulp is used in the corrugated part. Cardboard with a typical pulp yield of 65-70 wt% has a hemicellulose and lignin content of 19% and 18%, respectively[24].

Plastics: Clean non-coloured samples of LDPE, HDPE, PS, PP and PVC were obtained from two Norwegian plastic producers (Borealis and Norsk Hydro). Although the application of these plastics may overlap, they have different properties such as impact strength, density, aging and weathering, electric insulation properties and diffusion and permeability. The polymeric structure of both *LDPE* and *HDPE* is essentially a long chain of aliphatic hydrocarbons. The difference in density is due to chain branching. Polyethylene (PE) in general, is cheap and easy to process, and applications include heavy-duty sacks, refuse sacks, carrier bags, toys, electric cable insulation and general packaging[29]. *PP* has a slightly different structure than LDPE and HDPE with a methyl group (CH_3) in the repeating unit. *PS* is made from the styrene monomer and the repeating unit contains a benzene ring (C_6H_6). PP is often used as textile and "fast turnover food" packaging such as margarine tubs. PS is preferred when rigidity and low cost are important in products such as storage containers, toys and electrical equipment. For *PVC,* the methyl group of PP has been substituted with chlorine (Cl). Commercial PVC polymers are amorphous, slightly branched molecules with the monomer residues arranged in head-to-tail sequence. PVC has very wide application, from rigid piping and window frames to soft flexible foams.

Multi-materials: The juice carton was bought from the local store, and consists of 75wt% paperboard, 20wt% PE and 5wt% aluminium. Juice cartons are interesting from both an energy and material recovery point of view. For example, the aluminium can be recovered through thermal degradation of the paperboard and plastic at low temperatures and oxygen concentrations.

Table 2 shows the proximate analysis, ultimate analysis and higher heating values (HHV) of the MSW components. The fuel properties of the cellulosic fraction (paper/cardboard/wood) and plastics are quite different. Compared to the cellulosic fraction, which have a fixed carbon content of 5-10wt%, plastics have practically 100% volatiles, with the only exception of PVC (5wt% fixed carbon). The ultimate composition of paper and cardboard (on a dry ash free basis) is similar and comparable to wood (roughly 47wt% of C and O and 6wt% of H). The ash content for paper and cardboard varied from 1-28wt%, with corresponding HHV values of 19.3-10.4 MJ/kg and fixed carbon yields of 10.5-4.7wt%. The plastics PS, PP, LDPE and HDPE, however, had no ash and a HHV ranging from 42-47 MJ/kg. The higher HHV of these plastics compared to the cellulosic fraction is reflected in the ultimate composition, with much higher contents of hydrocarbons (85-93wt% C and 7-15wt% H) and no oxygen. PVC, on the other hand, has a similar content of hydrocarbons and consequently a similar HHV as the cellulosic fraction. The major difference between PVC and the cellulosic fraction with regards to the ultimate composition is the large content of chlorine in PVC (~48wt%) and a corresponding low oxygen content (6wt%). The contribution of each constituent (paperboard, PE and aluminium) of the juice carton is reflected in the results from the proximate analysis and HHV. The results of the proximate analysis is similar to cardboard, since the increased volatile matter on the account of PE is levelled off by the content of non-volatile aluminium. The HHV of 24.4 MJ/kg is higher than for paper due to the contribution of the higher heating values of PE and aluminium compared to paper/cardboard.

Table 2. Proximate analysis, ultimate analysis and heating values of paper, cardboard, spruce, juice carton and plastics. (n.a. = not available).

Sample	Proximate Analysis			Ultimate Analysis [20,30,40]						HHV (MJ/kg)
	VM (wt%)	Fix-C (wt%)	Ash (wt%)	C (wt%)	H (wt%)	O[a] (wt%)	N (wt%)	S (wt%)	Cl (wt%)	
Cellulosic fraction:										
Newspaper	88.5	10.5	1.0	52.1	5.9	41.86	0.11	0.03	n.a.	19.3
Cardboard	84.7	6.9	8.4	48.6	6.2	44.96	0.11	0.13	n.a.	16.9
Recycled paper	73.6	6.2	20.2[b] 22.4[c]	n.a.	n.a.	n.a.	n.a.	n.a.	n.a.	13.6
Glossy paper	67.3	4.7	28.0[b] 42.7[c]	45.6	4.8	49.41	0.14	0.05	n.a.	10.4
Spruce	89.6	10.2	0.2	47.4	6.3	46.2	0.07	n.a.	n.a.	19.3
Plastics:										
HDPE	100.0	0.0	0.0	86.1	13.0	0.90	n.a.	n.a.	n.a.	46.4
LDPE	100.0	0.0	0.0	85.7	14.2	0.05	0.05	0.00	n.a.	46.6
PP	100.0	0.0	0.0	86.1	13.7	0.20	n.a.	n.a.	n.a.	46.4
PS	99.8	0.2	0.0	92.7	7.9	0.00	n.a.	n.a.	n.a.	42.1
PVC	94.8	4.8	0.4	41.4	5.3	5.83	0.04	0.03	47.7	22.8
Multi-material:										
Juice carton	86.0	6.1	7.9	n.a.	n.a.	n.a.	n.a.	n.a.	n.a.	24.4

[a] Obtained by mass balance., [b] Ashed at 950°C.,[c] Ashed at 575°C.

2.2 Apparatus and Procedure

An SDT 2960 Simultaneous TGA-DTA from TA Instruments was used for the experimental study. The system is based on a dual-beam horizontal design in which each ceramic beam (arm) functions as one half of a DTA thermocouple pair, as well as part of a horizontal null-type balance. One arm accommodates the sample and measures its property changes. The other arm accommodates the reference (typically an appropriate amount of inert material such as aluminium oxide) and is used to generate the DTA (ΔT) measurement, as well as to correct the TGA measurement for temperature effects like beam growth. Detailed description of the equipment is given by Grønli[30]. A sample weight of 5 mg and a heating rate of 10°C/min were chosen based on studies investigating the influence of sample mass and heating rate[30,31].

High purity nitrogen was used for the experiments at a flow rate of 150 ml/min. The nitrogen was purged for 20 minutes, before starting the heating of the sample, to be sure of an atmosphere free of oxygen. The sample was then heated up to 110°C at a heating rate of 30°C/min in order to dry the sample. After a drying period of 30 minutes, the sample was heated up to the desired temperature (500 or 600°C) at the pre-selected heating rate of 10°C/min.

Experiments on mixtures of two and two components were performed in order to check possible interactions. In the mixture experiments paper was laid in the bottom of the sample cup and plastics at the top. This ensures the best possible mixing, because paper decomposes at a lower temperature and will have the possibility to interact with the plastics before it escapes the sample cup. The plastic will also melt prior or in the same temperature range when paper starts to decompose, so laying the plastic in the bottom would not give the paper the possibility to interact with the plastic. For the experiments with mixture of different paper qualities and mixture of different plastics, the components where not put in different layers, but thoroughly mixed. The experiments on mixtures and

single components are performed in exactly the same way with the same procedures. The experiments on mixtures were performed with a sample weight of 10 mg, while the experiments on single components were performed with a sample weight of 5 mg.

3 Results and discussion

3.1 Pyrolysis of the Cellulosic fraction

The normalised weight loss (TG curve) and rate of weight loss (DTG curve) for the cellulosic fraction are shown in Figure 1. The results show that the major weight losses of the cellulosic matter occur at 250-400°C, with maximum rate of weight losses between 355-371°C. The differences in remaining fraction at 450°C as shown in the TG curve is largely related to the difference in ash content. Subtracting the ash from the remaining residue at 450°C gives similar char fractions for all types of paper and cardboard. It is interesting to observe the similarity in DTG curves of newspaper and spruce. This is not surprising, however, since newspaper mainly consists of mechanical pulp with low ash content. A pronounced shoulder (first peak) prior to the cellulose peak (second peak) for newspaper, spruce and recycled paper can be seen from the DTG curves. This shoulder identifies the degradation of hemicellulose. For cardboard and glossy paper, however, the shoulder describing the hemicellulose degradation is less pronounced. The explanation of the less pronounced shoulder on the DTG curves for hemicellulose in cardboard and glossy paper can be attributed to the lower content of hemicellulose and/or catalytic effects. Catalytic effects caused by inorganic species such as ash and, in the case of cardboard, residues from the sulphate production process, may cause the decomposition of cellulose to occur at lower temperatures. This can make the separation of degradation of hemicellulose and cellulose less pronounced. The peak of the highest rate of mass loss for the DTG curves, which is cellulose, are for cardboard, glossy paper and recycled paper located at a somewhat lower temperature than for newspaper and spruce.

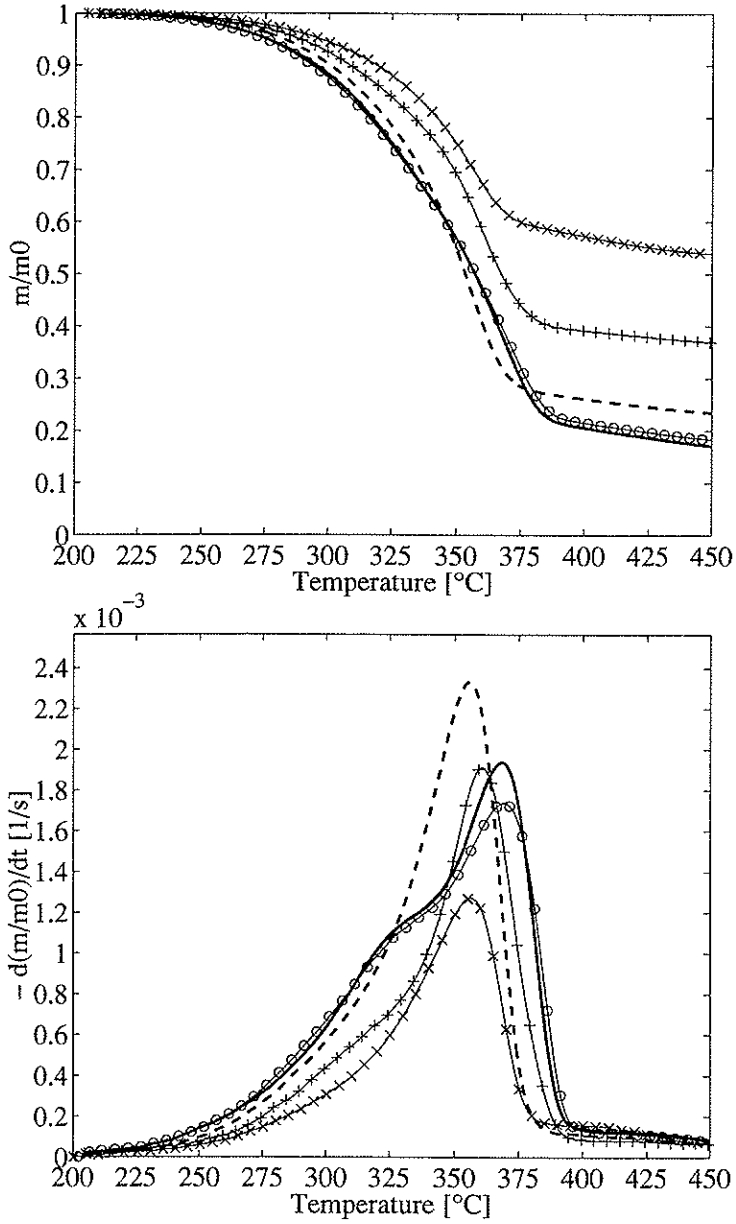

Figure 1. TG and DTG curves of: Spruce (———); Newspaper (-o-o-o-); Cardboard (- - - -); Recycled paper (++++); and Glossy paper (–x–x–x–).

Given that these materials consist of a similar cellulosic substance, indicates that catalytic effects are present. The flat tailing section observed above 400°C identifies the degradation of lignin.

3.2 Pyrolysis of Plastics

TG and DTG curves for the different plastics are shown in Figure 2. The pyrolytic degradation behaviour of PS, PP, LDPE and HDPE are quite similar with a rapid weight loss of hydrocarbons within a narrow temperature range (80-100°C), while PVC show a more complex degradation behaviour. The thermal degradation of PS, PP, LDPE and HDPE occur at 350-500°C, with maximum weight losses between 413-479°C, while the thermal degradation of PVC, in two major stages occurs at 200-380°C and 380-550°C. The first stage of degradation is connected to the release of the high amount of chlorine in PVC. This first step of degradation occurs in the same temperature range as for the hemicellulose and cellulose fractions of paper and cardboard. The second stage, which is believed to be the degradation of remaining hydrocarbons, occur at similar temperatures as for the other plastics. PVC separates from the other plastics not only by having a more complex degradation behaviour, but also by producing a char fraction.

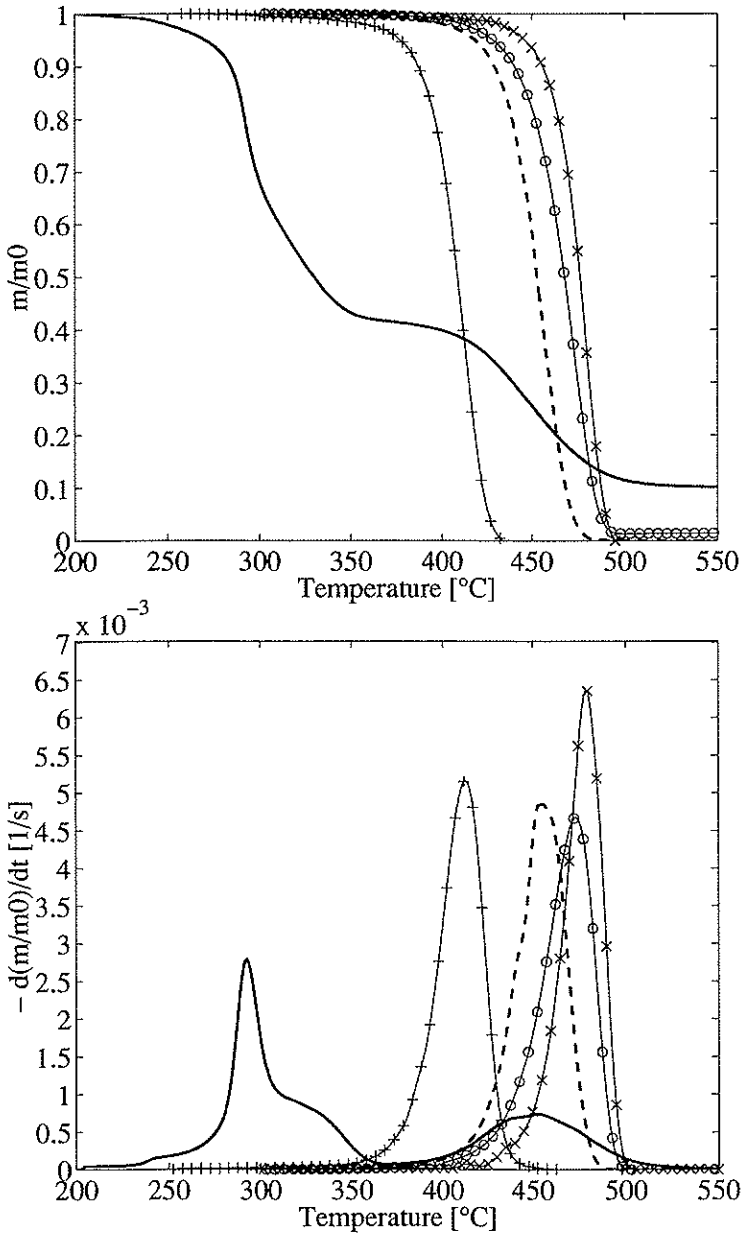

Figure 2. TG and DTG curves of: HDPE (–x–x–x–); LDPE (-o-o-o-); PP (- - - -); PS (++++); and UPVC (———).

3.3 Pyrolysis of Mixtures

A study on the behaviour of mixtures was also performed in order to check possible interactions between components. Mixtures of different paper/cardboard components, paper/cardboard and plastics and between different plastics were tested in the TGA, two at a time. Newspaper (low ash content) and glossy paper (high ash content) were chosen for this study, representing the paper fraction. LDPE and PVC were picked out to represent the plastic fraction. LDPE and PVC have a completely different degradation pattern and constitute a major share of the plastics found in MSW.

The only significant interaction observed between the different components, was between the cellulosic fraction and PVC. Experimentally obtained TG and DTG curves for a mixture of newspaper and PVC and the sum of the individual components are shown in Figure 3. The curves representing the sum of the individual components are derived by:

$$(m/m_0)_{SUM\ OF\ SINGLE\ COMPONENTS} = \sum_j Y_i \cdot (m/m_0)_i \qquad (1)$$

In Eq. 1, Y_i is the mass fraction of component i, $(m/m_0)_i$ is the normalised mass loss for component i as found from the single component experiments, j denotes the number of components in the actual mixture. The rate of weight loss for the sum of single components is derived in the same way as for the weight loss. A significant interaction is observed in the first stage of degradation at 250-370°C, while the second major stage of degradation (degradation of hydrocarbons in PVC) is not affected. The dehydrochlorination of PVC increases the reactivity of newspaper. At 325°C, the conversion of the sum of the single components is ~40 wt%, while the conversion of the mixture is 55 wt%. However, the interactions at lower temperatures have no significant impact on the degradation of remaining PVC and lignin from newspaper at higher temperatures.

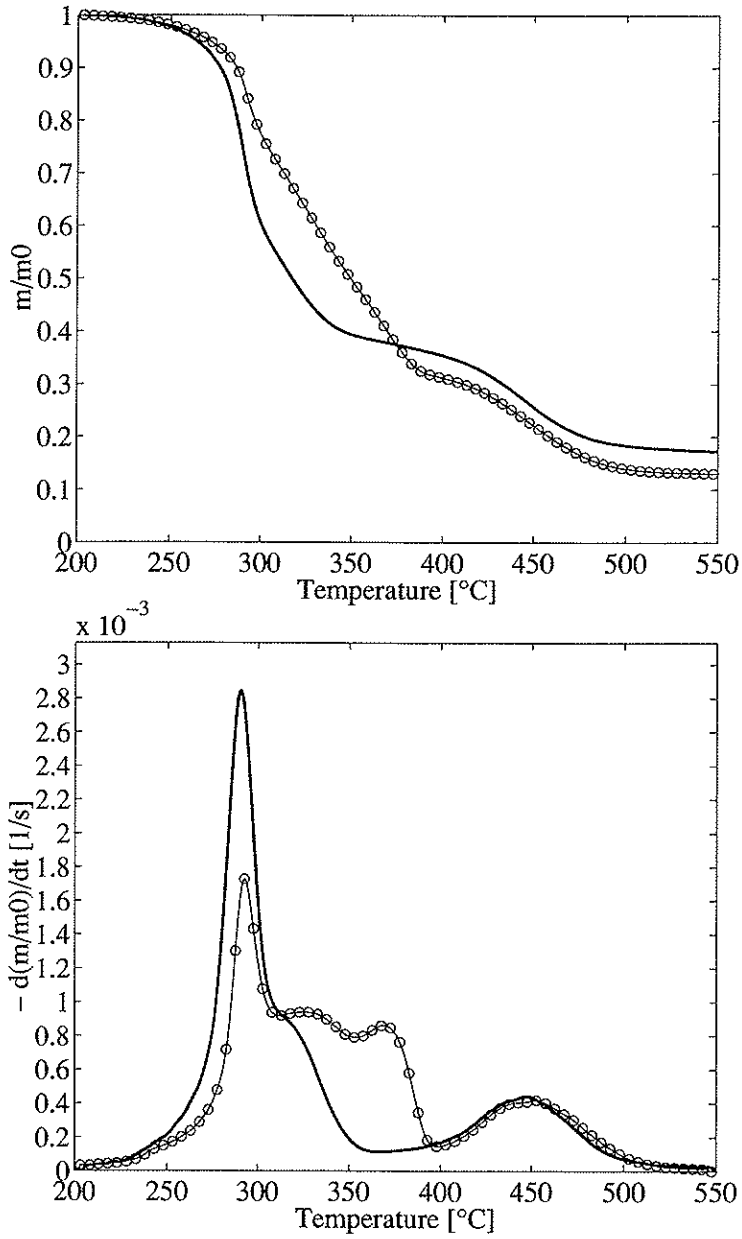

Figure 3. TG and DTG curves for mixture of PVC and Newspaper: Mixture (———); Sum of single components (-o-o-o-), 50 wt% of each.

The difference in remaining fraction at 550°C can be caused by irregularities between experiments and/or influence of the char formation of newspaper and/or PVC at lower temperatures. Another study investigating the co-pyrolysis of PVC with straw also found evidence of interaction during the dehydrochlorination step[32]. One probable explanation of the interaction between straw and PVC was that the liberated HCl may interact chemically with the cellulose, catalysing an acid hydrolysis type of reaction making it less stable. Further work in order to explain this phenomenon is needed.

4 KINETIC ANALYSIS

4.1 Kinetic Model

Although the pyrolysis of wood, paper and plastics may take place through a reaction network of parallel and competitive reactions, the DTG curves observed are quite simple and can be described by relatively simple mathematical models. PS, PP, LDPE and HDPE exhibit a sharp single DTG curve, which can be well described by a single reaction model. For the cellulosic fractions (including spruce) and PVC, however, the DTG curves contain shoulders and/or double peaks indicating that more than one reaction are involved. In this case, the overall decomposition can be described by a model of independent parallel reactions.

For the single reaction model, the rate of conversion can be described by:

$$\frac{d\alpha}{dt} = A \exp(-E/RT)(1-\alpha) \qquad (2)$$

In eq. 2, A and E are respectively the frequency factor and activation energy. α is the conversion (reacted fraction) which can be expressed by:

$$\alpha = \frac{1 - m}{1 - m_{char}} \qquad (3)$$

In eq. 3, m and m_{char} are the actual sample mass and char yield, normalised by the initial sample mass m_0, respectively.

If the material consists of more than one component and one assumes that each component decompose independently from each other, then the overall rate of conversion for *N* reactions can be described by:

$$-\frac{dm}{dt} = \sum_i c_i \frac{d\alpha_i}{dt} \qquad i = 1, 2, 3 .... N \qquad (4)$$

The separate conversion (reacted fraction) α_i for each component is given by:

$$\alpha_i = \frac{(m_{0,i} - m_i)}{(m_{0,i} - m_{char,i})} \qquad (5)$$

In eq. 5, $m_{0,i}$, m_i and $m_{char,i}$ are the initial sample mass, the actual sample mass and the final char yield (normalised with the initial sample mass, m_0) of component *i*, respectively. Note that the char yield in this case also includes ash. The components are all assumed to decompose individually according to:

$$\frac{d\alpha_i}{dt} = A_i \exp(-E_i/RT)(1 - \alpha_i) \qquad (6)$$

Coefficient c_i express the contribution of the partial processes to the overall mass loss, m_0-m_{char}:

$$c_i = m_{0,i} - m_{char,i} \qquad (7)$$

In our kinetic analysis, we used non-linear least squares (NLS) algorithms which identifies parameters (A_i, E_i, and c_i) that minimise values of the objective functions S_{DTG} given below.

$$S_{DTG} = \sum_{j=1}^{N} \left[\left(\frac{dm}{dt} \right)_j^{exp} - \left(\frac{dm}{dt} \right)_j^{calc} \right]^2 \qquad (8)$$

In eq 8, $(dm/dt)^{exp}$ is the experimentally observed DTG curve and $(dm/dt)^{calc}$ is the calculated DTG curve obtained by numerical solution of the kinetic differential equation with the given set of parameters. Subscript *j* denotes discrete values of (dm/dt).

4.2 Kinetic evaluation – Recycled paper, PVC and Juice carton as examples

Recycled paper has been taken as an example on how the cellulosic materials (wood, paper and cardboard) have been modelled. Figure 4 shows how recycled paper has been modelled with three independent parallel reactions according to the shape of the DTG curve. A calculation program has been used in order to determine the different reactions and calculating the kinetic data[33]. By looking at the shape of the DTG curve for recycled paper, it is possible to observe three reactions. The first shoulder (peak) is believed to be the degradation of hemicellulose. The second and third peaks (or shoulders) are believed to be the degradation of cellulose and lignin, respectively. All plastics, with the exception of PVC, have been modelled by a single reaction. PVC, however, is modelled with three independent reactions as shown in Figure 5. The thermal degradation of PVC is divided into two major steps. The first step is the dehydrochlorination step. Under the dehydrochlorination step, a portion of hydrocarbons in the form of benzene is released (first peak) together with HCl (second peak). Benzene is formed after the dehydrochlorination has proceeded for a while. The formed

conjugate double bonds form benzene by cyclization[34]. This theory is confirmed by a study using TGA and analysis of the evolved gases by mass spectrometry. Benzene was found in the evolved gases together with HCl[35]. Figure 6 shows how the juice carton has been modelled. For the juice carton, it is possible to separate the degradation of paperboard and polyethylene. The first three reactions describe the pyrolytic degradation of hemicellulose, cellulose and lignin, while the fourth reaction describes the degradation of polyethylene.

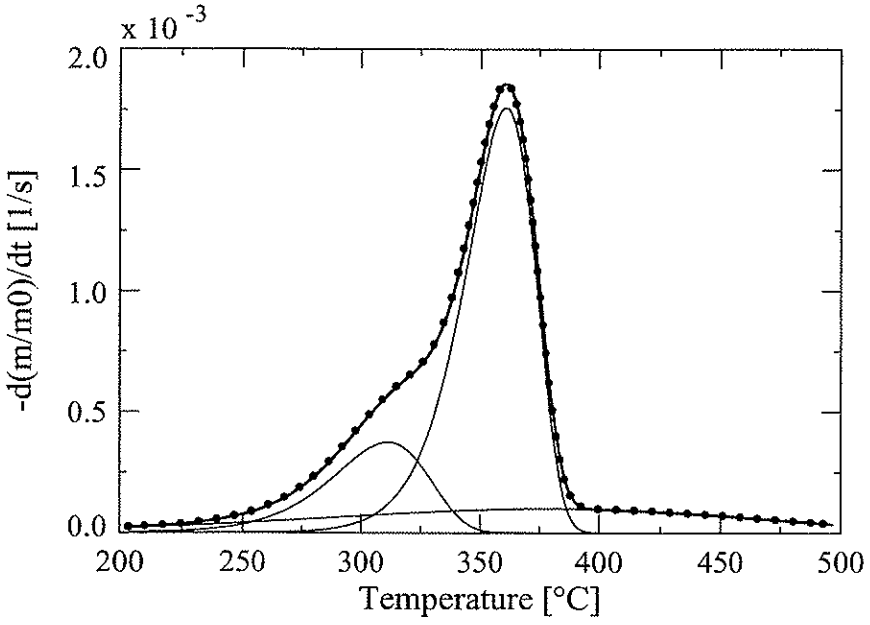

Figure 4. Kinetic evaluation of Recycled paper. Dots, the bold solid line, and the thin solid lines represent the experimental data (- dm^{exp}/dt), the calculated data (- dm^{calc}/dt), and the contributions of the partial reactions to - dm^{calc}/dt, respectively.

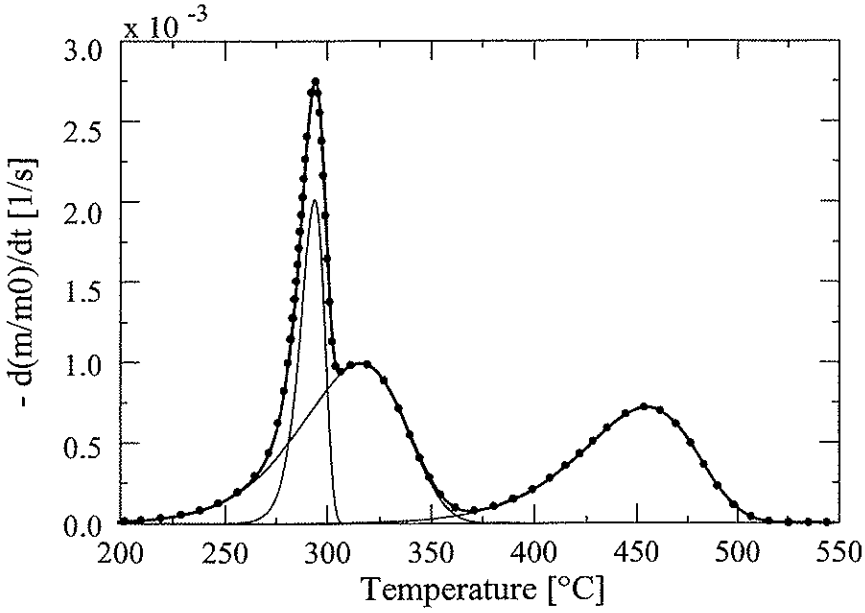

Figure 5. Kinetic evaluation of PVC. Dots, the bold solid line, and the thin solid lines represent the experimental data (- dm^{exp}/dt), the calculated data (- dm^{calc}/dt), and the contributions of the partial reactions to - dm^{calc}/dt, respectively.

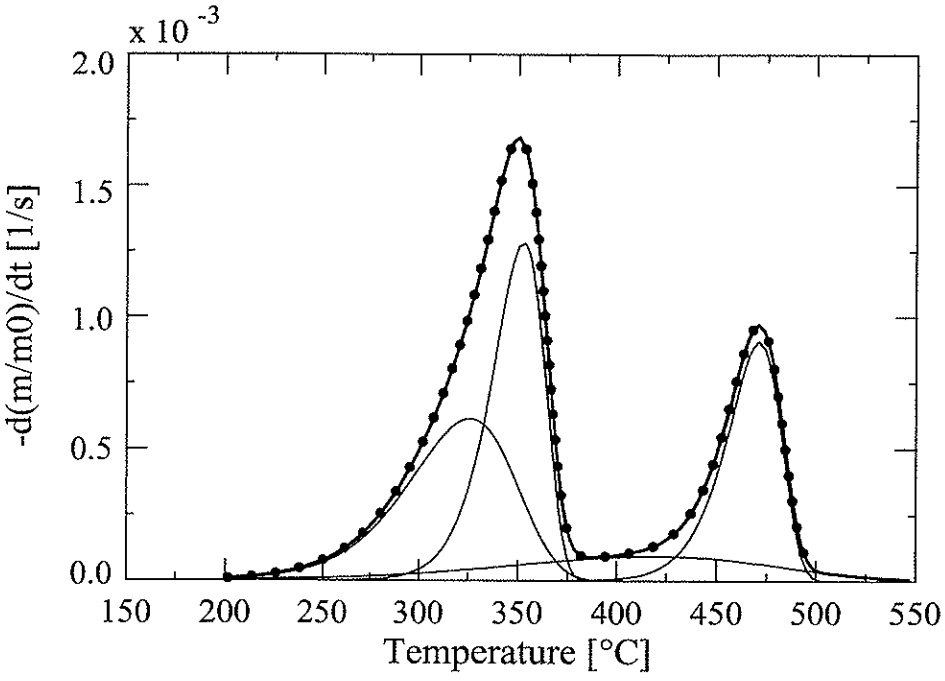

Figure 6. Kinetic evaluation of juice carton. Dots, the bold solid line, and the thin solid lines represent the experimental data (- dm^{exp}/dt), the calculated data (- dm^{calc}/dt), and the contributions of the partial reactions to - dm^{calc}/dt, respectively.

4.3 Kinetic Evaluation of the Cellulosic Fraction

Several considerations must be made when discussing the results from the experiments and calculations on chemical kinetics for the cellulosic fraction. Since the pyrolytic degradation has been modelled as a set of independent parallel reactions, it is important to understand the degradation behaviour of each chemically different component during pyrolysis. When trying to link the kinetic behaviour to the chemical composition, it is also necessary to be aware of differences in degradation behaviour due to catalytic effects or chemical and physical composition and structure. Comprehensive studies on the catalytic effects of inorganic substances in degradation of cellulosic substances have been

performed by other researchers[30,36,37]. In the present work, attempts were made to remove the inorganic substances by means of hot water washing at 80°C for two hours on newspaper and glossy paper, since other pre-treatment methods may alter the chemical composition of the sample by reducing the hemicellulose to cellulose ratio[36]. The results from the TGA experiments, however, revealed no significant effect. The explanation can be that this mild washing of the samples was not able to extract any significant amount of the inorganic substances, since these have strong physical bounds to the paper. Observing the samples after the washing process, support this explanation. Other researchers have shown that there exist a difference in char fraction and degradation temperature for cellulose, hemicellulose and lignin for different types of biomass. However, extracted hemicellulose and lignin will most likely behave differently from hemicellulose and lignin chemically bound together in wood or paper, since the extraction procedure always will change the chemistry[30].

Table 3 shows the results of the kinetic evaluation of the different MSW components. In the kinetic evaluation of the cellulosic fraction, the three observed degradation reactions separate from each other in different ways caused by differences in the chemical structure. The third peak or degradation of lignin is modelled over a very broad temperature range (typically 200-500°C). The first and second peaks or degradation of hemicellulose and cellulose, however, are modelled over a narrower temperature range. The degradation of cellulose is typically modelled between 275-400°C and for hemicellulose between 200-400°C. The major difference between the degradation of lignin and hemicellulose/cellulose is the broad temperature range under which the degradation takes place.

The average activation energy and conversion (c-value) of the observed degradation of hemicellulose (first peak) for all cellulosic materials is 110.3 kJ/mole and 24.7wt%, respectively. A standard deviation of 14 kJ/mole on the activation energy is relatively small, while the corresponding value for the

conversion is 11wt%, which is relatively large. The relatively large deviation in conversion for hemicellulose is caused by an overestimation (of the conversion) due to lack of a pronounced shoulder or peak in the case for newspaper and glossy paper. It is important, however, to notice that the reported conversions do not take into account that the ash content is different for the different samples. This means that for a direct comparison the conversion should be normalised by dividing it with the total reacted fraction (approximately 0.45 for glossy paper). Few data has been published on the degradation of hemicellulose, however, activation energies of 119 and 170 kJ/mole have been reported for hemicellulose from wood and straw, respectively[30,37]. The average activation energy for the second peak or degradation of cellulose for the cellulosic fraction is 244.8 kJ/mole with a standard deviation of 20.8 kJ/mole. Antal and Varhegyi[36] found that for a variety of different cellulosic substances a first order model with an activation energy of 238 kJ/mole accurately describes the pyrolytic degradation.

Table 3. Kinetic evaluation of the cellulosic fraction and plastics.

	First Peak			Second Peak			Third Peak		
	E (kJ/mole)	**log A (log s^{-1})**	**c (wt%)**	**E (kJ/mole)**	**log A (log s^{-1})**	**c (wt%)**	**E (kJ/mole)**	**log A (log s^{-1})**	**c (wt%)**
Cellulosic fraction:									
Newspaper	96.7	6.12	40.2	246.1	18.03	30.4	47.4	1.06	13
Cardboard	112.3	7.82	18.8	230.6	17.25	47.1	46.0	0.99	12.5
Recycled paper	136.2	10.11	11.0	214.0	15.67	41.4	36.2	0.14	12.9
Glossy paper	99.4	6.33	18.3	274.7	20.9	18.3	44.4	0.65	9.4
Spruce	109.8	7.35	33.9	255.2	18.85	34.2	41.3	0.62	16.9
Juice carton[a]	107.5	7.15	26.1	248.3	18.85	26.6	55.1	1.52	9.5
Average	***110.3***	***7.5***	***24.7***	***244.8***	***18.3***	***33.0***	***45.1***	***0.8***	***12.4***
Standard deviation	***14.0***	***1.4***	***10.9***	***20.8***	***1.8***	***10.3***	***6.3***	***0.5***	***2.8***
Plastics:									
HDPE	445.1	29.1	98.2	-	-	-	-	-	-
LDPE	340.8	21.98	96.3	-	-	-	-	-	-
PP	336.7	22.18	98.4	-	-	-	-	-	-
PS	311.5	21.84	98.1	-	-	-	-	-	-
PVC	388.2	34.13	19.3	110.4	7.59	37.7	149.8	8.5	31.6
Juice carton[b]	339.7	21.94	19.5						

[a] Only paperboard, [b] Only polyethylene.

An average activation energy of 45.1 kJ/mole and a standard deviation of 6.3 kJ/mole describe the pyrolytic degradation of lignin or third peak for the cellulosic fraction. The low activation energy is reflected by the complex structure and thus broad temperature range under which the degradation takes place. Grønli reported similar activation energy of lignin for different types of wood[30]. Glossy paper was modelled with four reactions in order to take into account the minor shoulder observed at ~400°C. This shoulder is believed to be degradation of additives such as pigment, binder and chemicals.

4.4 Kinetic Evaluation of Plastics

The pyrolytic degradation of PS, PP, LDPE and HDPE can be modelled as a single reaction. PVC, with its more complex degradation behaviour, is modelled with three reactions.

PS, PP, LDPE, HDPE. As shown in Table 3, the activation energies of PS, PP, LDPE and HDPE are 311.5, 336.7, 340.8 and 445.1 kJ/mole, respectively. The pyrolytic degradation of PS, PP and LDPE occurs between 350-450°C, 380 - 480°C and 400 - 500°C, respectively. Giving a similar temperature range of degradation of ~100°C. Hence, the major difference, which explains the variation in activation energy for PS, PP and LDPE, is the temperature level under which the degradation takes place. DTG peak temperatures (point of maximum rate of weight loss) are 413, 456 and 472°C for PS, PP and LDPE, respectively. The higher activation energy of HDPE compared to the other hydrocarbon plastics, however, can be explained by the narrower degradation temperature range (80°C) and the higher DTG peak temperature (479°C). The explanation of the observed difference between the different plastics is found in the chemical structure. PS, PP, LDPE and HDPE consists largely of C-C and C-H bonds, however, in the chain branching structure the C=C double bond may be present. The dissociation energy of the C-C, C-H and C=C bonds are 347, 414 and 611 kJ/mole, respectively[29]. Weaker

secondary bonds such as dipole forces, induction forces and dispersion forces are typically lower than 42 kJ/mole. All of these bond energies together give a picture on the level of activation energies expected for these plastics. However, differences in the chemical structure can alter the reactivity of the different plastics. The observed difference in thermal degradation of LDPE and HDPE may be caused by differences in chain branching, altering the distribution of the chemical bonds present to some extent. The bond energies of main chains or weak links are quite different for PS and LDPE/HDPE. The presence of the aromatic unit or benzene ring (C_6H_6) in PS causes the branching to be of a phenyl type, as opposed to LDPE and HDPE which have a methyl group (CH_3) as branch[38]. The presence of benzene may lower the bond energy for some of the bonds present in PS compared to LDPE and HDPE where the break down of the C-C bond is dominating[29]. Hence, the reactivity of PS is greater than the reactivity of LDPE and HDPE. The presence of the methyl group (CH_3) in the repeating monomer of PP can alter the properties of the polymer in a number of ways[29]. However, no specific explanation regarding the influence of the methyl group in terms of thermal degradation reactivity could be found. In the literature an activation energy of 172 kJ/mole was found for PS[20], 184-265 kJ/mole[19,20] for PP, 194-206 kJ/mole[20, 38] for LDPE and 233-326 kJ/mole[19,20] for HDPE. As this study and the study of others show, the activation energy is obviously influenced by the method used to calculate the activation energy and experimental equipment and procedures.

PVC. PVC separates from the other plastics by having a complex pyrolytic degradation behaviour. For PVC, three different reactions have been identified. The first peak is assumed to be the release of benzene during the dehydrochlorination. The second peak is assumed to be the dehydrochlorination and the third peak is assumed to be the degradation of the remaining hydrocarbons. The activation energy found for the degradation of hydrocarbons forming benzene is calculated to 388 kJ/mole with a DTG peak temperature of 294°C. The release of benzene (first peak) is modelled from 250-310°C. The dehydrochlorination of PVC takes place at

200 - 370°C. The activation energy calculated for the release of HCl is 110 kJ/mole and the DTG peak temperature is 316°C. A study of the ultimate composition of the residue from pyrolysis of PVC at 375°C showed that there was no significant amount of chlorine left, which confirms the dehydrochlorination reaction[39]. The bond energy for the breaking of the C-Cl bond is 339 kJ/mole, but neither this study nor other studies have been able to report activation energies close to the breaking of the primary C-Cl bond. Bockhorn et. al. [35] found an activation energy of 140 kJ/mole for the first degradation step of PVC (dehydrochlorination).

The third peak of the DTG curve describes the second step of the degradation of PVC. The calculated activation energy and DTG peak temperature is 150 kJ/mole and 455°C, respectively. The degradation occurs between 350-525°C. The third peak describes degradation of the remaining hydrocarbons. The chemical nature of the remaining hydrocarbons is not known and hence it is difficult to explain the activation energy of the second step of decomposition for PVC on basis of the chemical structure. However, others have reported activation energy of 260 kJ/mole for the second step of degradation[35].

4.5 Kinetic Evaluation of Juice Carton.

As shown in Figure 3, the juice carton is modelled with four reactions describing the degradation of hemicellulose, cellulose, lignin and PE. Kinetic data from evaluation of TGA experiments on multi-material beverage cartons (paperboard and LDPE) revealed that it was possible to obtain kinetic data similar to the individual materials. The calculated activation energies for the degradation of hemicellulose, cellulose, lignin and PE were 108, 248, 55 and 340 kJ/mole, respectively.

5 Conclusions

The pyrolysis characteristics and kinetics of 11 different components, representing the cellulosic fraction and plastics of MSW, have been investigated. Fundamental knowledge on the pyrolytic degradation behaviour of MSW components and mixtures thereof, is important in modelling, design and operation of thermal conversion systems (i.e. pyrolysis, gasification and combustion systems), since variations in MSW composition may influence the operational parameters and hence alter the formation and emission of pollutant species. The variations in fuel properties of the paper/cardboard and plastic components were relatively large. The ash content for different paper qualities and cardboard, varied from 1-28wt%, with corresponding HHV values of 19.3-10.4 MJ/kg and fixed carbon content of 10.5-4.7wt%. The plastics PS, PP, LDPE and HDPE were 100% volatile and HHV were between 42-47 MJ/kg. PVC, on the other hand, has a similar content of hydrocarbons and consequently a similar HHV as the cellulosic fraction (22.8 MJ/kg). The major difference between PVC and the cellulosic fraction with regards to the ultimate composition is that PVC has a chlorine content 48wt% and only 6wt% of oxygen.

Pyrolytic degradation behaviour and kinetics of MSW components were studied using TGA. It was found that paper and cardboard have a similar pyrolytic degradation behaviour as wood, occurring at 200-500°C. The DTG temperature peak was located at approximately 360°C. The degradation of PS, PP, LDPE and HDPE occurred at 350-500°C, while PVC had a completely different degradation behaviour, volatilising between 200°C and 525°C in two major steps. The cellulosic fraction of MSW was modelled as a set of three independent parallel reactions describing the degradation of hemicellulose, cellulose and lignin, with average activation energies of 111, 244 and 43 kJ/mole, respectively. PS, PP, LDPE and HDPE were all modelled as a single reaction describing the thermal degradation of the hydrocarbon polymers with activation energies of 312, 337, 341 and 445

kJ/mole, respectively. The degradation of PVC was modelled with three reactions describing the release of benzene during dehydrochlorination, dehydrochlorination and degradation of remaining hydrocarbons with activation energies of 388, 110 and 150 kJ/mole, respectively.

Possible interactions between different paper and plastic components in mixtures were also investigated. It was found that the reactivity of cellulosic matter was increased in a mixture with PVC.

6 Acknowledgement

The Nordic Energy Research Programme is acknowledged for financial support of this work.

7 References

1 Kulik, A. and Witoszek, A., *WPROST*, 1994, **4**, 36-37.

2 Temmink, H., *Biomass and Bioenergy*, 1995, **9**, 351-363.

3 Norwegian Pollution Control Authority, Our Common Environment - Waste, Report TA 664, 1992 (in Norwegian).

4 US Environmental Protection Agency, *Characterisation of Municipal Solid Waste in the United States – 1997 Update*, Report No. EPA 530-R-98-007, 1998.

5 Laughlin, K., IEA report Task 23, "The Management of residues from thermal processes", (in press), 2000.

6 Franklin, M. A., Report No. PB88 – 232780, Franklin Associates Ltd., USA, 1988.

7 Falnes, A. and Vinju, E., Report No. C402, Statistics Norway, Norway, 1997.

8 Kauffman, C.R., *in Wastetech '91: Canadian Waste Management Conference*, Toronto, 1991, 1-13.

9 Rigo, H. G. and Chandler, A. J., *in Proceedings of the National Waste Processing Conference*, ASME, 1994, 49-63.

10 Gort, R., Phd thesis ISBN 90-9008751-6, Twente University, The Netherlands, 1995.

11 Tillman, D. A., *in The Combustion of Solid Fuels & Wastes*, Academic Press, San Diego, USA, 1991.

12 Clarke, M. J., *Waste Age United States*, 1991, **May**, 105.

13 Rosseaux, P., *Biocycle*, 1989, **9**, 81.

14 Garcia, A. N., Marcilla, A., Font, R., *Thermochimica Acta,* 1995, **254**, 277.

15 Tsang, W. and Walker, J. A., *Resources and Conservation*, 1982, **9**, 355-365.

16 Krieger-Brockett, B., *in Proceedings from Nordic Seminar on Biomass Gasification and Combustion*, Norwegian University of Science & Technology, Norway, 1993.

17 Volkov, V. S., Khabenko, A. V., Ganzha, V. I., Dolmatov, S. A. and Prilepskaya, T. I., *International Polymer Science and Technology*, 1991, **10**, 36.

18 Wu, C-H, Chang, C-Y, Lin, J-P and Hwang, J-Y, *Fuel*, 1997, **12**, 1151-1157.

19 Fritsky, K. J., Miller, D. L. and Cernansky, N. P., *Journal of Air & Waste Management Association*, 1994, **44**, 1116-1123.

20 Wu, C-H, Chang, C-Y, Hor, J-L, Shih, S-M, Chen, L-W and Chang, F-W, *Waste Management*, 1993, **13**, 221-235.

21 Cozzani, V., Petarca, L. and Tognotti, L., 1995, *Fuel*, **6**, 903-912.

22 Agrawal, R. K., *in Compositional Analysis by Thermogravimetry*, ASTM STP 997, C.M. Earnest, Ed., American Society for Testing and Materials, Philadelphia, USA, 259-271, 1988.

23 Wenzl, H.F.J., *in The Chemical Technology of Wood*, Academic Press Inc., 1970.

24 Rydholm, S. A., *in Pulping Processes*, Interscience Publishers, USA, 1965.

25 Olsson, I., *in Papertypes for different use*, No. X-731, Swedens Forrest Industry Union, Markaryd, Sweden, 1986 (in swedish).

26 Hult, N., *in Coating of paper*, No. Y-308, Swedens Forrest Industry Union, Markaryd, Sweden, 1986 (in swedish).

27 Christensen, P. K., *Wood processing chemistry*, Compendium from Institute of Chemical Engineering, Norwegian University of Science and Technology, 1995 (in norwegian).

28 Rance, H. F., *in Handbook of Paper Science – Vol. 1*, Elsevier, The Netherlands, 1980.

29 Brydson, J.A., *in Plastics Materials*, Butterworth-Heinemann Ltd., Oxford, UK, 1995.

30 Grønli. M.G., Ph.D. thesis NTNU 1996:115, The Norwegian University of Science and Technology, 1996.

31 Grønli, M.G., Antal Jr., M.J. and Varhegy, G., *Ind. Eng. Chem. Res.*, 1999, **38**, 2238-2244.

32 McGhee, B., Norton, F., Snape, C. E. and Hall, P. J., *Fuel*, 1995, **1**, 28-31.

33 Austegard, A., Phd thesis NTNU 1997:78, The Norwegian University of Science and Technology, 1997.

34 Faximile from Ånund Ryningen at Hydro Porsgrunn Technical Centre-PVC, 02.03.98.

35 Bockhorn, H., Hornung, A., Hornung, U., Teepe, S. and Weichmann, J., *Combustion Science and Technology*, 1996, **116-117**, 129-151.

36 Antal, M. J. and Varhegyi, G., *Industrial & Engineering Chemistry Research*, 1995, **34**, 703-717.

37 Varhegyi, G., Szabo, P. and Antal M. J., *in Advances in Thermochemical Biomass Conversion*, Blackie Academic & Professional, GB, 1994.

38 Wu, C-H, Chang, C-Y, Hor, J-L, Shih, S-M and Chen, L-W, *International Symposium on Energy, Environment and Information Management*, Argonne National Laboratory, USA, 1992.

39 Wu, C-H, *The Canadian Journal of Chemical Engineering*, 1994, **4**, 644-650.

40 Sørum, L., Glarborg, P., Jensen, A., Skreiberg, Ø, and Dam-Johansen, K., *Combustion & Flame*, 2000 (in press).

3 Formation of NO from combustion of volatiles from MSW

3.1 Introduction

The aim of this section is to give a short introduction to NO formation mechanisms and the CHEMKIN program OPPDIF (opposed diffusion flame code) in connection to the work performed in Paper II.

3.1.1 NO mechanisms

In order to understand how to reduce NO emissions it is necessary to know how NO is formed. Parameters such as temperature, fuel nitrogen content, excess air ratio and residence time influence the formation of NO in MSW combustion systems. Three routes for formation of NO has been identified[1-2]:

1 The extended *thermal (or Zeldovich) mechanism* in which O, OH and N_2 species are at their equilibrium values and N atoms are in steady state:

$$O + N_2 \Leftrightarrow NO + N$$

$$N + O_2 \Leftrightarrow NO + O$$

$$N + OH \Leftrightarrow NO + H$$

Thermal NO originate from nitrogen in the combustion air at elevated temperatures.

2 Mechanisms whereby NO is formed more rapidly than predicted by the thermal mechanism above. Ignoring the processes that form CH radicals to initiate the mechanism, the *prompt* (Fenimore) pathways can be written:

$$CH + N_2 \Leftrightarrow HCN + N$$

$$C + N_2 \Leftrightarrow CN + N$$

where the first reaction is the primary path and the rate-limiting step in the sequence. For equivalence ratios less than ~1.2, the conversion of hydrogen cyanide, HCN, to form NO follows the following chain sequence:

$$HCN + O \Leftrightarrow NCO + H$$
$$NCO + H \Leftrightarrow NH + CO$$
$$NH + H \Leftrightarrow N + H_2$$
$$N + OH \Leftrightarrow NO + H$$

There is also the N_2O-intermediate route for NO formation. However, this route is only important in lean premixed combustion (low temperature).

Prompt NO also originates from nitrogen in the combustion air.

3 *Fuel nitrogen mechanism*, in which fuel-bound nitrogen is converted to NO through a very complex reaction path where both homogeneous and heterogeneous reactions, including catalytic reactions, may be of importance. In the combustion of fuels with bound nitrogen, the nitrogen in the parent fuel is rapidly converted to HCN and/or NH_3 and N_2. For HCN the remaining steps follow the prompt-NO mechanism described above. Figure 3.1 shows a reaction path diagram illustrating the major steps in prompt NO formation and conversion of fuel nitrogen (FN) to NO. Figure 3.2 outlines schematically the principal reactions by which ammonia is oxidised to nitric oxide and by which nitric oxide is converted to molecular nitrogen in flames.

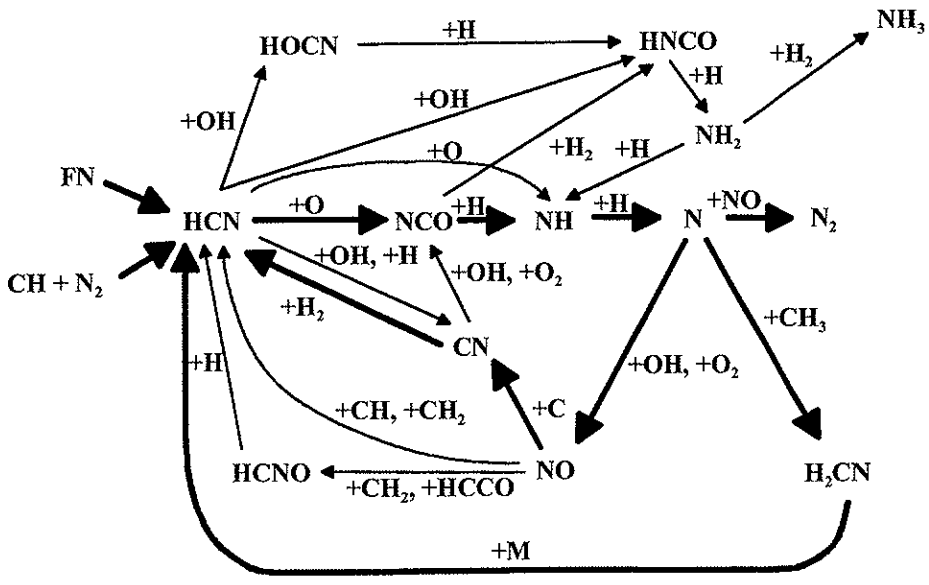

Figure 3.1 Reaction path diagram illustrating the major steps in prompt NO formation and conversion of fuel nitrogen (FN) to NO. The bold lines represent the most important reaction paths[2].

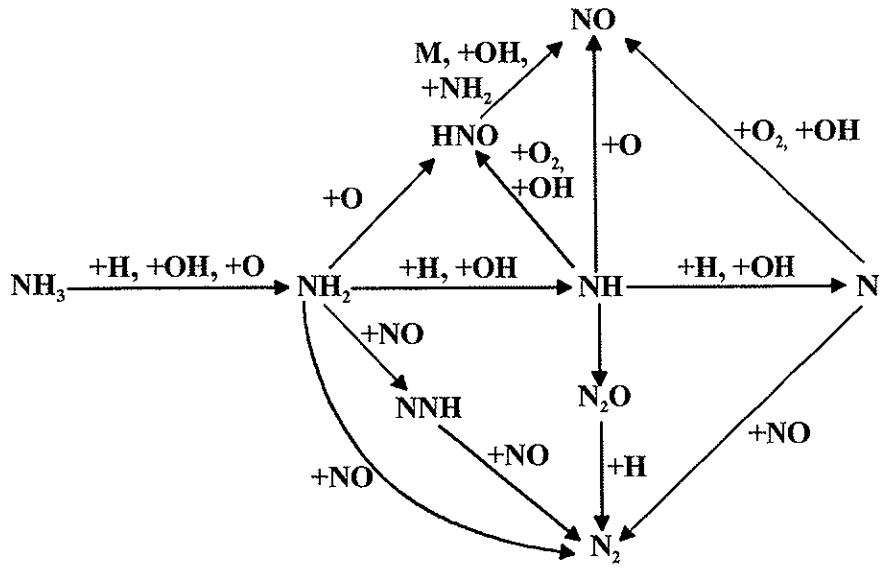

Figure 3.2 Reaction path diagram for the oxidation of ammonia in flames[2].

Nitrogen content and functionality of fuel-N in MSW together with the release of fuel nitrogen during pyrolysis are commented on in Paper II.

3.1.2 Opposed diffusion flame code in CHEMKIN (OPPDIF)

OPPDIF is a Fortran program that computes the diffusion flame between two opposing nozzles. The geometry consists of two concentric, circular nozzles directed towards each other, as shown in Figure 3.3.

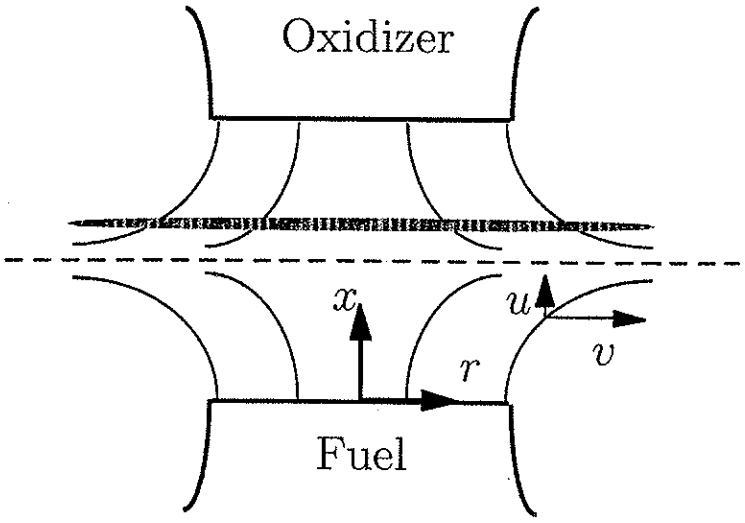

Figure 3.3 Principle drawing of the opposed diffusion flame code OPPDIF[3].

This configuration produces an axisymmetric flow field with a stagnation plane between the nozzles. The location of the stagnation plane depends on the momentum balance of the two streams. Fuel will diffuse through the stagnation plane to establish the flame in a stoichiometric mixture. A similarity transformation reduces the two-dimensional axisymmetric flow field to a one-dimensional problem. Assuming that the radial component of velocity is linear in radius, the dependent variables become functions of the axial direction only. OPPDIF predicts

the species, temperature, and velocity profiles in the core flow between the nozzles (excluding edge effects) (see Figure 3.4), hence allowing a detailed study of the diffusion flame chemistry.

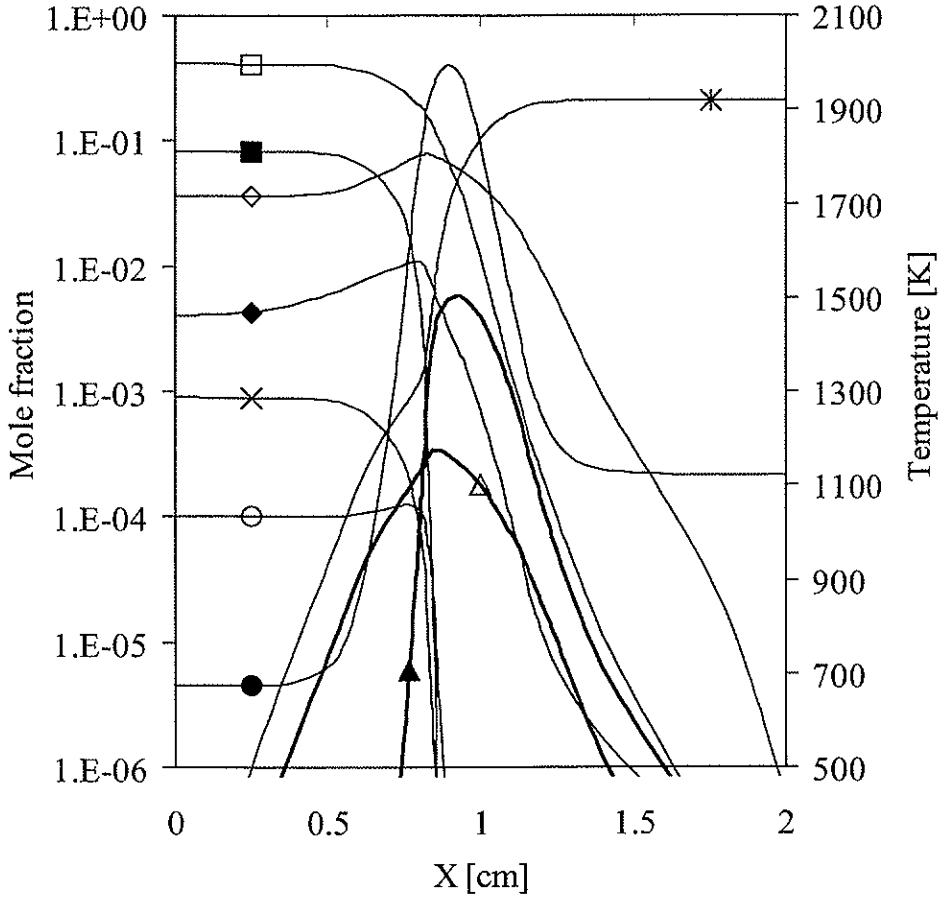

Figure 3. 4 Calculated temperature (●) and concentrations of species as a function of distance from the fuel nozzle for simulation on paper at 21 vol% oxygen and an oxidiser temperature of 1123 K. The concentrations are for CO (□), CH_4 (■), H_2O (◇), H_2 (◆), NH_3 (x), HCN (○), NO (△), OH (▲) and O_2 (∗).

3.2 References

1 Turns, S. R., An Introduction to Combustion – Concepts and Application, Mc Graw Hill, **1996**.

2 Miller, J. A. and Bowman, C. T., *Progress in Energy & Combustion Science*, Vol. 15, pp. 287-338, **1989**.

3 Lutz, A. E., Kee, R. J, Grcar, J. F. and Rupley, F. M., *OPPDIF: A Fortran Program for Computing Opposed-Flow Diffusion Flames*, Report No. SAND96-8243, Sandia National Laboratories, 1997.

3.3 Paper II

Formation of NO from Combustion of Volatiles from Municipal Solid Wastes

Authors:

Lars Sørum*, Peter Glarborg**, Anker Jensen**, Øyvind Skreiberg* and Kim Dam-Johansen**

*Norwegian University of Science & Technology, Institute of Thermal Energy and Hydropower

** Technical University of Denmark, Department of Chemical Engineering

Paper accepted for publication in the Scientific Journal ***Combustion & Flame***

Formation of NO From Combustion of Volatiles From Municipal Solid Wastes

LARS SØRUM* and ØYVIND SKREIBERG
Norwegian University of Science and Technology, Institute of Thermal Energy and Hydropower, N-7491 Trondheim, Norway

PETER GLARBORG, ANKER JENSEN, and KIM DAM-JOHANSEN
Technical University of Denmark, Department of Chemical Engineering, DK-2800 Lyngby, Denmark

An experimental and theoretical study has been performed on the formation of NO in the combustion of volatiles from municipal solid wastes. Single components and their mixtures were burned in a small-scale, fixed-bed reactor. Numerical simulations using the opposed flow diffusion flame program OPPDIF were performed to obtain a further understanding of the experimental results. Conversion factors for fuel-N to NO were determined for single components of newspaper, cardboard, glossy paper, low-density polyethylene (LDPE), and poly(vinylchloride) (PVC) and their mixtures, using gases with oxygen concentrations of 12, 21, and 40 vol %. For single components experiments at 100 vol % oxygen were also performed. The conversion factors for paper and cardboard varied from 0.26 to 0.99. The conversion factor for LDPE and PVC varied from 0.71 to 10.09 and 0.04 to 0.37, respectively. Conversion factors higher than 1.0 in the case of LDPE clearly show that NO is formed by thermal and/or prompt mechanisms. For mixtures, calculated conversion factors (based on a weighted sum of the conversion factors for single components) were compared with the experimentally determined conversion factors. Mixtures of paper and cardboard only gave different conversion factors with 40 vol % of oxygen. For mixtures of paper/cardboard and plastics, however, significant differences in the conversion factors were observed at all oxygen concentrations, when comparing experiments on a mixture of paper and plastics with the weighted sum of the single components. The explanation is found in the different combustion properties for paper/cardboard and plastic, which in this case make the formation of thermal NO from LDPE more favorable for the single component than in mixtures with other components. The simulations with OPPDIF confirmed the trends observed experimentally, and allowed an assessment of the contribution of the different mechanisms of NO formation.

INTRODUCTION

In recent years, waste management has become increasingly complex. Earlier, Municipal Solid Waste (MSW) was sent to landfill sites, which was considered the most economic way of handling MSW. However, in the last 2 decades awareness of the environmental hazards and a lack of landfill sites have promoted an increased number of alternative waste treatment systems. Today, MSW management systems are complex and a product of several different factors. Factors influencing the choice of MSW management systems are composition of the waste, environmental, and economical aspects, and also infrastructure (i.e., type of housing, access to landfill sites, etc.). Material recovery and reuse, combustion with energy recovery, composting, and landfilling are the most common parts of today's waste management system. There is an international trend towards increasing the reuse and recycling of waste. The increased recycling of materials, such as paper, plastic, and beverage cartons may influence the performance of combustion systems. The increased complexity of MSW management systems makes detailed characterization of MSW components necessary. The trend today is to classify waste into categories depending on composition. Classification of waste as a fuel with a certain quality and composition will make it easier for operators and manufacturers of combustion plants to assess the consequences of burning different wastes. To do this, fundamental knowledge of the combustion properties of the different components and possible interactions in mixtures should serve as a basis for these decisions.

Reducing the emission of nitrogen oxides (NO_x) from burning MSW and Refuse Derived Fuel (RDF) is one of the challenges in this field. NO_x abatement is generally divided into two

*Corresponding author. E-mail: lars.sorum@energy.sintef.no

COMBUSTION AND FLAME 123:000–000 (2000)

Published by Elsevier Science Inc.

0010-2180/00/$–see front matter
PII S0010-2180(00)00194-2

categories. Primary measures involve treatment prior to or during the combustion process and are not considered to be part of the air pollution control (APC) system. Generally, there are a wide range of primary reduction techniques, such as staged air combustion, reduced excess air (improved mixing), reburning, flue gas recirculation, and combustion with pure oxygen. Pickens [1] reported that typical baseline NO_x emission levels for commercial moving grate and stoker incinerators were 350–600 mg/Nm^3 at 7 vol % oxygen. Emissions of nitric oxides are generally lower from fluidized beds than with grates for two reasons: the combustion temperature is lower and the excess air level is lower (typically 50% lower excess air) [2]. Primary measures can achieve up to 70% reduction. However, secondary measures, which are part of the APC system, are often necessary [3].

A nitrogen content of 0.45 wt % is typical for MSW [4, 5]. For paper and plastics, typical nitrogen contents of 0.11–0.8 and 0.3–0.85 wt %, respectively, have been reported [4, 5]. Chemically paper and cardboard consists of three main constituents, namely hemicellulose, cellulose, and lignin [6]. Aho et al. [7] concluded that nitrogen in fuels with a high O/N ratio, such as wood, can mainly be found in pyrrolic forms. Nitrogen, however, might also be found in additives, such as color ink and binders. Bowman [8] stated that for fossil fuels the conversion of fuel N to NO is strongly dependent on the fuel–air ratio and on combustion temperature, and only slightly dependent on the identity of the parent nitrogen compound. Typically, of the NO_x formed during the combustion of waste, nitric oxide (NO) is the major component, with a much smaller fraction, usually less 5% of the total NO_x, appearing as nitrogen dioxide (NO_2) and an almost insignificant amount of nitrous oxide (N_2O) [9]. Abbas [9] also stated that 5–15% of the total NO is formed by the thermal NO mechanism, while up to 5% is formed in the prompt mechanism. The remaining NO is formed through conversion of fuel N to NO (fuel NO). The objective of this study was to investigate the formation of NO in detail for different components of MSW such as paper, cardboard, and plastics and their mixtures. The mechanisms of NO formation have been studied experimentally and with numerical simulations, investigating the influence of oxygen concentration and temperature and mass of sample. The focus has been on determining typical conversion levels and trends for NO formation from different MSW components in a small-scale laboratory furnace and not on absolute emission levels for MSW combustion plants.

EXPERIMENTAL METHODS

Five components of MSW were investigated in this study, both as single components and in mixtures. Newspaper (NP), glossy paper (GP), and cardboard (CB) were chosen as representatives of the cellulosic paper/cardboard fraction of MSW. Low-density polyethylene (LDPE) taken from a white-colored plastic bag and poly(vinylchloride) (PVC) taken from a gray-colored piece of a solid plate were chosen to represent the plastic fraction. Table 1 shows results from a C/H/N/S/Cl analysis of both fresh samples and char formed at 1123 K and a proximate analysis of each component. The proximate analysis was performed according to ASTM standards for RDF. These standards specify 848 K for the determination of ash and 1223 K for measuring volatile matter. However, to be sure of closing the mass balance for the proximate analysis, determination of ash was also performed at 1223 K. Only GP experienced a significant weight loss between 848 and 1223 K (ash content reduced from 44 to 27 wt %). The ultimate analysis of NP, CB, and GP shows similar results. The nitrogen contents of NP, CB, and GP were 0.11, 0.11, and 0.14 wt %, respectively. However, it should be noted that the carbon content of the char for GP was ~40% lower than for NP and CB. The proximate analysis shows that the ash content of GP is 27 wt %, whereas the ash content in NP and CB is 0.6 and 1.2 wt %, respectively. Comparing GP to NP and CB, less moisture, volatile matter, and fixed carbon for GP were observed. PVC and LDPE have a similar low content of nitrogen with 0.04 and 0.05 wt %, respectively. The nitrogen content in PVC and LDPE can originate from compounding ingredients such as stabilizer, plasticizer, extenders, fillers, pigment, etc., because the original polymers does not contain nitrogen. It is known, for example, that

TABLE 1

C/H/O/N/S/Cl (Dry Ash Free) Analysis of Fresh Samples and Char Formed at 1123 K and Proximate Analysis

Sample	C (wt %)	H (wt %)	O[a] (wt %)	N (wt %)	S (wt %)	Cl (wt %)
Fresh samples						
Newspaper	52.1	5.9	41.86	0.11	0.03	n.d.
Cardboard	48.6	6.2	44.96	0.11	0.13	n.d.
Glossy paper	45.6	4.8	49.41	0.14	0.05	n.d.
LDPE	85.7	14.2	0.05	0.05	0.00	n.d.
PVC	41.4	5.3	5.83	0.04	0.03	47.7
Char						
Newspaper	92.3	1.3	6.29	0.11	n.d.	n.d.
Cardboard	85.4	1.2	13.32	0.08	n.d.	n.d.
Glossy paper	56.7	0.6	42.7	<0.05	n.d.	n.d.
PVC	71.4	1.9	1.0	<0.05	n.d.	25.7

	Ash (wt %)	Volatile Matter (wt %)	Fixed Carbon (wt %)	Moisture (wt %)
Newspaper	0.6	80.5	11.0	7.9
Cardboard	1.2	81.9	10.3	6.6
Glossy paper	27.0	65.1	4.4	3.5
LDPE	2.1	97.6	0.0	0.3
PVC	4.2	81.4	14.4	0.0

n.d. = not determined.
[a] O obtained by difference.

stabilizer for PVC contains nitrogen [10]. Otherwise, the ultimate and proximate analysis of PVC and LDPE shows different characteristics. PVC has ~50 wt % of chlorine, whereas LDPE consists of carbon and hydrogen. PVC has a fixed carbon content of almost 15%, while LDPE has 100% volatile matter on an ash-free basis.

Pellets of the different components and mixtures of components were prepared. Paper and plastic were cut into small pieces (~5 × 5 mm) and compressed. The components constituting the mixture pellets were mixed thoroughly before compression. The thorough mixing and compression increases the possibility of interactions between the different components. The pellets were ~12 mm in diameter with varying heights, depending on the material, ranging typically from 8–25 mm.

The combustion experiments were performed in an electrically heated small-scale fixed bed reactor, a schematic drawing of which is shown in Fig. 1. The top section consists of an outer steel tube and an inner alumina tube to prevent reactions catalyzed by steel in the freeboard. The pellets were put in a cylinder (i.d. 13 mm; height 54 mm), which was open at the top, allowing pyrolysis gases and tars to escape and enter the reactor. The solid wall and the height of the cylinder do not allow oxygen to react with the sample inside the cylinder. Hence, this study only investigates the formation of NO from combustion of the volatile material in the fuel (volatile fraction 85–100% on a dry ash free basis). Heterogeneous reactions (oxidation of char) were not examined in this study. An inconel wire fastened the cylinder to the top screw. The cylinder with the sample was lowered into the reactor just above the air distribution plate, which had 127 holes of diameter 0.55 mm. The reactor had seven separately controlled heating elements—two in the bottom section (preheating of oxidizer), and five in the top section. The heating elements were controlled so that the freeboard section was as isothermal as possible.

Figure 2 shows the experimental setup. High purity N_2 and O_2 were delivered from pressur-

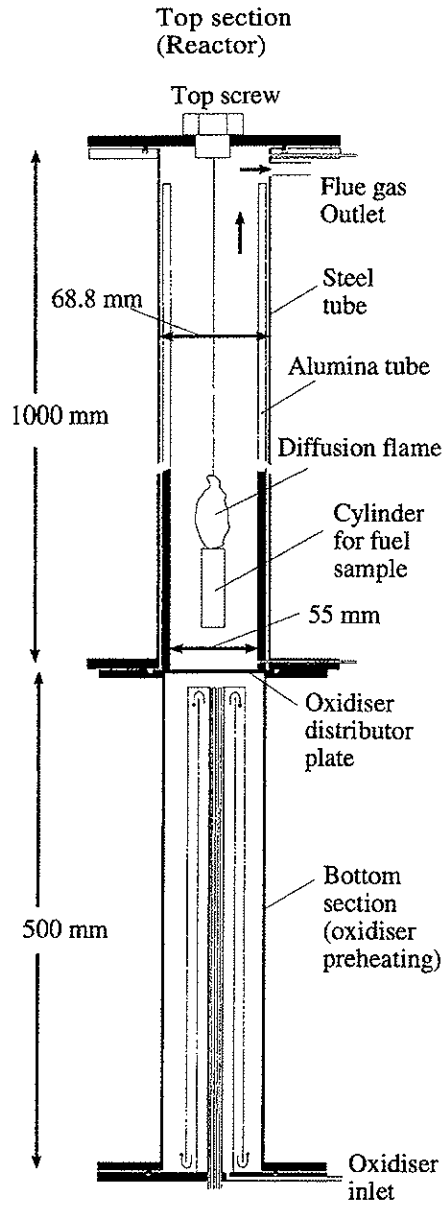

Fig. 1. Schematic drawing of reactor.

ized cylinders connected with a pressure control valve. A mass flow controller controlled the flow rate of each gas, before the gases were mixed in the mixing vessel. The mixed gas was fed to the bottom of the reactor for preheating. The flue gas was sampled at the top of the reactor by sending it through a small cyclone to remove particles. A sample line from the cyclone delivered gas to the analyzers. The pump and mass flow controllers ensured a constant flow to the analyzers. A particle filter and a condenser were connected to the sample line prior to the pump to remove fine particles and water from the flue gas. The analyzers were connected in series. Oxygen was measured with a paramagnetic (Hartmann & Braun Magnos 3) analyzer, CO_2 and CO were measured with infrared (Hartmann & Braun analyzers URAS 4 and URAS 3G) analyzers, respectively. Nitric oxide was measured by the nondispersive ultraviolet absorption technique (Hartmann & Braun Radas 2 analyzer). Sulphur dioxide was also measured by an ultraviolet absorption analyzer (NGA 2000 MLT). The concentrations of O_2, CO_2, CO, NO_x, and SO_2 were continuously recorded by a data acquisition system every 0.5 s. The typical uncertainty in all these measurements was a maximum deviation of 1% of the range of each analyzer.

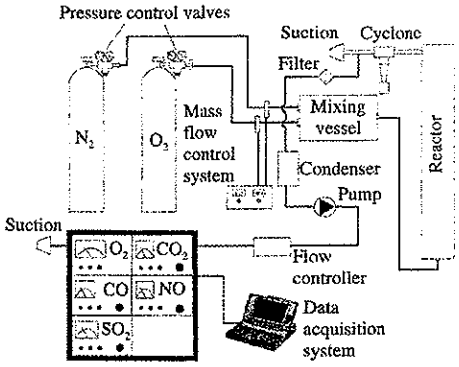

Fig. 2. Experimental setup.

Table 2 shows the experimental matrix for this investigation. Samples heavier than 0.12 g (0.2 g in the mixture with paper/cardboard and PVC) for LDPE were not used, because the reactor was not big enough to handle the sudden release of hydrocarbon volatiles from this fuel. Samples above 0.12 g gave problems from a lack of oxygen causing incomplete combus-

TABLE 2

Experimental Matrix

Component	Sample Mass (g)	Temperature Range (K)	O_2 Concentration in Oxidizer (vol %)
Single components			
Newspaper	0.2–2.0[a]	973–1123[b]	12, 21, 40, 100[d]
Cardboard	2.0	1123	12, 21, 40, 100
Glossy paper	2.0	1123	12, 21, 40, 100
LDPE	0.05–0.2[a]	973–1123[c]	12, 21, 40, 100[e]
PVC	2.0	1123	12, 21, 40, 100
Mixture of paper/cardboard	2.0	1123	12, 21, 40
20–80% Newspaper			
10–70% Cardboard			
10–70% Glossy paper			
Mixture of plastics	0.2	1123	12, 21, 40
33–67% LDPE			
33–67% PVC			
Mixture of paper/cardboard and plastics	2.0	1123	12, 21, 40
15–60% Newspaper			
10–55% Cardboard			
10–55% Glossy paper			
10% LDPE			
10–55% PVC			

[a] Variation of sample weight performed at 1123 K and 21 vol % O_2.
[b] Variation of temperature performed with a sample weight of 2.0 g.
[c] Variation of temperature performed with a sample weight of 0.12 g.
[d] Variation of O_2 concentration performed with a sample weight of 2.0 g and temperature of 1123 K.
[e] Variation of O_2 concentration performed with a sample weight of 0.12 g and temperature of 850°C.

tion, resulting in high values of CO. Increasing the flow of oxidizer did not promote complete oxidation, because this also reduced the residence time. The variations in compositions for the different mixtures of paper, cardboard, and plastics in Table 2 reflect the typical composition of MSW and RDF [11, 12, 14]. However, compositions outside this range were also studied.

The measurements from the combustion experiments were analyzed and the conversion factor for volatile fuel nitrogen to NO was calculated for each experiment, from integrating the transient [NO] over time. Equation 1 describes how the conversion factor for the volatile nitrogen was calculated.

$$\text{NO/fuel} - N = V/(m_0 \cdot X_N/M_N) \cdot \sum [\text{NO}] \cdot \Delta t \quad (1)$$

In Eq. 1, V [Nm^3/s] is the constant gas flow rate, m_0 [g] is the initial mass of the sample on a dry basis, X_N [−] is the initial mass fraction of volatile nitrogen in the sample, M_N [g/mol] is the atomic weight of nitrogen, [NO] [mol/Nm^3] is the transient NO concentration and Δt [s] is the time interval for recording of data. The conversion of fuel N to NO can be considered as a two-step process. The first step (in this case pyrolysis in the cylinder) will convert volatile nitrogen to intermediate products, such as HCN and NH_3. The second step is the conversion of the intermediate products to NO. Some of the volatile nitrogen will also be converted to N_2 in both steps; however, Eq. 1 calculates the total conversion of volatile nitrogen to NO.

The reproducibility of the experiments was checked, both for single components and for mixtures. Three experiments in succession, under identical experimental conditions, were performed. Figure 3 shows the emission level of NO as a function of time for three experiments on NP and LDPE. These concentrations were quite well repeated for both NP and LDPE. The conversion factor was calculated for each of these experiments, and a standard deviation in the conversion factor of 3.6 and 3.7% was found

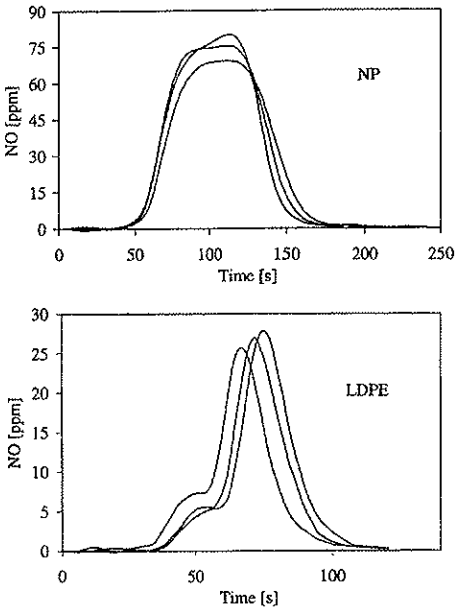

Fig. 3. Repeatability tests of NO emission level for NP and LDPE. Sample mass m_{NP} = 2.0 g and m_{LDPE} = 0.12 g; reactor temperature T = 1123 K; O_2 concentration = 21 vol %.

for NP and LDPE, respectively. Standard deviations of 2.5 and 1.9% were found for a chosen composition of mixture of paper/cardboard and a mixture of paper/cardboard and plastics, respectively.

EXPERIMENTAL RESULTS

Experiments were performed on single particles of NP, CB, GP, LDPE, and PVC, as well as with mixtures of only paper/cardboard, mixtures of plastics and mixtures of paper/cardboard and plastics.

Single Components

Figure 4 shows [NO] from the five different components in this study. NP and CB have similar [NO] profiles. The overall profiles for GP, LDPE, and PVC, however, are significantly lower. The differences between the components can be explained by differences in fuel properties; elemental composition, devolatilization behavior, and in the case of LDPE, the sample's mass is also of great importance (0.12 g vs. 2.0 for the other fuels). For PVC and LDPE, small but significant amounts of NO was observed at all oxygen concentrations prior to the major formation of NO. After a detailed study of the data, minor oxygen consumption was also observed. A small blue and yellow flame was observed before the major combustion took place. The minor formation of NO for PVC and LDPE may, therefore, partly be explained by a minor release of volatiles creating a small flame before the main combustion took place. However, other factors such as a release of a larger amount of volatile nitrogen and higher flame temperature in the first stage of devolatilization compared to the second stage can explain the observed NO formation.

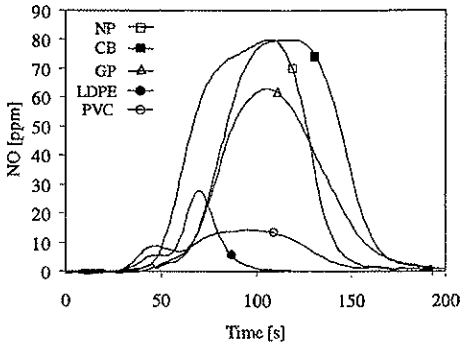

Fig. 4. Transient emissions levels of NO for the different components in this study. Sample weight equals 2.0 g with the exception of LDPE (sample weight = 0.12 g). Reactor temperature = 1123 K, and O_2 concentration = 21 vol %.

Figure 5 shows $[CO_2]$ and $[O_2]$ for experiments on 0.12 g of LDPE and 2.0 g of NP; NP has a burnout time of ~2 min, while the burnout time for LDPE is ~30 s. The observed difference in burnout time is explained by different devolatilization rates and masses of sample. The peak oxygen consumption for LDPE is slightly higher than for NP. The oxygen consumption is controlled by the devolatilization rate and composition of the pyrolysis gas. The stoichiometric oxygen requirements calculated from their elemental compositions for LDPE (consisting of hydrogen and carbon) and NP (with a high yield of oxygen) are 209 and 83 mol/kg_{fuel}, respec-

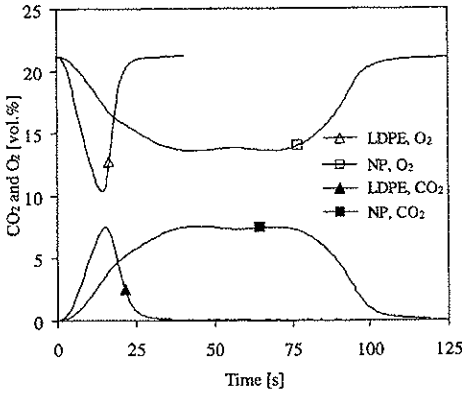

Fig. 5. CO_2 and O_2 levels for experiments on LDPE and newspaper. Reactor temperature is 1123 K and O_2 concentration is 21 vol %. m_{LDPE} = 0.12 g and m_{NP} = 2.0 g.

tively. These values are similar to the calculated oxygen consumption for experiments on LDPE and NP at base-case conditions (21 vol % oxygen and 1123 K), being 238 and 78 mol/kg_{fuel}. Taking the weight of the volatile fraction of the samples into consideration, the total number of mol of oxygen needed for complete combustion of LDPE and NP are 0.029 and 0.133, respectively. Given similar release rate of volatiles, the burnout time would be ~14 times higher for NP than for LDPE, while the actual burnout time ratio is ~4. Although the release rate is significantly lower, the peak oxygen consumption is higher for LDPE than for NP. Hence, a lower release rate of volatiles and higher oxygen requirement for LDPE, explains the different oxygen consumption curves.

Table 3 shows the calculated conversion factors for single components as a function of oxygen concentration. Only minor differences in the conversion factors were observed from 12 to 21 vol % O_2. Therefore, it was decided to run experiments with oxygen concentrations above 21 vol % O_2, which should result in a more intense flame with a higher temperature, thereby forming thermal NO. Three experiments were conducted for each oxygen concentration, except for 100% O_2, where one experiment was performed on each sample. Average values for the conversion factor and standard deviation are shown in Table 3.

The fraction of volatile nitrogen is usually determined by subtracting the remaining nitrogen content in the char (as determined from the proximate and ultimate analysis) from the nitrogen content of the parent fuel. However, conditions for devolatilization of nitrogen may vary for different fuels and conditions. To validate the use of a proximate and ultimate analysis to determine the fixed content of a certain element, a mass balance for carbon was calculated for each of the experiments (C in fresh sample vs. C in char, CO, and CO_2). Using the ultimate analysis on fresh samples, char formed at 1123 K and measured CO and CO_2 values closes the mass balances for carbon well (within ±10 wt %). The results also showed that the major part of the volatile C is found in CO_2 (>95%). PVC

TABLE 3

Average Conversion Factors (NO/Fuel N) for Single Components of 2.0 g as a Function of Oxygen Concentration in Oxidizer at a Reactor Temperature of 1123 K

	Newspaper	Cardboard	Glossy paper	LDPE[a]	PVC
O_2 (vol %)	(NO/fuel N) STDEV (%)	(NO/fuel N) STDEV (%)	(NO/fuel N) STDEV (%)	(NO/fuel N) STDEV (%)	(NO/fuel N) STDEV (%)
12	0.49	0.48	0.27	1.60	0.21
	1.3	2.4	1.6	9.8	6
21	0.54	0.53	0.26	1.96	0.23
	3.7	0.9	1.8	3.7	10.2
40	0.99	0.86	0.32	10.09	0.37
	2.4	2.6	4	7.2	6.9
100[c]	0.50	0.42	0.23	0.71 (0.38)[b]	0.04

[a] Sample size 0.12 g.
[b] Sample size 2.0 g.
[c] Only one experiment.

produces the largest fraction of CO from volatile C (~5% of volatile C), while corresponding values for other samples are typically 0–3%.

The conversion factors for NP are 0.49, 0.54, and 0.50 at 12, 21, and 100 vol % oxygen, respectively. The corresponding values for CB are 0.48, 0.53 and 0.42. At 40 vol % O_2 the conversion factor increases to 0.99 for NP and 0.86 for CB, which is approximately a 80% increase from 21 vol % oxygen for NP and a 60% increase for CB. These results show that NO formation is more sensitive to combustion temperature caused by a higher oxygen concentration, than to a higher availability of oxygen. In other words, very similar behavior was observed for NP and CB for all oxygen concentrations. Skreiberg et al. [13] reported a conversion factor of ~0.3 and 0.45 at 11 and 21 vol % oxygen for a spruce sample of 700 mg at 1073 K in the same reactor as in this study. However, the conversion factor was based on total conversion of the fuel (volatiles and char) and not only on volatiles, as in this study.

Glossy paper, however, behaves differently with conversion factors of 0.27, 0.26, and 0.23 at 12, 21 and 100 vol % oxygen. When increasing the oxygen concentration from 21 to 40 vol % O_2, a small increase in conversion factor from 0.23 to 0.32 was observed. Comparing the conversion factors at 12, 21, and 100 vol % O_2 for GP with NP and CB, the conversion factor for GP is approximately a factor of two lower. The explanation may be that the GP sample contained more iron than NP and CB [14]. Mori et al. [15] studied the effect of iron catalysts on the fate of fuel nitrogen during coal pyrolysis; they concluded that an iron content of 0.2–0.7 wt % promoted both the formation of N_2 and lower yields of HCN, NH_3, N-containing oil, tar, and char. However, the very high amount of ash in GP may also contain other catalytic species and have the same effect as iron on the conversion of fuel nitrogen.

The large conversion factors for LDPE clearly indicate the production of thermal NO and possibly also prompt NO. The conversion factor increased by ~500% when the oxygen concentration was increased from 21 to 40 vol %. The prompt NO mechanism is important with fuel-rich conditions [16], so this large increase in the conversion factor can mainly be explained by a larger formation of thermal NO due to a higher combustion temperature with more O_2 present. PVC shows similar behavior to GP: the conversion factor increased by ~60% from 21 to 40 vol % O_2. However, the conversion factor with 100% O_2 is close to zero. One of the most important differences between PVC and the other fuels used in this study is the high content of chlorine. The low conversion factor with pure O_2 implies that the formation of NO at lower O_2 concentrations is by the thermal and/or prompt mechanism. However, due to high concentrations of chlorine in PVC, the formation mechanism for NO is more complex, and presently not fully understood, even though several studies have investigated the effect of chlorine in combustion processes [17–20].

The oxidation of CO by the hydroxyl radical (OH) is much faster than steps involving O_2 or O [16]. However, the fuels in this study contain sufficient hydrogen to produce hydroxyl radicals, so the oxidation of CO becomes fast and incomplete combustion is avoided. This is confirmed by the low CO emissions observed at all oxygen concentrations for all components.

The influence of the sample's mass was investigated for NP and LDPE. The conversion factor for NP increased from 0.50 to 0.59 when its mass was reduced from 2.0 to 0.2 g with 21 vol % oxygen. For LDPE the conversion factor increased from 2.05 to 2.73, with a reduction in sample mass from 0.2 to 0.05 g. Care should be taken interpreting these results, because different variables are coupled. A smaller sample results in lower consumption of oxygen and more excess air. A smaller sample also increases the uncertainty in the calculation of the conversion factor.

For NP and LDPE, the influence of reactor temperature was investigated: a decrease from 1123 to 973 K resulted in a decrease in conversion factor from 0.50 to 0.45 for NP and from 1.96 to 1.89 for LDPE. These experiments were performed with 21 vol % oxygen and samples of 2.0 and 0.12 g were used for NP and LDPE, respectively. The differences in fuel N content for the components in this study are minor; therefore, the reduction in conversion when increasing the nitrogen content, as stated in the literature [21], is considered of minor importance.

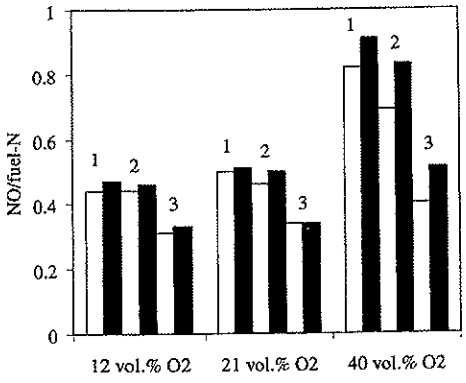

Fig. 6. Conversion factor for mixtures of paper as a function of O_2 concentration in inlet gas. White bars denotes experiments on a pellet of the mixture. Black bars denote the conversion calculated factor from single components. 1: NP = 80 wt %, CB = 10 wt %, GP = 10 wt %; 2: NP = 20 wt %, CB = 70 wt %, GP = 10 wt %; 3: NP = 20 wt %, CB = 10 wt %, GP = 70 wt %.

Mixtures

The conversion factors for the experiments on pellets of mixtures were compared to the conversion factors calculated for an imaginary pellet built up from the weighted contributions of each component's conversion factor. The experiments on mixtures and single components were performed in exactly the same way with a mass of 2.0 g, except for experiments on single particles of LDPE, where a sample of 0.12 g was used. The conversion factor for the imaginary pellet is described by:

$$(\text{NO/fuel} - N)_{\text{SUM OF SINGLE COMPONENTS}} = \sum_j Y_i \cdot (\text{NO/fuel } N)_i \quad (2)$$

In Eq. 2, Y_i is the mass fraction of component i, $(\text{NO/fuel N})_i$ is the conversion factor for component i as found from the single-component experiments, and j denotes the number of components in the actual mixture.

The experiments on mixtures of paper and cardboard gave some interesting results at 40 vol % O_2. As shown in Fig. 6, the conversion factor for the mixture at 40 vol % O_2 was ~10–20% lower than the value calculated from the single components. This indicates that the lower conversion factor for the mixture is mainly caused by a lower temperature, and hence, less contribution from thermal NO. The lower temperature can be explained by differences in the measured transient oxygen consumption for the different fuels, and hence, the devolatilization rate. The oxygen consumption for the single components had somewhat different profiles and maximum values. The transient oxygen consumption for the mixture is a function of composition. However, at this high inlet oxygen concentration, a difference in the transient oxygen consumption, and hence, temperature, might influence the NO emissions significantly, because a large fraction of the NO is formed thermally. For experiments at 12 and 21 vol % O_2 the differences in the conversion factors for mixtures and the calculated sum of single components were minor, being within the experimental error. For all experiments on mixtures of paper and cardboard, no influence of a special component could be detected when the fraction of each component was varied.

Interpretation of the experimental results on mixtures of LDPE and PVC was somewhat more difficult, due to the small mass leading to a higher degree of uncertainty. The results showed no clear trends with oxygen concentration or mixture ratio, indicating little or no interaction between the two components.

Figure 7 shows the conversion factors for different mixtures of paper and plastic compared with calculated values. All the mixtures of paper and plastics show conversion factors lower than estimated from the single components. The major reason is that the contribution from LDPE in the mixture is not as much as expected. In fact, the conversion factor for LDPE as a single component exceeds unity for all oxygen concentrations, clearly indicating a contribution from thermal or possibly prompt NO. The conditions for thermal NO are not as favorable for the mixture as for the single component. An indication on the difference in flame temperature for the different fuels is the adiabatic flame temperature. The adiabatic flame temperature is the maximum combustion temperature, which will be higher than those actually attained in the reactor, given that there will be significant radiative heat losses. However, it is useful as an indicator of differences

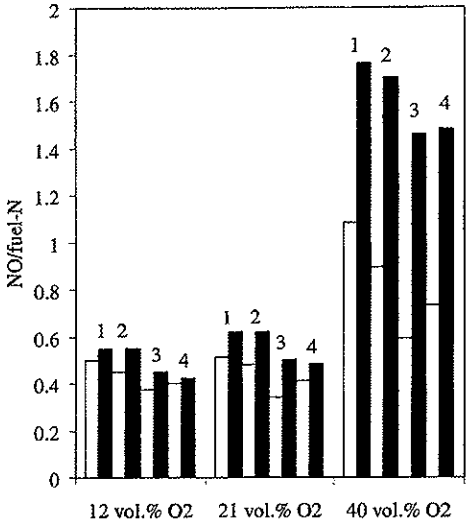

Fig. 7. Conversion factors for mixtures of paper and plastic as a function of O_2 concentration in inlet gas. White bars denote experiments on mixtures. Black bars denote the conversion factor calculated from single components. 1: NP = 60 wt %, CB = 10 wt %, GP = 10 wt %, LDPE = 10 wt %, PVC = 10 wt %; 2: NP = 15 wt %, CB = 55 wt %, GP = 10 wt %, LDPE = 10 wt %, PVC = 10 wt %; 3: NP = 15 wt %, CB = 10 wt %, GP = 55 wt %, LDPE = 10 wt %, PVC = 10 wt %; 4: NP = 15 wt %, CB = 10 wt %, GP = 10 wt %, LDPE = 10 wt %, PVC = 55 wt %.

between fuels and mixtures of different fuels, and not as a quantitative measure of combustion temperature, and hence, NO formation. Equilibrium calculations with CHEMKIN III [22] were performed with the same oxygen concentrations as for the experiments. For LDPE, the major pyrolysis product is ethene (C_2H_4) [23]. Ethene was used in the equilibrium calculations simulating the combustion of LDPE. For paper, the following composition of the pyrolysis gas was used [24]: 0.4 vol % H_2, 41.1% CO, 46.6% CO_2, 8.3% CH_4, and 3.6% H_2O. For PVC, a pyrolysis gas corresponding to the elemental composition was used: 60 vol % C_2H_4 and 40 vol % HCl. Calculations were also made for a mixture of paper and plastics, with a composition corresponding to 80 wt % paper, 10% PVC, and 10% LDPE. The mixture had the following gas composition: 0.3 vol % H_2, 31.6% CO, 35.9% CO_2, 6.4% CH_4, 18% C_2H_4, 5% HCl, and 2.8% H_2O. Table 4 shows the calculated adiabatic flame temperatures for the different fuels at the same oxygen concentrations at different fuel/air ratios. The oxygen concentrations correspond to those used in the experiments, while $\lambda = 3$ corresponds to the maximum λ observed for NP at base case conditions with maximum oxygen consumption. Initial temperatures of 673 K for paper and mixture of paper and plastics and 773 K for LDPE and PVC were used according to their devolatilization temperatures, as observed from a thermogravimetric analysis of the different components. Increasing λ from 1.5 to 3.0 decreases the adiabatic flame temperatures for paper, LDPE, and the mixture by 472, 638, and 571 K, respectively. An adiabatic temperature difference at $\lambda = 1.0$ increasing from 259 to 621 K when increasing the oxygen concentration from 12 to

TABLE 4

Adiabatic Flame Temperatures for Pyrolysis Gas from Paper, LDPE, PVC, and Mixture of Paper and Plastics at Different Oxygen Concentrations in Oxidizer and λ

Sample	12 vol % O_2	21 vol % O_2	40 vol % O_2	100 vol % O_2
$\lambda = 1.0$				
Paper	1840	2174	2417	2598
LDPE	2099	2556	2912	3219
PVC	2001	2472	2833	3131
Mixture	1936	2350	2655	2897
λ (at 21 vol % O_2)	1.5	2.0	2.5	3.0
Paper	1955	1749	1597	1483
LDPE	2260	1973	1768	1622
PVC	2155	1867	1667	1524
Mixture	2073	1816	1634	1502

100 vol % is observed when comparing paper and LDPE. PVC has a slightly lower adiabatic flame temperature than LDPE at all oxygen levels. A temperature difference of 163 to 322 K when increasing the oxygen concentration from 12 to 100 vol % oxygen is observed when comparing the mixture to LDPE. Knowing that the formation of thermal NO increases exponentially with temperature, starting at approximately 1600–1700 K [25], a small temperature change will significantly alter the yield of thermal NO. The relative temperature contribution of LDPE in the flame of the volatile fraction of the mixture is, therefore, not as large as if one summarizes the weighted conversion factors for the single components. This is especially evident for experiments at 40 vol % O_2, where the conversion factor of LDPE as a single component is very high (see Table 3). No clear trend towards a reduced conversion factor for mixtures with a high content of PVC was observed.

MODELING

The opposed flow diffusion flame code in Chemkin III [22] and OPPDIF [26] was used for a parametric study and for comparison with *trends* observed in the experimental study. OPPDIF is a Fortran code, which computes the steady-state solution for axisymmetric diffusion flames between two opposing nozzles. The one-dimensional model predicts the species, temperature, and velocity in the core flow between the nozzles (excluding edge effects). Several aspects of opposed-flow or counterflow diffusion flames, such as flame structure, extinction limits, and burning velocities, have been studied numerically and experimentally [27–34]. Mechanisms for NO formation in opposed-flow diffusion flames have also been investigated. The contributions from thermal, prompt [35], and N_2O mechanisms have been identified for different fuels under different conditions [36, 37]. Turns [38] has reviewed the formation of NO_x in nonpremixed flames, and concluded that research was needed into several aspects of NO formation in both laminar and turbulent jet flames. However, no literature was found on the formation of NO during the combustion of pyrolysis gases from paper or plastics.

Methods

The experimental setup is a coflow system, whereas the OPPDIF program describes an opposed-flow system; consequently, differences in residence time and flame structure may occur. However, in laminar diffusion flames, the chemistry, independent of flow arrangements (coflow vs. opposed-flow system), occurs in the flame close to or at stoichiometric conditions. The important parameters in the simulation of an opposed flow diffusion flame include the velocities of the two gas flows and the separation between the two nozzles; these two parameters characterize the residence time. A typical velocity in an experiment with NP was estimated to be ~20 cm/s for the whole pyrolysis period for the gas flowing out of the cylinder, and ~40 cm/s for the oxidizer. In this study, the distance between the nozzle was kept constant at 2.0 cm, whereas the exit velocities were varied with a constant fuel/oxidizer ratio of 0.5 similar to the experiments. Keeping the velocity gradient (i.e., strain rate) constant, when changing the separation distance and velocities of the fuel and oxidizer can be used as a control parameter. However, due to differences between experimental and simulation conditions, using the strain rate as a parameter in the parametric study would not further explain the experimental results. The temperature of the fuel (pyrolysis gas) is 673 K for simulating the burning of paper, and 773 K for plastic (C_2H_4). These temperatures were found from a thermogravimetric analysis (TGA) of the components. The TGA study gave the degree of degradation as a function of temperature, not taking into account the possible influence of heat and mass transfer. The temperature of the oxidizer in the simulations was 1123 K unless indicated otherwise.

The kinetic reaction schemes used for simulations on paper and plastic are slightly reduced subsets of the chemical kinetic model for hydrocarbon/NO interactions proposed by Glarborg et al. [39]. The reaction mechanism used for paper had 39 species, with a total of 239 reversible reactions, while that for plastic (taken as C_2H_4) involved 43 species, with a total of 258 reversible reactions. The pyrolysis gas composition for paper/cardboard was estimated from

the literature. For paper, an average of all gas compositions obtained from a study of the pyrolysis of paper and cardboard, with the exception of two experiments performed at low temperature, was used [24]. The minor amount of hydrocarbons was taken into account as CH_4 in the gas composition. The tar fraction was assumed to crack, yielding a gas of the same composition as the primary gas: 0.4 vol % H_2, 41.1% CO, 46.6% CO_2, 8.3% CH_4, and 3.6% H_2O. This gas composition was used in all simulations, unless otherwise mentioned. The content of NH_3 and HCN was not measured in the above-mentioned study.

Little information on the release of fuel nitrogen during the pyrolysis of MSW components or biomass has been found. Ammonia is believed to be the dominant fuel N product from pyrolysis of low rank fuels (biomass, peat, lignite, and low-rank coals) [40]. However, for bituminous coals and anthracites, HCN is the dominant nitrogenous product of pyrolysis. Others [41] have found for the pyrolysis of different biomasses and coals, that the HCN/NH_3 ratio decreased with increasing O/N ratio for the parent fuel. However, for O/N ratios above 20, the HCN/NH_3 ratio was relatively constant at ~0.15. For pine bark, which has an O/N ratio similar to paper, the HCN/NH_3 ratio was found to be 0.1 [41]. The total conversion of fuel N to NH_3 and HCN during pyrolysis shows large variations. An investigation of the formation of NH_3 and HCN from the pyrolysis of peat, coal, and bark at low heating rates showed that all fuels produced more NH_3 than HCN [42]. It was further found that increasing the heating rates resulted in a higher conversion of fuel N to NH_3 and HCN. The fraction of nitrogen remaining in the char after pyrolysis ranged from 15 wt % for peat to 70 wt % for bark. The heating rate and devolatilization temperature play important roles in the devolatilization of fuel N. Previous studies [43] have shown that char from coal will be enriched in nitrogen at a low degree of devolatilization, i.e., during heating to a low final temperature or at very short residence times. At higher devolatilization temperatures, nitrogen is released faster than the volatiles, so the final nitrogen content of the char may be lower than that of the parent coal. The same study stated that the amounts of NH_3 and HCN released during pyrolysis depend on a number of factors, most importantly coal type, heating rate, final temperature, and residence time.

Based on the information found in the literature, the HCN/NH_3 ratio was set to 1/9 for the simulations on pyrolysis gas from paper. Estimating the conversion of volatile fuel N to NH_3 and HCN is difficult. Leppälahti [42] stated that for peat, which has a similar volatile fraction of fuel N as paper, the conversion to NH_3 was between 17–24 wt %, and that the conversion to HCN was between 3 to 9 wt % of the initial fuel N. As observed in the ultimate analysis of char from newspaper (see Table 1), 15% of the nitrogen in paper remains in the char. Furthermore, it is assumed that 50% of the remaining volatile nitrogen is converted to N_2 either before escaping the pellet or inside the cylinder. Based on the elemental composition of the fuel, the above ratio of HCN/NH_3 of 1/9 and the assumption that 50% of the volatile nitrogen is converted to N_2, the concentrations of NH_3 and HCN in the pyrolysis gas from paper were set to 900 and 100 ppmv, respectively. For all simulations the calculated conversion factor means the conversion of NH_3 and HCN (in the pyrolysis gas) to NO.

For the simulation of LDPE, C_2H_4 was chosen as a fuel corresponding to the content of carbon and hydrogen in the fuel and experimental data [23].

Simulations of Paper

The temperature and concentrations of species, as a function of the distance X from the fuel nozzle, for simulations of the pyrolysis gas from paper are shown in Fig. 8. The peak temperature is observed slightly to the fuel side. OPPDIF estimates the flame thickness by assuming that the flame starts where the temperature equals the fuel temperature plus 10% of the maximum temperature increase. The end point of the flame is estimated the same way using the temperature of the oxidizer as a starting point. A flame thickness of ~6 mm was estimated using this method. Consumption of the species CO, CH_4, and NH_3 is observed in Fig. 8, when the fuel is entering the flame region; formation of HCN and NO is observed

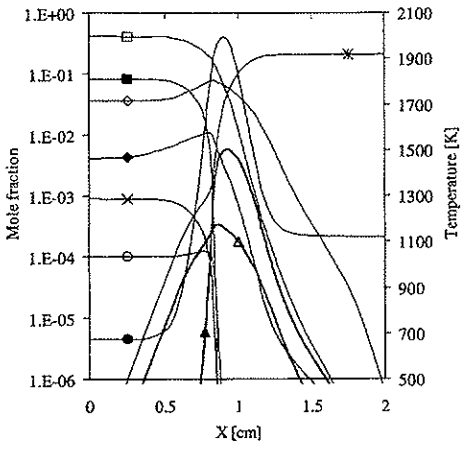

Fig. 8. Calculated temperature (●) and concentrations of species as a function of distance from the fuel nozzle for simulation on paper at 21 vol % oxygen and an oxidizer temperature of 1123 K. The concentrations are for CO (□), CH_4 (■), H_2O (◇), H_2 (◆), NH_3 (×), HCN (○), NO (△), OH (▲), and O_2 (*).

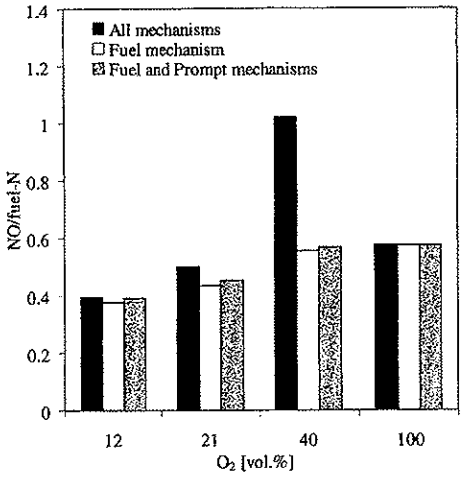

Fig. 9. Contribution of fuel, prompt, and thermal mechanisms to the conversion factor (conversion of HCN and NH_3 to NO) for simulations on pyrolysis gas from paper at different oxygen concentrations. Oxidizer temperature = 1123 K.

in the first section of the flame on the fuel side. The peak formation of NO is observed on the fuel side at a temperature slightly lower than the peak temperature. At the point of peak formation of NO, most of the NH_3 and HCN have been consumed.

Figure 9 shows the contributions of fuel, prompt, and thermal NO_x mechanisms to the conversion factor for paper at different oxygen concentrations in the oxidizer. The initiating reactions for the thermal and prompt NO_x mechanisms were removed from the reaction scheme for the respective calculations. A peak temperature of 2260 K was observed for simulations at 40 vol % oxygen, whereas the peak temperature at 21 vol % oxygen was 2000 K. This increase in temperature is the main reason for the high contribution from thermal NO_x at 40 vol % oxygen. An increased oxygen concentration results in a larger conversion factor when only considering fuel nitrogen for the simulations on paper. The conversion factor for experiments with pure oxygen, however, was more similar to the values obtained at 12 and 21 vol % oxygen. The minor formation of prompt NO observed in Fig. 9 can be explained by the observed formation of HCN in Fig. 8. The rest of the amount of NO derives mainly from the fuel nitrogen species, NH_3, and HCN, and a minor amount of thermal NO.

To investigate the effect of different concentrations and HCN/NH_3 ratios, a sensitivity study was performed. Table 5 shows the concentrations of HCN and NH_3, and the calculated

TABLE 5

Sensitivity Study on the Effect of Different NH_3 and HCN Concentrations for Simulations on Paper

Gas	Base case (vol %)	Comp. 1 (vol %)	Comp. 2 (vol %)	Comp. 3 (vol %)	Comp. 4 (vol %)	Comp. 5 (vol %)	Comp. 6 (vol %)
HCN	0.01	0.005	0.015	0.02	0.05	0.00	0.10
NH_3	0.09	0.045	0.135	0.18	0.05	0.10	0.00
NO/fuel N	0.50	0.72	0.41	0.35	0.50	0.56	0.47

TABLE 6

Variations in Pyrolysis Gas Composition and Conversion Factors for Sensitivity Study for Simulations on Paper

Gas	Base case (vol %)	Comp. 1 (vol %)	Comp. 2 (vol %)	Comp. 3 (vol %)	Comp. 4 (vol %)	Comp. 5 (vol %)
H_2	0.40	0.52	0.32	0.30	0.39	0.40
CO	41.1	41.08	53.43	30.36	39.98	40.64
CO_2	46.5	46.40	36.74	60.45	45.24	45.97
CH_4	8.30	8.30	6.56	6.13	10.79	8.21
H_2O	3.60	3.60	2.85	2.66	3.50	4.68
HCN	0.01	0.01	0.01	0.01	0.01	0.01
NH_3	0.09	0.09	0.09	0.09	0.09	0.09
NO/fuel N	0.50	0.50	0.56	0.47	0.56	0.50

conversion factor for the different simulations on pyrolysis gas from paper. The oxygen concentration in the oxidiser nozzle was 21 vol %, and the temperature of the oxidiser was 1123 K. These results indicate that the total concentrations of NH_3 and HCN have a significant effect on the conversion factor, while the NH_3/HCN ratio is of minor importance. At a constant NH_3/HCN ratio, a decreasing conversion factor with increasing concentrations of HCN and NH_3 is observed. This agrees with other work [21]. It is also interesting to observe that a larger fraction of NH_3 than HCN is converted to NO. A sensitivity study on the pyrolysis gas composition was also performed to investigate the effects of changing composition. Table 6 shows the variations in composition and conversion factors for the pyrolysis gas used in the sensitivity study. An oxidizer temperature of 1123 K and 21 vol % of O_2 were used. The concentrations used in this sensitivity study reflect the range of compositions found in the literature [24]. The concentrations of HCN and NH_3 were held constant. Even with these fairly large variations in composition (each case adds 30% to the selected component, consequently adjusting the concentrations of the other components), the conversion factor varies very little: it deviated by a maximum of 12% from the base case.

Three cases with different velocities for the fuel and oxidizer were simulated for four different oxygen concentrations in the oxidizer and at three different temperatures. In addition, a comparison with the experimental results on NP was made. The results are shown in Figs. 10 and 11. The fuel/oxidizer velocity ratio was estimated from experiments. As can be seen from Figs. 10 and 11, a velocity of 40 cm/s for fuel and 80 cm/s (40/80 velocity ratio) for oxidizer provides the best agreement with the experimental trend observed for NP. The increase in conversion factor for the 20/40 velocity ratio as a function of oxygen concentration, observed in Fig. 10, is generally overestimated. However,

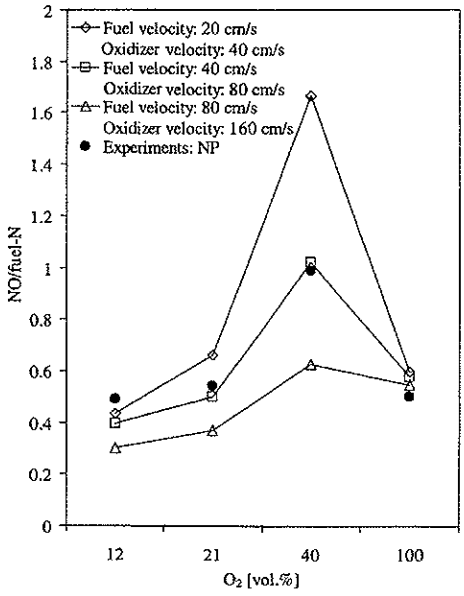

Fig. 10. Comparison of conversion factor at different oxygen concentrations for simulations of pyrolysis gas from paper (conversion of HCN and NH_3 to NO) with different nozzle velocities and experiments on newspaper. Oxidizer temperature = 1123 K.

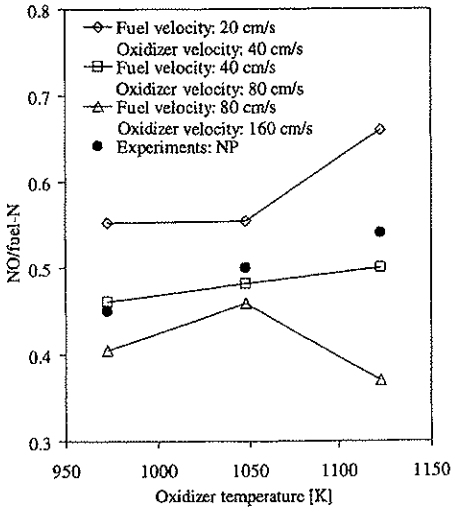

Fig. 11. Comparison of conversion factor at different temperatures for simulations of pyrolysis gas from paper (conversion of HCN and NH_3 to NO) with different nozzle velocities and experiments on NP. Oxygen concentration is 21 vol %.

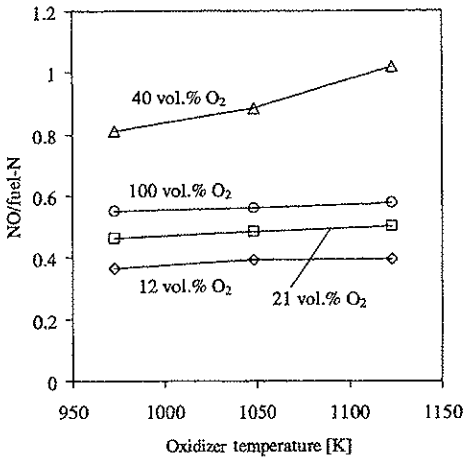

Fig. 12. Influence of temperature and oxygen concentration on conversion factor (conversion of HCN and NH_3 to NO) for simulations of pyrolysis gas from paper.

the conversion factors for both the 40/80 and the 80/160 velocity ratio show a similar trend as the experimental data for NP with regards to a change in oxygen concentration. However, comparing the conversion factor with experiments on NP as a function of temperature shows that the trend of increasing conversion factor with increasing temperature is not reflected for the 80/160 velocity ratio. Based on these results, the 40/80 velocity ratio was chosen for further simulations.

Figure 12 shows the influence of temperature and oxygen concentration in the oxidizer on the conversion factor for simulations on pyrolysis gas from paper. A minor increase is observed with increasing temperature at all oxygen concentrations. A major jump in conversion factor is observed when the oxygen concentration is increased from 21 to 40 vol %, caused by the formation of thermal NO due to a higher flame temperature. It is also interesting to observe that the conversion factor for pure oxygen is similar to that for 21 vol % oxygen. This is also consistent with the experimental results. The reason is that thermal NO cannot be formed at 100% oxygen, due to the absence of nitrogen, which again indicates that NO formed at 12 and 21 vol % oxygen is mainly fuel NO. It can also be observed that NO formation at 40 vol % oxygen is more temperature dependent, because a large portion of the NO formed is from the thermal mechanism.

Figure 13 compares conversion factors as a

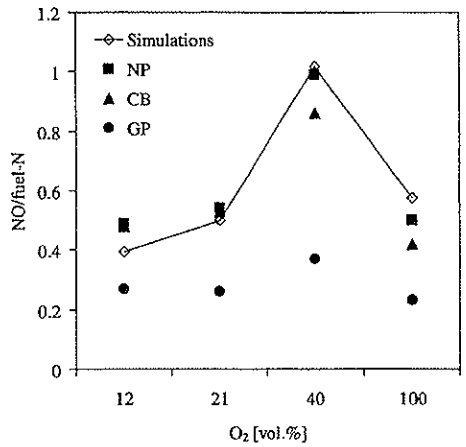

Fig. 13. Comparison of conversion factors as a function of oxygen concentration in the oxidizer for simulations of pyrolysis gas from paper (conversion of HCN and NH_3 to NO) and experiments on NP, CB, and GP. Oxidizer temperature = 1123 K.

function of oxygen concentration in the oxidizer, for simulations on pyrolysis gas from paper and experiments on paper and cardboard. The experimental trends are well simulated, especially for NP and CB. The conversion factor for GP, however, is less influenced by an increase in oxygen concentration than observed in the simulations.

Simulations on Plastic

The simulations for plastic, taken as C_2H_4 in the case of LDPE, including NH_3 and HCN, are more difficult to interpret, because only the initial fuel consumption occurs in the opposed flow diffusion flame. Compared to the volatiles from paper with a lower hydrocarbon yield and higher levels of inert species, the volatiles from a plastic have a much higher stoichiometric oxygen requirement. The limited availability of oxygen in the opposed flow diffusion flame reduces the conversion of fuel to a small value. Therefore, performing simulations with HCN and NH_3 in the fuel gave no valuable results due to large *formation* of HCN and NH_3 rather than their *consumption*. The HCN and NH_3 are formed from reactions in the prompt mechanism [44], which plays an important role in this flame due to the high level of hydrocarbons. Therefore, simulations were performed with only C_2H_4 as fuel, and hence, including only thermal and prompt NO. Experiments on LDPE indicated that the major source of NO was thermal and possibly prompt NO. Due to the high stoichiometric air requirement for C_2H_4, the simulations in OPPDIF were sensitive to the nozzle velocities for the oxidizer and fuel. This is the reason for not performing all simulations with the same velocities as for the simulations for paper.

Attempts were made to simulate the combustion of pyrolysis gas from PVC, assuming the gas was HCl and C_2H_4. However, even a very small concentration of HCl caused the simulations to fail. Therefore, simulations including chlorine were excluded from this study.

Figure 14 shows the emission index for various oxygen concentrations in the oxidizer and velocities in the fuel and oxidizer for simulations on C_2H_4 and experiments on LDPE. The

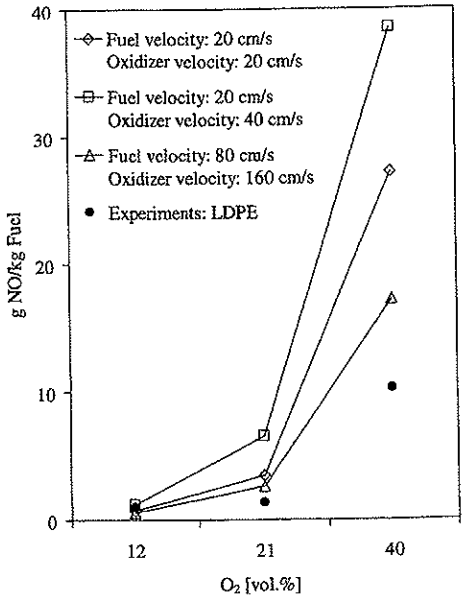

Fig. 14. Emission index (g NO/kg fuel) as a function of oxygen concentration of oxidizer and nozzle velocities. Comparison of simulations using C_2H_4 and experiments on LDPE. The experimental values are subtracted the contribution from fuel NO.

emission index for the experiments is described by:

$$EI_{NO} = \left(\frac{M_{NO}}{M_N}\right) \cdot \left(\frac{V}{m_0 \cdot X_N / M_N}\right) \cdot \sum [\mathrm{NO}] \cdot \Delta t \cdot Y_N \qquad (3)$$

In Eq. 3, M_{NO} [g/mol] is the molecular weight of nitric oxide and Y_N [gN/kg_{Fuel}] is the weight fraction of nitrogen in the fuel on a dry ash free basis. In Fig. 14, the contributions from fuel NO have been subtracted from the experimental values for LDPE. The contribution from fuel NO was estimated by subtracting the NO formed in pure oxygen, assuming that this is the contribution from fuel nitrogen. This contribution of fuel NO should be considered a maximum value, because the high oxygen concentration would result in a higher conversion of fuel N to NO than for a lower oxygen concentration.

The emission index for simulations on plastic was calculated by integrating the production

rate of NO multiplied with the molecular weight of NO over the control volume for the total distance from 0 to L (the distance between nozzles) and dividing this by the corresponding value for the actual fuel consumption. The emission index for the simulations can be described by:

$$EI_{NO} = \frac{\int_0^L W_{NO}\omega_{NO}\,dx}{-\int_0^L W_F\omega_F\,dx} \qquad (4)$$

In Eq. 4, W_{NO} and W_F are the molecular weights of NO and fuel, respectively; ω_{NO} and ω_F are the production rates of NO and the actual consumption rate of fuel. Further explanation of the emission index is given by Takeno [45]. As observed in Fig. 14, the experimental trend of the emission index increasing with the oxygen concentration in the oxidizer is confirmed by the simulations. It is also observed that the influence of velocities and velocity ratio of fuel and oxidizer increases with increasing oxygen concentration. The calculated emission index for experiments on LDPE and simulations on C_2H_4 at 21 vol % oxygen are of the same order of magnitude as found by Turns [38] for a C_2H_4 jet flame in air. Changes in emission index with velocity may be explained by changes in the flame structure causing parameters such as strain rate and residence time to change.

CONCLUSIONS

An experimental and theoretical study of NO formation from the combustion of volatiles from different components (paper, cardboard and plastics) of MSW and their mixtures has been performed. The experiments were performed in a laboratory furnace, while simulations were made with the CHEMKIN code OPPDIF for an opposed-flow diffusion flame.

Experiments and simulations on the combustion of volatiles from paper/cardboard show that NO is mainly formed from the fuel nitrogen. For the plastics LDPE and PVC, however, the experiments show that NO mainly originates from the thermal and possibly the prompt NO mechanisms.

Increased formation of NO is observed for newspaper, cardboard, glossy paper, PVC, and LDPE, when increasing the oxygen concentration in the oxidizer from 12 to 40 vol %. Increasing the temperature of the oxidizer from 973 to 1123 K led to more NO from newspaper and LDPE. Simulations with OPPDIF confirmed these trends.

The measured conversion factor for fuel N to NO for mixtures of paper and cardboard was compared to the conversion factor calculated from single components at 12, 21, and 40 vol % oxygen. A significant difference between the measured and calculated conversion factor was only found at 40 vol % oxygen, when the measured conversion factor for the mixture was 10–20% lower than the calculated value. This indicates that temperature differences and the contribution of thermal NO mainly cause the differences.

The comparison of the conversion factor for experiments on mixtures of paper/cardboard and plastics vs. the weighted sum of single components showed a higher conversion factor for the sum of single components at all oxygen concentrations, but especially with 40 vol % oxygen. The reason for this difference is mainly that the conditions for forming thermal NO from LDPE as a single component are less favorable when LDPE is part of the mixture, due to a lower flame temperature and a consequential decrease in thermal NO from LDPE in the mixture.

The Nordic Energy Research Programme is acknowledged for financial support, while the CHEC (Combustion and Harmful Emission Control) group at the Technical University of Denmark are acknowledged for making their laboratory facilities available and for technical support during this work.

REFERENCES

1. Pickens, R. D., *J. Hazardous Mater.* 47:201 (1996).
2. Patel, N. M., Wheeler, P., and Ohlsson, O., *Fluidised Bed Combustion of Municipal Solid Waste*, Status Report for the International Energy Agency, 1994.
3. Farrow, R. L., Fisk, G. A., Hartwig, C. M., Hurt, R. H., Ringland, J. T., and Swansiger, W. A., *Technical*

Resource Document for Assured Thermal Processing of Wastes, Report No. SAND94-8240 UC-1414, Sandia National Laboratory, USA, 1994, p. 117.
4. Sandgren, J., Heie, Aa., and Sverud, T., *Emissions from Waste Management of Municipal Solid Waste*, Report 96:16, Norwegian Pollution Control Authority, Norway, 1996, (in Norwegian).
5. Tillman, D. A., *The Combustion of Solid Fuels & Wastes*, Academic Press, New York, 1991.
6. Rydholm, S. A., *Pulping Processes*, Interscience Publishers, New York, 1965.
7. Aho, M. J., Hämäläinen, J. P., and Tummavuori, J. L., *Combust. Flame* 95:22–30 (1993).
8. Bowman, C. T., *Proc. Comb. Inst.* 24:859–878 (1992).
9. Abbas, T., Costen, P., and Lockwood, F. C., *A Review of Current NOx Control Methodologies for the Municipal Solid Waste Combustion Process*, 4th European Conference on Industrial Furnaces and Boilers, 1997.
10. Brydson, J. A., in *Plastics Materials*, Butterworth-Heinemann Ltd., Oxford, UK, 1995, p. 317.
11. Franklin, M. A., *Characterisation of Municipal Solid Waste in the United States 1960–2000 (Update 1988)*, Report No. PB88-232780, Franklin Associates Ltd., USA, 1988.
12. Kauffman, C. R., *Wastetech '91: Canadian Waste Management Conference*, Toronto, 1991, pp. 1–13.
13. Skreiberg, Ø., Glarborg, P., Jensen, A., and Dam-Johansen, K., *Fuel* 76:671–682 (1997).
14. Rigo, H. G., and Chandler, A. J., *Proceedings of the National Waste Processing Conference*, ASME, 1994, pp. 49–63.
15. Mori, H., Asami, K., and Ohtsuka, Y., *Energy Fuels* 10:1022–1027 (1996).
16. Turns, S. R., *An Introduction to Combustion—Concepts and Applications*, McGraw-Hill, Singapore, 1996, p. 143.
17. Linak, W. P., and Wendt, J. O. L., *Combust. Sci. Technol.* 115:69–82 (1996).
18. Yang, M. H., Hamins, A., and Puri, I. K., *Combust. Flame* 98:107–122 (1994).
19. Roesler, J. F., Yetter, R. A., and Dryer, F. L., *Combust. Flame* 100:495–504 (1995).
20. Roesler, J. F., Yetter, R. A., and Dryer, F. L., *Combust. Sci. Technol.* 120:11–37 (1996).
21. Skreiberg, Ø., Hustad, J. E., and Karlsvik, E., in *Developments in Thermochemical Biomass Conversion* (Bridgewater and Boocock, Eds.), Blackie Academic & Professional, 1997.
22. Kee, R. J., Rupley, F. M., Meeks, E., and Miller, J. A., *CHEMKIN III: A Fortran Chemical Kinetics Package for the Analysis of Gas-Phase Chemical and Plasma Kinetics*, Report No. SAND96-8216, Sandia National Laboratories, USA, 1996.
23. Westerhout, R. W. J., Waanders, J., Kuipers, J. A. M., and Swaaij, P. M., *Ind. Eng. Chem. Res.* 37:2293–2300 (1998).
24. Helt, J. E., Agrawal, R. K., and Myles, K. M., *Pyrolysis of Municipal Solid Waste*, Report No. ANL/CNSV-54 DE87 002352, Argonne National Laboratory, USA, 1985.
25. Necker, P., *Überblick über die NOx-Minderungsmassnamen in Europa*, Proceedings of NOx-Symposium Karlsruhe, Universität Karlsruhe, D1/D44, 1985.
26. Lutz, A. E., Kee, R. J., Grcar, J. F., and Rupley, F. M., *OPPDIF: A Fortran Program for Computing Opposed-Flow Diffusion Flames*, Report No. SAND96-8243, Sandia National Laboratories, 1997.
27. Hamins, A., and Seshadri, K., *Proc. Comb. Inst.* 20: 1905–1913 (1984).
28. Dixon-Lewis, G., and Missaghi, M., *Proc. Comb. Inst.* 22:1461–1470 (1988).
29. Tanoff, M. A., Smooke, M. D., Osborne, R. J., Brown, T. M., and Pitz, R. W., *Proc. Comb. Inst.* 26:1121–1128 (1996).
30. Bloor, M. I. G., David, T., Dixon-Lewis, G., and Gaskell, P. H., *Proc. Comb. Inst.* 21:1501–1509 (1986).
31. Smooke, M. D., Puri, I. K., and Seshadri, K., *Proc. Comb. Inst.* 21:1783–1792 (1986).
32. Dixon-Lewis, G., David, T., Gaskell, P. H., Fukutani, S., Jinno, H., Miller, J. A., Kee, R. J., Smooke, M. D., Peters, N., Effelsberg, E., Warnatz, J., and Behrendt, F., *Proc. Comb. Inst.* 20:1893–1904 (1984).
33. Papas, P., Glassman, I., and Law, C. K., *Proc. Comb. Inst.* 25:1333–1339 (1994).
34. Brown, T. M., Tanoff, M. A., Osborne, R. J., Pitz, R. W., and Smooke, M. D., *Combust. Sci. Technol.* 129:71–88 (1997).
35. Drake, M. C., and Blint, R. J., *Combust. Flame* 83:185–203 (1991).
36. Nishioka, M., Kondoh, Y., and Takeno, T., *Proc. Comb. Inst.* 26:2139–2145 (1996).
37. Nishioka, M., Nakagawa, S., Ishikawa, Y., and Takeno, T., *Combust. Flame* 98:127–138 (1994).
38. Turns, S. R., *Prog. Energy Combust. Sci.* 21:361–385 (1995).
39. Glarborg, P., Alzueta, M. U., Miller, J. A., and Dam-Johansen, K., *Combust. Flame* 115:1–27 (1998).
40. Hämäläinen, J. P., Aho, M. J., and Tummavuori, J. L., *Fuel* 73:1894–1898 (1994).
41. Aho, M. J., Hämäläinen, J. P., and Tummavuori, J. L., *Combust. Flame* 95:22–30 (1993).
42. Leppälahti, J., *Fuel* 74:1363–1368 (1995).
43. Johnsson, J. E., *Fuel* 73:1398–1415 (1994).
44. Miller, J. A., and Bowman, C. T., *Prog. Energy Combust. Sci.* 15:295 (1989).
45. Takeno, T., and Nishioka, M., *Combust. Flame* 92:465–468 (1993).

Received 5 January 2000; revised 5 July 2000; accepted 15 August 2000.

4 The fate of heavy metals in MSW combustion

4.1 Introduction

This section will give a short introduction to mechanisms related to heavy metal behaviour in grate fired systems for MSW and the use of global equilibrium analysis (GEA) in such systems.

4.1.1 Heavy metal mechanisms in MSW combustion

Mechanisms related to the behaviour of heavy metals in MSW combustion in a grate fired unit is shown in Figure 4.1. Heavy metals are usually present in MSW as inorganic compounds. Many of these compounds are not affected by the combustion environment and pass through the incinerator unchanged in the bottom ash. The combustion air (usually fed to the incinerator through the grate) will entrain a fraction of the smaller ash particles while the remaining material is removed from the combustion chamber as residual ash. The quantity of material entrained is a function of the size, shape, and density of the ash particles as well as the incinerator operating conditions.

Some metals and metal species found in the waste materials are volatile and vaporise under the conditions that occur near the burning waste. The vaporised heavy metals diffuse into the flue gas stream, which then carries them through the incinerator system. As the flue gas is cooled, the vapours condense both homogeneously (also called *nucleation*, i.e. formation of new particles directly from the gas phase) to form new particles and heterogeneously on the surfaces of the entrained ash particles (also called *condensation,* i.e. particle growth caused by mass transfer from the gas phase to an existing condensed phase).

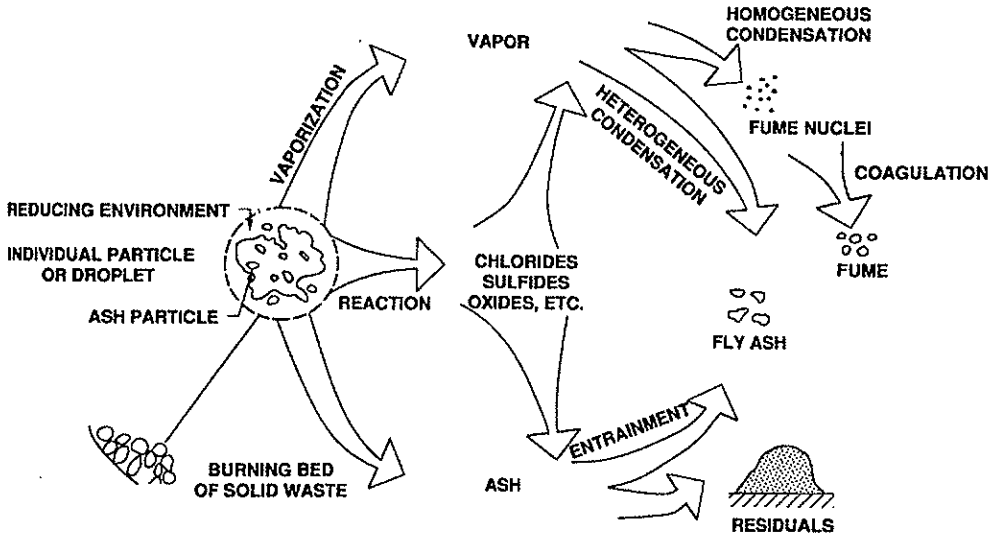

Figure 4.1 Mechanisms of heavy metals during combustion of waste in a grate fired unit[1].

Homogeneous condensation produces particles typically less than 1 μm in diameter. Heterogeneous condensation also tends to favour small particles due to their high surface area to weight ratio. Thus, the small, entrained particles have higher concentration of volatile metals than the original waste. Particle growth due to particle adhesion or agglomeration, i.e. changing the particle size distribution, while conserving the total volume (or mass) of particles is called *coagulation.* Metal containing materials may react in the waste combustion system. Two types of reactions have been observed. In the first type, reactive elements released during the combustion of organic materials in the waste combine with the metals. Chlorine is the most common of these reactive constituents. The second class of reactions occurs because of the formation of a high temperature, reducing environment near the burning waste. A reducing environment may be formed in nearly all waste combustion systems although the incinerator may be operated at overall excess air conditions. The reactions principally involve the reduction of metal oxides. The newly formed compounds often volatilise more readily than the original species. Once the vapours diffuse away from the waste and encounter lower temperatures

and higher oxygen concentrations, they undergo secondary reactions, convert back to their original, more refractory forms and condense. Both homogeneous and heterogeneous condensation occurs[1-2].

Barton et. al.[1] identified several parameters that influence the partitioning of heavy metals in MSW combustion systems. Parameters found to have a strong impact on heavy metal partitioning were:

- Furnace temperature
- MSW chlorine content
- Flue gas cleaning system operation

Other parameters predicted to have a weaker impact on heavy metal behaviour were:

- MSW sulphur content
- Gas residence time
- Entrained particle size distribution
- Local oxygen concentration
- Concentration of entrained particles
- Gas cooling rate
- Specific flue gas cleaning device operating parameters

4.1.2 Global equilibrium analysis (GEA)

Global equilibrium analysis uses the word global, because only global parameters such as pressure, temperature and total composition are taken into account – no local conditions (e.g. pressure or temperature gradients), are considered. The system is at its final state, where all possible reactions – homogeneous and heterogeneous – have reached equilibrium[3]. Thus, the actual combustion system

considered is regarded as an equilibrium reactor at known temperature and pressure, as shown in Figure 4.2.

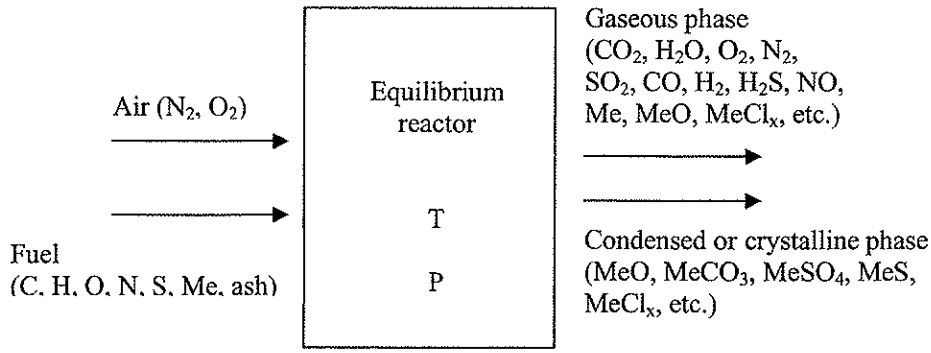

Figure 4.2 The system approach in Global Equilibrium Analysis. Me denote a metal[4].

Determination of the composition of a multiphase multicomponent system is performed, by minimising the total content of Gibbs free energy in the system. The Gibbs free energy is, under the conditions of constant absolute temperature (T) and pressure (P), given as:

$$\frac{G^t}{R \cdot T} = \sum_{i=1}^{N} n_i \cdot \left(\frac{G_{fi}^o}{R \cdot T} + \ln(a_i) \right) \qquad (4.1)$$

In eq. (4.1), G symbolises a Gibbs energy, superscript t denotes total, R is the universal gas constant, n_i is the number of moles of component i, a_i is the activity of component i, subscript f_i denotes formation of component i and N is the total number of chemical species.

As an illustration, the total Gibbs free energy for a gas phase containing N chemical species may, under the conditions of constant T and P, be written as[3]:

$$(G')_{T,P} = G(n_1, n_2, ..., n_N) \qquad (4.2)$$

where n_i is the number of moles of the *i'th* component in the gasphase. The equilibrium composition of the gasphase is determined by a set of n_i – values ($\underline{n}$) that minimises the function G^t, within the constraints of the mass-balances of the system.

To perform a GEA the total composition of the system must be specified in addition to the temperature, the pressure and a list of chemical species possibly present in the system (see Figure 4.2).

In the present work the total composition of the system with respect to the main elements – C, O, H, S and N – is determined by specifying a fuel and an air excess number (λ).

For a fuel with the general main component molar composition $C_\alpha H_\beta S_\gamma N_\delta O_\varphi.(H_2O)_\mu$ the stoichiometric reaction between the fuel and oxygen from the air is given by equation (4.3):

$$C_\alpha H_\beta S_\gamma N_\delta O_\varphi.(H_2O)_\mu \text{ (cr)} + (\alpha+\beta/4+\gamma+\delta/2-\varphi/2)O_2 \text{ (g)} \rightarrow \alpha CO_2 \text{ (g)} + (\beta/2+\mu)H_2O \text{ (g)} + \gamma SO_2 \text{ (g)} + \delta NO \text{ (g)} \qquad (4.3)$$

assuming all nitrogen in the fuel converted to nitric oxide. (g) denotes gas phase and (cr) denotes the crystalline state.

The stoichiometric air requirement is given by:

$$L_{min} = \frac{\alpha + \frac{\beta}{4} + \gamma + \frac{\delta}{2} - \frac{\varphi}{2}}{Y^{I}(O_2)} \qquad (4.4)$$

In eq. (4.4), $Y^{I}(O_2)$ is the mole fraction of oxygen in air. Finally the air excess number (λ) is defined by:

$$\lambda = \frac{L}{L_{min}} \qquad (4.5)$$

L is the actual air supply in eq. (4.5).

When used on combustion systems GEA has several limitations:

- In low temperature (T<800 K) zones of the combustion system (e.g. around the electrostatic precipitator), the reactions rates may be too slow to reach equilibrium, even for long residence times.

- In the furnace (flame) zone, mixing phenomena may introduce local conditions, e.g. temperature and/or composition gradients, not taken into account in GEA.

- Phenomena like adsorption, chemisorption (to take up and chemically bind a substance onto the surface of another substance) and capillary condensation (e.g. condensation in a capillary structure of fly ash) are not taken into account in GEA.

- All relevant chemical species occurring in the real combustion system must be taken into account, otherwise the output from the GEA may be misleading.

Thus when used on real combustion systems, care must be taken when interpreting the results of GEA.

4.2 References

1 Barton, R. G, Clark, W. D. and Seeker, W. R., *Comb. Sci. and Tech.*, **74**, pp. 327-342, 1990.

2 Linak, W. P. and Wendt, J. O. L., *Prog. Energy Combust. Sci.*, **19**, pp. 145-185, 1993.

3 Frandsen, F. J., Phd Thesis, Technical University of Denmark, Department of Chemical Engineering, 1995

4 Backman, R., Nordic Phd Course on Equilibrium Chemistry in Combustion Systems, Aabo Academy University, Aabo, Finland, Sept, 1992.

4.3 Paper III

Heavy Metal Partitioning

in a

Municipal Solid Waste Incinerator

Authors:

Lars Sørum*, Morten Fossum**, Egil Evensen*** and Johan E. Hustad*

*Norwegian University of Science & Technology, Institute of Thermal Energy and Hydropower

**SINTEF Energy Research, Department of Thermal Energy

*** Trondheim Energy Board, Department of District Heating

Paper presented at and in the Proceedings of the *Fifth Annual North American Waste to Energy Conference*, Research Triangle Park, North Carolina, April 22-25, 1997.

INTRODUCTION

Waste Management in Norway

Norway has the following priorities for management of municipal solid waste (MSW)[1]:

1) Reduce waste generation and toxic components in waste
2) Encourage re-use, recycling and energy recovery
3) Secure an environmentally safe management of residues

MSW consists of household waste and waste from the service and trade industry delivered to municipal waste treatment plants or recycling schemes. In 1995, a total of 2.7 million tons of MSW (1.26 million tons of household waste and 1.44 million tons of waste from service and trade industry) was handled as follows[2]: 68% was deposited on landfills, 18% was combusted, 13% recycled and 1% composted. Combustion of MSW is handled in five larger plants with energy recovery located in different cities in Norway. In addition, a new incinerator for MSW is planned. This incinerator will have to meet the new emission regulations given by the European Union which are more stringent than the present regulations. Hence, Norway is moving towards more stringent regulations, leading to an increased interest in the environmental aspects of MSW incinerators.

Heimdal Heating Central (HHC)

One of the largest MSW incinerators in Norway is situated in Trondheim and is owned and operated by Trondheim Energy Company (TEV). HHC consists of two lines each with a maximum capacity of 6.5 tonne/hour. The furnaces are moving grate units delivered by VonRoll, Switzerland. The flue gas cleaning system consists of an electrostatic precipitator (ESP) and a wet scrubber. The MSW incinerator is a base load energy production unit in a district heating system. In

1996, a total of 85600 tonne of MSW was incinerated in this plant with a heat production equivalent to 222 GWh. Figure 1 show a sketch of the incinerator.

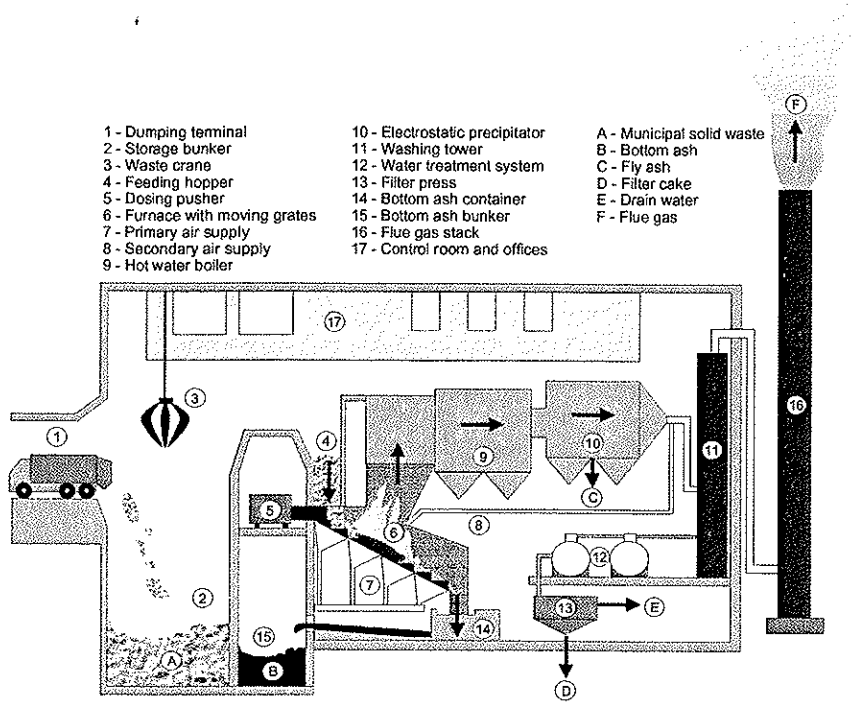

Figure 1. Sketch of the waste incinerator with major parts and mass fluxes indicated.

The MSW is delivered by trucks to a bunker for storage and mixing. The waste is collected from the bunker and into the feeding hopper by a waste crane. The waste is fed to the furnace by a dosing pusher. While the waste is transported through the furnace by a moving grate, primary air is supplied for combustion from below the grates and from the side walls. The sidewalls are cooled and insulated with refractory. Recirculated flue gas is injected into the flame above the grate before the flue gas enters the secondary combustion chamber. The flue gas first flows through a hot water generator and the ESP, which removes dust particles, before it

enters the wet scrubber. In the wet scrubber, the flue gas pass through a quencher which reduces the temperature before it enters the wet scrubber where most of the pollutants in gas phase are removed. The water from the scrubber is first treated in a neutralization tank and then in a flocculation tank where particles are separated from the scrubber water. Then the scrubber water passes a sediment reactor where the solid phase is collected in the bottom. The solid phase is transported to a filter press where filter cakes are made. The water from the cleaning process is filtered in a sand filter and a ion exchanger system, before it goes to the drain. The clean flue gas is emitted through the 70 meter high stack. The bottom ash is deposited on a landfill, while the ESP dust and filter cakes are deposited in a landfill as hazardous waste.

Objective of the project

During 1995, TEV carried out an investigation program to examine the residues from the incinerator. Primary attention was on the heavy metals in the bottom ash, fly ash and the landfill leachate. The program was conducted in order to establish more information about characteristics of the residues and thus be able to undertake a sounder evaluation of the environmental aspects of the final treatment of these products. This program was supplementary to the emission analysis done periodically for the flue gas and drain water. The objective of this work has been to establish knowledge about the partitioning of heavy metals through the incinerator and calculate the concentrations of heavy metal in the input MSW. A comparison of the results obtained from this study with other studies such as the WASTE Program (Burnaby)[3] and Brunner/Mönch[4] is of interest to see equalities and differences in the heavy metal partitioning through the incinerator and also the estimated heavy metal concentrations of the input MSW. All of the three different MSW incinerators (HHC, Burnaby, Brunner/Mönch) have similar furnaces (moving grate), but different cleaning systems.

Heavy metal characteristics

Heavy metals are environmental toxics which accumulates in the environment. Heavy metals do not break down, but will remain in the environment forever. Cadmium, lead, mercury, vanadium, chromium, nickel, copper, zinc and arsenic are the most important heavy metals found in emissions from combustion of MSW. Cadmium, lead and mercury got most attention due to their relative toxicity[5,6]. Some of the heavy metals, especially cadmium, can deposit in the soil and be absorbed by plants. Mercury can be transformed into methyl mercury in sediments and be accumulated in the food chain, especially through fresh water. Excessive levels of heavy metals can provoke a number of health effects. Excessive amounts of lead and mercury are especially dangerous with regards to damage to the nervous system and fetal life. Lead can also give cardiovascular diseases and anaemia. Excessive amounts of cadmium can damage the kidney after long term exposure and accumulating in the body[6,7]. In order to reduce emissions of heavy metals and other pollutant emissions, the Norwegian government has signed several agreements, both national and international, which have the aim of reducing emissions in the future. For example: the Parliament report on national reduction of 70% of 13 selected environmental toxics, the North Sea Declaration states that the emission of 40 selected substances to both air and water shall be reduced and the Montreal Protocol include reduction of ozone destructive substances.

EXPERIMENTAL METHODS AND PROCEDURES

The experiments performed during this investigation were mainly conducted in 1995 and 1996. The input MSW has the average composition given in Table 1[9].

Table 1. Average composition of MSW delivered to HHC[9].

COMPONENT	FRACTION [wt%]
Paper	30
Food wastes	17
Plastic, textiles,rubber, leather	6
Wood	8
Glass	7
Metal	12
Other combustibles	6
Other non-combustibles	14
Total	**100**

The waste originates from the urban and rural areas in and around Trondheim municipality. The degree of material recovery of different components is estimated to[9]: paper 35%, food waste 22%, plastic/textiles/rubber 11%, glass 25%, metals 63% and other non-combustibles 50%. The total material recovery rate from MSW is estimated to 30%. In the sections below, a description of the sampling and experimental methods and procedures are explained.

Mass Balance

In this study the mass balance has been established for bottom ash, filter ash and filter cake. All of the values are mean values taken over a whole year and are on a dry basis.

All of the MSW delivered to the incinerator is weighed before dumped into the waste bunker. The weight of the waste is continuously recorded every year. The bottom ash, filter ash (ESP dust) and filter cakes are always weighed (on a wet basis) before sent to the landfill. However, the average moisture content has been determined for each of the different residues. All residues were expressed on a dry basis for the mass balance. The amount of flue gas has been calculated by measuring the flow through the stack with a pitot tube and micromanometer according to the Norwegian standard method (NS 4862). All of the moisture from the input waste was considered leaving with the flue gas.

Chemical Analysis

Chemical analysis of the different waste streams have been done according to different standard tests methods. The heavy metals presented in this investigation is mercury (Hg), zinc (Zn), chromium (Cr), cadmium (Cd), lead (Pb) and iron (Fe). Some of the residues and the flue gas has also been analysed for other heavy metals such as arsenic (As), nickel (Ni) and copper (Cu).

Bottom ash. For ten weeks samples were taken every Monday, Wednesday and Friday. The samples were taken from the bottom ash conveyor belt with a spade. Particles larger than 50 mm were sieved out and magnetic metals were removed with a magnet. Other easy visible pieces of metal was also picked out. The samples were air dried for 70 hours at 20°C before shipment to the laboratory, in order to enable crushing of the ash before analysis. Every sampling day six samples, each of approximately 2 kg, were taken with 1-1.5 hours intervals. The samples from one day were mixed and split into two parts and a sample of approximately 4 kg was sent to the laboratory for chemical analysis and another sample was analyzed for grain size distribution. The samples were sent to a certified laboratory in The Netherlands, Tauw Milieu bv, and the chemical analysis was done according to the standard test method ICP NPR 6425 for cadmium, chromium, lead and zinc; mercury was determined by the Cold Vapour-method NEN 5779. Full details of the chemical analysis of bottom ash are given in the report from Kummeneje[10].

The amount of iron in the bottom ash was determined by sieving and magnet separation test in a pilot plant with a capacity of 36 tons/hour[11]. Approximately six tons of bottom ash was handled in the sieving/magnet separation test. The bottom ash was first sieved on 50 mm sieve and this fraction was put through the magnet separator to determine the magnetic fraction. The rest fraction after sieving (<50 mm) was also separated for magnetic materials in the same system. The total amount of magnetic materials from the magnetic separation test was considered as iron.

Filter Ash. Samples of approximately 2 kg were taken once a week for three weeks. The samples were taken in the intermediate container below the conveyor belt from the filter ash bin. The samples were stored in plastic bags just above room temperature in order to prevent interaction with the surroundings before shipment to the laboratory. The laboratory, Tauw Milieu bv in The Netherlands, is certified for these chemical analysis. ICP-method NPR 6425 was used to determine the content of cadmium, chromium, iron, lead and zinc. The Cold Vapour-method NEN 5779 was used to determine the content of mercury. Full description of these chemical analysis of the filter ash is given in the report by Kummeneje[12].

Filter Cakes. Some samples of the filter cakes from the washing process were analyzed with Atom Absorption Spectrophotometry (AAS) to determine the content of lead, zinc and chromium [13]. Iron was estimated from values found in the literature. The content of mercury and cadmium was determined by measuring the difference in concentration in the water before and after the water cleaning process. For a whole year one sample was taken every day and all of the samples from one week were put together and analysed. The NS4768 and NS4781 methods were used to determine the content of mercury and cadmium in the samples.

Drain Water. The drain water has been analyzed for mercury, cadmium and lead according to Norwegian standard methods NS4768, NS4781 and NS4781. The amount of iron, zinc and chromium was estimated on the basis of values found in the literature.

Flue Gas. The Norwegian standard method NS 4863 was used to determine the content of lead, cadmium, mercury and chromium in the flue gas. The procedure is described in a SINTEF report[14]. The content of iron and zinc was estimated on basis of values found in the literature. Four samples of the flue gas were taken for chemical analysis.

Sources of error in mass balances

In addition to the usual measurement inaccuracy's connected to every measurement done in this investigation, the closure of the mass balance also represent a source of error. Since the measurement inaccuracy's are given by the standarized measurement methods, those will not be commented on further. However, the mass balance closure need further explanation. The examination of the bottom ash, filter ash, filter cakes, drain water and flue gas has served different purposes. In addition to the determination of heavy metal balances and concentrations in input MSW, determination of heavy metal concentrations in residues and flue gas with regards to soil, water and air pollution has been one of TEV's objectives with these investigations. All of the measurements used in the mass balances has, therefore not been performed within the same period of time and with different sampling rates. However, this investigation has tried to give relatively long term mass balances and determined the concentrations of heavy metals in input MSW on basis of these findings. Short term investigations within the same time period has both the advantages and disadvantages of stable conditions with regards to operational parameters and composition of input MSW. The closure of the mass balances is therefore more likely to happen in investigations with parallel sampling of the residues and flue gas rather than sampling in series. However, the heavy metal balances and concentrations in input MSW is also a function of the variations in operational conditions and composition of input MSW. More extensive investigations with sampling in parallel would be very interesting and would provide a more complete picture of the mass balances and concentrations of heavy metals in input MSW. The cost of such comprehensive measurements is one of the major problems.

HEAVY METAL PARTITIONING THROUGH THE INCINERATOR

The results of the mass balance, heavy metal partitioning through the incinerator, heavy metal content in the residues and flue gas are presented in the sections

below. Further, calculated heavy metal concentrations in the input MSW on the basis of the heavy metal content of the residues and flue gas are presented.

Mass Balance

The result of the mass balance is given in figure 2. The figure show that 83 % of the input MSW is converted to CO_2 and H_2O and is emitted as moist flue gas. The mass flux of bottom ash was found to be 16.5 % and the mass flux of filter ash was 0.37 %. The dust found in the filter cakes was almost negligible (0.02%). Brunner and Mönch[4] found in their investigation a bottom ash portion of 20.5% and a flue gas portion of 77%. The flux of filter ash was the same as this study.

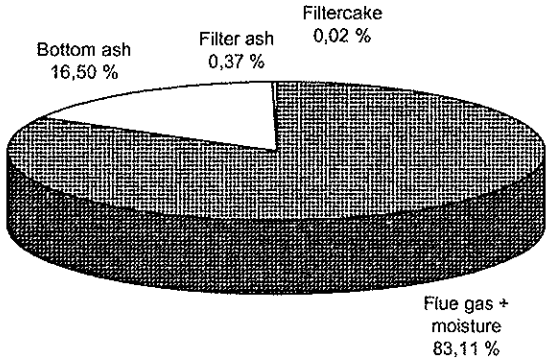

Figure 2. Overall mass balance for the MSW incinerator (dry basis).

Heavy Metal Balance

Figure 3 and table 2 show the heavy metal balance between the different residues and flue gas for the incinerator.

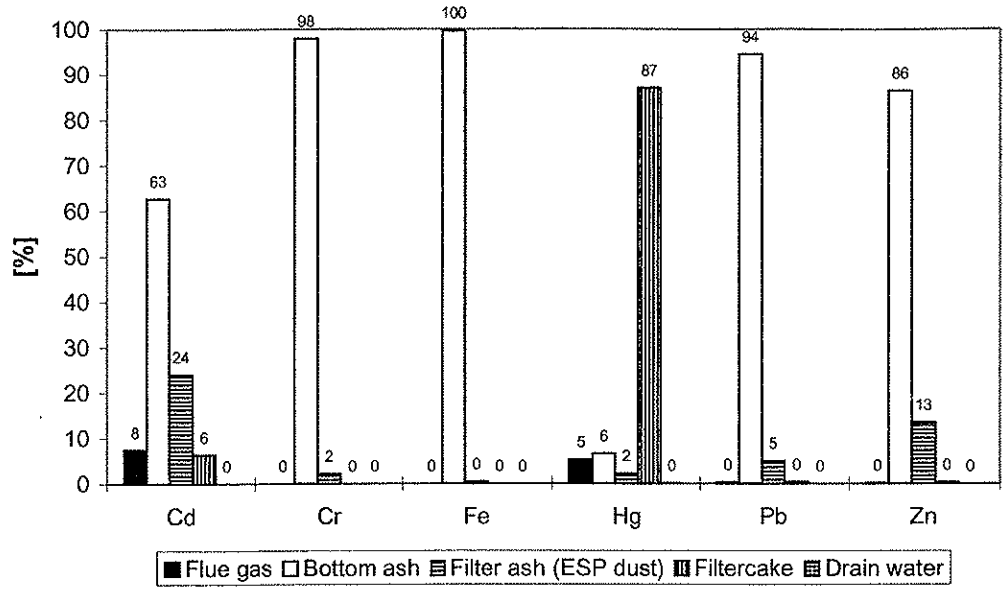

Figure 3. Heavy metal balances for the MSW incinerator.

Table 2. Concentrations in residues, flue gas and waste and heavy metal balance.

	Cd	Cr	Fe	Hg	Pb	Zn
Concentration in residues, flue gas and waste						
Flue gas [mg/Nm^3 dry]@11%O_2	0.057	0.00075	0	0.013	0.162	0.159
Bottom ash [mg/kg dry]	19	125	53250	0.62	2513	5464
Filter ash [mg/kg dry]	323	127	9833	8	5833	37667
Filtercake [mg/kg dry]	1331	10	2600	5805	7027	8567
Drain water [Tg/m^3]	1.3	0.9	0	3.6	48.1	100
Input MSW [mg/kg]	5	21.1	8823	1.6	439	1044
Heavy metal balance for the combustion plant						
Flue gas [kg/year]	32.7	0.44	0	7.2	91.8	76.3
Bottom ash [kg/year]	272	1788	761768	9	35950	78165
Filter ash [kg/year]	104	41	3154	3	1871	12083
Filtercakes [kg/year]	27.7	0.2	54.1	120.8	146.2	178.3
Drain water [kg/year]	0.02	0.02	0	0.06	0.83	1.7
Input MSW [kg/year]	434	1829	764954	139	38061	90515

Cadmium (Cd). Cadmium is a quite volatile metal in a combustion context with a boiling point of 767°C. Figure 3 show that 63% of the cadmium remain in the bottom ash, 24% is captured in the filter ash, 8% is emitted with the flue gas, 6% is captured in the scrubber (filter cakes) and virtually nothing is emitted via the drain water. In this study 37% of the cadmium was evaporated from the combustion process and entered the flue gas cleaning system. Several other studies on the evaporation of cadmium from MSW incinerators have been done and they have shown quite different results. The Brunner and Mönch[4] investigation stated that only 12% of the cadmium remained in the bottom ash, while the Burnaby project[3] could report an even lower content of cadmium in the bottom ash (3.7%). A Swedish investigation[15] of four different MSW incinerators found large variations in cadmium remaining in the bottom ash, varying from 13 to 83%. These large variations can originate from two different important parameters, namely combustion temperature and chlorine content in the waste. Cadmium has a boiling point which is close to the combustion temperature and the content of cadmium in the bottom ash will be dependent on the operating furnace temperature. The operating furnace temperature is a parameter which is strongly dependent on furnace construction, MSW composition and fuel/air ratio. Of these parameters the fuel/air ratio is the easiest to control. Two important factors in the evaporation of cadmium are: chlorine available to form cadmium-chloride and the chemical form of cadmium. With chlorine present, cadmium can form relatively volatile chlorides that will follow the hot flue gases[16]. When the temperature drops, volatile cadmium adsorbs on the relatively small particles which have the largest surface area. The emission of cadmium will therefore be highly dependent on the efficiency of the flue gas cleaning system and it's ability to capture particle emissions.

Table 2 shows the heavy metal balance, the estimated heavy metal content in input MSW and concentrations of heavy metals for the different residues and the flue gas. The total yearly input of cadmium for the incinerator is 434 kg and 33 kg is leaving with the flue gas. The total efficiency of the flue gas cleaning system

regarding cadmium is 80% (63% in ESP and 17% in scrubber) in this study. The Burnaby study[3] which had a flue gas cleaning system consisting of a conditioning tower, reactor with lime injection and fabric filter showed an efficiency of 99.8% for cadmium. The Brunner and Mönch[4] study which only had a electrostatic precipitator as flue gas cleaning system had an efficiency factor of 86% for cadmium.

Of the heavy metals in this investigation, cadmium is the one with the highest portion emitted through the stack. The calculated cadmium concentration in MSW was 5 mg/kg. The calculated cadmium concentration in MSW in the Burnaby project[3] was 13.5 mg/kg while Brunner and Mönch[4] reported 8.7 mg/kg. The city of Trondheim is currently implementing a source separation system where environmentally harmful waste such as electrical and electronic waste is separated and sent to a special landfill site for hazardous waste. A study has shown that electrical and electronic waste contributes with a large fraction of cadmium in MSW[17]. The effect of separating this fraction from the input MSW will be followed with great interest.

Chromium (Cr). Chromium with a boiling point of 2672°C can be regarded as a non-volatile heavy metal from a MSW combustion point of view. This is also shown by the results of the heavy metal balance for the combustion plant (table 2). Of the total input of 1829 kg/year to the incinerator, nothing is emitted through the stack. Approximately 2% is captured in the flue gas cleaning system the rest is left in the bottom ash. The Burnaby study reported that 93% of the chromium was left in the bottom ash. Only 0.06% was emitted with the flue gas, the rest was captured in the flue gas cleaning system. Calculated concentration of chromium in MSW is 21.1 mg/kg. The Burnaby project[3] calculated the chromium concentration in MSW to 92.5 mg/kg.

Iron (Fe). Like chromium iron can be regarded as a non-volatile heavy metal in MSW combustion, with a boiling point of 2750°C. From the input of 764954 kg/year virtually nothing is emitted through stack or drain water, 0.4% is captured in the flue gas cleaning system while the rest is found in the bottom ash. Brunner and Mönch[4] found in their study 99% of the iron in the bottom ash and 1% in the filter ash, while 0.02% were stack emissions. Calculated iron concentration in MSW in this study was 8823 mg/kg.

Mercury (Hg). Mercury is the most volatile of the heavy metals with a boiling point of 357°C. The volatile behaviour of mercury was confirmed in this study with only 6% remaining in the bottom ash. Mercury content in the bottom ash between 0.2-19% has been found in other studies[3,4,15]. Mercury differs from the other heavy metals by the fact that it is in gas-phase in a combustion plant[16]. Mercury is converted to a gaseous metal and gaseous chloride salt in the combustion process. The flue gas cleaning system had an efficiency of 95% for mercury. The wet scrubber captured 92% of the volatile mercury. Brunner/ Mönch[4] had a mercury removal efficiency of 25% with electrostatic precipitator, while the Burnaby study[3] had an efficiency of 40% where practically all captured mercury was found in the fabric filter. The calculated concentration of mercury in MSW in this study was 1.6 mg/kg, which is exactly the same concentration as a similar mercury balance study gave in 1994[18]. Other studies have indicated mercury concentrations in the range of 0.7 - 1.5 mg/kg[3,4,19]. Given the volatile nature of mercury, emphasis should be put into removing mercury containing waste from the input MSW in order to reduce mercury emission to the environment. A study has shown that electrical and electronic waste contributes with a large fraction of mercury in MSW[17]. The potential for reduction of mercury entering the incinerator by removing the electrical and electronic waste fraction should therefore be considerable.

Lead (Pb). Lead, with a boiling point of 1750°C, should in combustion of MSW normally be considered as a non-volatile metal. However, studies have shown that

small portions of chlorine in the waste will decrease the volatility temperature with several hundred degrees[20]. From the total of 38061 kg/year input of lead to the incinerator, 94% is captured in the bottom ash, 5% is captured in the flue gas cleaning system and 0.2% is stack emission. Other studies have shown a large variation of lead in the bottom ash ranging from 58 to 89%[3,4,15]. This and other studies have shown that most of the volatile part of lead is captured on ash particles and cleaned in the filter units. The calculated concentration of lead in MSW was 439 mg/kg. Other studies have reported values in the range of 160 to 430 mg/kg[3,4,19]. As for cadmium and mercury, lead is also strongly represented in the older electronic and electrical waste fraction although not relatively as much as mercury and cadmium. The combination lead and PVC (resin PVC contains over 50% of chlorine[21]) is highly possible for the electronic and electrical waste fraction, giving an increase in the volatile release of lead in the combustion process.

Zinc (Zn). Zinc, with a boiling point of 907°C, is one of the more volatile metals in this investigation. Zinc is also the heavy metal with largest yearly stack emissions (76 kg/year). Most of the zinc was found in the bottom ash (86%), while most of the residual 14% is captured in the flue gas cleaning system. Only 0.1% is emitted through the stack. This study differ from other studies with a large portion of the zinc remaining in the bottom ash. Other studies[3,4] have reported 42 and 51% of zinc in the bottom ash, but like this study most of the volatile fraction of zinc is captured in the ESP. The large variation in volatility can be ascribed to differences in combustion temperature due to the relatively low boiling point which is in the area of the combustion temperature. The calculated concentration of zinc in MSW was 1044 mg/kg while others have reported 1873 and 2000 mg/kg[3,4].

CONCLUSIONS

In this study most of the cadmium (63%), zinc (86%), lead (94%), chromium (98%) and iron (100%) was found in the bottom ash. The filter ash captured most of the volatile cadmium (24%), zinc (13%), lead (5%) and chromium (2%). The wet scrubber captured most of the mercury (87%). From these results it is evident that a large portion of the heavy metals are captured in the bottom ash compared to other studies, indicating a relatively low combustion temperature. The calculated concentrations of heavy metal in the input MSW was 1.6 mg/kg for mercury, 5 mg/kg for cadmium, 1044 mg/kg for zinc, 439 mg/kg for lead, 21.1 mg/kg for chromium and 8823 mg/kg of iron. Long term monitoring of the flue gas and residues seem to be a better and easier way to measure the content of heavy metals in MSW rather than sampling the input waste. Reduction in heavy metal emissions is expected after implementation of source separation of environmental harmful waste including electronic and electrical waste in 1997. The potential for reduction of mercury is confirmed by the relatively high concentration in MSW compared to other studies. The continuing work on identifying and separation of MSW fractions with large concentrations of heavy metals seem to be an important method to reduce heavy metal emissions further. Improved flue gas cleaning systems, furnace constructions and combustion control will also contribute to reduced emissions. This work has contributed to a better understanding of the behaviour of heavy metals in MSW combustion and given complementary understanding of the efficiency of various flue gas cleaning systems for different heavy metals.

REFERENCES

1. Department of the Environment, Norwegian Parliament Statement No. 44 (1991-1992), Initiative for reduced waste amounts, increased recycling and a secure waste management, Department of the Environment, Oslo, 1992, p. 65 (in Norwegian).

2. Official Statistics of Norway, We are still producing more waste, Weekly Statistics No. 39, Official Statistics of Norway, Kongsvinger, 1996, p. 4 (in Norwegian).

3. The WASTE Program, Waste Analysis, Sampling, Testing and Evaluation (WASTE Program): Effect of Waste Stream Characteristics on MSW Incineration: The Fate and Behaviour of Metals, Final report of the Mass Burn MSW Incineration Study (Burnaby, B.C.), Vol. 1, summary report, 1993, p. 76.

4. Brunner, P. H., Mönch, H., "The Flux of Metals Through Municipal Solid Waste Incinerators", Waste Management & Research, 4(1):105-119 (1986).

5. Scholdager, J., Air Pollution - Emission, Diffusion, Settling and Effects, Lecture Presentation in The Course Energy Technology at Norwegian University of Science and Technology (NTNU), Trondheim, 1990.

6. World Health Organization, Heavy Metal and PAH Compounds from Municipal Incinerators, Report from WHO Meeting Florence 12-16 oct. 1987, Copenhagen, 1988, p. 67.

7. Øverli, J.M., Energy and Environment - Global and International Challenges, Statoil, Environment Project Publication No. 2, Trondheim,1990, p. 31 (in Norwegian).

8. Berntsen, T., Environmental Political Statement - 1995, Department of the Environment, Oslo, 1995, p. 126 (in Norwegian).

9. Trondheim Municipality, Waste Management Plan for Trondheim Municipality 1996-1999, Trondheim, 1996, p. 107 (in Norwegian).

10. Gilde, T., Heimdal Varmesentral - Chemical Analysis of Slag - Results of Chemical Analysis of Slag and Leachate.Kummeneje a.s., Trondheim, 1995, p. 11 (in Norwegian).

11. Skjæveland, R., HVS-Waste Combustion - Characterization of slag with regards to separation of iron, preliminary experiments, Norwegian University of Science and Technology (NTNU) - Department of Geology and Rock and Mineral Engineering, Trondheim, 1996, p. 28 (in Norwegian).

12. Gilde, T., Heimdal Varmesentral - Chemical Analysis of Electrostatic Precipitator Dust - Results of Chemical Analysis of Filterdust and Leachate, Kummeneje a/s, Trondheim, 1995, p. 6 (in Norwegian).

13. Mathillas, F. R., Analysis and Characterization of filtercakes from the flue gas cleaning system of the waste combustion plant, Project work, Norwegian University of Science and Technology (NTNU) - Department of Geology and Rock and mineral Engineering, Trondheim, 1995, p. 36 (in Norwegian).

14. Horrigmo, W., Vassbotn, T., Flatberg, H., Emission Measurements at Heimdal Waste Incinerator 1995, STF84 F96402, SINTEF Energy, Department of Thermal Energy and Hydropower, Trondheim, 1995, p. 34 (in Norwegian).

15. Soma, M. H., What Kind of Emissions Do We Get from Waste Combustion, Technical Winterweek 1986, EG61b, The Association of Norwegian Chartered Engineers, Oslo, 1986, p. 31 (in Norwegian).

16. Benestad, C., Braastad, G., Normann, H. H., et. al., Combustion Plants - Instructions for Officials in Charge, 95:13, The Norwegian Environmental Protection Agency, Oslo, 1995, p. 86 (in Norwegian).

17. Department of the Environment, Collection and Treatment of Waste from Electrical and Electronic Products, T-1135 ISBN 82-457-0100-9, Department of the Environment, Oslo, 1996, p. 64 (in Norwegian).

18. Evensen, E., Assessment of the Mercury-Balance of the Combustion Plant, EE/EB/450, Trondheim Energy Board, Trondheim, 1995, p. 3 (in Norwegian).

19. Halmø, T., Solid Waste, Tapir, Trondheim, 1984, p. 316 (in Norwegian).

20. Federal Register, US EPA, Guidance on Metals and Hydrogen Chloride Controls for Hazardous Waste Incinerators, 1989.

21. C-H. Wu, C-Y. Chang, J-L. Hor, S-M. Shih, L-W. Chen, F-W. Chang, "On the Thermal Treatment of Plastic Mixtures of MSW: Pyrolysis Kinetics", Waste Management, 13:15 (1993).

4.4 Paper IV

Combustion of Municipal Solid Waste
—
Fate of Heavy Metals

Authors:

Lars Sørum*, Flemming J. Frandsen** and Johan E. Hustad*

*Norwegian University of Science & Technology,
Institute of Thermal Energy and Hydropower

** Technical University of Denmark,
Department of Chemical Engineering

Paper Submitted to the Scientific Journal ***Combustion Science & Technology***

ABSTRACT

The aim of this study has been to investigate the fate of the heavy metals As, Cd, Cr, Cu, Hg, Ni, Pb, and Zn in a grate furnace for combustion of MSW, from the combustion zone to the flue gas cleaning system, using equilibrium calculations. Focus has been on the influence of varying MSW composition and operational parameters such as fuel/air ratio and temperature. Equilibrium distributions at 950-1600 K, under reducing and oxidising conditions on the grate, showed that Cd, Hg and Pb are fully volatilised. However, Cr is found to be stable in solid phase, in the entire temperature range. The partitioning of Cd, Cr, Hg and Pb show no significant influence, while As, Cu, Ni and Zn are strongly influenced by one or more of the parameters; temperature, fuel/air and chlorine/metal ratios. The availability of sulphur and chlorine largely influenced the condensing behaviour and chemistry for many of the heavy metals as they follow the flue gas path from the furnace to the flue gas cleaning system. One important observation is the shift from solid phase chlorides to sulphates at temperatures below 900 K for Pb and Zn, when increasing the sulphur availability. Pb and Zn sulphates being less corrosive in boiler systems than the respective chlorides.

INTRODUCTION

The large amounts and inhomogeneous nature of municipal solid waste (MSW) combined with the awareness of environmental consequences connected to waste disposal have lead to development of complex waste management systems. Material reuse and recycling, anaerobic digestion, composting and combustion with energy recovery are some of the methods that are used in addition to landfills. Paper, plastics, wet organic waste (wood, grass, food wastes, etc.) are the major components of the combustible fraction of MSW. However, the composition of the waste subject to energy recovery can vary largely between countries and within each country depending on factors such as standard of living and waste management policy. This variation in composition of the fuel may influence the operational parameters of combustion plants and alter the formation and emission of pollutant species.

One of the challenges in MSW combustion is the emission of heavy metals. Heavy metals may be harmful to the environment and humans when exposed to concentrations above what can be found in the natural environment. From the work of Heie and Sørum (1997), Frandsen (1995) and Nussbaumer (1994), it is clear that the heavy metal concentration in MSW compared to other solid fuels such as biomass and coal is relatively high. In addition, the work of Clarke (1991), Sandgren and Heie (1996) and Rigo and Chandler (1994) shows that variations in heavy metal concentrations in MSW are large, also within each fraction of MSW. Heavy metals in MSW combustion may evaporate, react or show no response (Lee (1988)). In order to decrease emissions of heavy metal species to the environment from any of the mass flows from a combustion plant for MSW (i.e. flue gas, fly ash, bottom ash, etc.), knowledge is needed on the behaviour of heavy metals in the combustion zone on the grate and in the flue gas from the furnace to filter. The partitioning of the different heavy metals and the chemistry of the heavy metals bound in the ashes determines the concentration and the potential of leachability

when utilising the bottom or fly ash for other purposes than landfilling. Knowledge on the volatile and condensing behaviour of heavy metal species in a combustion plant is important in order to assess the emission potential of heavy metal species. Heavy metal species condensing on very small particles or aerosols, which typically are formed late in the cooling process of the flue gas, have a larger potential to escape through the stack as larger particles will be captured by the flue gas cleaning system (Obernberger (1998)). Research has also shown that certain heavy metal species such as lead and zinc chlorides are highly corrosive and therefore unwanted in the boiler system (Krause (1989)). A study performed by Ghorishi and Gullett (1997) showed that the knowledge of the chemical form of mercury, when entering the flue gas cleaning system is important, in order to chose the right sorbent for removal of mercury. Hence, there are several reasons why knowledge on the partitioning and chemistry of heavy metal species in MSW combustion plants are needed.

Several studies using equilibrium calculations to investigate the behaviour of heavy metals in combustion systems have been performed. Equilibrium analysis was used by Wu (1993) to determine the speciation of six metals during combustion of methane in air, doped with chlorine, at high temperatures. The effect of temperature and chlorine content was investigated. Verhulst (1996) studied the thermodynamic behaviour of metal chlorides and sulphates at typical conditions found in waste incineration furnaces. Frandsen et. al. (1994) performed an extensive review of the equilibrium distribution of a large number of metals at typical coal gasification and combustion conditions. Barton et. al. (1988) performed a sensitivity study on selected heavy metals (lead, zinc, copper, chromium and vanadium) investigating the influence of parameters such as temperature, chlorine content, sulphur content, residence time, entrained particle size distribution and saturation ratio (i.e. the ratio of the actual concentration to the equilibrium concentration in the vapour phase).

Common for all the above-mentioned work on equilibrium distribution of heavy metals in thermal fuel conversion systems is that no ash species are included. Ash species may interact chemically with heavy metals to form, for instance, silicates, aluminates and/or aluminosilicates and thereby influence the distribution and volatility of heavy metals in combustion of MSW. In addition, more knowledge and understanding of the distribution and chemical composition of heavy metals under the conditions of MSW combustion is needed. The objective of this study is therefore to investigate the influence of varying operational parameters and MSW compositions on the equilibrium distribution at typical combustion conditions in a grate furnace. Ash species are included to investigate possible interactions between heavy metals and ash species. Focus is on the influence of temperature, Cl/metal- and S/metal ratios, fly ash content and fuel/air ratio.

CALCULATION METHOD

The program MINGTSYS (Frandsen et. al. (1994)) was used for the global chemical equilibrium analyses. The program minimises the total Gibbs energy (G(T)) for a given system of selected species. Thermodynamic data were taken from the GFE-DBASE version 2.0. The Gibbs free energy function is defined as:

$$GFE_i(T) = -\left(\frac{G_i^0(T) - H_{298,i}^0}{T}\right) \qquad (1)$$

In Eq. 1, G_i^0 is the standard Gibbs free energy for component i, $H^0_{298,i}$ is the enthalpy at 298 K for component i and T is the temperature. GFE functional expressions (eq. (1)) are used to calculate G(T). Further documentation on the GFE-DBASE is described by Frandsen et. al. (CALPHAD 1996). Global equilibrium analysis (GEA) has several limitations when used on a combustion system. The residence time need to be long enough, or the temperature must be high enough, to ensure that all reactions reaches equilibrium. A turbulent flame

may introduce local conditions e.g. temperature and/or composition gradients which are not taken into account in a GEA. Physical adsorption, chemisorption and capillary condensation phenomena are not taken into account. No mixing models, in order to describe non-ideal behaviour between heavy metals and ash species, have been used in this study. The reason for not using an overall applicable mixing model that will give a description of how heavy metals and heavy metals and ash species mix is that at present no such model exists. In spite of the above-mentioned limitations, the method of determining stable phases, assuming global equilibrium, is at present the only computational possibility for generating knowledge about the chemistry of heavy metals in combustion systems. Another reason for using GEA on thermal conversion systems is the lack of kinetic data for heavy metal reactions. Few thermodynamic data are available for species containing more than one heavy metal. Verhulst (1996) and Ljung and Nordin (1997) showed that there were no interaction between arsenic (As), cadmium (Cd), chromium (Cr), copper (Cu), mercury (Hg), nickel (Ni), lead (Pb) and zinc (Zn). These are the same heavy metals as considered in this study, therefore, each heavy metal has been considered separately. Including all relevant species involved in the combustion process and using the best available thermodynamic data is important, otherwise the results may be misleading (Frandsen (1995)). Frandsen et. al. (1996) compared four different thermodynamic packages for calculation of equilibrium distribution for the oxidative thermal conversion of coal. The major differences between the four thermodynamic packages were caused by differences in the list of species included and in the thermodynamic data.

This study will focus on a comparison of *trends* observed from experimental investigations in literature with GEA on the volatile behaviour at the grate and condensation in the flue gas by performing a comprehensive parametric study. In addition, generating additional knowledge on heavy metal chemistry in MSW combustion is another important aspect of this work.

Species Included in Calculations

A comprehensive list of ash and heavy metal species and possible interactions between ash components and heavy metals are included in these investigations. Included are the heavy metals As, Cd, Cr, Cu, Hg, Ni, Pb, Zn and the ash species Aluminium (Al), Calcium (Ca), Iron (Fe) and Silicone (Si). The eight heavy metals included in this study are the same which are subjected to emission restrictions as given by the Norwegian Pollution Control Authority on MSW combustion (Benestad et. al. (1995), with the exception of manganese (Mn). Mn has been replaced with Zn due to the lack of experimental data for comparison purposes. Zn is of special interest due to the relatively large content in MSW and the potential corrosive behaviour. Ash species have only been included to make interactions between ash species and heavy metals possible. Other ash species such as Potassium (K), Sodium (Na) and Phosphorous (P) could have been included as they might compete with the heavy metals on the access to sulphur (S) and chlorine (Cl). However, the access to S and Cl for the heavy metals is investigated by performing a parametric study varying the content of S and Cl. The distribution of ash species is not subject to any discussion in this work unless there is an interaction with any of the heavy metals.

In order to come up with two systems for equilibrium calculations, one for *reducing* conditions and one for *oxidising* conditions, a comprehensive set of species were included in the initial calculations using a typical ultimate composition for MSW. After a reduction of the original set of species to include only the species that were actually involved in the equilibrium chemistry (even at very small concentrations), two sets of species were established, one for reducing conditions and one for oxidising conditions. The combustion products, ash and heavy metal species are listed in the Appendix in Tables 1-3.

INPUT PARAMETERS AND PARAMETRIC STUDY

A "typical" composition for European/US MSW has been used to calculate the elemental and heavy metal concentrations. The composition being 33.1 wt% of paper and cardboard, 6.5% plastics, 24.4% wet organic waste, 6.4% glass, 3.7% metals, 12.6% of other combustibles (wood, rubber, leather, textiles) and a rest fraction of 13.3% (ash, sand, stones, fines, etc). Table 4 shows the ultimate analysis and heavy metal concentrations for the chosen composition of MSW based on literature values (Sandgren and Heie (1996), Rigo and Chandler (1994) and Laughlin (2000)).

Table 4. Ultimate analysis of base case composition for MSW.

Element	Composition [wt%]	Element	Concentration [g/ton]
C	25.29	As	18.2
H	3.39	Cd	40.9
O	18.06	Cr	55.7
N	0.48	Cu	462.9
S	0.17	Hg	1.1
Cl	0.56	Ni	28.4
Moisture	24.82	Pb	136.0
Ash	27.24	Zn	1713.7

The conditions investigated in this study reflect those of a commercial grate furnace. Details of typical grate furnaces and flue gas cleaning systems (FGCS) are provided by Sørum et. al. (1997) and Rigo and Chandler (1994). Table 5 shows the elemental composition of fuel and oxidiser for base case (BC) calculations. The only difference between the reducing and oxidising conditions on the grate is the fuel/air ratio. In order to investigate how the distribution of heavy metals changes as a function of temperature from the furnace to the filter (cooling of flue gas) an additional set of calculations were performed under oxidising conditions. In these

calculations it was assumed that 3 wt% of the total ash content followed the flue gas as fly ash through the boiler to the electrostatic precipitator (ESP) (Sørum et. al. (1997)).

Table 5. Elemental composition of fuel and oxidiser for " base case" calculations.

Input parameters	Grate (Reducing)	Grate (Oxidising)	Flue Gas (Oxidising)
C [mole]	21.1	21.1	32.7
H [mole]	61.5	61.5	80.2
O [mole]	53.8	85.5	172.3
N [mole]	108.3	227.9	530.8
S [mole]	0.05	0.05	0.08
Cl [mole]	0.16	0.16	0.25
λ	0.6	1.3	1.9
Ash [wt%]	27.2	27.2	0.8
Temp. [K]	950-1600	950-1600	300-1600
Al [mole]	0.234	0.234	0.007
Ca [mole]	3.426	3.426	0.103
Fe [mole]	2.153	2.153	0.065
Si [mole]	0.300	0.300	0.009
As [mole]	$2.430 \cdot 10^{-4}$	$2.430 \cdot 10^{-4}$	$2.430 \cdot 10^{-4}$
Cd [mole]	$3.637 \cdot 10^{-4}$	$3.637 \cdot 10^{-4}$	$3.637 \cdot 10^{-4}$
Cr [mole]	$1.072 \cdot 10^{-3}$	$1.072 \cdot 10^{-3}$	$1.072 \cdot 10^{-3}$
Cu [mole]	$7.290 \cdot 10^{-3}$	$7.290 \cdot 10^{-3}$	$7.290 \cdot 10^{-3}$
Hg [mole]	$5.615 \cdot 10^{-6}$	$5.615 \cdot 10^{-6}$	$5.615 \cdot 10^{-6}$
Ni [mole]	$4.843 \cdot 10^{-4}$	$4.843 \cdot 10^{-4}$	$4.843 \cdot 10^{-4}$
Pb [mole]	$6.565 \cdot 10^{-4}$	$6.565 \cdot 10^{-4}$	$6.565 \cdot 10^{-4}$
Zn [mole]	$2.620 \cdot 10^{-2}$	$2.620 \cdot 10^{-2}$	$2.620 \cdot 10^{-2}$

Calculations with a composition simulating Refuse Derived Fuel (RDF) were also performed in order to study the influence of differences in the elemental composition (C/H/O/N) and ash content. No significant influence on the equilibrium distribution was discovered when performing calculations with MSW versus RDF on the grate. In the flue gas, however, a varying ash content had a

significant influence on the equilibrium distribution for all heavy metals in this study, except Hg. The content of Cl, S and heavy metals were kept the same for MSW and RDF in these calculations for comparison purposes.

In MSW combustion there are two important factors controlling the fate of heavy metals; waste composition and operational parameters such as air supply and temperature profile through the combustion plant. A parametric study has therefore been performed in order to investigate the effect of these parameters at typical conditions for MSW grate combustion. Table 6 shows the extent of the parametric study. The Cl/Cl_{BC} ratio denotes the actual number of moles of Cl used in the calculations to the number of moles at base case conditions. On an as received mass basis the chlorine and sulphur content of the waste is varied between 0.06-5.7wt% and 0.02 and 1.7 wt%, respectively. The flyash content is varied between 1-6 wt% of the total ash concentration of the waste.

Table 6. Calculation matrix.

Parameters	Grate (Reducing)	Grate (Oxidising)	Flue Gas (Oxidising)
Cl/Cl_{BC}	0.1-10	0.1-10	0.1-10
S/S_{BC}	0.1-10	0.1-10	0.1-10
Ash/Ash_{BC}	-	-	0.3-2.0
λ	0-0.9	1.2-1.9	1.1-1.9

RESULTS AND DISCUSSION

Previous experimental studies have shown large variations in partitioning in similar incinerators for MSW for the eight heavy metals focused upon in this study. These large variations in volatile behaviour may be explained by several factors such as variations in MSW composition, operational conditions and measurement

techniques and methods. The results from the GEA calculations will be presented and discussed in separate parts; *one* covering the distribution of metals on the grate (950 to 1600 K) and *one* covering the distribution of metals from the furnace to filter (300 to 1600 K). On the grate, the major focus will be on the volatile behaviour, while the systems describing the conditions from furnace to filter will focus both on chemistry and condensation of the heavy metals. An adiabatic flame temperature of ~ 1500 K was calculated using the base case fuel composition and λ =1.9. In addition, Gort (1995) showed that a maximum temperature of ~1600 K was obtained in the reaction front of MSW in a packed bed. Therefore a maximum temperature of 1600 K was chosen for both systems. The lower temperature (950 K) on the grate reflects the point where all components of MSW are volatilised and only fixed carbon is left. For the system covering the conditions from furnace to filter, 300 K is chosen in order to be on the low side of temperatures observed when entering the filter system (typically 500 K).

Conditions On The Grate

Calculations on the grate using both a reducing and an oxidising system have been performed at base case conditions. The results from these base case calculations are shown in Figure 1 for reducing conditions and in Figure 2 for oxidising conditions. When interpreting the results it is important to know the equilibrium distribution of chlorine and sulphur, since these species will affect the distribution of the heavy metals. The equilibrium distribution for base case calculations for reducing and oxidising conditions on the grate and oxidising conditions in the flue gas are shown in Figure 6 in the Appendix. At base case reducing conditions, chlorine is present as $CaCl_2$ (cr) (cr = solid phase) and gaseous HCl (g) (g = gas phase) up to 1050 K. From 1050 K, HCl (g) is the dominating species, whereas for oxidising conditions, HCl (g) is the dominating species with minor amounts of Cl (g) (< 1.5% (mol/mol)) at higher temperatures.

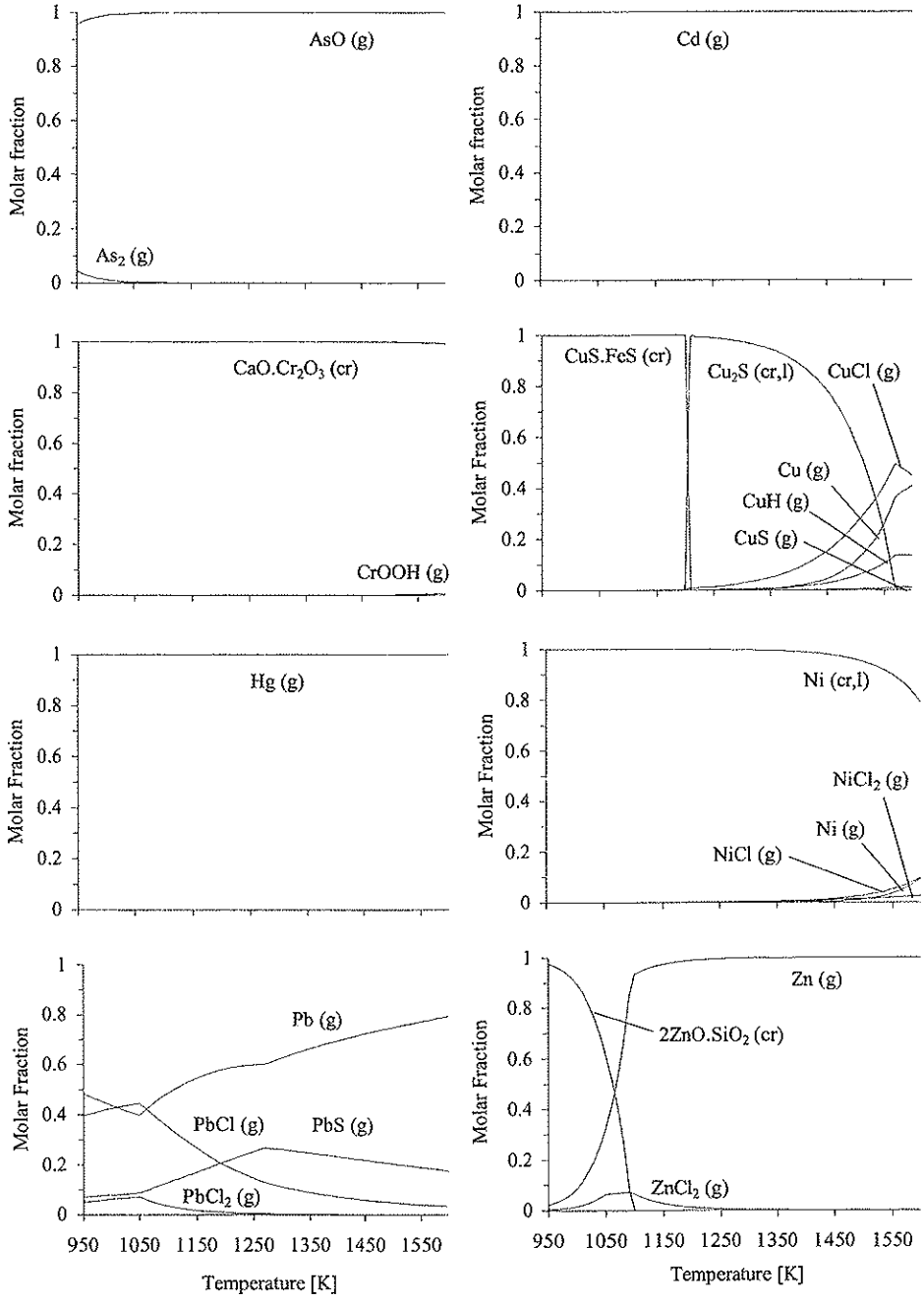

Figure 1. Equilibrium distribution of As, Cd, Cr, Cu, Hg, Ni, Pb and Zn at reducing conditions on the grate ($\lambda = 0.6$).

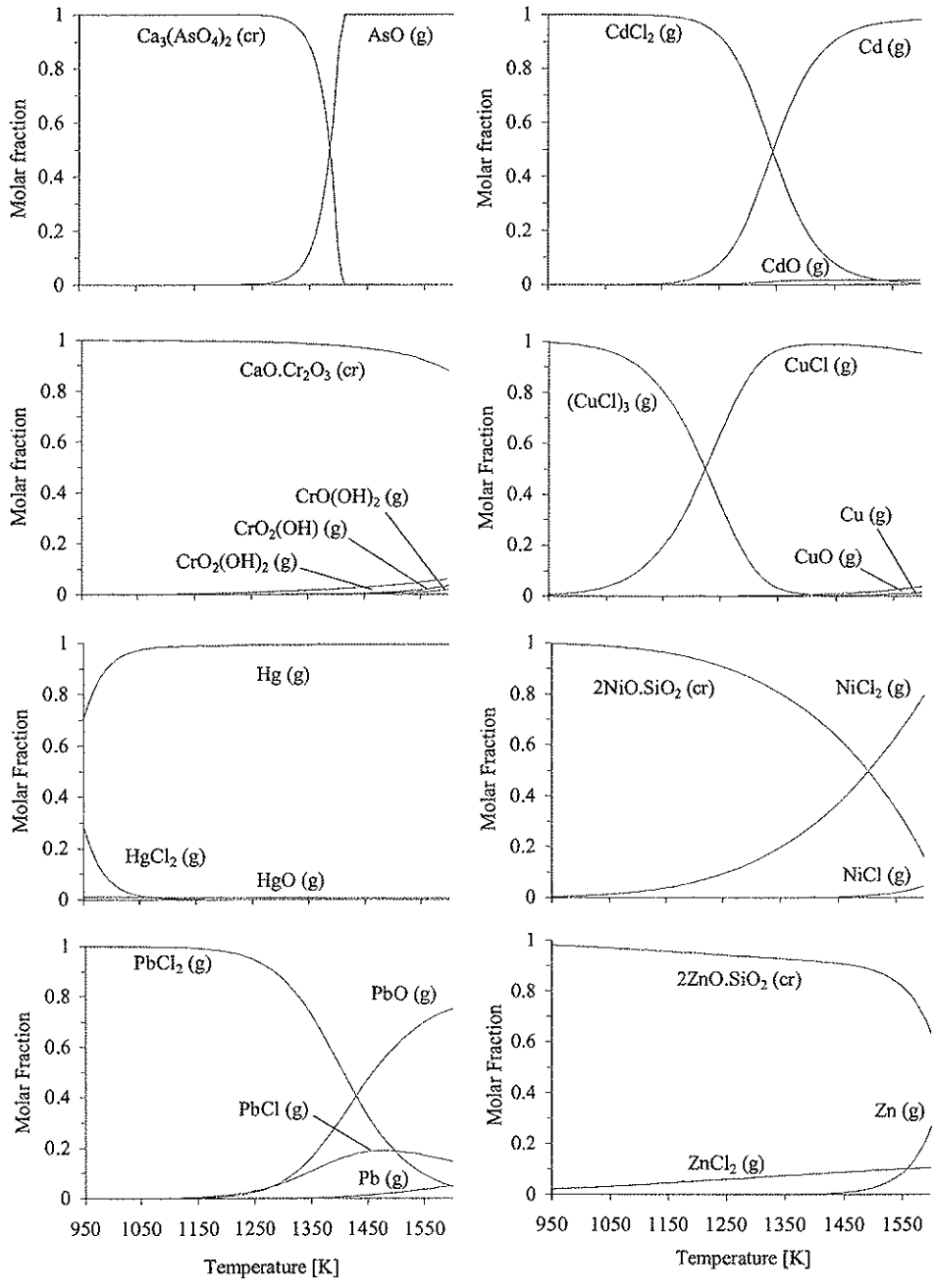

Figure 2. Equilibrium distribution of As, Cd, Cr, Cu, Hg, Ni, Pb and Zn at oxidising conditions on the grate. $\lambda = 1.3$.

The sulphur distribution for reducing conditions is dominated by CaS (cr) and H_2S (g) up to 1270 K, from where H_2S (g) is the dominating species. Minor amounts of COS (g), SO_2 (g) and HS (g) (< 3.5% (mol/mol)) are also observed. The sulphur distribution for oxidising conditions is completely different. $CaSO_4$ (cr) is the stable phase below 1250 K, from where it gradually changes to SO_2 (g), which is the dominating S-containing species above 1400 K.

As. Under reducing conditions, As is present as AsO (g) with only a small amount of As_2 (g) (< 3.5% (mol/mol)) below 1050 K. Under oxidising conditions, however, As is stable as $Ca_3(AsO_4)_2$ (cr) up to approximately 1300 K. From 1300 K to 1400 K the stable form of As gradually changes to AsO (g). The difference may be explained by the equilibrium distribution of Ca. Under reducing conditions the dominant Ca species is CaO (cr), whereas under oxidising conditions the dominant species is CaO (cr,l) (cr,l = condensed liquid phase). In order to test the hypothesis that the Ca distribution determines the interaction between As and Ca, CaO (cr), was removed from the calculations for reducing condition. After the removal of CaO (cr), Ca was bound as CaO (l) and minor amounts of $CaCl_2$ (cr) and CaS (cr). In this latter case $Ca_3(AsO_4)_2$ (cr) was present at lower temperatures (below 1000 K) together with AsO (g). Removing CaO (l) in addition to CaO (cr) resulted in a similar equilibrium distribution as observed for oxidising conditions. Verhulst et. al. (1996) found that As_2O_5 (cr), was the stable phase up to about 800 K, from where it volatilises between 800 and 1300 K to As_4O_6 (g). Above 1300 K AsO (g) was the dominant species. Frandsen et. al. (1994) found similar results as Verhulst under the conditions of coal combustion, however As_4O_6 (g) was only present between 750 to 900 K, from where AsO (g) becomes the stable species. Wu (1993) found that the equilibrium distribution for As in an oxidising system was As_2O_5 (cr) at lower temperatures and $AsCl_3$ (g) at higher temperatures. However, Verhulst, Frandsen and Wu did not include $Ca_3(AsO_4)_2$ (cr) in their studies. In addition, Wu did not include As_4O_6 (g) in his study. Rigo and Chandler (1994) found that 50 wt% of As remained in the bottom ash during combustion of MSW in

a grate fired system. This indicates that the volatility of As is strongly dependent upon the MSW composition and operational parameters such as fuel/air ratio and temperature.

Cd. Cd (g) is the stable phase for Cd under reducing conditions at 950-1600 K. At oxidising conditions the stable phase is $CdCl_2$ (g) up to approximately 1150 K, where it gradually changes to Cd (g) and a minor amount of CdO (g) (< 2 % (mol/mol)) up to 1600 K. These distributions are fairly "classical" and has been observed also for coal gasification and combustion as reported by Frandsen et. al. (1994). Ljung and Nordin (1997) also reported similar equilibrium distribution behaviour during combustion of biomass. No significant interaction between ash species and Cd could be detected. The distribution of Cd among Cd (g), CdO (g) and $CdCl_2$ (g) is governed by the reactions: $CdCl_2$ (g) + H_2O (g) $\Leftrightarrow$ CdO (g) + 2HCl (g) and CdO (g) $\Leftrightarrow$ Cd (g) + ½ O_2 (g), where CdO (g) will dissociate into Cd (g) and O_2 (g) at temperatures above 1000 K according to Frandsen et. al. (1994). The literature reports very varying degree of volatility of Cd in real grate combustion plants for MSW. Several studies on similar grate combustion plants for MSW, reports the extremes of Cd volatile fraction to be between 17 to 83 wt% (Soma (1986) and Rigo and Chandler (1994)). This varying degree of volatilisation is not observed in this work, as Cd is entirely volatilised in the investigated temperature range. Water-cooled grates (Sørum et. al. (1996)) versus air-cooled grates (Rigo & Chandler (1994)), causing a lower temperature on the grate, may be one of the reasons for the large variations in the volatile behaviour of Cd.

Cr. Cr does only to a very small degree volatilise under the given temperature range. This is also observed in practice in real combustion plants, where Rigo and Chandler (1994) and Sørum et. al. (1997) states that ~ 95 wt% of Cr will remain in the bottom ash. $CaO.Cr_2O_3$ (cr) is the dominant species for both reducing and oxidising systems, with small amounts of oxides (< 10 % (mol/mol)) are formed starting at approximately 1250 K for the oxidising system. In the reducing system,

the CrOOH (g) oxide is barely visible above 1550 K. The equilibrium distribution for Cr is not significantly influenced changing from reducing to oxidising conditions

Cu. The volatile behaviour for Cu is largely altered when changing from reducing to oxidising conditions. At reducing conditions, Cu is present as sulphides in solid phase as CuS.FeS (cr) (valid up to 1200 K) and Cu_2S (cr,l) (from 1200 K). A gradual increase in the chloride CuCl (g) is observed from approximately 1200 K, up to approximately 50% (mol/mol). From 1350 K, the amounts of Cu (g) and CuH (g) increases up to a maximum of 45 and 15% (mol/mol) at 1600 K, respectively. At oxidising conditions Cu is only present in gas phase. First as $(CuCl)_3$ (g), which gradually decomposes to CuCl (g) from 950 K. Minor amounts of CuO (g) and Cu (g) (< 4% (mol/mol)) can be observed at higher temperatures (above 1450 K). The results found for oxidising conditions are similar to those found by Verhulst et. al. (1996) at typical conditions for MSW combustion. Values found in the literature reports that 89–96 wt% of Cu remained in the bottom ash (Rigo and Chandler (1994) and Brunner and Mönch (1986)).

Hg. Hg is present only in gas phase for both reducing and oxidising conditions. The distribution of species, however, is different. At reducing conditions, only Hg (g) is present, while at oxidising conditions up to 28% (mol/mol) of $HgCl_2$ (g) is observed in the lower temperature range (below 1100 K). However, Hg (g) is the dominant species at oxidising conditions as well. A small amount of HgO (g) (< 1% (mol/mol)) is also observed for the entire temperature range. The difference between the reducing and the oxidising system can be found by looking at the Cl distribution. Cl in the reducing system is partly bound as $CaCl_2$ (cr) up to 1050 K from where HCl is the only significant species. This means that in competition with HCl (g) for chlorine, mercury does not form chlorides. In competition with $CaCl_2$ (cr), however, mercury chloride is formed. The equilibrium distribution for oxidising conditions is "classical" and has been found by other researchers such as

Frandsen et. al. (1994) and Verhulst et. al. (1996) for coal and waste combustion, respectively. Experimental studies on the volatile behaviour of Hg in grate combustion plant states that up to 19 wt% will remain in the bottom ash (Rigo and Chandler (1994) and Soma (1986)). The relatively large amount of Hg remaining in the bottom ash in some studies may be found in unburned fractions of the fuel.

Ni. The major part of Ni is present as the stable condensed elemental nickel Ni (cr,l), for the reducing system at 950-1600 K. Small amounts (< 10% (mol/mol)) of chlorides in gas phase and Ni (g) is observed above 1400 K. Under oxidising conditions the dominant species is $2NiO.SiO_2$ (cr). However, increasing amounts of chlorides in gas phase, especially $NiCl_2$ (g), is observed already at 950 K, with a maximum of approximately 80% (mol/mol) at 1600 K. The availability of oxygen may explain the formation of $2NiO.SiO_2$ (cr) in the oxidising system rather than Ni (cr,l) as observed in the reducing system, since Si is bound as SiO_2 (cr,l) for both systems. Rigo and Chandler (1994) found that 98 wt% of Ni remained in the bottom ash.

Pb. The distribution of Pb under reducing and oxidising conditions are quite different. At lower temperatures (<1050 K), at reducing conditions, Pb (g) and lead chlorides are dominating. Above 1050 K, the amount of Pb (g) gradually increases on the expense of lead chlorides. An increasing amount of PbS (g) is observed up to approximately 1270 K, from where it starts to gradually decrease with increasing temperature. The sharp edges observed in the $PbCl_x$ (g) curves at 1050 K may be explained by looking at the chlorine balance of the system. At 1050 K the solid phase $CaCl_2$ (cr) disappears and chlorine is present as HCl (g). As for Hg, the formation of chlorides of Pb in competition with HCl (g) as opposed to $CaCl_2$ (cr) will decrease with increasing temperature. $PbCl_4$ (g) was added in an additional calculation for the reducing system, but no influence was found. In the oxidising system $PbCl_2$ (g) is the stable phase at temperatures below 1150 K. From approximately 1150 K an increasing amount of PbO (g) and PbCl (g) is observed.

A minor amount of Pb (g) (< 5% (mol/mol)) is observed from approximately 1400 K. In order to check the possible influence of $PbCl_4$ (g) on the equilibrium distribution of Pb this species was added in an additional calculation. This calculation showed that $PbCl_4$ (g) was the dominating species up to about 1300 K. However, $PbCl_4$ (g) was also the only Pb species at room temperature (300 K) and was therefore excluded from these calculations. The literature shows a large variation in the volatility of Pb. Reported extreme values of the fraction of Pb remaining in the bottom ash, (Brunner and Mönch (1986), Barton et. al. (1990) and Sørum et. al. (1997)), varied from 58-94 wt%. Srinivasachar et. al (1989) stated that the use of an additive (no description of the additive was given) gave very promising results for controlling lead aerosol emissions and minimising lead chloride deposition due to decreased volatility.

Zn. At 950 K the silicate $2ZnO.SiO_2$ (cr) is the dominant species under reducing conditions. However, it gradually decreases with increasing temperature to zero at 1100 K, from where Zn (g) is the dominant stable phase. A minor amount of $ZnCl_2$ (g) is observed from 950 to 1250 K. Under oxidising conditions, $2ZnO.SiO_2$ (cr) is the dominant species for the entire temperature range. However, Zn (g) is sharply increasing from 1450 K to 1600 K to a maximum of 26% (mol/mol). A minor amount of $ZnCl_2$ (g) (< 10% (mol/mol)), linearly increasing from 950 to 1600 K is also observed. The difference between reducing and oxidising condition is related to the oxidation of Zn into $2ZnO.SiO_2$ (cr). Lowering the excess air will force $2ZnO.SiO_2$ (cr) to decompose into Zn (g) and O_2 (g) in order to maintain the equilibrium. The experimental work of Rigo and Chandler (1994) and Sørum et. al. (1997) showed that 37-86 wt% of Zn remained in the bottom ash. Since chlorides of Zn in deposits are highly unwanted in the boiler, efforts should be made to decrease the volatility for Zn on the grate. The influence of different parameters such as temperature, availability of sulphur and chlorine and fuel/air ratio on the volatility is therefore of great importance for Zn.

Influence of S/S_{BC} ratio

The S/S_{BC} ratio was varied from 0.1 to 10 on a molar basis, keeping all other concentrations constant as given by base case composition. No changes in the distribution of heavy metal species were observed for the oxidising system when varying the S/S_{BC} ratio from 0.1 to 10. In the reducing system, only Cu, Ni and Pb experienced changes in equilibrium distribution.

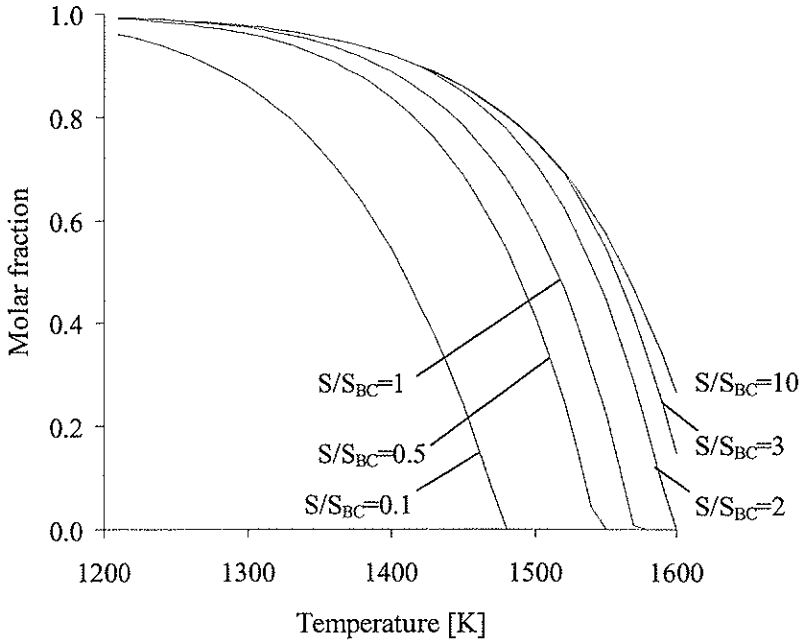

Figure 3. Influence of the S/S_{BC} ratio on the volatility of Cu_2S (cr,l) as a function of temperature.

As shown in Figure 3, a less volatile behaviour is observed for Cu with increasing S/S_{BC} ratio. Cu_2S (cr,l) becomes more and more dominant in the higher temperature range (1400 to 1600 K) on the expense of CuCl (g), Cu (g) and CuH (g). At a S/S_{BC} ratio of 0.1, Cu_2S (cr,l) is fully volatilised at 1480 K. At a S/S_{BC} ratio of 10, however, there is still 26% (mol/mol) left in the condensed phase at 1600 K. Only a

minor increase is observed for CuS (g) in the temperature range 1500 to 1600 K at high S/S_{BC} ratios. At a S/S_{BC} ratio of 0.1, Cu_2S (cr,l) is also dominant in the lower temperature range, with a minor amount of CuS.FeS (cr) present.

The only significant effect on the equilibrium distribution of Ni, when varying the S/S_{BC} ratio is a shift from Ni (cr,l) to Ni_3S_2 (cr,l) at approximately 1520 K for a S/S_{BC} ratio above 3. The volatile behaviour of Ni_3S_2 (cr,l), however is similar to Ni (cr,l) at lower S/S_{BC} ratios.

For Pb the distribution of chlorides PbCl (g) and $PbCl_2$ (g) stay constant when varying the S/S_{BC} ratio from 0.1 to 10. The amount of PbS (g) increases on the expense of Pb (g) as the S/S_{BC} ratio increases, however there is always more Pb (g) in the system than PbS (g).

Influence of Cl/Cl_{BC} ratio

The influence of the Cl/Cl_{BC} ratio gave different results for the reducing and oxidising systems and is therefore discussed separately.

Reducing system

The equilibrium distribution of As, Cd, Cr and Hg in the reducing system is not influenced by a changed content of Cl compared to base case.

Cu becomes more volatile when the Cl/Cl_{BC} ratio increases. At a 0.1 Cl/Cl_{BC} ratio, 13% (mol/mol) of Cu is still in solid phase as Cu_2S (cr,l) at 1600 K, a significant amount of Cu (g) and minor amounts of CuCl (g), CuH (g) and CuS (g) are observed above 1500 K. At a Cl/Cl_{BC} ratio of 10, however, Cu_2S (cr,l) is fully volatilised at 1420 K. At this ratio the chloride CuCl (g) is sharply increasing from 1200 K, and becomes the dominant species above 1400 K. Minor amounts of Cu (g) and CuH (g) is also observed in the higher temperature range from approximately 1400 K. It is interesting to observe that when increasing the Cl/Cl_{BC}

ratio from 0.1 to 10, Cu becomes more volatile, which is the inverse effect on the volatile behaviour of Cu for a similar increase in the S/S_{BC} ratio. One should, however, be aware of the combined effect or S/Cl ratio. When the S/S_{BC} ratio is changed from 0.1 to 10 or the Cl/Cl_{BC} ratio is changed from 10 to 0.1, this corresponds to a change in the S/Cl ratio from 0.034 to 3.4. However, the investigation of the combined effect or S/Cl ratio is beyond the scope of this study.

Ni also becomes more volatile when increasing the Cl/Cl_{BC} ratio from 0.1 to 10. At a Cl/Cl_{BC} ratio of 0.1 and a temperature of 1600 K, 90% (mol/mol) of Ni is stable as Ni (cr,l), with minor amounts of Ni (g) and NiCl (g) (<10% (mol/mol)) present. Increasing the ratio to 10, causes Ni (cr,l) to be fully volatilised at 1450 K and chlorides to dominate the equilibrium distribution at temperatures above 1400 K.

Even though Pb is present in gas phase for all Cl/Cl_{BC} ratios, the equilibrium distribution changes. At Cl/Cl_{BC} ratios below 1.0, the distribution of Pb is dominated by Pb (g) and PbS (g), and below 1250 K also PbCl (g). Increasing the Cl/Cl_{BC} ratio above 1.0 leads to an increase in the amount of the lead chlorides PbCl (g) and $PbCl_2$ (g). However, Pb (g) is still the dominating species above 1450 K.

The volatile behaviour of Zn is not significantly altered even when changing the Cl/Cl_{BC} ratio from 0.1 to 10. However, the amount of $ZnCl_2$ (g) increases with increasing Cl/Cl_{BC} ratio on the expense of Zn (g), especially below 1400 K. Zn (g) is the dominating species at all Cl/Cl_{BC} ratios above 1250 K.

Oxidising system

The equilibrium distribution of As and Cr is not influenced by varying the Cl/Cl_{BC} ratio from 0.1 to 10. The volatile behaviour of Cd, Hg and Pb is not significantly altered under the same range of variations, but the chlorides $CdCl_2$ (g), $HgCl_2$ (g) and $PbCl_2$ (g) decompose at higher temperatures when increasing the Cl/Cl_{BC} ratio.

Meaning that only the gas phase chemistry is affected. For Cd a very small amount (< 3.5% (mol/mol)) of $CdO.SiO_2$ (cr) is observed at 950 to 970 K at a Cl/Cl_{BC} ratio of 0.1. The volatile behaviour of Cu, Ni and Zn is highly dependent on the Cl/Cl_{BC} ratio.

Insignificant influence when varying the Cl/Cl_{BC} ratio from 1.0 to 10 on the volatile behaviour of Cu is observed, meaning that Cu only is present in gas phase. However, at lower ratios the species CuO (cr) becomes more and more dominant in the lower temperature range. At a Cl/Cl_{BC} ratio of 0.1, CuO (cr) is the dominant species up to 1250 K. At 1300 K, Cu is only stable in the gas phase.

Ni shifts from being stable as 2NiO.SiO2 (cr) over the entire temperature range at a Cl/Cl_{BC} ratio of 0.1 to being almost fully volatilised, at a Cl/Cl_{BC} ratio of 10, with 2NiO.SiO2 (cr) only being present from 950 to 1030 K (decreasing from 67 to 0% (mol/mol)). Increasing the Cl/Cl_{BC} ratio, decompose 2NiO.SiO2 (cr) at lower temperatures and increase the amount of $NiCl_2$ (g).

Zn shows a volatile behaviour similar to Ni, when varying the Cl/Cl_{BC} ratio. With the exception of the presence of Zn (g) (less than 30% (mol/mol)) above 1450 K, Zn is stable as $2ZnO.SiO_2$ (cr) over the entire temperature range at a Cl/Cl_{BC} ratio of 0.1. Increasing the Cl/Cl_{BC} ratio makes the presence of $ZnCl_2$ (g) more and more dominating. Zn is only present in gas phase at a Cl/Cl_{BC} ratio of 10, with $ZnCl_2$ (g) as the stable phase over the entire temperature range.

Effects of varying fuel/air ratio

The equilibrium distribution of the different heavy metals was not largely altered, varying λ from 1.2 to 1.9 for the oxidising system. The volatility of Cd, Hg, Ni and Pb was not changed at all, while the observed effects on the other heavy metals are different from metal to metal. Zn becomes less volatile when increasing λ. At λ=1.2 and a temperature of 1600 K, there is 22% (mol/mol) of $2ZnO.SiO_2$ (cr) in

the system, while at λ=1.9 this has increased to 71% (mol/mol) on the expense of Zn (g). The decreasing volatility of Zn is only observed in the higher temperature range, above 1450 K. The effect on the volatility of Zn in a real combustion plant would be enhanced since lowering λ also will increase the combustion temperature. Given the possibility of forming highly corrosive condensed zinc chlorides in the flue gas it is preferable to have Zn bound as $2ZnO.SiO_2$ (cr) in the bottom ash. At λ=1.9 a part of Cu is present in solid phase as CuO (cr) (decreasing from 50 to 0% (mol/mol) from 950 to 1010 K). This is the only significant effect on the volatile behaviour of Cu when increasing λ. Cr becomes more volatile as the amount of gaseous chromium oxides increases with increasing λ. At 1600 K the amount of $CaO.Cr_2O_3$ (cr) gradually decreases from 96% (mol/mol) at λ=1.2 to 71% at λ=1.9. For As the major effect of an increase in λ from 1.2 to 1.9 is that the equilibrium distribution has been shifted 70 K to a higher temperature. Meaning that an increasing in λ makes As slightly less volatile.

At reducing conditions, when varying λ from 0 to 0.9, the volatile behaviour of As, Cd, Cr, Hg and Pb are not significantly changed. Ni becomes slightly more volatile at temperatures above 1400 K, when increasing λ, due to the decomposition of Ni (cr,l) to $NiCl_x$ (g) and Ni (g). The equilibrium distribution also becomes more complex at λ=0.9 as compared to λ=0, with the presence of Ni_3S_2 (cr,l) between 1150 and 1300 K and Ni chlorides at higher temperatures. Cu and Zn become less volatile with increasing λ. At λ = 0, Cu and Zn is fully volatilised at 1350 and 1000 K, respectively, while the corresponding temperatures at λ=0.9 are 1550 and 1150 K.

Conditions From Furnace To Filter

The temperature of the flue gas when it enters the flue gas cleaning system is important in order to evaluate the amount of condensed heavy metals. This temperature might vary, but in the following discussion a temperature in the range

300-500 K has been assumed. Due to the uncertainty on the fraction of heavy metals that will remain in the bottom ash, it has further been assumed that all metals are fully volatilised and found in the flue gas with the same amount as in the MSW. The results from the equilibrium calculations are compared to full-scale measurements performed in two different studies performed by Rigo and Chandler (1994) and Sørum et. al. (1997), below only referred to as Rigo and Sørum. In the study of Rigo, the combustion plant consisted of an inclined grate furnace followed by boiler sections, a conditioning tower, lime injection reactor and a fabric filter. The combustion plant in the study of Sørum consisted of a water-cooled inclined grate furnace, followed by a boiler section and an electrostatic precipitator (ESP) and a wet scrubber system. The equilibrium distribution of all heavy metals simulating the conditions from the furnace to the filter is shown in Figure 4.

As. As is found stable as $Ca_3(AsO_4)_2$ (cr), when cooling the flue gas from 1300 K to approximately 300 K. From 1300 K to 1400 K the stable form of As gradually changes to AsO (g). Above 1400 K, AsO (g) is the only stable phase of As. This means that As following the flue gas should condense and be captured corresponding to the efficiency of the ESP or fabric filter, provided sufficient residence time and specific surface area. Rigo observed this behaviour for As, where the major volatile fraction of As was captured in the fabric filter residue in the combustion plant, and less than 1 wt% escapes through the stack.

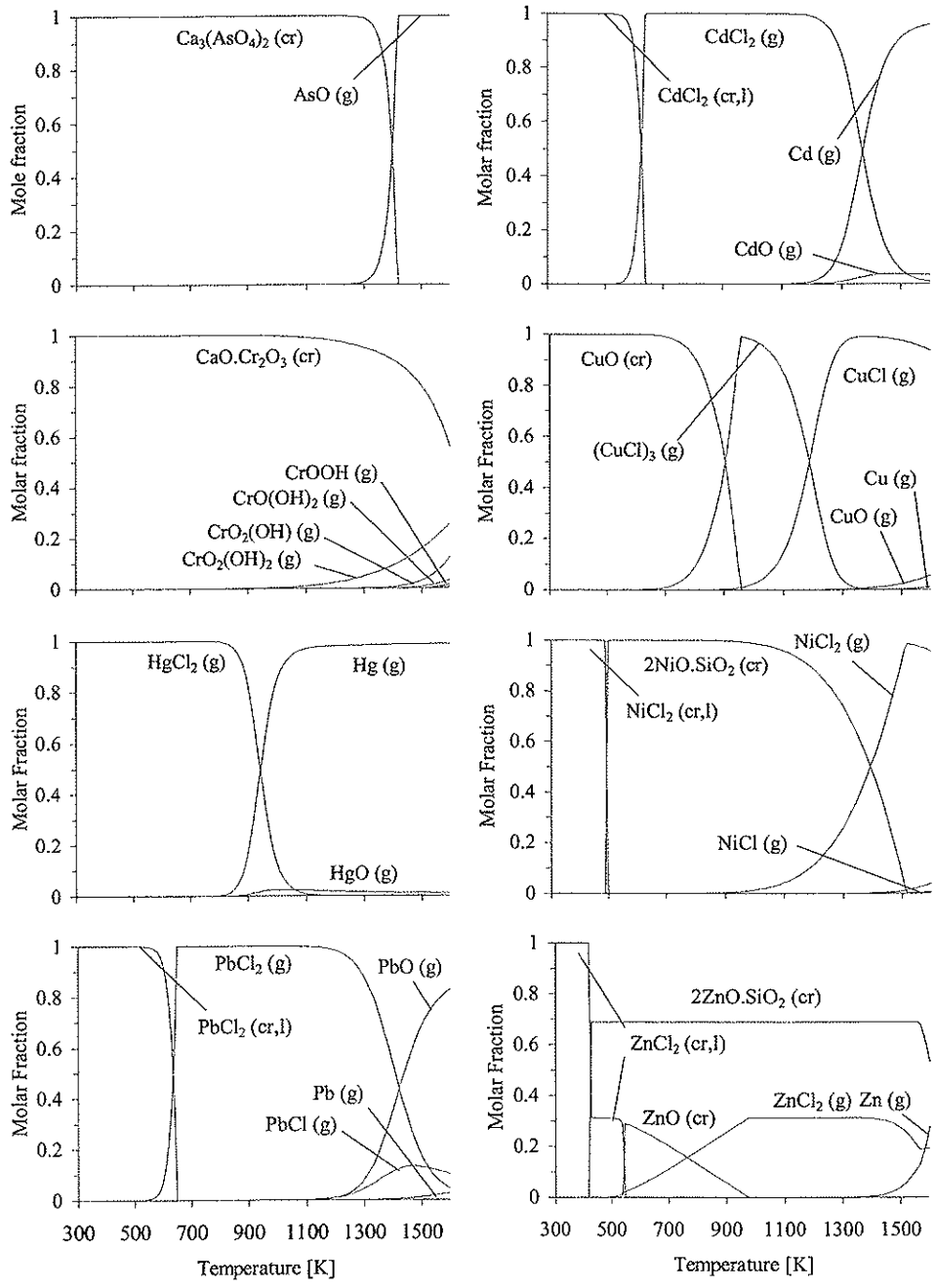

Figure 4. Equilibrium distribution of As, Cd, Cr, Cu, Hg, Ni, Pb and Zn at oxidising conditions in the flue gas ($\lambda = 1.9$).

Cd. $CdCl_2$ (cr,l) is the stable phase in the lower temperature range from 300 to 600 K. From 600 K the stable phase changes sharply to $CdCl_2$ (g), which is stable until 1200 K. From 1200 K, the stable phase gradually changes to Cd (g) and a minor amount of CdO (g) (< 3% (mol/mol) from 1300 K) up to 1600 K. Similar to As, the volatile fraction of Cd should be captured in the ESP or fabric filter corresponding to the efficiency, assuming a temperature of 500 K, when entering the flue gas cleaning system (FGCS). However, 500 K is close to where Cd starts to condense and a slightly higher temperature might cause parts of Cd to pass through the FGCS and enter the stack. Cd may also condense on aerosols, which might not be captured by the filter system. Rigo found that 96 wt% of the volatile part of Cd is captured in the fabric filter, while Sørum found that 25 wt% of the volatile Cd escapes through the stack. The reason for this difference may be found in the fact that in the study of Rigo, 96 wt% of Cd is volatile, while the corresponding value in the study of Sørum is 41 wt%. In addition the concentration of Cd in the MSW is a factor of 2.4 higher in the study of Rigo compared to the study of Sørum. Given similar operational conditions and efficiencies of FGCS, this means that the concentration of Cd in the flue gas would be ~ 6 times higher. However, Hasselriis and Licata (1996) stated that even a substantial spiking of Cd in the feed resulted in only marginal changes in stack emission. Given a constant stack emission of Cd, means that a lower concentration of Cd in the flue gas will increase the fraction of Cd escaping through the stack. The relatively low temperature of condensation for Cd increases the possibility for condensation on aerosols, since aerosols are formed at low temperatures in the boiler.

Cr. Cr is only volatile in significant extent at high temperatures i.e. above 1500 K, where the amounts of gaseous oxides start to increase. $CaO.Cr_2O_3$ (cr) is the dominant species from 300 to 1500 K. At 1600 K, ~ 40% (mol/mol) of the chromium is volatilised. In the study of Sørum, 99.6 wt% of Cr remained in the bottom ash. All significant amount of volatile chromium (0.4 wt%) of Cr was captured in the ESP. Rigo experienced the same behaviour with all significant

volatile amount of Cr being captured in the FGCS and boiler hoppers. In other words, at 500 K, Cr is present in solid phase, as also the equilibrium calculations have shown.

Cu. There are three dominant stable phases for Cu. CuO (cr) is stable from 300 to 700 K, from where the amount of $(CuCl)_3$ (g) gradually increases. $(CuCl)_3$ (g) is the dominant species from 900 to 1200 K. From 900 K, the amount of CuCl (g) gradually increases and becomes the dominant species from 1200 to 1600 K. Minor amounts of CuO (g) and Cu (g) can be observed at high temperatures. Rigo showed that the major amount of the volatile fraction of Cu was captured on fly ash particles in the boiler hoppers (1/3) and in the fabric filter (2/3). At 500 K, the equilibrium calculations showed that Cu was present in solid phase as CuO (cr).

Hg. Hg is stable in gas phase for the entire temperature range with two dominant stable phases. $HgCl_2$ (g) is the stable phase from 300 to 800 K, from where it gradually shifts to Hg (g) and a small amount of HgO (g) (<1.8% (mol/mol)). Mercury is the most volatile of the metals in this study. Equilibrium calculations and experimental investigations confirm this. In the studies of Rigo and Sørum, almost all Hg was volatilised. In the study of Rigo, a dry scrubbing system (lime injection) was used, capturing ~ 40 wt% of the volatile Hg. In the study of Sørum a wet scrubbing system was used and the corresponding capture of Hg was ~ 90 wt%. Although neither of the systems used in the two studies are specifically intended to remove mercury they have a removal effect. This indicates that the capture efficiency of Hg is closely related to the type of FGCS.

Ni. Ni is present as the thermodynamically stable, condensed $NiCl_2$ (cr,l) in the temperature range 300-500 K. From 500 to 900 K, $2NiO.SiO_2$ (cr) is the stable phase, which gradually decreases to zero from 900 to 1520 K, while the amount of $NiCl_2$ (g) increases, being the dominant species at higher temperatures. Minor amounts of NiCl (g) and Ni (g) (< 5% (mol/mol) is observed above 1400 K. Of the

2 wt% of Ni in the study of Rigo not found in the bottom ash, approximately 60 wt% was captured on fly ash particles in the boiler hoppers while the remaining 40 wt% was captured in the fabric filter. The volatile fraction of Ni may be volatilised on the grate and consequently condensed and/or it might follow the fly ash. This confirms the non-volatile behaviour of Ni as shown from the equilibrium calculations.

Pb. The highly corrosive species $PbCl_2$ (cr,l) is the stable phase from 300 to 550 K, from 550 to 650 K the stable phase shifts to $PbCl_2$ (g). In the higher temperature range from 1100 to 1600 K, $PbCl_2$ (g) gradually decomposes, while the amount of PbO (g) increases and dominates above 1400 K. Minor amounts of PbCl (g) and Pb (g) (< 15% (mol/mol)) are also observed in the higher temperature range. A calculation including $PbCl_4$ (g) showed that this species had a large influence on the equilibrium distribution. $PbCl_4$ (g) was the single significant stable species from 300 to 1200 K and the dominating species up to 1300 K. This volatile behaviour at low temperatures is not experienced in real combustion plants where most of the volatile Pb is captured on fly ash particles. Hence $PbCl_4$ (g) was left out of the calculations. In the studies of Rigo and Sørum almost all of the volatile Pb is captured on fly ash particles in the filter systems.

Zn. Zn has a fairly complex equilibrium distribution. Starting with $ZnCl_2$ (cr,l) as the stable phase from 300 to 440 K, from where the stable phases is divided between $ZnCl_2$ (cr,l) and the silicate $2ZnO.SiO_2$ (cr) in a approximately 30/70 ratio up to 550 K. The amount of $2ZnO.SiO_2$ (cr) keeps stable at ~ 70% (mol/mol) up to 1570 K from where it gradually decreases to 55% (mol/mol) at 1600 K. From 550 to 980 K the remaining 30% (mol/mol) of Zn gradually shifts from the solid phase ZnO (cr) to the gaseous chloride $ZnCl_2$ (g) as the stable phase. The amount of $ZnCl_2$ (g) gradually decreases as the amount of Zn (g) increases from 1400 K. the studies of Rigo and Sørum showed that the volatile fraction of Zn is condensed on fly ash particles and captured in the filter systems.

Influence of S/S_{BC} ratio

No significant change in equilibrium distribution or volatile behaviour is observed at S/S_{BC} ratios lower than 1.0. For calculations at a S/S_{BC} ratio of 1.5 and higher, the equilibrium distribution for all metals with the exception of Hg changes. Figure 5 shows how the distribution of As, Cd, Cr, Cu, Ni, Pb and Zn have changed at a S/S_{BC} ratio of 2.0. $Ca_3(AsO_4)_2$ (cr) is no longer the stable solid phase, but As_2O_5 (cr) has taken over. As_2O_5 (cr) is more volatile than $Ca_3(AsO_4)_2$ (cr) making As fully volatilised at 860 K, instead of 1430 K for $Ca_3(AsO_4)_2$ (cr) at base case conditions. As_4O_6 (g) is observed as an intermediate species between 810-960 K, before AsO (g) becomes the only stable phase. The explanation of the shift from $Ca_3(AsO_4)_2$ (cr) to As_2O_5 (cr) when increasing the S/S_{BC} ratio is found in the fact that at a S/S_{BC} ratio of 2.0 there is enough S to bind Ca as $CaSO_4$ (cr) completely, while at a S/S_{BC} ratio of 1.0 Ca is only partly bound as $CaSO_4$ (cr) and partly CaO (cr,l). As opposed to when Ca is bound only as $CaSO_4$ (cr), parts of Ca will bind as $Ca_3(AsO_4)_2$ (cr) in competition with CaO (cr,l).

Cd becomes less volatile when increasing the S/S_{BC} ratio from 1.0 to 1.5 due to the shift to the thermally more stable cadmium sulphate ($CdSO_4$ (cr)) from the less stable cadmium chloride ($CdCl_2$ (cr,l)) as the stable phase at lower temperatures. At base case conditions $CdCl_2$ (cr,l) is fully volatilised at 650 K, however at a S/S_{BC} ratio of 2.0, where $CdSO_4$ (cr) is the stable phase, Cd is fully volatilised at 870 K. The equilibrium distribution above 900 K is the same for both S/S_{BC} ratios. Cd gets slightly less volatile when increasing the S/S_{BC} ratio from 1.5 to 10 as $CdSO_4$ (cr) decomposes at higher temperatures.

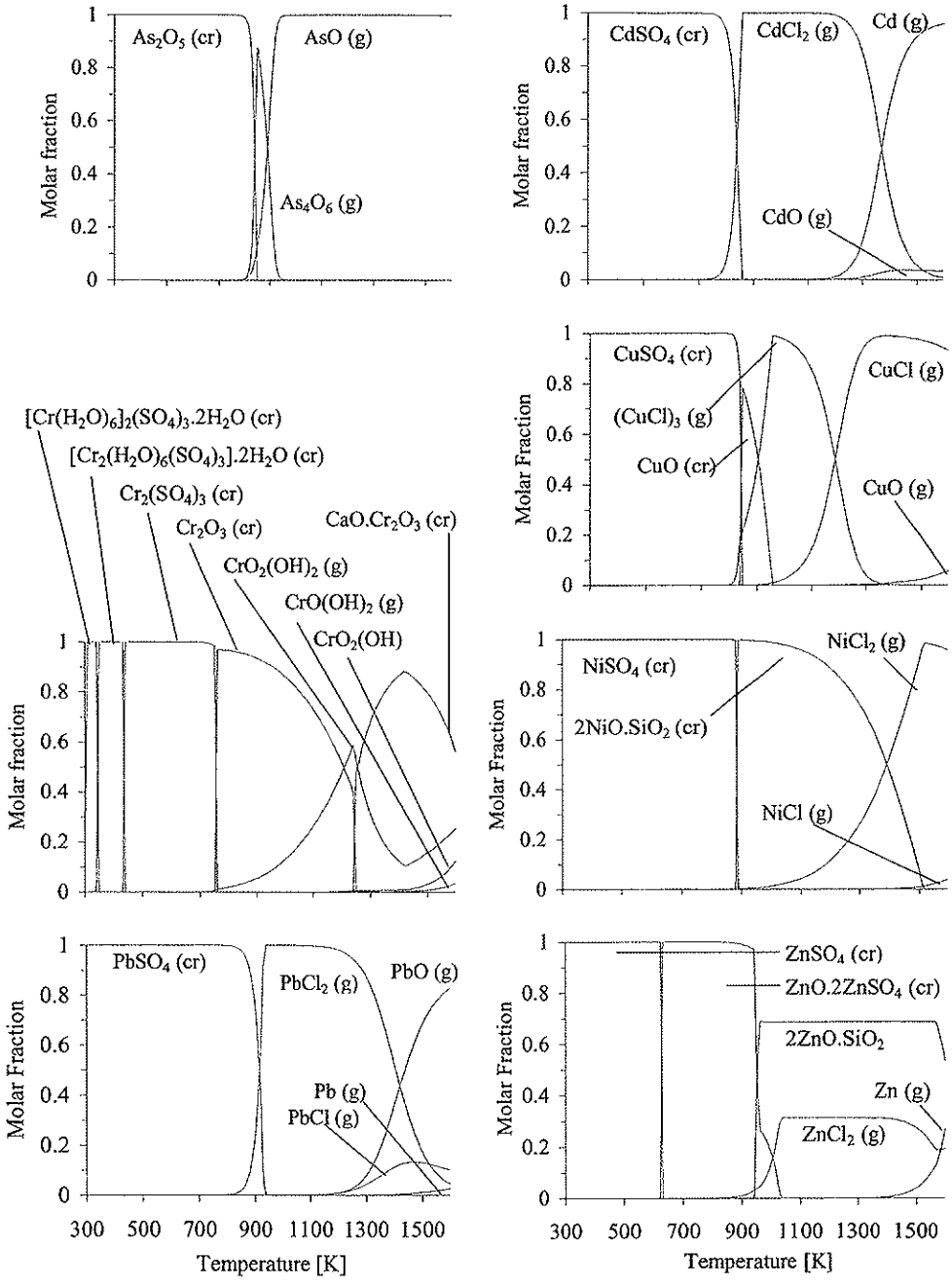

Figure 5. Equilibrium distribution of As, Cd, Cu, Cr, Ni, Pb and Zn at a S/S_{BC} ratio of 2.0.

The equilibrium distribution of Cr is strongly altered for S/S_{BC} ratio from 1 to 2 as can be observed in Figure 5. Instead of $CaO.Cr_2O_3$ (cr) being the dominant stable phase with an increasing amount of chromium oxides at higher temperatures at base case conditions, a major change in the equilibrium distribution is observed. At lower temperatures chromium forms two hydrated sulphate compounds: $[Cr(H_2O)_6]_2(SO_4)_3.2H_2O$ (cr) (below 350 K) and $[Cr_2(H_2O)_6(SO_4)_3].2H_2O$ (cr) (between 350 and 430 K). At 450 K, the solid non-hydrated sulphate, $Cr_2(SO_4)_3$ (cr), is formed and remains stable up to 770 K, from where Cr_2O_3 (cr) becomes the dominating stable phase. This distribution at lower temperatures is similar to the one Frandsen et. al. (1994) reported for combustion of coal. At higher temperatures, however, the equilibrium distribution is different, one of the reasons being that $CaO.Cr_2O_3$ (cr) was not included in the study of Frandsen et. al. Starting from 770 K, Cr_2O_3 (cr) gradually decomposes, forming $CrO_2(OH)_2$ (g). At 1240 K, however, a radical shift in equilibrium distribution occurs. The solid phase changes from Cr_2O_3 (cr) to $CaO.Cr_2O_3$ (cr) and the amount of this species increases at the expense of $CrO_2(OH)_2$ (g), up to 1430 K, from where it gradually decomposes into several gaseous chromium oxide species. The sudden shift of solid phase at 1240 K is connected to the decomposition of $CaSO_4$ (cr) into $CaCl_2$ (g). The decomposition of $CaO.Cr_2O_3$ (cr) above 1430 K may be connected to the partial shift of the solid phase of Ca to CaO (cr,l).

The volatile behaviour of Cu is not significantly altered when increasing the S/S_{BC} ratio from 1.0 to 10. At low temperatures, $CuSO_4$ (cr) is the stable phase at a S/S_{BC} ratio from 1.5 and higher, with a narrow temperature area of CuO (cr) after $CuSO_4$ (cr) has decomposed fully ($CuSO_4$ (cr) $\rightarrow$ CuO (cr) + SO_2 + ½ O_2). Increasing the S/S_{BC} ratio from 1.5 to 10, $CuSO_4$ (cr) goes from being fully volatilised at 830 to 920 K. CuO (cr) is fully volatilised at 970 K at all S/S_{BC} ratios, but the temperature range where it is stable becomes more narrow with higher S/S_{BC} ratio. Above temperatures of 970 K, the equilibrium distribution is not altered when varying the S/S_{BC} ratio. Ni shows the same behaviour as was observed

for Cu. The volatile behaviour is not altered when varying the S/S_{BC} ratio, but at lower temperatures (below 900-950 K), Ni is now stable as the solid sulphate, $NiSO_4$ (cr). Pb, however, becomes less volatile with increasing S/S_{BC} ratio. The shift from $PbCl_2$ (cr,l) to $PbSO_4$ (cr,l) (observed at S/S_{BC} ratio from 1.5) as the stable solid phase increases the temperature where Pb is fully volatilised from 660 to ~ 900 K, as the sulphate is stable at higher temperatures than the chloride. A further increase in S/S_{BC} ratio from 1.5 to 10 increases the temperature where Pb is fully volatilised with 80 K. Even though increasing the S/S_{BC} ratio from 1.0 to 1.5 shifts the stable phase of Zn at lower temperatures from chlorides and silicates to sulphates the volatility is not largely altered. However, at a S/S_{BC} ratio of 1.0 and lower, $ZnCl_2$ (g) is gradually increasing from 0 to 31% (mol/mol) from 510 tom 980 K, while at S/S_{BC} ratio of 1.5 $ZnCl_2$ (g) is increasing from 0 to 31% (mol/mol) from 820 tom 1020 K. Increasing the S/S_{BC} ratio further from 1.5 to 10 increases the temperature where the sulphate $ZnO.2ZnSO_4$ (cr) is fully decomposed from 1020 to 1110 K. Above 1100 K there is no significant difference in equilibrium distribution for Zn when varying the S/S_{BC} ratio. Especially for Pb and Zn the shift from condensed chlorides to sulphates at S/S_{BC} ratios equal or higher than 1.5 is important information since this may decrease deposit corrosion in the boiler (Krause (1989)).

Influence of Cl/Cl_{BC} ratio

As and Cr show no effect of a varying Cl/Cl_{BC} ratio. All other metals have to a varying degree effect of changing the Cl/Cl_{BC} ratio. Although the gaseous chlorides decompose at higher temperatures when increasing the Cl/Cl_{BC} ratio for Cd, Hg and Pb, there is no effect on the volatile behaviour. Cu, Ni and Zn become more volatile with increasing Cl/Cl_{BC} ratio. Increasing the Cl/Cl_{BC} ratio from 1.0 to 10 lower the temperature where Cu, Ni and Zn are fully volatilised from 970, 1520 and 1670 K to 670, 1000 and 780 K, respectively. A lower temperature of condensation will increase the possibility of heavy metal species condensing on

very small particles or aerosols, which might escape the filter system and consequently be emitted through the stack.

Influence of Ash/Ash_{BC} ratio

Increasing the ash/ash_{BC} ratio from 1.0 to 2.0 does only have effect on the equilibrium distribution for Zn. $2ZnO.SiO_2$ (cr) becomes more dominant on the expense of $ZnCl_2$ (cr,l), CuO (cr) and $ZnCl_2$ (g), below 1500 K, when increasing the ash/ash_{BC} ratio from 1.0 to 2.0. Decreasing the ash/ash_{BC} ratio, however, give significant changes in the equilibrium distribution for all metals with the only exception of Hg. The changes are similar to those described when increasing the S/S_{BC} ratio to 1.5 or higher, were a shift from heavy metal chlorides to sulphates was observed at lower temperatures. Hence reducing the flyash content may reduce corrosion in deposits due to the shift from Pb and Zn chlorides to sulphates.

Influence of λ

The only significant effect of changing λ from 1.1 to 1.9, is that Cu becomes slightly less volatile (temperature where CuO (cr) is fully volatilised increases from 870 to 970 K) and that Cr becomes slightly more volatile. Cr becomes more volatile because increasing the excess air number will force $CaO.Cr_2O_3$ (cr) to decompose into gaseous chromium oxides in order to maintain equilibrium.

CONCLUSIONS

The lack of knowledge on the fate of As, Cd, Cr, Cu, Hg, Ni, Pb and Zn at typical conditions for MSW combustion has motivated this work. The fate of these metals has been studied using equilibrium calculations. As opposed to similar studies in this field, ash species are included in order to investigate possible interactions with the heavy metals. These heavy metals behaves differently with respect to the volatility and re-condensation at combustion conditions in a grate furnace. The heavy metals also responded differently to changes in MSW composition and operational parameters. Thus, no overall conclusion applicable to all heavy metals

is provided. The conclusions are divided in two separate parts; one considering the conditions on the grate and one considering the conditions in the flue gas as it is transported from the furnace to the filter.

On the grate

The equilibrium calculations investigating the volatile behaviour on the grate shows that Cd, Hg and Pb is fully volatilised between 950 and 1600 K. Cr, however, is stable in solid phase practically over the entire temperature range. Only a small amount is volatilised at high temperatures. No influence on the volatility of Cr was observed when changing the sulphur or chlorine content. Cd, Hg and Pb showed no response, while Cr became slightly more volatile at higher temperatures with decreasing fuel/air ratio.

The volatile behaviour of As, Cu and Zn is largely altered when shifting from reducing to oxidising conditions. Whereas As and Zn become less volatile when shifting from reducing to oxidising conditions, Cu becomes more volatile. Changing the sulphur content only resulted in a change for Cu, making it less volatile with increasing sulphur content at reducing conditions.

At reducing conditions the volatile behaviour of As and Zn is not influenced by changes in the chlorine content, while Cu become more volatile when increasing the content of chlorine. At oxidising conditions, Cu (at low chlorine content) and Zn becomes more volatile, while As experienced no change when increasing the chlorine content.

Although the equilibrium distribution changed, Ni experienced no change in the volatile behaviour when varying the sulphur content. Ni did, however, become more volatile when increasing the chlorine content, while varying λ did not significantly alter the volatile behaviour of Ni. These observations apply both for reducing and oxidising conditions.

Furnace to Filter

Investigation of the condensing behaviour of the heavy metals as they pass through the boiler and enter the flue gas cleaning system on their way to the stack (500–300 K), revealed that only Hg was present in gas phase.

Increasing the Cl/Cl_{BC} ratio from 1.0 to 10 lower the temperature where Cu, Ni and Zn are fully volatilised from 970, 1520 and 1670 K to 670, 1000 and 780 K, respectively. A lower temperature of condensation will increase the possibility of heavy metal species condensing on very small particles or aerosols, which might escape the filter system and consequently be emitted through the stack.

Solid phase interaction between As and Cr with Ca and silicates of Ni and Zn were identified. In the case of As at oxidising conditions, the formation of $Ca_3(AsO_4)_2$ (cr) was dependent on the S/Ca ratio. A high S/Ca ratio, which is obtained by a high sulphur content or low concentration of fly ash in the flue gas, will favour the formation of As_2O_5 (cr) rather than the less volatile $Ca_3(AsO_4)_2$ (cr). A low S/Ca ratio will on the other hand favour the formation of $Ca_3(AsO_4)_2$ (cr). Another important consequence of increasing the sulphur/chlorine ratio in the flue gas (S/S_{BC} ratios equal or higher than 1.5), is the shift from solid phase metal chlorides to sulphates for Cd, Cr, Cu, Ni, Pb and Zn at lower temperatures. In the case of Pb and Zn, a shift from the highly corrosive species $PbCl_2$ (cr,l) and $ZnCl_2$ (cr,l) to $PbSO_4$ (cr) and $ZnSO_4$ (cr) may reduce corrosion in the boiler sections significantly in a combustion plant for MSW. Increasing the sulphur/chlorine ratio in the flue gas may be obtained by removing waste with high chlorine content such as PVC, or reducing the fly ash content. At high fly ash content the sulphur is bound to the ash as $CaSO_4$ (cr) up to 1300 K. Reducing the fly ash content will increase the amount of available sulphur to form heavy metal sulphates.

REFERENCES

Barton, R. G.; Maly, P. M.; Clark, W. D.; Seeker, W. R., (1988), Prediction of the fate of toxic metals in waste incineration, In *Proceedings of ASME 13th National Waste Processing Conference.*

Barton, R. G., Clark, W.D. and Seeker, W. R., (1990), Combustion Science and Technology, **74**, 327-342.

Benestad, C. Braastad, G., Normann, H. H., Færden, T., Nåmdal, S., Moe, M. and Hoel, A., (1995), Combustion plants – a guide for officials in charge, Norwegian Pollution Control Authority, Report 95:13.

Brunner, P.; Mönch H., (1986), *Waste Management and Research*, **4**, 105-119.

Clarke, M. J., (1991), *Waste Age United States*, **May**, 105-118.

Frandsen, F. J.; Dam-Johansen, K.; Rasmussen, P. (1994), *Prog. Energy Combust. Sci.*, **20**, 115-138.

Frandsen, F. J., (1995), Ph.D. Thesis, Technical University of Denmark.

Frandsen, F. J., Erickson, T. A., Kühnel, V., Helble, J. J. and Linak, W. P. (1996), Equilibrium Speciation of As, Cd, Cr, Hg, Ni, Pb and Se in Oxidative Thermal Conversion of Coal – A Comparison of Thermodynamic Packages, *Technical report no. 9620*, Technical University of Denmark.

Frandsen, F. J., Dam-Johansen, K., Rasmussen, P. (1996), GFE-DBASE - A Pure Component Trace Element Thermochemical Database, CALPHAD; **20** (2), 175 - 229.

Ghorishi, B.; Gullett, B. K. (1997), An Experimental Study on Mercury Sorption by Activated Carbons and Calcium Hydroxide, *Proceedings of the Fifth Annual North American Waste-to-Energy Conference*, Apr 22-25, North Carolina, USA.

Gort, R., (1995), Phd Thesis, Twente University, The Netherlands.

Hasselriis, F. and Licata, A. (1996), *Journal of Hazardous Materials*, **47**, 77-102.

Heie, Aa; Sørum, L. (1997), Interconsult Report 3924.003.

Krause, H. H. (1989), Corrosion by chlorine in waste-fuelled boilers, *In Proceedings of the International Conference on Fireside Problems While Incinerating Municipal and Industrial Waste.*

Laughlin, K. (2000), IEA report Task 23, "The Management of residues from thermal processes", in press.

Lee, C. C. (1988), *J. Air Poll. Contr. Assoc*, **38**, 941-945.

Ljung, A.; Nordin, A. (1997), *Environ. Sci. Technol.*, **31**, 2499-2503.

Nussbaumer, T. (1994), Emissions from biomass combustion, *Proceedings of IEA Biomass Combustion Conference*, Cambridge.

Obernberger, I. (1998), Ashes and particulate emissions from biomass combustion - Formation, characterization, evaluation and treatment, TU Graz, Austria, ISBN 3-7041-0254-7.

Rigo, H. G.; Chandler, A. J. (1994), Metals in MSW - Where are they and where do they go in an incinerator?, *Proceedings of the National Waste Processing Conference*, ASME, USA.

Sandgren, J.; Heie, Aa.; Sverud, T. (1996), Norwegian pollution control authority (SFT) Report 96:16.

Soma, M. H. (1986), What Kind of Emissions Do We Get from Waste Combustion, Technical Winterweek 1986, EG61b, The Association of Norwegian Chartered Engineers, Oslo, p. 31.

Srinivasachar, S., Boni, A. and Bryers, R. W. (1989), Partitioning of chlorides and Sulfates of lead during Incineration: Thermochemical calculations, *In Proceedings of the International Conference on Fireside Problems While Incinerating Municipal and Industrial Waste.*

Sørum, L.; Fossum, M.; Evensen, E.; Hustad, J. E. (1997), Heavy Metal Partitioning in a Municipal Solid Waste Incinerator, *Proceedings of the Fifth Annual North American Waste-to-Energy Conference*, Apr 22-25, North Carolina, USA.

Verhulst, D.; Buekens, A.; Spencer, P. J.; Eriksson, G. (1996), *Environ. Sci. Technol.*, **30**, 50-56.

Wu, C. Y.; Biswas, P. (1993), *Combustion and Flame*, **93**, 31-40.

APPENDIX

Species used in calculations

Table 1. Combustion products species used for both reducing and oxidising conditions. All species are valid up to 2000 K.

Combustion Products				
CH_4 (g)	HCN (g)	H_2S (g)	NOCl (g)	OH (g)
CO (g)	HCl (g)	H_2S_2 (g)	NO_2 (g)	O_2 (g)
CO_2 (g)	HNO (g)	H_2SO_4 (g)	NO_2Cl (g)	S (g)
COS (g)	HNO_3 (g)	NH (g)	N_2 (g)	SO (g)
Cl (g)	HS (g)	NH_2 (g)	N_2H_4 (g)	SO_2 (g)
ClO (g)	H_2 (g)	NH_3 (g)	N_2O (g)	SO_3 (g)
Cl_2 (g)	H_2O (g)	NO (g)	O (g)	C (cr)*

* Only included in calculations on reducing system.

Table 2. Ash species. All ash species are valid up to 2000 K.

Aluminium	Silicon	Calcium	Iron
Al (g)	**Si (g)**	**Ca (g)**	**Fe (g)**
AlCl (g)	**SiCl (g)**	**CaCl (g)**	**FeCl (g)**
$AlCl_2$ (g)	**$SiCl_2$ (g)**	**$CaCl_2$ (g)**	**$FeCl_2$ (g)**
$AlCl_3$ (g)	**$SiCl_2H_2$ (g)**	**CaO (g)**	**$FeCl_3$ (g)**
AlO (g)	**$SiCl_3$ (g)**	**Ca(OH) (g)**	**FeO (g)**
Al(OH) (g)	**$SiCl_4$ (g)**	**$Ca(OH)_2$ (g)**	**$Fe(OH)_2$ (g)**
AlO_2 (g)	**SiH (g)**	**CaS (g)**	FeS (g)
AlS (g)	**SiH_4 (g)**	*Ca_2 (g)*	Fe_2Cl_4 (g)
OAlCl (g)	**SiO (g)**	$CaCl_2$ (cr)[b]	FeO (cr)
OAl(OH) (g)	**SiO_2 (g)**	$CaCl_2$ (l)[b]	FeO (l)[b]
Al_2 (g)	**Si_2 (g)**	CaO (cr)	$FeS_{0.877}$ (cr)[b]
Al_2Cl_6 (g)	**Si_3 (g)**	CaO (l)	*Fe_2O_3 (cr)*
Al_2O (g)	**SiO_2 (cr,l)**	*CaO (cr,l)*	*Fe_3O_4 (cr)*
Al_2O_2 (g)		CaS (cr)	**$FeO.Cr_2O_3$ (cr)[a]**
Al_2O_3 (cr,l)		*$CaSO_4$ (cr)*	

Bold: Species used for both reducing and oxidising conditions.
Normal: Species used only for reduced conditions.
Italic: species used only for oxidising conditions.
[a] Only used in calculations with Cr.
[b] Used up to 1200 K.

Table 3. Heavy metal species used in calculations.

Species	Temperature	Species	Temperature
As (g)	2000	**$CrO_2(OH)_2$ (g)**	3000
$AsCl_3$ (g)	2000	**$CrO(OH)_4$ (g)**	3000
AsH_3 (g)	2000	**$Cr(OH)_6$ (g)**	3000
AsO (g)	2000	CrS (g)	2000
AsS (g)	1500	Cr (cr)	2000
As_2 (g)	2000	**$CrCl_2$ (cr,l)**	1500
As_3 (g)	2000	$CrCl_3$ (cr)	1000
As_4 (g)	2000	**Cr_2O_3 (cr)**	2000
As_4O_6 (g)	*2000*	CrS (cr)	2000
As_2O_3 (cr,l)	*700*	**$Cr_2(SO_4)_3$ (cr)**	*780*/1000
As_2O_5 (cr)	*1000*	*$[Cr(H_2O)_6]_2(SO_4)_3.2H_2O$*	540
$Ca_3(AsO_4)_2$ (cr)	*1700*	*$[Cr(H_2O)_6]_2(SO_4)_3.3H_2O$*	540
		$[Cr(H_2O)_6]_2(SO_4)_3.4H_2O$	540
Cd (g)	2000	*$[Cr(H_2O)_6]_2(SO_4)_3.5H_2O$*	540
$CdCl_2$ (g)	2000	*$[Cr_2(H_2O)_6(SO_4)_3].2H_2O$*	540
CdO (g)	2000	**$CaO.Cr_2O_3$ (cr)**	1900
CdS (g)	2000		
Cd (cr,l)	1000	**Cu (g)**	2000
$CdCl_2$ (cr,l)	1200	**CuCl (g)**	2000
CdO (cr)	*1700* /1200	**CuH (g)**	2000
$CdO.Al_2O_3$ (cr)	1200	**CuO (g)**	2000
$CdO.SiO_2$ (cr)	*1700* /1200	CuS (g)	2000
$Cd(OH)_2$ (cr)	1200	**Cu_2 (g)**	2000
CdS (cr)	*1700*/1200	**$(CuCl)_3$ (g)**	2000
$CdSO_4$ (cr)	*1300*/1200	**CuCl (cr,l)**	1400
		CuO (cr)	1300
Cr (g)	2000	$CuO.Al_2O_3$ (cr)	1400
$CrCl_2$ (g)	2000	$CuO.Fe_2O_3$ (cr)	1300
$CrCl_2O_2$ (g)	2000	**CuS.FeS (cr)**	1200
$CrCl_3$ (g)	2000	**$CuSO_4$ (cr)**	1000
$CrCl_4$ (g)	2000	$Cu_2O.Al_2O_3$ (cr)	1200
CrO (g)	2000	$Cu_2O.Fe_2O_3$ (cr)	1600
Cr(OH) (g)	3000	Cu_2S (cr,l)	2000
CrO_2 (g)	2000	**Cu_5FeS_4 (cr)**	1200
$Cr(OH)_2$ (g)	3000		
CrOOH (g)	3000		
CrO_3 (g)	2000		
$Cr(OH)_3$ (g)	3000		
$CrO(OH)_2$ (g)	3000		
$Cr(OH)_4$ (g)	3000		
CrO_2OH (g)	3000		
$CrO(OH)_3$ (g)	3000		
$Cr(OH)_5$ (g)	3000		

Table 3. Continued.

Species	Temperature	Species	Temperature
Hg (g)	2000	**Pb (g)**	2000
HgCl (g)	2000	**PbCl (g)**	2000
$HgCl_2$ (g)	2000	**$PbCl_2$ (g)**	2000
HgH (g)	2000	**PbO (g)**	2000
HgO (g)	2000	PbS (g)	2000
HgS (g)	2000	**Pb_2 (g)**	2000
$HgCl_2$ (cr,l)	1500	Pb (l)	2000
HgO (cr)	1000	**$PbCl_2$ (cr,l)**	2000
Hg_2Cl_2 (cr)	1500	**PbO (cr,l)**	2000
		$PbO.SiO_2$ (cr)	1800
Ni (g)	2000	**$2PbO.SiO_2$ (cr)**	1800
$Ni(CO)_4$ (g)	2000	PbS (cr)	1800
NiCl (g)	2000	**$PbSO_4$ (cr,l)**	1800
$NiCl_2$ (g)	2000	**Pb_3O_4 (cr)**	1500
NiO (g)	2000		
Ni (cr,l)	2000	**Zn (g)**	2000
$NiCl_2$ (cr,l)	1400	**$ZnCl_2$ (g)**	2000
NiO (cr)	2000	ZnS (g)	2000
$NiO.Al_2O_3$ (cr)	2000	Zn (cr,l)	1100
NiS (cr,l)	2000	*$ZnCl_2$ (cr,l)*	900
NiS_2 (cr,l)	2000	**ZnO (cr)**	2000
$NiSO_4$ (cr)	1200	**$ZnO.SiO_2$ (cr)**	2000
$NiO.Fe_2O_3$ (cr)	1500	ZnS (cr,S)	1300
$2NiO.SiO_2$ (cr)	1800	**$ZnSO_4$ (cr)**	1500
Ni_3S_2 (cr,l)	2000	**$2ZnO.SiO_2$ (cr)**	2000
		$ZnO.2ZnSO_4$ (cr)	1200

Bold: Species used for both reducing and oxidising conditions.
Normal: Species used only for reducing conditions.
Italic: species used only for oxidising conditions.

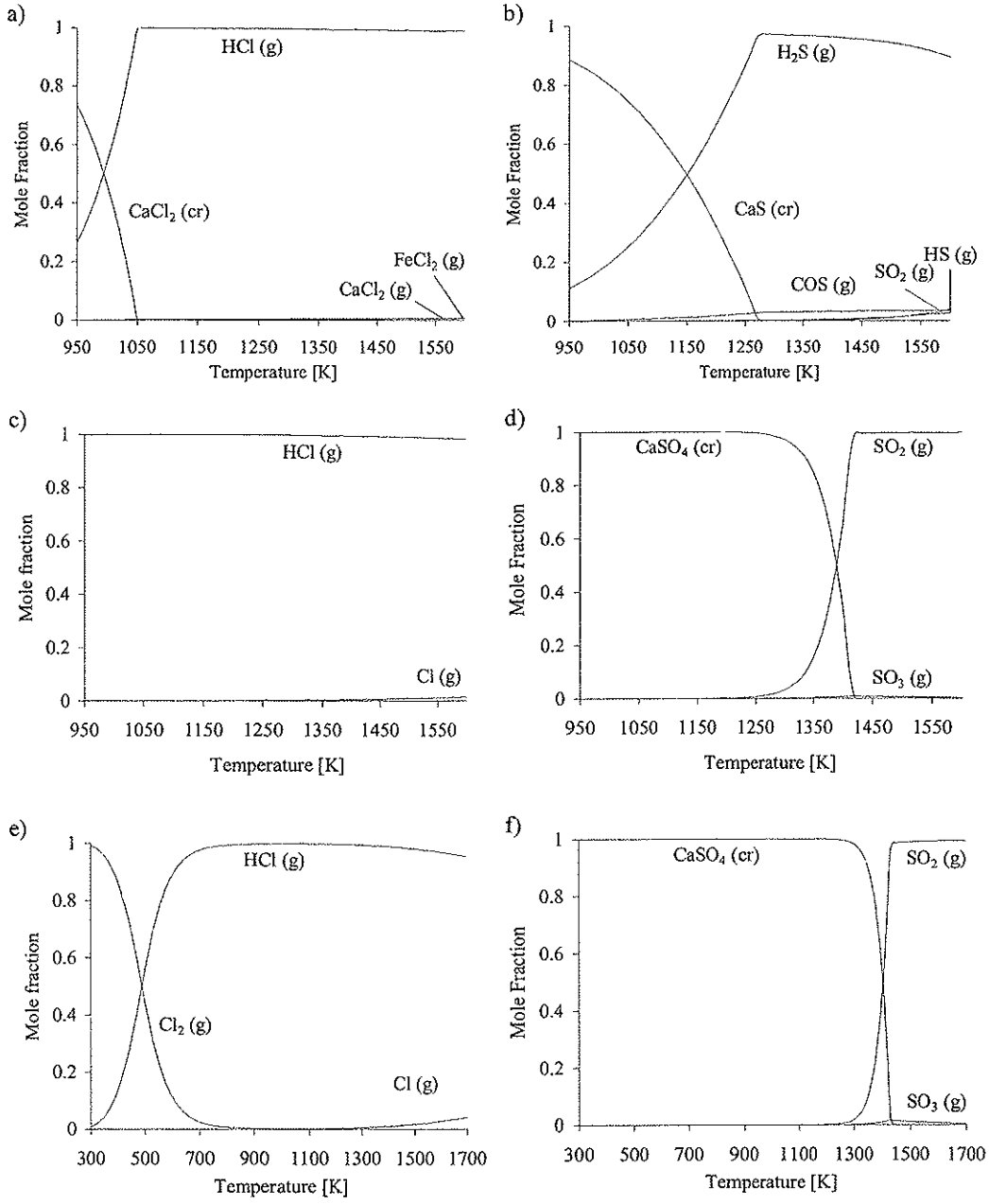

Figure 6. Chlorine and sulphur balance for the three different base case calculations. a) and b): reducing conditions on grate, c) and d): oxidising conditions on grate, e) and f): oxidising conditions in flue gas.

5 Further work

MSW is a complex fuel consisting of various components with different properties and chemical composition at different mixture ratios. Knowing how to reduce harmful pollutant emissions and optimise operational conditions requires detailed knowledge regarding all aspects of MSW combustion. It is the author's opinion that the need for research in the field of MSW combustion is considerable. The complex fuel, varying compositions, and stricter and stricter emission requirements makes design and operation of combustion plants a challenge. In general, some important subjects related to thermal conversion of MSW are:

- Modelling of MSW combustion. Development of models describing the devolatilisation of the solid fuel and the subsequent gas phase combustion.

- Further development of primary NO_x reduction methods applicable in MSW combustion.

- Environmental consequences of burning different waste fractions/components and mixtures thereof.

- Electricity efficiency in energy recovery from MSW (i.e. increase steam temperature and pressure (need for new corrosion resistant materials in boilers), new processes like gasification and pyrolysis (combined cycle))

The need for further work particularly related the three subjects investigated in detail in this thesis are:

- Experimental data on pyrolysis gas composition from MSW components and mixtures thereof are needed. The influence of parameters such as final temperature and heating rates should be investigated.

- Further investigation of NO formation and formation mechanisms for MSW components and mixtures as a function of process parameters such as temperature, residence time, oxygen concentration, etc. in order to be able to assess different primary NO_x reduction techniques in detail (e.g. the conversion of fuel nitrogen to HCN, NH_3 and N_2).

- Kinetic data on heavy metal reactions in MSW combustion is needed.

- Experimental investigations of the influence of parameters such as temperature, oxygen concentrations, sulphur and chlorine, on the volatile and re-condensation behaviour of heavy metals in MSW combustion will give new and valuable data.

- Equilibrium calculations on heavy metals not included in this study, that are included in the new emission requirements for MSW combustion plants (i.e. titanium (Ti), cobalt (Co), vanadium (V), tin (Sn), antimony (Sb), and manganese (Mn)).

- Include more ash species (e.g. phosphorus (P), sodium (Na) and potassium (K)) in equilibrium calculations.

Appendix A: Paper V

Future Industrial and Municipal Waste Management in Poland – "The Polish Challenge"

In Proceedings of the Fifth International Conference on Energy and Environment, Cairo, Egypt, 1996.

Editors: Abdul Latif El-Sharkawy and Ralph H. Kummler

FUTURE INDUSTRIAL AND MUNICIPAL WASTE MANAGEMENT IN POLAND - "THE POLISH CHALLENGE"

Janusz Nowakowski*, Lars Sørum**, Johan E. Hustad**
* Technical University of Szczecin, Department of Heat Engineering
Al. Piastow 19, PL-70-310 Szczecin, Poland
** Norwegian University of Science and Technology
Department of Thermal Energy and Hydro Power
Kolbjørn Hejes v. 1A, N-7034 Trondheim, Norway

Abstract

Poland now face a very interesting discussion on modern waste treatment methods, although the waste problems are very old. This paper presents a total waste management view from the formation process to recycling, utilisation and landfilling. The average municipal solid waste (MSW) annual per capita generation in Poland is 250 kg per person, which is half of the waste amount generated in Norway and one third of the amount in USA. The present low per capita generation, large variations in MSW properties and an expected growth in the standard of living make the decisions regarding future Polish waste management systems very important. Waste management must be handled carefully to prevent a rapid growth of waste generation - this is the "Polish challenge", both now and for the future. Three different possibilities for future waste management systems for rural areas, small cities and larger cities are discussed in the paper.

1. INTRODUCTION

The amount of MSW in Poland has increased with 80 vol% from 1975 to 1992 [1]. The economy system in Poland changed to market economy in 1989 and since there has been a stagnation period on waste generation. The composition of MSW in Poland is different from other (western) countries, distinguished with a lower content of paper and plastics and a higher content of organic and inorganic waste. However, these characteristics are expected to be more comparable in the future.

The paper is divided into two parts - the first part presents the state-of-the-art in Polish waste generation, characterisation and waste management. The second part presents the government plans for future waste management systems and three different possibilities for future waste management systems for rural areas, small cities and large cities. Since 98,7% of MSW generated in Poland today is landfilled [1] and lack of landfill sites is expected for the future, it seems necessary to employ other methods for volume reduction of waste in the future. Energy estimations for different treatment methods of MSW are performed.

Since household waste is a very small percentage (typically in Europe 6-10%) [2] of total waste created, it is apparent that individuals only can have a small impact on overall waste volumes generated and that the largest contribution to reducing waste must come from government waste policy and manufacturing industry, agriculture and from the construction and demolition sectors. The only influence individuals have on waste generation is to buy less, buy longer life products and to re-use items.

The average MSW per capita generation in Poland is 250 kg per person a year, which is one third of the amount generated in USA [3] and half the amount generated in Norway [4]. Previous studies have shown that the variation in waste properties is large in Poland so waste management must be handled very carefully.

Laws, rules and regulations should create possibilities for a good and proper environmental protection. This includes proper waste management systems and providing basic directions and constraints concerning water, ground, and air pollution. The appropriate waste management hierarchy should set specific succession in decision making on Ministry and Parliament level [5]:

1. Minimise waste generation
2. Recycling
3. Utilisation (thermal destruction and energy recovery, composting)
4. Landfilling

Waste management is controlled under the 1980 Environment Protection Act (EPA) and a number of Cabinet Decrees [1]. The EPA defines wastes, states the responsibilities of waste generators and the duties of local government offices, together with penalties and fines for breaches of the regulations. The EPA is supported by new directives (investment and non-investment enterprises) established in 1995 by the Parliament, which are aimed at decreased landfilling of waste, neutralising of hazardous waste and economical use of waste (mainly waste from energy production) [5]. The governmental bodies responsible for waste management in Poland are [1]:

- Ministry of Environment Protection, Natural Resources and Forestry,
- Ministry of Physical Planning and Construction,
- Ministry of Health and Social Welfare,
- Ministry of Industry.

The information flow between ministries, local communities and councils up to ministry and back, and a competent financial system must function well to implement any ideas. The governmental and local authorities efforts and money can, however, be in vain if the communities do not collaborate for the best results. Education and information play a significant role for each individual's understanding of the waste management problem. It is impossible for the government to control all parts of the country, therefore the local authorities are very important. Only the councils having all of the data and knowledge of the communities' needs are able to make the correct decision for their region.

A free market and people's wish to live in a clean world, country and region should force environmental friendly activities, supported by governmental policy. A master plan and strategy study for regions are elaborated by consulting the proper expertise and by co-ordinating the work with councils. The next step in the decision making is to find a financial source. There is a possibility to take credit from a national, private or international financing institution (bank). After a feasibility study the project together with the bank's credits goes to realisation and then to exploitation.

2. PRESENT WASTE MANAGEMENT AND CHARACTERISATION

The waste is divided into three different categories namely municipal waste, industrial waste and special/hazardous waste. This chapter gives a presentation of definitions, amounts, composition and present waste management systems for the three different types.

Municipal Waste

Municipal waste is consistent with municipal solid waste (MSW) and municipal liquid waste. MSW is household waste and institutional/commercial waste. In general it is all waste collected by each municipality, industrial and hazardous waste excluded. Figure 1 shows that the total amount of MSW accumulated from 1975 to 1992 is 712 mill m^3. The definition of city is an administrative one and there are 835 cities in Poland. In 1992 the amount of MSW in Polish cities or urban areas was 47 mill. m^3/yr, with an average of 1.23 m^3 per capita per annum and variation between housing types and between cities with different housing stock [1]. Average density is approximately 200 kg/m^3 [1,6]. The Polish MSW is in general characterised by low effective heating value and combustion is not possible without pre-treatment. Table I shows the characteristics of Polish MSW for three areas with different population density.

There is a distinct difference between these three categories, where cities and small cities have the largest per capita generation. Cities have a higher heating value for the waste as a result of higher paper, plastic and food waste content and lower content of inorganic material. Smaller cities have slightly higher heating value than rural areas due to the same factors as mentioned above, but the per capita generation is 67% higher for small cities than for rural areas. Due to more waste from institutions, shops, hotels, etc. the generation would be larger and the composition would be distinguished by a higher content of paper, plastic and food waste as it gets more urban. A culture for re-use of paper and plastics for combustion and also the use of food wastes for compost in rural areas could explain some of the differences in composition.

The variation in composition for MSW is dependent on several factors [1]. Seasonality, heating system (ash content in MSW), standard of living, packaging, overcrowding (recycling/composting is difficult).
MSW collection in Poland is carried out by the Public Cleansing Enterprise of each community's environmental protection department, or by private enterprises authorised by them. The service covers urban areas, but it is estimated that between 20% and 40% of rural areas are covered at best. The average service coverage factor for Poland was 55% in 1990 [1]. Collection methods for MSW vary, but there is an emphasis on use of large containers in apartment blocks and at special collection points. The frequency of collection is 2 to 3 times per week from apartment buildings, and weekly from scattered housing areas, detached houses and suburban buildings. There are currently three methods in use for treatment and disposal of MSW in Poland, namely landfilling, composting and recycling. In 1992 the 47 million m^3 of MSW generated were disposed as follows [1]:

- Landfilling 98.7 %
- Composting 1.3 %
- Recycling Negligible post-consumer

There are currently some pilot projects carried out on recycling of not separated glass and paper in selected areas in Poland. At the end of 1995, contracts were signed for the construction of Poland's first glass recycling plant in the city of Kutno [7].
The generation of municipal liquid waste or sewage sludge in 1993 was 14.9 mill m^3 [5]. Sewage sludge is presently for rural areas treated at source, smaller cities have treatment plants (biogas, chemical and biological treatment) and larger cities dump the sewage sludge (into rivers, landfilling).

Industrial Waste.

The waste generated during any production process by small and large factories which can not be used in further processes are named "industrial waste". The waste "producers" are responsible for removing, collecting and managing of the refuse. The waste management system should therefore be a part of the production line. Poland generated in 1993 120,5 million tons of industrial waste that was treated as follows:

- 53,6 % Utilised for site levelling, filling of mining excavations, building and road industry
- 0,3 % Neutralised
- 46,1 % Landfilled, dumped on heaps and in sediment ponds

As we can see almost half of the generated industrial waste was landfilled which will increase the problem with lack of landfill sites. Accumulated amount of industrial waste was in 1993 1834,9 million ton [5]. The industrial waste composition is as follows [5]:

- 42,6 % Mining refuse
- 30,0 % Floatation sludge
- 15,0 % Fly ash/slag from energy prod.
- 4,4 % Metallurgical slag
- 3,0 % Phospho-gypsum
- 2,0 % Sodium industry refuse
- 0,4 % Metallurgic gas cleaning sludge and dust
- 0,4 % Waste water treatment plant sludge,
- 0,3 % Calcium carbide,
- 1,9 % Others.

Special / Hazardous Waste.

Waste which is dangerous for human life or health or for environment due to its origin, chemical or biological composition or other properties like: toxic, flammable, explosive or radioactive, are named special / hazardous wastes [6]. The producers of hazardous refuses are mainly chemical industry and hospitals. There exists a few hospital waste incineration plants nearby hospitals, some are just incinerating hospital refuse and some are able to produce steam and hot water for hospital needs.
In 1993 the Polish industry produced 3,44 million tons of hazardous waste where 66,2 % were economically used, 0,9 % were specially neutralised and the rest was dumped. 1369 dumping sites have accumulated 258,24 million tons of special / hazardous waste (1993) [5]. The hazardous waste producers are specially equipped and trained for safety handling and transport, also in the case of an emergency.

3. FUTURE WASTE MANAGEMENT SYSTEMS - "THE POLISH CHALLENGE"

Future waste management systems in Poland should be based on a socio-economic correct treatment of waste as a resource and problem. Where economic aspects concerning both investment

costs and pay back time for different treatment systems should be compared to environmental aspects such as air, soil and water pollution and the potential costs for solving these problems for the different waste management systems. Poland's economy and energy infra-structure should also be taken into consideration when new waste management systems are planned.

Figure 2 shows the development of per capita generation of MSW from 1975 to 1992. From 1992 to 2010 we have made three different scenarios for the per capita generation. Since Poland has a very low per capita generation, there is a very good opportunity to level out this development for the future and for 2010 may be reach a per capita generation of 300 kg/yr (scenario I). This is an increase of 20% compared to 1992 and could be a realistic goal for 2010. Since Poland is a country in great development and will probably, after a stabilisation period with implementation of market economy in 1989, again increase their per capita generation towards the year 2010 due to an expected increase in standard of living. Scenario II and III which is typical generation for western countries should be avoided. The assumed increase in standard of living will also be a major factor for the changes in composition of MSW in the future. It is assumed that there will be an increase in combustible matter and a higher calorific value and a decrease in moisture content.

Poland's starting point for implementation of new waste management systems is very good due to the low per capita generation and it is possible to enforce the first law in the waste management hierarchy namely minimisation of waste generation.

The estimation of future generation of industrial waste is more complex. Industrial waste comes mainly from coal mining and an increase in living standard should give an increase in energy consumption and hence an increase in industrial waste. On the other hand export of coal could decrease due to carbondioxide taxes for instance, and hence the industrial waste generation could level out or even decrease. Therefore, any assumption on industrial waste generation for the future is not included.

Waste management systems for Poland are divided into three different categories dependent on population density. The reason for that is that Poland have a distinct difference in composition and also generation of MSW for areas with different population density and hence a need for different waste management systems. Industry and industrial waste are also dependent on population density, where agriculture waste dominates the rural areas, wood waste from wood processing and waste from food producers dominates the smaller cities and waste from coal mining dominates the coal basin (larger) cities.

The government have the following future plans for waste management within year 2000 [5]: Build 2 incineration plants with capacity of 600 ton/day each for MSW. Build 10 composting plants with capacity of 100 ton/day each. Implement source separation collecting systems in 20 communities. Build 10 large regional dumping sites and numerous communal dumping sites. Build 3 regional neutralising plants with capacity 20 ton/day each for hazardous waste. Organise 20 regional systems for neutralising of hospital waste. Build 10 installations to locate mining and waste from energy production in mining excavations (30 million ton/year). Build installation for generating market gypsum from flue gas desulfurisation products.

Waste Management in Rural Areas

Due to the low coverage factor for collecting MSW (20-40%) and large amount of illegal landfill sites, waste should to a great extent be source separated and utilised at source in rural areas. MSW generation in rural areas is 60 vol% less compared to small and larger cities. The composition is distinguished by a high content of inorganic materials and fines (0-10mm) and low content of food wastes, paper and plastics. The waste has a low heating value due to the low content of combustible matter (12 weight%), therefore collection of rural MSW for combustion would be very expensive due to several factors such as:

- Collecting distances
- Small quantities
- Processing
- Poor quality of waste

A process scheme for a waste management system for rural areas is shown in figure 3. Sewage sludge is collected in a collecting tank and transported to small or larger cities for treatment. MSW should be source separated. Glass which is one of the five main components of rural MSW is subjected to recycling and should be collected in a separate container. Paper should be combusted at source for heating purposes during the cold period, which is the present common practice. Otherwise paper could be collected in a separate container for recycling. Plant and animal origin food wastes and remaining organic wastes

according to table 1 should be composted at source. Many people in rural areas already compost organic wastes today, so this should be easy to implement. The rest fraction after utilisation of organic, glass and paper wastes should be collected and landfilled.
We have focused on making a simple realistic system which could be implemented without too much efforts and investments put into a new waste management system.
In rural areas agriculture could be looked upon as "industry" and a source separation of different wastes into three different categories would be suitable. Plant origin wastes and food wastes should be composted at source. Straw which today is burnt out in the fields should be utilised for energy production. The straw should be transported to small or larger cities for energy recovery, because it is not possible to utilise straw for energy recovery in an economic way in rural areas. There is presently a collaboration between Poland and Denmark on utilisation of straw for energy recovery.

Waste Management in Small Cities

Higher population density and a larger fraction of combustible components makes small cities suitable for a more integrated waste management system with source separation, recycling and RDF (Refuse Derived Fuel) production. RDF processing facilities will become more common in the future because of the increasing interest in material recovery from waste. Figure 4 shows a proposed waste management system for small cities. Sewage sludge from rural areas and smaller cities should be treated at a biogas plant. The gas should be utilised for electricity and heat production and the rest fraction from processing should be used as fertiliser. Small cities should sort out glass from MSW at source for recycling. The rest should be handled at a RDF processing facility [8,9]. In general the RDF processing facilities processes the waste to a combustible fraction, wet organic fraction and a metal fraction [9]. The combustible fraction could also include wet organic waste in order to increase the energy output from RDF and decrease the rest fraction from processing [10]. The industry could also deliver pre-sorted combustible waste to the RDF processing facility and receive RDF fuel in return at a reasonable price. This fuel could be used for co-combustion in already existing coal firing plants (fluidized bed, grate firing). The RDF fuel should be densified and classified to meet the requirements for use in co-combustion with coal [11]. RDF fuel is also suitable for combustion in a fluidized bed alone [12]. Fluff RDF could be used for grate firing or in a fluidized bed with the advantage of one processing step less (densifying). The residue from combustion of RDF should be landfilled.
Metals sorted out from the RDF facility should be landfilled, but in the future recycling could be an option. Wet organic waste if not utilised for combustion, should be composted.
Industrial waste should be source separated and the combustible fraction could either cover energy needs without any upgrading or it could be sent to the RDF facility for upgrading. Residues from combustion of combustible fraction should be properly landfilled. The rest fraction from source separation of industrial waste should also be landfilled.
Hazardous waste should be taken care of with a special collecting system and transported to larger cities for treatment.
Straw collected in rural areas should be utilised for energy production in special designed boilers for straw combustion (low exit furnace temperatures) and the energy should be used for district heating.

Waste Management in Larger Cities, Urban Areas.

The MSW composition in larger cities is characterised by a larger content of paper, plastics and food wastes and a lower content of inorganic material than the case is for rural areas and small cities. The heating value is higher due to the above mentioned factors. Industrial waste in larger cities mostly consist of waste from coal and energy industry. Larger cities and urban areas in Poland are characterised by many high-rise buildings which were built in 1970s and 1980s with limited possibilities for source separation of MSW. Just one vertical tunnel per stairway enables people to get rid of different kinds of waste into one container. The high population density in these areas makes source separation of wastes and subsequent re-use, recycling and composting very difficult.
Figure 4 shows a proposed waste management system for larger cities.
Sewage sludge from larger cities and rural areas is collected in tanks and then transported to a biogas production plant. Sewage sludge together with green wastes are processed for biogas production. The biogas production is an anaerobic process which mainly produces methane (50-65%) and carbon dioxide.

A gas motor fuelled by biogas is driving an electricity generator and heat can also be recovered through a heat exchanger. The multifunctional system with a relatively simple technique and relative low investment cost for biogas production and utilisation serves the following advantages: energy production, improvement of sanitation, control of erosion by recycling organic matter into soil, degradation of toxic components. The total conversion efficiency is between 20 and 40%. Volume reduction for a biogas plant is between 65 to 90 % [13,14].

MSW in larger cities is not subjected to source separation but is transported directly to a RDF processing facility. For utilisation of MSW for energy production one need pre-treatment due to the low effective heating value of raw MSW. The RDF plant for larger cities should consist of grinding, sieving, magnetic metal separator and a ballistic separator. This system will increase the heating value of MSW by taking out metals, fines (mostly ashes) and the heavy fraction (glass, stones, remaining metals, ceramics, etc.). Heavy fraction and fines together with metals should be landfilled and RDF utilised for energy recovery. Residue from combustion should also be landfilled. As pointed out in figure 5 energy from combustion of RDF can be utilised in a steam turbine for electricity production with an efficiency factor between 30 to 33%, utilised in a combined heat and power plant one would have an efficiency factor between 50 to 60%. For district heating one would typically have an efficiency factor around 80%. To choose between these different methods one would have to take into consideration the energy infrastructure in the actual area and future demands for energy. Figure 5 has marked with a dotted line that gasification of pre-treated MSW as a high-technology process is an opportunity for the future. The product gas from gasification offers a wide range of possibilities for utilisation: production of industrial heat or steam, gaseous fuel for generation of electric power, substitute gas for natural gas and as a synthesis gas for production of liquid fuels or chemicals. The advantage of gasification compared to direct combustion is a higher electricity production efficiency (up to 45%), if the power is generated in a combined cycle (gas turbine, steam turbine and generator). Since gasification is not a well developed process and have high investment costs and because of the relative low prices of other energy carriers, this will be a technique for the future[15,16].

Industrial waste should be treated as industrial waste in smaller cities is treated, with source separation and energy recovery, but here most of the waste is non-combustible and this is landfilled.

Energy recovery from straw collected in rural areas is also a possibility for larger cities.

Hazardous waste for larger cities should be collected and treated at treatment plant which meets the environmental standards for pollutants. One or two larger plants should be built located nearby the largest industrial areas, where most of the producers of special/hazardous waste are situated.

There are several different treatment methods for hazardous waste; for instance chemical treatment, physical treatment, biological treatment, landfill and several different thermal destruction methods. Decision on which method or methods that should be used is dependent on: amounts and composition of waste, economy, politics, technical solutions and even feelings. Feelings are involved because no one wants to have a treatment plant for hazardous waste close to where they live and people want a method that is environmental friendly, so the public opinion have to be taken into consideration. The Polish hazardous waste is mainly generated from hospitals and chemical industries and therefore there is a need for both thermal treatment method for volume reduction and destruction/decomposing of toxic/infected waste and a need for a well controlled landfill site for non-organic hazardous waste. The most common thermal destruction method for hazardous waste is combustion and this would be the most suitable method for Poland at this stage. In addition to combustion there is plasma pyrolysis, which decomposes the waste at a very high temperature, 5000-12000 °C. This technology is, however, new and still in development [17]. The pyrolysis alternative is in figure 5 marked with a dotted line as possibility for the future.

5. ENERGY ESTIMATIONS

Poland consumed 3950 PJ of primary energy in 1993 [18], the energy calculations will be refereed to this figure.

1 ton of average composition MSW [19,20] was used for the energy estimation:

C_{wh} = 9,0 MJ / kg total amount of MSW was 8,2 million ton in 1993

Landfill Gas Production (LFG).

The period for LFG production in a typical landfill is between 25 and 30 years (taken t = 25).

$G_t = 183,6 (1 - 10^{-0,03 * 25}) = 151 \ m^3 / ton$ (1)

$C_l = 18 \ MJ / m^3$

$E_l = G_t * C_l : 25 = 108,7 \ MJ / ton$ and 0.89 PJ/y (2)

LFG production and utilisation is restricted by the following decreasing energy conversion factors [1]:

- only larger landfill sites can use gas extraction systems, it means that the share of landfill sites that can be used for LFG extraction and utilisation is 60 - 80% of total registered landfills
- approximately 50% of generated LFG can be extracted
- utilisation method

The total energy conversion factor for LFG production and utilisation is between 2 - 5 %.

Biogas Production.

Period for biogas production is between 10 and 30 days and average biogas yield is 145 m^3 /ton.

$C_b = 22,3 \ MJ / m^3$

$E_b = 145 * C_b = 3234 \ MJ / ton$ and 26,6 PJ/y (3)

Biogas production is characterised by energy conversion efficiency between 25 - 60% depending on feedstock. The total energy conversion factor for biogas production and utilisation is between 12 - 54%.

RDF Production.

Two different methods for RDF production [19] are used for energy estimations:

a) RDF production without food wastes in combustible fraction. Mass reduction is 21%, which gives us 210 kg of RDF from one ton of waste.

$C_{pa} = 16,5 \ MJ / kg$

$E_p = 210 * C_{pa} = 3465 \ MJ / ton$ and 28,4 PJ/y (4)

b) RDF production including food wastes in combustible fraction. Mass reduction is 58%, which gives us 580 kg of RDF from one ton of waste.

$C_{pb} = 12,6 \ MJ / kg$

$E_p = 580 * C_{pb} = 7308 \ MJ / ton$ and 59,9 PJ/y (5)

RDF production is characterised by conversion efficiency between 40-80% depending on method and feed-stock. The total energy conversion factor for RDF production and utilisation is between 22- 64%.

Straw for Energy Purposes.

Straw can be regarded both as biomass and as waste from agriculture production. In Poland it is mostly considered as waste. For combustion of straw one should use special constructed boilers with large combustion chambers and heating area to avoid high temperature corrosion because of the high content of alkalies. The feeding system should be adapted for burning straw in ballots and a gas cleaning system should be implemented. Energy recovery from straw would also give a net reduction of pollutants. The straw production in Poland was 14 million ton in 1994 [21].

C_s = 14,3 MJ / kg

$E_s = 14 * C_s$ = 200 PJ/y (6)

Utilisation Methods.

Different utilisation methods are shown in figure 5, each of these methods are characterised by different efficiency factors, so the final energy amount can be different depending on the method used. The preliminary assessments were carried out in reference to the total energy contained in wastes, which will not be achieved since the conversion efficiency is lower than 100%, in some cases much lower. The most common utilisation methods for energy recovery from waste, as mentioned above, are:

1. Combustion of gaseous fuels in a gas boilers with relatively high combustion efficiency for heat production up to 95%.
2. Fuelling (gaseous fuels) of gas engines to produce mechanical / electrical energy and heat with total efficiencies between 50 - 70%.
3. Combustion of solid fuels (RDF, straw, RDF mixed with coal or wood) in moving grate furnaces to produce hot water for district heating purposes with efficiency about 80%,
4. Combustion of solid fuels (RDF, straw, RDF mixed with coal or wood) in moving grate furnaces or fluidized bed furnaces to generate heat, process steam and electricity with efficiencies between 55 - 70%.

If sum up the energy in wastes (2)+(6) or (3)+(6) or (4)+(6) or (5)+(6), the average calculated energy in wastes will be 228,9 PJ/y and 28,9 PJ/y (without straw). Multiplied with an average conversion factor of 30% for MSW and add 200 PJ/y for straw multiplied with an conversion factor of 80% the result is 168,7 PJ/y. This is 4,3% of the primary energy consumption in Poland. The calculated energy in MSW using different methods and an efficiency factor of 30% is 8,67 PJ/y, in comparison to only LFG production and utilisation which gives 0,03 PJ/y.

6. CONCLUSIONS

Poland have a good opportunity to control the development of annual per capita generation of MSW and preserve the present low level if proper waste management systems are implemented. Due to the large variations in properties for Polish MSW and an expected growth in the standard of living, it is important to handle waste management carefully. Different and more integrated waste management systems for the future for both industrial and municipal waste are suggested for rural areas, smaller cities and larger cities.

7. NOMENCLATURE

C_b	biogas calorific value,	E_b	calculated energy in biogas,
C_l	LFG calorific value,	E_l	calculated energy in LFG,
$C_{pa,b}$	RDF calorific value,	E_p	calculated energy in pellets,
C_s	straw calorific value,	E_s	calculated energy in straw,
C_{wh}	higher waste calorific value,	G_t	LFG yield (t - yielding time),

8. ACKNOWLEDGEMENTS

The authors would like to thank the Norwegian Foreign Department (East-Europe Secretariat) for funding of this work.

REFERENCES

1. *The Energy Potential of Landfill Sites in Poland*, Thermie Programme Action BM 25/Dec.1994
2. PRISM, World Resource Foundation, Information sheet on waste minimisation, 1996
3. EPA Waste Characterisation Report, Franklin Assoc., 1994
4. *Waste Statistics, Municipal Waste 1992*, Official Statistics of Norway, 1994
5. *Waste Management and Treatment, Strategies and Methods*, International Symposium proceedings, April 26-28, 1995, Miedzyzdroje, Poland
6. Szymanski K.: *Gospodarka I Unieszkodliwianie Odpadow Komunalnych*, Koszalin 1994
7. Warmer Bulletin No 48/1996, p. 3
8. Rosvold H.: *Fab fra Djupvik Behandlingsanlegg, Analyse, Produksion og Bruk*, SINTEF Report

No STF15 A92052, Trondheim, Norway, 1992
9. Rosvold H.: *Erfaringer med Produksion og Anvendelse av Fab, Grinda-Sande Modellen*, SINTEF Report No STF15 A90079, Trondheim, Norway, Dec.1990
10. Eley M.H., Guinn G.R.: *A New Processing System for the Production of Improved Refuse Derived Fuel and Recyclables from Municipal Solid Waste*, National Waste Processing Conference Proceedings, ASME 1994
11. Duckett J.E.: *The Changing Role of Standards in the Marketing of RDF*, FACT-Vol. 13, Refuse Derived Fuel (RDF): Quality, Standards and Processing, ASME 1991
12. Patel N.M., Wheeler P.,Ohlsson O.O.: *Fluidised Bed Combustion of Municipal Solid Waste*, Task XI: MSW Conversion to Energy, Activity: MSW and RDF Combustion,IEA Bioenergy Agreement, 1994
13. Kozmienski- Thome, K.J.:*Recycling in Developing Countries.* Berlin 1982
14. Kozmienski- Thome, K.J.:*Recycling International.* Berlin 1984
15. *Gasification of Waste, Evaluation of the Waste Processing Facilities of the Thermoselect and TPS/Greve.* The EWAB Programme, Netherlands Organisation for Energy and Environment
16. Rensfelt E., Ostman A.: Task X. Biomass Utilisation, Biomass Thermal Gasification and Gas Turbines Activity, Sub-Task 6 - *Gasification of Waste,* IEA Biomass Agreement
17. Røkke N.A.: *Flere Teknikker Finnes*, J. Teknisk Ukeblad No 14/1989, pp. 24-25
18. *BP Statistical Review of World Energy*, British Petroleum Company p.l.s.1995
19. Sørum L., Hustad J.E.: *Forbrenning av Avfall i Polen - Dr.Ing. Utdanning*, SINTEF Report No STF12 A95045, Trondheim, Norway, Dec.1995
20. Kulik A., Witoszek A.: *Zapach Pieniedzy*, J. Wprost No. 4, 1994, pp. 36-37
21. 2nd International Workshop on Biofuels proceedings, Gdansk, Poland, 1995

TABLES

TABLE I: CHARACTERISTICS OF MSW IN POLAND (AVERAGE DATA 1980-1992) [1]

Characteristics	Unit	Cities	Small cities	Rural areas
Per capita generation	kg/yr	196	200	120
Composition				
0-10 mm	weight%	10.3	28	21
Plant origin food wastes	weight%	29.7	11.5	3.7
Animal origin food wastes	weight%	3.7	2.5	0.8
Paper & Cardboard	weight%	22.6	8.5	3.5
Plastic	weight%	7.3	2.5	1.0
Textile	weight%	2.9	2.5	1.5
Glass	weight%	10.6	12.5	10.0
Metals	weight%	4.1	5.5	8.5
Remaining organic wastes	weight%	3.7	11.0	18.1
Remaining inorganic wastes	weight%	5.1	15.5	32.0
Combustion Properties				
Moisture*	weight%	49.5	34	32
Combustible matter*	weight%	22.6	16	12
Noncombustible matter*	weight%	27.9	50	56
Higher calorific value**	kJ/kg	9027	2450	1927
Fertile properties				
Organic matter	weight%	43.8	24.5	17.5
Organic carbon	% C	20.7	12.9	7.9
Organic nitrogen	% N	1.2	0.5	0.4
Organic phosphorus	% P_2O_5	0.7	0.6	0.5
Total potassium	% K_2O	0.4	0.1	0.1

* as received ** dry basis

FIGURES

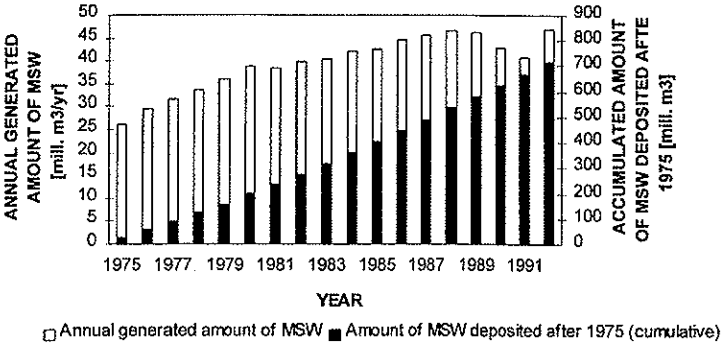

Fig. 1. Annual and Accumulated Amounts of MSW in Poland [1]

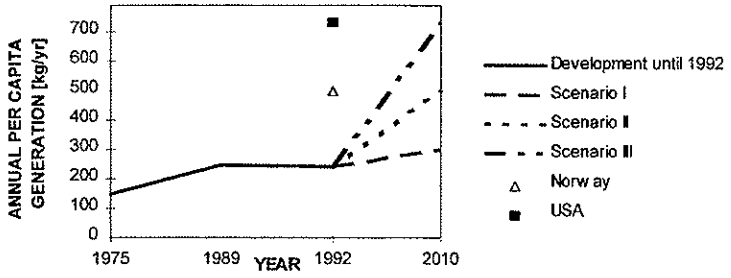

Fig. 2. MSW Generation Development and Future Scenarios

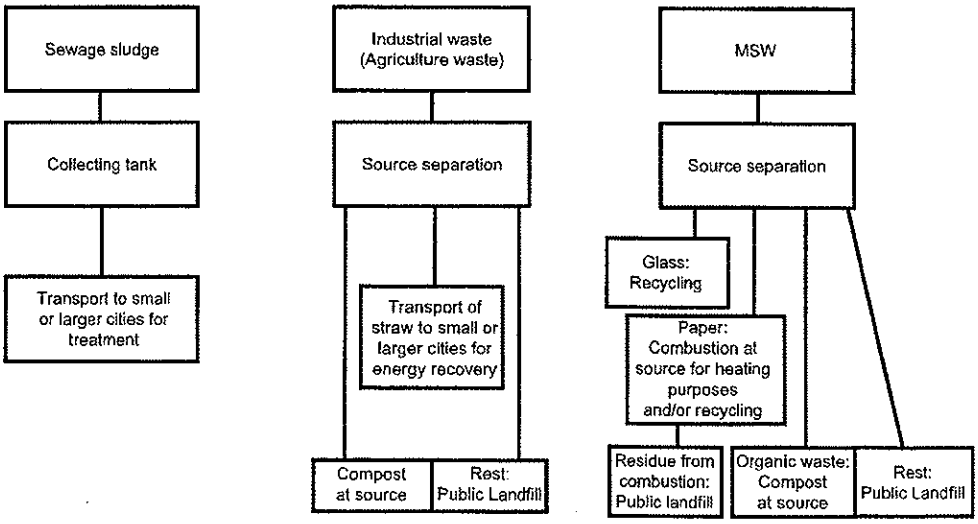

Fig. 3. Waste Management System for Rural Areas

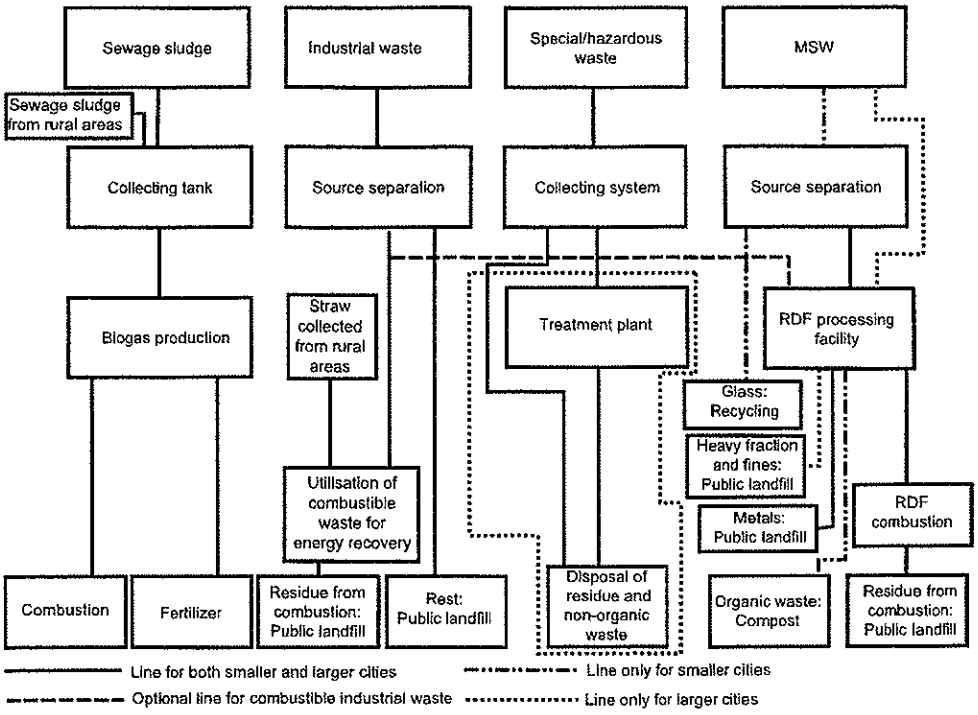

Fig.4. Waste Management Systems for Small and Larger Cities

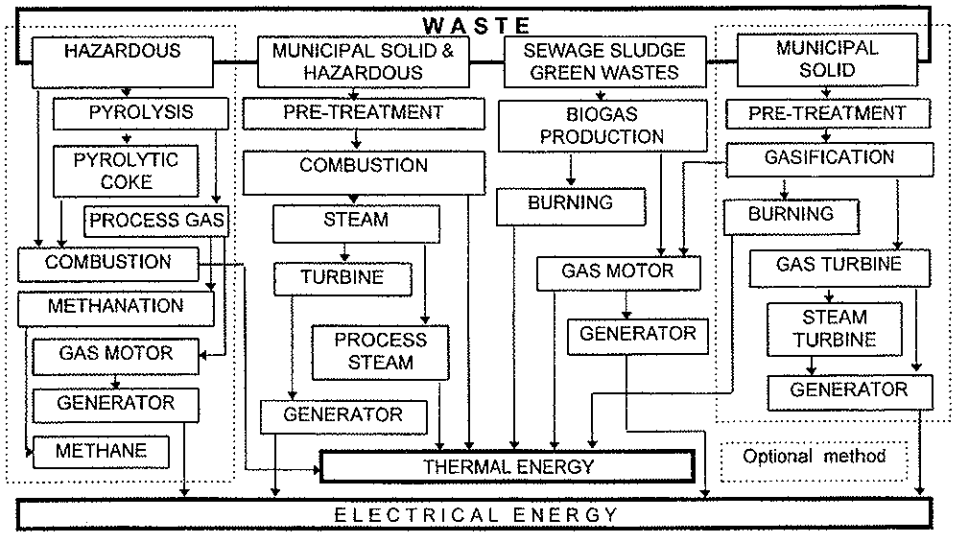

Fig.5. Thermoutilisation Methods

Appendix B:

TG and DTG curves of wet organic wastes, car tyres and textiles

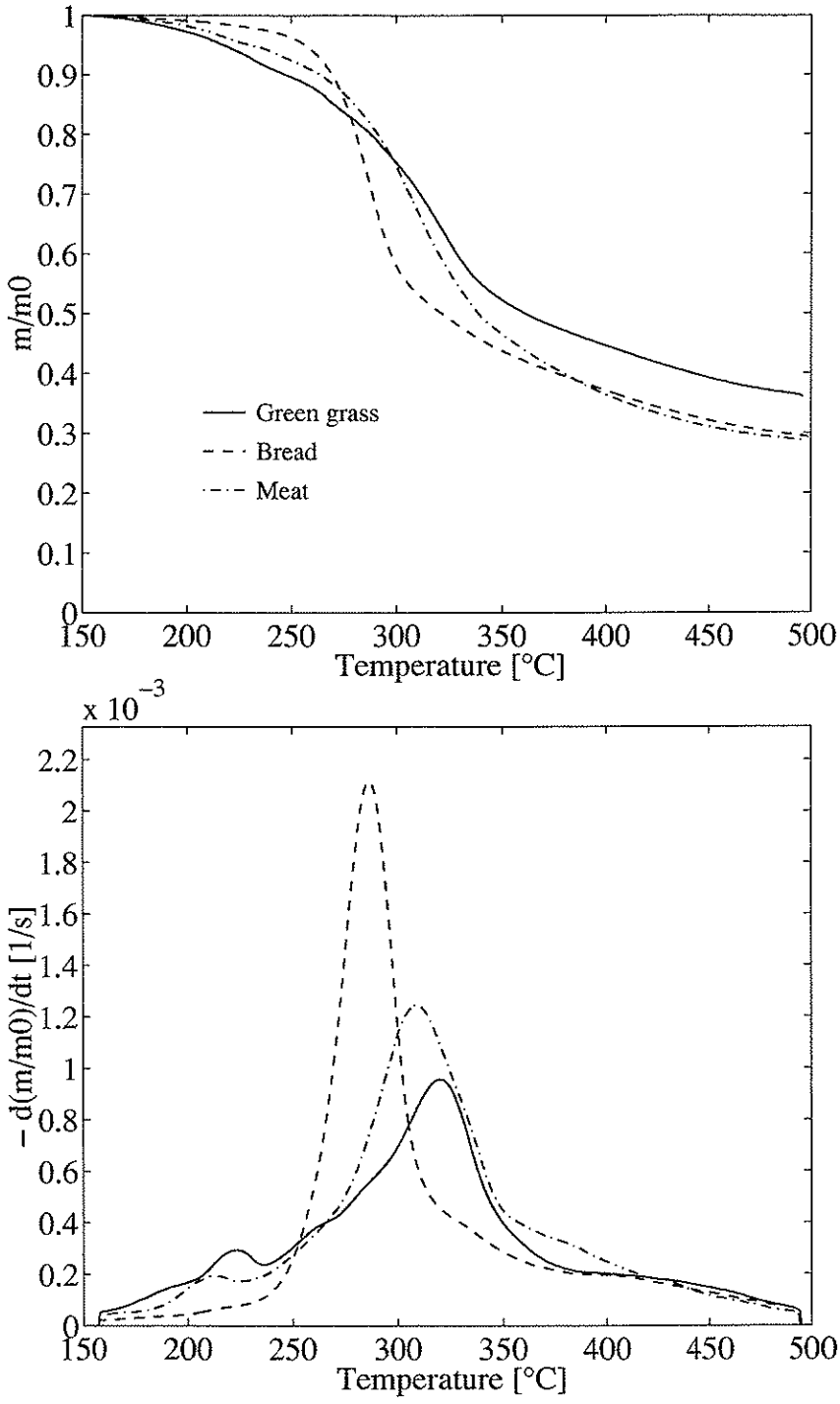

Figure B. 1 TG and DTG curves for green grass, meat and bread.

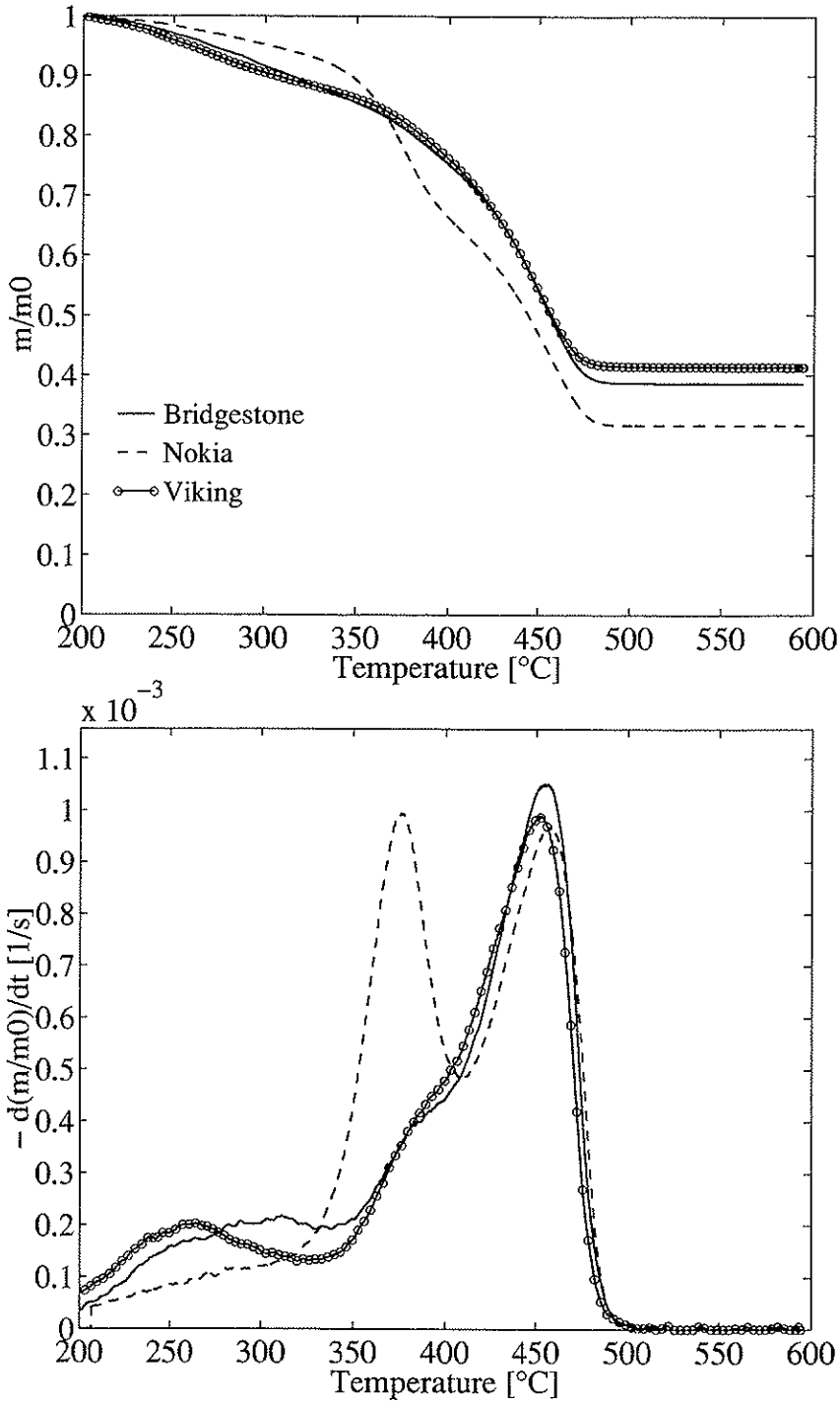

Figure B. 2 TG and DTG curves for Bridgestone, Nokia and Viking car tyres.

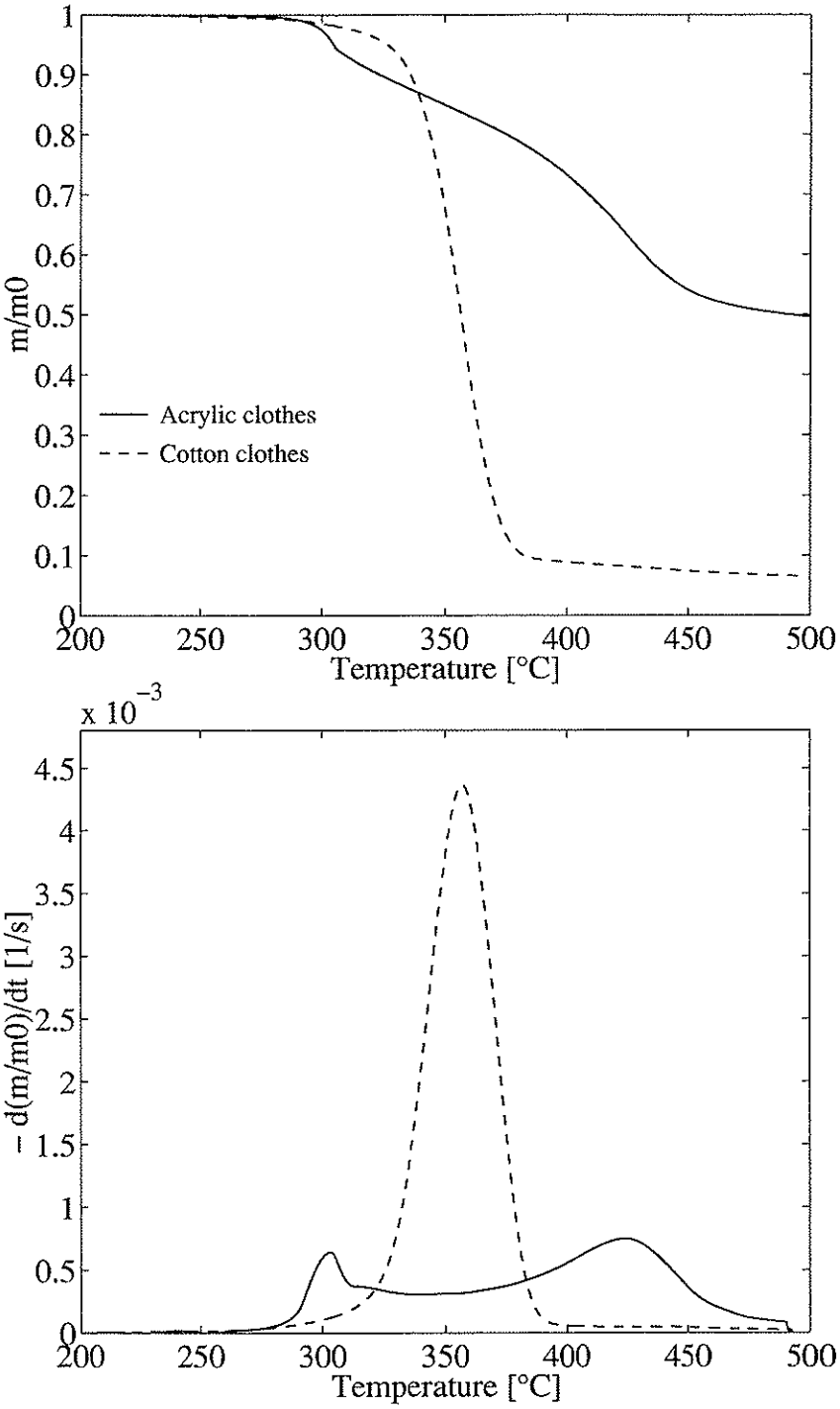

Figure B. 3 TG and DTG curves for cotton and acrylic clothes.

Appendix C:

Summary of Experimental Data Obtained in the NO Study (Part II)

The columns in the following table shows (in succession) the experimental number, share of Newspaper, Cardboard, Glossy paper, LDPE and PVC, reactor temperature, oxygen content of oxidiser, residence time for oxidiser in reactor, sample weight, char + ash weight and conversion factor for fuel nitrogen to NO.

Exp. no.	Newspaper [%]	Cardboard [%]	Glossy paper [%]	LDPE [%]	PVC [%]	Temp. [°C]	O_2 [vol.%]	Residence time [s]	Batch weight [g]	Char+ash weight [g]	NO/Fuel-N
N100	100	0	0	0	0	850	100	2.41	2.00	0.350	0.50
N411	100	0	0	0	0	850	12	2.41	2.00	0.307	0.50
N412	100	0	0	0	0	850	12	2.41	2.00	0.329	0.49
N413	100	0	0	0	0	850	12	2.41	2.00	0.307	0.49
N414	100	0	0	0	0	850	21	2.41	2.00	0.315	0.53
N415	100	0	0	0	0	850	21	2.41	2.00	0.309	0.52
N416	100	0	0	0	0	850	21	2.41	2.00	0.310	0.56
N417	100	0	0	0	0	850	40	2.41	2.00	0.312	0.98
N418	100	0	0	0	0	850	40	2.41	2.00	0.319	0.97
N419	100	0	0	0	0	850	40	2.41	2.00	0.294	1.01
NT1	100	0	0	0	0	700	21	2.78	2.00	0.347	0.45
NT2	100	0	0	0	0	775	21	2.58	2.00	0.331	0.50
NT3	100	0	0	0	0	850	21	2.41	2.00	0.310	0.51
Nv11	100	0	0	0	0	850	21	2.41	0.20	0.026	0.60
Nv12	100	0	0	0	0	850	21	2.41	0.20	0.028	0.59
Nv13	100	0	0	0	0	850	21	2.41	0.20	0.028	0.57
Nv2	100	0	0	0	0	850	21	2.41	0.60	0.092	0.57
Nv3	100	0	0	0	0	850	21	2.41	1.00	0.151	0.55
Nv4	100	0	0	0	0	850	21	2.41	2.00	0.328	0.56
C100	0	100	0	0	0	850	100	2.41	2.00	0.334	0.42
C421	0	100	0	0	0	850	12	2.41	2.00	0.334	0.50
C422	0	100	0	0	0	850	12	2.41	2.00	0.334	0.48
C423	0	100	0	0	0	850	12	2.41	2.00	0.337	0.47
C424	0	100	0	0	0	850	21	2.41	2.00	0.333	0.53
C425	0	100	0	0	0	850	21	2.41	2.00	0.327	0.52
C426	0	100	0	0	0	850	21	2.41	2.00	0.332	0.52
C427	0	100	0	0	0	850	40	2.41	2.00	0.316	0.84
C428	0	100	0	0	0	850	40	2.41	2.00	0.323	0.87
C429	0	100	0	0	0	850	40	2.41	2.00	0.320	0.88
G100	0	0	100	0	0	850	100	2.41	2.00	0.904	0.23
G431	0	0	100	0	0	850	12	2.41	2.00	0.888	0.27
G432	0	0	100	0	0	850	12	2.41	2.00	0.913	0.26
G433	0	0	100	0	0	850	12	2.41	2.00	0.908	0.27
G434	0	0	100	0	0	850	21	2.41	2.00	0.913	0.26
G435	0	0	100	0	0	850	21	2.41	2.00	0.906	0.25
G436	0	0	100	0	0	850	21	2.41	2.00	0.906	0.26
G437	0	0	100	0	0	850	40	2.41	2.00	0.905	0.30
G438	0	0	100	0	0	850	40	2.41	2.00	0.893	0.33
G439	0	0	100	0	0	850	40	2.41	2.00	0.916	0.33
Mpa211	50	40	10	0	0	850	12	2.41	2.00	0.365	0.46
Mpa212	50	40	10	0	0	850	21	2.41	2.00	0.363	0.48
Mpa214	50	40	10	0	0	850	21	2.41	2.00	0.357	0.50
Mpa215	50	40	10	0	0	850	21	2.41	2.00	0.357	0.50
Mpa213	50	40	10	0	0	850	40	2.41	2.00	0.364	0.74
Mpa221	20	70	10	0	0	850	12	2.41	2.00	0.371	0.44
Mpa222	20	70	10	0	0	850	21	2.41	2.00	0.372	0.46
Mpa223	20	70	10	0	0	850	40	2.41	2.00	0.357	0.69
Mpa231	80	10	10	0	0	850	12	2.41	2.00	0.356	0.44
Mpa232	80	10	10	0	0	850	21	2.41	2.00	0.353	0.50
Mpa233	80	10	10	0	0	850	40	2.41	2.00	0.347	0.82
Mpa241	20	10	70	0	0	850	12	2.41	2.00	0.690	0.31
Mpa242	20	10	70	0	0	850	21	2.41	2.00	0.678	0.34
Mpa243	20	10	70	0	0	850	40	2.41	2.00	0.714	0.40
Mpa251	20	40	40	0	0	850	12	2.41	2.00	0.528	0.36
Mpa252	20	40	40	0	0	850	21	2.41	2.00	0.528	0.41
Mpa253	20	40	40	0	0	850	40	2.41	2.00	0.513	0.61
Mpa261	50	10	40	0	0	850	12	2.41	2.00	0.526	0.38
Mpa262	50	10	40	0	0	850	21	2.41	2.00	0.523	0.41
Mpa263	50	10	40	0	0	850	40	2.41	2.00	0.527	0.64

Exp. no.	Newspaper [%]	Cardboard [%]	Glossy paper [%]	LDPE [%]	PVC [%]	Temp. [°C]	O_2 [vol.%]	Residence time [s]	Batch weight [g]	Char+ash weight [g]	NO/Fuel-N
l100	0	0	0	100	0	850	100	2.41	0.14	0.000	0.71
l1002	0	0	0	100	0	850	100	2.41	2.00	0.000	0.38
l441	0	0	0	100	0	850	12	2.41	0.12	0.000	1.42
l442	0	0	0	100	0	850	12	2.41	0.13	0.000	1.68
l443	0	0	0	100	0	850	12	2.41	0.12	0.000	1.71
l444	0	0	0	100	0	850	21	2.41	0.12	0.000	2.02
l445	0	0	0	100	0	850	21	2.41	0.12	0.000	1.97
l446	0	0	0	100	0	850	21	2.41	0.12	0.000	1.88
l447	0	0	0	100	0	850	40	2.41	0.12	0.000	10.14
l448	0	0	0	100	0	850	40	2.41	0.12	0.000	9.34
l449	0	0	0	100	0	850	40	2.41	0.12	0.000	10.78
lt1	0	0	0	100	0	700	21	2.78	0.13	0.000	1.89
lt2	0	0	0	100	0	775	21	2.58	0.12	0.000	2.01
lt3	0	0	0	100	0	850	21	2.41	0.12	0.000	2.08
lv151	0	0	0	100	0	850	21	2.41	0.05	0.000	2.97
lv152	0	0	0	100	0	850	21	2.41	0.05	0.000	2.63
lv153	0	0	0	100	0	850	21	2.41	0.06	0.000	2.61
lv6	0	0	0	100	0	850	21	2.41	0.10	0.000	2.22
lv7	0	0	0	100	0	850	21	2.41	0.16	0.000	1.65
lv8	0	0	0	100	0	850	21	2.41	0.21	0.000	2.05
mpl311	0	0	0	67	33	850	12	2.41	0.18	0.011	0.63
mpl321	0	0	0	50	50	850	12	2.41	0.19	0.017	0.95
mpl322	0	0	0	50	50	850	12	2.41	0.18	0.016	1.02
mpl323	0	0	0	50	50	850	12	2.41	0.19	0.017	0.82
mpl3211	0	0	0	67	33	850	21	2.41	0.18	0.011	1.29
mpl3221	0	0	0	50	50	850	21	2.41	0.19	0.017	1.27
mpl3222	0	0	0	50	50	850	21	2.41	0.18	0.017	1.29
mpl3223	0	0	0	50	50	850	21	2.41	0.19	0.017	1.16
mpl3231	0	0	0	33	67	850	21	2.41	0.18	0.022	0.99
mpl331	0	0	0	33	67	850	12	2.41	0.18	0.022	0.95
mpl3311	0	0	0	67	33	850	40	2.41	0.18	0.011	6.21
mpl3321	0	0	0	50	50	850	40	2.41	0.19	0.017	4.85
mpl3322	0	0	0	50	50	850	40	2.41	0.19	0.017	4.06
mpl3323	0	0	0	50	50	850	40	2.41	0.19	0.017	4.33
mpl3331	0	0	0	33	67	850	40	2.41	0.19	0.022	2.28
p100	0	0	0	0	100	850	100	2.41	2.00	0.413	0.04
p451	0	0	0	0	100	850	12	2.41	2.00	0.390	0.23
p452	0	0	0	0	100	850	12	2.41	2.00	0.372	0.21
p453	0	0	0	0	100	850	12	2.41	2.00	0.386	0.20
p454	0	0	0	0	100	850	21	2.41	2.00	0.379	0.26
p455	0	0	0	0	100	850	21	2.41	2.00	0.386	0.23
p456	0	0	0	0	100	850	21	2.41	2.00	0.386	0.21
p457	0	0	0	0	100	850	40	2.41	2.00	0.424	0.35
p458	0	0	0	0	100	850	40	2.41	2.00	0.395	0.40
p459	0	0	0	0	100	850	40	2.41	2.00	0.391	0.38

Exp. no.	Newspaper [%]	Cardboard [%]	Glossy paper [%]	LDPE [%]	PVC [%]	Temp. [°C]	O_2 [vol.%]	Residence time [s]	Batch weight [g]	Char+ash weight [g]	NO/Fuel-N
mpp131	15	10	10	10	55	850	12	2.41	2.00	0.386	0.40
mpp132	15	10	10	10	55	850	21	2.41	2.00	0.401	0.41
mpp133	15	10	10	10	55	850	40	2.41	2.00	0.400	0.73
mpp161	15	10	32.5	10	32.5	850	12	2.41	2.00	0.507	0.37
mpp162	15	10	32.5	10	32.5	850	21	2.41	2.00	0.412	0.39
mpp163	15	10	32.5	10	32.5	850	40	2.41	2.00	0.484	0.66
mpp171	60	10	10	10	10	850	12	2.41	2.00	0.360	0.50
mpp172	60	10	10	10	10	850	21	2.41	2.00	0.351	0.51
mpp173	60	10	10	10	10	850	40	2.41	2.00	0.364	1.08
mpp181	37.5	32.5	10	10	10	850	12	2.41	2.00	0.366	0.54
mpp182	37.5	32.5	10	10	10	850	21	2.41	2.00	0.366	0.47
mpp184	37.5	32.5	10	10	10	850	21	2.41	2.00	0.363	0.49
mpp185	37.5	32.5	10	10	10	850	21	2.41	2.00	0.354	0.49
mpp183	37.5	32.5	10	10	10	850	40	2.41	2.00	0.374	1.00
mpp191	15	32.5	32.5	10	10	850	12	2.41	2.00	0.467	0.44
mpp192	15	32.5	32.5	10	10	850	21	2.41	2.00	0.439	0.42
mpp193	15	32.5	32.5	10	10	850	40	2.41	2.00	0.452	0.86
mpp1101	37.5	10	10	10	32.5	850	12	2.41	2.00	0.370	0.50
mpp1102	37.5	10	10	10	32.5	850	21	2.41	2.00	0.390	0.43
mpp1103	37.5	10	10	10	32.5	850	40	2.41	2.00	0.366	0.69
mpp1111	15	10	55	10	10	850	12	2.41	2.00	0.569	0.37
mpp1112	15	10	55	10	10	850	21	2.41	2.00	0.531	0.34
mpp1113	15	10	55	10	10	850	40	2.41	2.00	0.586	0.59
mpp1121	15	32.5	10	10	32.5	850	12	2.41	2.00	0.389	0.44
mpp1122	15	32.5	10	10	32.5	850	21	2.41	2.00	0.393	0.42
mpp1123	15	32.5	10	10	32.5	850	40	2.41	2.00	0.379	0.73
mpp1131	15	55	10	10	10	850	12	2.41	2.00	0.369	0.45
mpp1132	15	55	10	10	10	850	21	2.41	2.00	0.363	0.48
mpp1133	15	55	10	10	10	850	40	2.41	2.00	0.351	0.89
mpp1151	37.5	10	32.5	10	10	850	12	2.41	2.00	0.446	0.43
mpp1152	37.5	10	32.5	10	10	850	21	2.41	2.00	0.450	0.42
mpp1153	37.5	10	32.5	10	10	850	40	2.41	2.00	0.445	0.74

Appendix D:

Kinetic Reaction Schemes used for Paper and Plastics in the NO Study

```
!
  ! *****************************************************
  ! *   Hydrocarbon/nitrogen mechanism for simulations  *
  ! *   on PAPER in OPPDIF                              *
  ! *   Reference: Glarborg, Alzueta, Dam-Johansen,Miller *
  ! *   Comb Flame, submitted (4/97)                    *
  ! *   revised Oct 22, 1997                            *
  ! *                                                   *
  ! *****************************************************
  !
ELEMENTS
H O C N AR
END
SPECIES
CO CO2 NO HCN
H O OH HO2 O2 H2 H2O2 H2O
CH2O HCO CH3O CH2OH
CH4 CH3 CH2 CH2(S) CH C
NO2 HNO
NH3 NH2 NH N N2H2 NNH N2O
HCN CN NCO HNCO HOCN HCNO
AR N2
END
THERMO
CH2(S)              83194H   2C   1    0    0G   300.000  4000.000 1400.00    0 1
 0.40752106E+01 0.15779120E-02-0.10806129E-06-0.84592437E-10 0.14033284E-13    2
 0.50007492E+05-0.15480316E+01 0.35932946E+01 0.13151238E-02 0.30756846E-06    3
 0.42637904E-09-0.34178712E-12 0.50451547E+05 0.17780241E+01                   4
CH2                 83194H   2C   1    0    0G   300.000  4000.000 1400.00    0 1
 0.39737520E+01 0.16097502E-02-0.10785119E-06-0.86399922E-10 0.14301196E-13    2
 0.45608973E+05 0.75549729E-01 0.36872995E+01 0.15066403E-02 0.69679857E-07    3
 0.23537297E-09-0.19397147E-12 0.45863672E+05 0.20267601E+01                   4
HNO                 pg9601H   1N   1O   1     G  0300.00   5000.00  1000.00      1
 0.03615144E+02 0.03212486E-01-0.01260337E-04 0.02267298E-08-0.01536236E-12    2
 0.11769108E+05 0.04810264E+02 0.02784403E+02 0.06609646E-01-0.09300223E-04    3
 0.09437980E-07-0.03753146E-10 0.12025976E+05 0.09035629E+02                   4
HCN                 110193H   1C   1N   1     G  0300.00   4000.00  1000.00      1
 0.03426457E+02 0.03924190E-01-0.01601138E-04 0.03161966E-08-0.02432850E-12    2
 0.01485552E+06 0.03607795E+02 0.02417787E+02 0.09031856E-01-0.01107727E-03    3
 0.07980141E-07-0.02311141E-10 0.01501044E+06 0.08222891E+02                   4
HNCO                110193H   1C   1N   1O   1G  0300.00   4000.00  1400.00      1
 0.06545307E+02 0.01965760E-01-0.01562664E-05-0.01074318E-08 0.01874680E-12    2
-0.01664773E+06-0.01003880E+03 0.03858467E+02 0.06390342E-01-0.09016628E-05    3
-0.01898224E-07 0.07651380E-11-0.01562343E+06 0.04882493E+02                   4
HOCN                110193H   1C   1N   1O   1G  0300.00   4000.00  1400.00      1
 0.06022112E+02 0.01929530E-01-0.01455029E-05-0.01045811E-08 0.01794814E-12    2
-0.04040321E+05-0.05866433E+02 0.03789424E+02 0.05387981E-01-0.06518270E-05    3
-0.01420164E-07 0.05367969E-11-0.03135335E+05 0.06667052E+02                   4
NCO                 110193C   1N   1O   1     G  0300.00   4000.00  1400.00      1
 0.06072346E+02 0.09227829E-02-0.09845574E-06-0.04764123E-09 0.09090445E-13    2
 0.01359820E+06-0.08507293E+02 0.03359593E+02 0.05393239E-01-0.08144585E-05    3
-0.01912868E-07 0.07836794E-11 0.01462809E+06 0.06549694E+02                   4
END
```

```
REACTIONS
   !
   ! *****************************************
   ! *   H2/O2 Subset                        *
   ! *   ref: nh2+no2 paper (IJCK), except   *
   ! *        where noted                    *
   ! *****************************************
   !
1.     O+OH=O2+H                      2.0E14 -0.40      0
2.     O+H2=OH+H                      5.0E04  2.67   6290
3.     OH+H2=H2O+H                    2.1E08  1.52   3450
4.     2OH=O+H2O                      4.3E03  2.70  -2486
5.     H+H+M=H2+M                     1.0E18 -1.00      0
       H2O/0/
6.     H+H+H2O=H2+H2O                 6.0E19 -1.25      0
7.     H+O+M=OH+M                     6.2E16 -0.60      0
       H2O/5/                                           .
8.     H+OH+M=H2O+M                   1.6E22 -2.00      0
       H2O/5/
9.     O+O+M=O2+M                     1.9E13  0.00  -1788
       H2O/5/
10.    H+O2+M=HO2+M                   2.1E18 -1.00      0 ! *
       H2O/10/  N2/0/
11.    H+O2+N2 = HO2+N2               6.7E19 -1.42      0 ! *
12.    H+HO2=H2+O2                    4.3E13  0.00   1411
13.    H+HO2=2OH                      1.7E14  0.00    874
14.    H+HO2=O+H2O                    3.0E13  0.0    1721
15.    O+HO2=O2+OH                    3.3E13  0.0       0
16.    OH+HO2=H2O+O2                  1.9E16 -1.0       0
17.    HO2+HO2=H2O2+O2                4.2E14  0.0   11982
       DUP
18.    HO2+HO2=H2O2+O2                1.3E11  0.0   -1629
       DUP
19.    H2O2+M=OH+OH+M                 1.3E17  0.0   45500
       H2O/5/
20.    H2O2+H=HO2+H2                  1.7E12  0.0    3755
21.    H2O2+H=OH+H2O                  1.0E13  0.0    3576
22.    H2O2+O=OH+HO2                  6.6E11  0.0    3974
23.    H2O2+OH=H2O+HO2                7.8E12  0.0    1330
       DUP
24.    H2O2+OH=H2O+HO2                5.8E14  0.0    9560 ! +
       DUP
   !
   ! *****************************************
   ! *   CO Subset                           *
   ! *****************************************
   !
25.    CO+O+M=CO2+M                   6.2E14  0.0    3000 ! nbs86
       H2O/5/
26.    CO+OH=CO2+H                    1.5E07  1.3    -758 ! gla86
27.    CO+O2=CO2+O                    2.5E12  0.0   47700 ! nbs86
28.    HO2+CO=CO2+OH                  5.8E13  0.0   22934 ! gla86
   !
   ! *****************************************
   ! *   CH2O/HCO Subset                     *
   ! *****************************************
   !
29.    CH2O+M=HCO+H+M                 3.3E16  0.0   81000 ! gla86
       H2O/5/
30.    CH2O+H = HCO+H2                1.3E08  1.62   2166 ! CEC94
31.    CH2O+O=HCO+OH                  1.8E13  0.00   3080 ! nbs86
32.    CH2O+OH=HCO+H2O                3.4E09  1.18   -447 ! nbs86
33.    CH2O+HO2 = HCO+H2O2            3.0E12  0.00  13000 ! cec92
34.    CH2O+O2 = HCO+HO2              6.0E13  0.00  40660 ! cec92
35.    HCO+M=H+CO+M                   1.9E17 -1.0   17000 ! tim87
       H2O/5/
36.    HCO+H=CO+H2                    1.2E13  0.25      0 ! lrev (harding,21st)
37.    HCO+O=CO+OH                    3.0E13  0.000     0 ! cec92
```

```
38.    HCO+O=CO2+H                      3.0E13  0.000     0 ! cec92
39.    HCO+OH=H2O+CO                    1.0E14  0.00      0 ! cec92
40.    HCO+O2=HO2+CO                    7.6E12  0.0     400 ! tim88
  !
  ! ********************************************
  ! *   CH4/CH3/CH2/CH/C Subset                *
  ! ********************************************
  !
41.    CH3+H(+M)=CH4(+M)                1.3E16 -0.63    383 ! GRI-MECH2.11
       LOW/1.75E33  -4.76 2440.0/
       TROE/0.783  74.0 2941.0 6964.0/
       H2O/8.57/ N2/1.43/
42.    CH4+H=CH3+H2                     1.3E04  3.00   8040 ! cec92
43.    CH4+O=CH3+OH                     1.0E09  1.5    8600 ! nbs86
44.    CH4+OH=CH3+H2O                   1.6E06  2.10   2460 ! war84
45.    CH4+HO2=CH3+H2O2                 1.8E11  0.00  18700 ! nbs86
46.    CH4+O2=CH3+HO2                   7.9E13  0.00  56000 ! ski72
47.    CH3+H=CH2+H2                     9.0E13  0.00  15100 ! gla86
48.    CH2(S)+H2=CH3+H                  7.2E13  0.0       0 ! cec92
49.    CH3+O=CH2O+H                     8.4E13  0.0       0 ! cec92
50.    CH3+OH=CH2+H2O                   7.5E06  2.0    5000 ! m
51.    CH2(S)+H2O=CH3+OH                3.0E15 -0.6       0 ! car/wag95,hack/hggw 88
52.    CH2OH+H=CH3+OH                   1.0E14  0.0       0 ! m
53.    CH3O+H=CH3+OH                    1.0E14  0.0       0 ! m
54.    CH3+HO2 = CH3O+OH                8.0E12  0.00      0 ! Tro92
55.    CH3+O2=CH3O+O                    2.9E13  0.0   30480 ! yu/fre95
56.    CH3+O2=CH2O+OH                   1.9E12  0.0   20315 ! yu/fre95
57.    CH3+CH2O = CH4+HCO               7.8E-8  6.10   1967 !+cec94
58.    CH3+HCO = CH4+CO                 1.2E14  0.00      0 !+nbs86
59.    CH2+H=CH+H2                      1.0E18 -1.56      0 ! gla86
60.    CH2+O=CO+H+H                     5.0E13  0.0       0 ! lrev
61.    CH2+O=CO+H2                      3.0E13  0.0       0 ! lrev
62.    CH2+OH=CH+H2O                    1.1E07  2.0    3000 ! m
63.    CH2+OH=CH2O+H                    2.5E13  0.0       0 ! m
64.    CH2+O2=CO+H2O                    2.2E22 -3.3    2867 ! dom92,m
65.    CH2+O2=CO2+H+H                   3.3E21 -3.3    2867 ! dom92,m
66.    CH2+O2=CH2O+O                    3.3E21 -3.3    2867 ! dom92,m
67.    CH2+O2=CO2+H2                    2.6E21 -3.3    2867 ! dom92,m
68.    CH2+O2=CO+OH+H                   1.6E21 -3.3    2867 ! dom92,m
69.    CH2+CO2=CH2O+CO                  1.1E11  0.0    1000 ! gla86
70.    CH2+CH4 = CH3+CH3                4.3E12  0.0   10030 ! boh85
71.    CH2(S)+M=CH2+M                   1.0E13  0.0       0 ! m
       H/0/ H2O/0/ N2/0/ AR/0/
72.    CH2(S)+N2=CH2+N2                 1.3E13  0.0     430 ! Hayes, 1996
73.    CH2(S)+AR=CH2+AR                 1.5E13  0.0     884 ! Hayes, 1996
74.    CH2(S)+H=CH2+H                   2.0E14  0.0       0 ! m
75.    CH2(S)+H2O=CH2+H2O               3.0E13  0.0       0 ! WAGNER
76.    CH2(S)+H=CH+H2                   3.0E13  0.0       0 ! nbs86
77.    CH2(S)+O=CO+H+H                  3.0E13  0.0       0 ! nbs86
78.    CH2(S)+OH=CH2O+H                 3.0E13  0.0       0 ! nbs86
79.    CH2(S)+O2=CO+OH+H                7.0E13  0.0       0 ! m
80.    CH2(S)+CO2=CH2O+CO               3.0E12  0.0       0 ! nbs86
81.    CH2(S)+CH4=CH3+CH3               4.3E13  0.0       0 ! nbs86
82.    CH+H=C+H2                        1.5E14  0.0       0 ! m
83.    CH+O=CO+H                        5.7E13  0.0       0 ! gla86
84.    CH+OH=HCO+H                      3.0E13  0.0       0 ! m
85.    CH+OH=C+H2O                      4.0E7   2.0    3000 ! m
86.    CH+O2=HCO+O                      3.3E13  0.0       0 ! cec92
87.    CH+H2O=CH2O+H                    5.7E12  0.0    -751 ! cec92
88.    C+OH=CO+H                        5.0E13  0.00      0 ! m
89.    C+O2=CO+O                        2.0E13  0.00      0 ! gla86
```

```
!
! ****************************************************
! *   H/N/O subset                                   *
! *   taken from [nh2no2] except where noted         *
! ****************************************************
!
90.    H+NO+M=HNO+M                      2.7E15  0.0     -600 ! bau73
       H2O/10/  O2/1.5/ H2/2/ CO2/3/ N2/0.0/
91.    H+NO+N2=HNO+N2                    7.0E19 -1.50       0 ! see text
92.    NO+O+M=NO2+M                      7.5E19 -1.41       0 !
       N2/1.7/   O2/1.5/  H2O/10/
93.    HO2+NO=NO2+OH                     2.1E12  0.00    -479 !
94.    NO2+H=NO+OH                       8.4E13  0.0        0 !
95.    NO2+O=NO+O2                       3.9E12  0.0     -238 !
96.    NO2+NO2=NO+NO+O2                  1.6E12  0.0    26123 !
97.    HNO+H=H2+NO                       4.5E11  0.72     655 !
98.    HNO+O=NO+OH                       1.0E13  0.0        0 ! +
99.    HNO+OH=NO+H2O                     3.6E13  0.0        0 !
100.   HNO+O2=HO2+NO                     1.0E13  0.0    25000 !
101.   HNO+HNO=N2O+H2O                   9.0E08  0.0     3100 ! *
102.   HNO+NH2=NH3+NO                    3.63E6  1.63   -1252 ! lin96
103.   NH3+M = NH2+H+M                   2.2E16   0     93470 ! +
104.   NH3+H=NH2+H2                      6.4E05  2.39   10171 !
105.   NH3+O=NH2+OH                      9.4E06  1.94    6460 ! *
106.   NH3+OH=NH2+H2O                    2.0E06  2.04     566 !
107.   NH3+HO2=NH2+H2O2                  3.0E11  0.0    22000 !
108.   NH2+H=NH+H2                       4.0E13  0.00    3650 !
109.   NH2+O=HNO+H                       6.6E14 -0.50       0 !
110.   NH2+O=NH+OH                       6.8E12  0.         0 !
111.   NH2+OH=NH+H2O                     4.0E06  2.      1000 !
112.   NH2+HO2=NH3+O2                    1.0E13  0.0        0 !
113.   NH2+NO=NNH+OH                     8.9E12 -0.35       0 ! bodenstein
114.   NH2+NO=N2+H2O                     1.3E16 -1.25       0 ! bodenstein
       DUP
115.   NH2+NO=N2+H2O                    -8.9E12 -0.35       0 !
       DUP
116.   NH2+NO2=N2O+H2O                   3.2E18 -2.2        0 !
117.   NH2+NH2=N2H2+H2                   8.5E11  0.         0 !
118.   NH2+NH=N2H2+H                     5.0E13  0.         0 !
119.   NH2+N=N2+H+H                      7.2E13  0.         0 !
120.   NH+H=N+H2                         3.0E13  0.         0
121.   NH+O=NO+H                         9.2E13  0.         0
122.   NH+OH=HNO+H                       2.0E13  0.         0
123.   NH+OH=N+H2O                       5.0E11  0.50    2000
124.   NH+O2=HNO+O                       4.6E05  2.      6500 !
125.   NH+O2=NO+OH                       1.3E06  1.5      100 !
126.   NH+NO=N2O+H                       2.9E14 -0.4        0 !
       DUP
127.   NH+NO=N2O+H                      -2.2E13 -0.23       0
       DUP
128.   NH+NO=N2+OH                       2.2E13 -0.23       0
129.   NH+NO2=N2O+OH                     1.0E13  0.         0
130.   NH+NH=N2+H+H                      2.5E13  0.         0
131.   NH+N=N2+H                         3.0E13  0.         0
132.   N+OH=NO+H                         3.8E13  0.         0
133.   N+O2=NO+O                         6.4E09  1.      6280
134.   N+NO=N2+O                         3.3E12  0.30       0
135.   N2H2+M=NNH+H+M                    5.0E16  0.     50000
       H2O/15/ O2/2/ N2/2/ H2/2/
136.   N2H2+H=NNH+H2                     5.0E13  0.      1000
137.   N2H2+O=NH2+NO                     1.0E13  0.         0
138.   N2H2+O=NNH+OH                     2.0E13  0.      1000
139.   N2H2+OH=NNH+H2O                   1.0E13  0.      1000
140.   N2H2+NO=N2O+NH2                   3.0E12  0.         0
141.   N2H2+NH2=NH3+NNH                  1.0E13  0.      1000
142.   N2H2+NH=NNH+NH2                   1.0E13  0.      1000
143.   NNH=N2+H                          1.0E7   0.         0 ! bodenstein
```

```
144.   NNH+H=N2+H2                      1.0E14  0.        0
145.   NNH+O=N2+OH                      8.0E13  0.        0
146.   NNH+O=N2O+H                      1.0E14  0.        0
147.   NNH+O=NH+NO                      5.0E13  0.        0
148.   NNH+OH=N2+H2O                    5.0E13  0.        0
149.   NNH+O2=N2+HO2                    2.0E14  0.        0 ! bodenstein
150.   NNH+O2=N2+O2+H                   5.0E13  0.        0 ! bodenstein
151.   NNH+NO=N2+HNO                    5.0E13  0.        0
152.   NNH+NH2=N2+NH3                   5.0E13  0.        0
153.   NNH+NH=N2+NH2                    5.0E13  0.        0
154.   N2O+M=N2+O+M                     4.0E14  0.    56100
       N2/1.7/   O2/1.4/ H2O/12/ CO/1.5/  CO2/3/
155.   N2O+H=N2+OH                      3.3E10  0.     4729
       DUP
156.   N2O+H=N2+OH                      4.4E14  0.    19254
       DUP
157.   N2O+O=NO+NO                      6.6E13  0.    26630 ! nbs91
158.   N2O+O=N2+O2                      1.0E14  0.    28000 ! nbs91
159.   N2O+OH=N2+HO2                    1.3E-2  4.72  36561 ! Mebel,Lin IJCK 1996
160.   N2O+OH=HNO+NO                    1.2E-4  4.33  25081 ! Mebel,Lin IJCK 1996
161.   N2O+NO=NO2+N2                    5.3E05  2.23  46281 ! Mebel,Lin IJCK 1996
  !
  ! ****************************************************
  ! *  cyanide subset                                  *
  ! ****************************************************
  !
162.   CN+H2=HCN+H                      3.0E05  2.45   2237 !
163.   HCN+O=NCO+H                      1.4E04  2.64   4980
164.   HCN+O=NH+CO                      3.5E03  2.64   4980
165.   HCN+O=CN+OH                      2.7E09  1.58  29200
166.   HCN+OH = CN+H2O                  3.9E06  1.83  10300 !
167.   HCN+OH=HOCN+H                    5.9E04  2.40  12500
168.   HCN+OH=HNCO+H                    2.0E-3  4.      1000
169.   HCN+OH=NH2+CO                    7.8E-4  4.      4000
170.   CN+O=CO+N                        7.7E13  0.         0 !
171.   CN+OH=NCO+H                      4.0E13  0.         0 !
172.   CN+O2=NCO+O                      7.5E12  0.      -389 !
173.   CN+CO2=NCO+CO                    3.7E06  2.16  26884 !
174.   CN+NO2=NCO+NO                    5.3E15 -0.752   344 !
175.   CN+NO2=CO+N2O                    4.9E14 -0.752   344 !
176.   CN+NO2=N2+CO2                    3.7E14 -0.752   344 !
177.   CN+HNO=HCN+NO                    1.8E13  0.00       0
178.   CN+HNCO=HCN+NCO                  1.5E13  0.         0 !
179.   HNCO+M=NH+CO                     1.1E16  0.    86000 !
180.   HNCO+H=NH2+CO                    2.2E07  1.7    3800 !
181.   HNCO+O=HNO+CO                    1.5E08  1.57  44012 !
182.   HNCO+O=NH+CO2                    9.8E7   1.41   8524 !
183.   HNCO+O=NCO+OH                    2.2E6   2.11  11425 !
184.   HNCO+OH=NCO+H2O                  6.4E05  2.      2563 !
185.   HNCO+HO2=NCO+H2O2                3.0E11  0.     22000 !
186.   HNCO+O2=HNO+CO2                  1.0E12  0.     35000 !
187.   HNCO+NH2=NH3+NCO                 5.0E12  0.      6200 !
188.   HNCO+NH=NH2+NCO                  3.0E13  0.     23700 !
189.   HOCN+H=NCO+H2                    2.0E07  2.      2000 !
190.   HOCN+O=NCO+OH                    1.5E04  2.64    4000 !
191.   HOCN+OH=NCO+H2O                  6.4E05  2.      2563 !
192.   HCNO+H=HCN+OH                    1.0E14  0      12000 !
193.   HCNO+O=HCO+NO                    2.0E14  0.         0 !
194.   HCNO+OH=CH2O+NO                  4.0E13  0.         0 !
195.   NCO+M=N+CO+M                     3.1E16 -0.50  48000 !
196.   NCO+H=NH+CO                      5.0E13  0.         0 !
197.   NCO+O=NO+CO                      4.7E13  0.         0 !
198.   NCO+OH=NO+HCO                    5.0E12  0.     15000 !
199.   NCO+O2=NO+CO2                    2.0E12  0.     20000 !
200.   NCO+H2=HNCO+H                    7.6E02  3.      4000 !
201.   NCO+HCO=HNCO+CO                  3.6E13  0.         0 !
202.   NCO+NO=N2O+CO                    6.2E17 -1.73     763 !
203.   NCO+NO=N2+CO2                    7.8E17 -1.73     763 !
```

```
204.   NCO+NO2=CO+NO+NO                2.5E11   0.      -707 !
205.   NCO+NO2=CO2+N2O                 3.0E12   0.      -707 !
206.   NCO+HNO=HNCO+NO                 1.8E13   0.         0 !
207.   NCO+N=N2+CO                     2.0E13   0.         0 !
208.   NCO+NCO=N2+CO+CO                1.8E13   0.         0 !
  !
  ! ****************************************************
  ! *  subset for CxHyOz+nitrogen species reactions     *
  ! *  (see paper for refs)                             *
  ! ****************************************************
  !
209.   CO+NO2 = CO2+NO                 9.0E13   0.     33779 !
210.   CO+N2O=N2+CO2                   3.2E11   0.     20237 !
211.   CO2+N=NO+CO                     1.9E11   0.      3400 !
212.   CH2O+NCO=HNCO+HCO               6.0E12   0.         0 !
213.   HCO+NO=HNO+CO                   7.2E12   0.         0 !
214.   HCO+NO2 = H+CO2+NO              8.4E15  -0.75    1930 !
215.   HCO+HNO=CH2O+NO                 6.0E11   0.      2000 !
216.   CH4+CN=CH3+HCN                  6.2E04   2.64    -437 !
217.   NCO+CH4 = CH3+HNCO              9.8E12   0.00    8120 !
218.   CH3+NO=HCN+H2O                  1.5E-1   3.523   3950 !
219.   CH3+NO=>HCN+OH+H                1.5E-1   3.523   3950 ! ***
220.   CH3+NO2=CH3O+NO                 1.4E13   0.         0 !
221.   CH2+NO=HCN+OH                   2.2E12   0.      -378 !
222.   CH2+NO=HCNO+H                   1.3E12   0.      -378 !
223.   CH2+NO2=CH2O+NO                 5.9E13   0.         0 !
224.   CH2+N=HCN+H                     5.0E13   0.         0 !
225.   CH2+N2=HCN+NH                   1.0E13   0.     74000 !
226.   CH2(S)+NO=HCN+OH                2.0E13   0.         0 !
227.   CH2(S)+NO=CH2+NO                1.0E14   0.         0 !
228.   CH2(S)+HCN=CH3+CN               5.0E13   0.         0 !
229.   CH+NO2=HCO+NO                   1.0E14   0.         0 !
230.   CH+NO = HCN+O                   4.8E13   0.00       0 !
231.   CH+NO = HCO+N                   3.4E13   0.00       0 !
232.   CH+NO = NCO+H                   1.9E13   0.00       0 !
233.   CH+N=CN+H                       1.3E13   0.         0 !
234.   CH+N2=HCN+N                     3.7E07   1.42   20723 !
235.   CH+N2O=HCN+NO                   1.9E13   0.      -511 !
236.   C+NO=CN+O                       2.0E13   0.         0 !
237.   C+NO=CO+N                       2.8E13   0.         0 !
238.   C+N2=CN+N                       6.3E13   0.     46019 !
239.   C+N2O=CN+NO                     5.1E12   0.         0 !
END

NOTE:  A units: mole-cm-sec-K, E units: cal/mole
□
```

```
!
  ! ****************************************************
  ! *   Hydrocarbon/nitrogen mechanism for simulations *
  !  *   of plastic in OPPDIF                           *
  ! *   Glarborg, Alzueta, Dam-Johansen,Miller         *
  ! *   Comb Flame, submitted (4/97)                   *
  ! *   revised Oct 22, 1997                           *
  ! *   CH4+H; CH2+CO2; H+NO+N2; NH3+O; CN+CO2; HNCO+H *
  ! ****************************************************
  !
ELEMENTS
H O C N CL AR
END
SPECIES
CO CO2 NO HCN
H O OH HO2 O2 H2 H2O2 H2O
CH2O HCO
CH2 CH2(S) CH C CH4
C2H4 C2H3 C2H2 C2H C2
CH2CO HCCO
NO2 HNO
NH3 NH2 NH N N2H2 NNH N2O
CN NCO HNCO HOCN
HCL CL
AR N2
END
THERMO
C2H5                 83194H   5C   2    0    0G   300.000  4000.000 1400.00    0 1
 0.87349157E+01 0.54537677E-02-0.37647177E-06-0.31297920E-09 0.52844000E-13    2
 0.10265269E+05-0.23104086E+02 0.24398923E+01 0.13747212E-01-0.85500653E-06    3
-0.31469924E-08 0.93754355E-12 0.13158588E+05 0.13099146E+02                   4
C2H3                 83194H   3C   2    0    0G   300.000  4000.000 1400.00    0 1
 0.71861677E+01 0.34552682E-02-0.29435373E-06-0.20681942E-09 0.36797774E-13    2
 0.32229627E+05-0.15977573E+02 0.24955740E+01 0.10269993E-01-0.10226917E-05    3
-0.27594382E-08 0.96919825E-12 0.34232813E+05 0.10614626E+02                   4
C2H                  83194H   1C   2    0    0G   300.000  4000.000 1400.00    0 1
 0.52086663E+01 0.12875765E-02-0.10398387E-06-0.67526325E-10 0.11751871E-13    2
 0.64697773E+05-0.53721781E+01 0.39396334E+01 0.32114412E-02-0.39412765E-06    3
-0.74782530E-09 0.27493521E-12 0.65224684E+05 0.17814000E+01                   4
CH2(S)               83194H   2C   1    0    0G   300.000  4000.000 1400.00    0 1
 0.40752106E+01 0.15779120E-02-0.10806129E-06-0.84592437E-10 0.14033284E-13    2
 0.50007492E+05-0.15480316E+01 0.35932946E+01 0.13151238E-02 0.30756846E-06    3
 0.42637904E-09-0.34178712E-12 0.50451547E+05 0.17780241E+01                   4
CH2                  83194H   2C   1    0    0G   300.000  4000.000 1400.00    0 1
 0.39737520E+01 0.16097502E-02-0.10785119E-06-0.86399922E-10 0.14301196E-13    2
 0.45608973E+05 0.75549729E-01 0.36872995E+01 0.15066403E-02 0.69679857E-07    3
 0.23537297E-09-0.19397147E-12 0.45863672E+05 0.20267601E+01                   4
CH3CN               111596H   3C   2N   1    0G   300.000  3000.000 1000.00    0 1
 0.23924046E+01 0.15618873E-01-0.79120497E-05 0.19372333E-08-0.18611956E-12    2
 0.84999377E+04 0.11145236E+02 0.25197531E+01 0.13567523E-01-0.25764077E-05    3
-0.30893967E-08 0.14288692E-11 0.85533762E+04 0.10920868E+02                   4
CH2CN               111596H   2C   2N   1    0G   300.000  3000.000 1000.00    0 1
 0.46058146E+01 0.94485160E-02-0.47116329E-05 0.11389957E-08-0.10828942E-12    2
 0.29171486E+05 0.10084415E+01 0.25296724E+01 0.18114138E-01-0.18960575E-04    3
 0.11944583E-07-0.32544142E-11 0.29592293E+05 0.10993441E+02                   4
OCHCHO              120596H   2C   2O   2    0G   300.000  3000.000 1000.00    0 1
 0.49087462E+01 0.13182673E-01-0.71416730E-05 0.18461316E-08-0.18525858E-12    2
-0.27116386E+05 0.59148768E+00 0.25068862E+01 0.18899139E-01-0.10302623E-04    3
 0.62607508E-09 0.88114253E-12-0.26427374E+05 0.13187043E+02                   4
C2H2OH HCCO TRAN    121196H   3C   2O   1    0G   300.000  3000.000 1000.00    0 1
 0.57206843E+01 0.10704185E-01-0.50358494E-05 0.11324499E-08-0.10086621E-12    2
 0.12849424E+05-0.47081776E+01 0.81498282E-01 0.31640644E-01-0.34085361E-04    3
 0.18978838E-07-0.41950165E-11 0.14060783E+05 0.22908977E+02                   4
C2H5CO    burcat  T 9/92C   3H   5O   1    0G   298.150  5000.000 1000.00      1
 0.30445698E+01 0.23236429E-01-0.86317936E-05 0.14799550E-08-0.96860829E-13    2
-0.61787211E+04 0.13122302E+02 0.67368294E+01-0.26945299E-02 0.49927017E-04    3
-0.50025808E-07 0.15011503E-10-0.65703366E+04-0.23398732E+01-0.43321855E+04    4
C2H5CHO   burcat  T 9/92C   3H   6O   1    0G   273.150  5000.000 1000.00      1
```

```
 0.33137982E+01 0.26619606E-01-0.10475596E-04 0.18815334E-08-0.12761310E-12    2
-0.25459603E+05 0.96608447E+01 0.76044596E+01-0.86403564E-02 0.73930097E-04    3
-0.79687398E-07 0.28004927E-10-0.25489789E+05-0.67643691E+01-0.23097645E+05    4
CH3CN             111596H   3C   2N   1    0G   300.000  3000.000 1000.00    0 1
 0.23924046E+01 0.15618873E-01-0.79120497E-05 0.19372333E-08-0.18611956E-12    2
 0.84999377E+04 0.11145236E+02 0.25197531E+01 0.13567523E-01-0.25764077E-05    3
-0.30893967E-08 0.14288692E-11 0.85533762E+04 0.10920868E+02                  4
CH2CN             111596H   2C   2N   1    0G   300.000  3000.000 1000.00    0 1
 0.46058146E+01 0.94485160E-02-0.47116329E-05 0.11389957E-08-0.10828942E-12    2
 0.29171486E+05 0.10084415E+01 0.25296724E+01 0.18114138E-01-0.18960575E-04    3
 0.11944583E-07-0.32544142E-11 0.29592293E+05 0.10993441E+02                  4
HNO               pg9601H   1N   1O   1    G  0300.00   5000.00  1000.00      1
 0.03615144E+02 0.03212486E-01-0.01260337E-04 0.02267298E-08-0.01536236E-12    2
 0.11769108E+05 0.04810264E+02 0.02784403E+02 0.06609646E-01-0.09300223E-04    3
 0.09437980E-07-0.03753146E-10 0.12025976E+05 0.09035629E+02                  4
HCN               110193H   1C   1N   1    G  0300.00   4000.00  1000.00      1
 0.03426457E+02 0.03924190E-01-0.01601138E-04 0.03161966E-08-0.02432850E-12    2
 0.01485552E+06 0.03607795E+02 0.02417787E+02 0.09031856E-01-0.01107727E-03    3
 0.07980141E-07-0.02311141E-10 0.01501044E+06 0.08222891E+02                  4
HNCO              110193H   1C   1N   1O   1G  0300.00   4000.00  1400.00      1
 0.06545307E+02 0.01965760E-01-0.01562664E-05-0.01074318E-08 0.01874680E-12    2
-0.01664773E+06-0.01003880E+03 0.03858467E+02 0.06390342E-01-0.09016628E-05    3
-0.01898224E-07 0.07651380E-11-0.01562343E+06 0.04882493E+02                  4
HOCN              110193H   1C   1N   1O   1G  0300.00   4000.00  1400.00      1
 0.06022112E+02 0.01929530E-01-0.01455029E-05-0.01045811E-08 0.01794814E-12    2
-0.04040321E+05-0.05866433E+02 0.03789424E+02 0.05387981E-01-0.06518270E-05    3
-0.01420164E-07 0.05367969E-11-0.03135335E+05 0.06667052E+02                  4
NCO               110193C   1N   1O   1    G  0300.00   4000.00  1400.00      1
 0.06072346E+02 0.09227829E-02-0.09845574E-06-0.04764123E-09 0.09090445E-13    2
 0.01359820E+06-0.08507293E+02 0.03359593E+02 0.05393239E-01-0.08144585E-05    3
-0.01912868E-07 0.07836794E-11 0.01462809E+06 0.06549694E+02                  4
O2*               dummy O   2    0    0    G  0300.00   4000.00  1400.00      1
 0.06072346E+02 0.09227829E-02-0.09845574E-06-0.04764123E-09 0.09090445E-13    2
 0.01359820E+06-0.08507293E+02 0.03359593E+02 0.05393239E-01-0.08144585E-05    3
-0.01912868E-07 0.07836794E-11 0.01462809E+06 0.06549694E+02                  4
NO*               dummy O   1N   1    0    G  0300.00   4000.00  1400.00      1
 0.06072346E+02 0.09227829E-02-0.09845574E-06-0.04764123E-09 0.09090445E-13    2
 0.01359820E+06-0.08507293E+02 0.03359593E+02 0.05393239E-01-0.08144585E-05    3
-0.01912868E-07 0.07836794E-11 0.01462809E+06 0.06549694E+02                  4
END


REACTIONS
   !
   ! ********************************************
   ! *   H2/O2 Subset                           *
   ! *   ref: nh2+no2 paper (IJCK), except      *
   ! *        where noted                       *
   ! ********************************************
   !
1.     O+OH=O2+H                      2.0E14 -0.40      0
2.     O+H2=OH+H                      5.0E04  2.67   6290
3.     OH+H2=H2O+H                    2.1E08  1.52   3450
4.     2OH=O+H2O                      4.3E03  2.70  -2486
5.     H+H+M=H2+M                     1.0E18 -1.00      0
       H2O/0/
6.     H+H+H2O=H2+H2O                 6.0E19 -1.25      0
7.     H+O+M=OH+M                     6.2E16 -0.60      0
       H2O/5/
8.     H+OH+M=H2O+M                   1.6E22 -2.00      0
       H2O/5/
9.     O+O+M=O2+M                     1.9E13  0.00  -1788
       H2O/5/
10.    H+O2+M=HO2+M                   2.1E18 -1.00      0 ! *
       H2O/10/  N2/0/
11.    H+O2+N2 = HO2+N2               6.7E19 -1.42      0 ! *
12.    H+HO2=H2+O2                    4.3E13  0.00   1411
```

```
13.    H+HO2=2OH                          1.7E14  0.00    874
14.    H+HO2=O+H2O                        3.0E13  0.0    1721
15.    O+HO2=O2+OH                        3.3E13  0.0       0
16.    OH+HO2=H2O+O2                      1.9E16 -1.0       0
17.    HO2+HO2=H2O2+O2                    4.2E14  0.0   11982
       DUP
18.    HO2+HO2=H2O2+O2                    1.3E11  0.0   -1629
       DUP
19.    H2O2+M=OH+OH+M                     1.3E17  0.0   45500
       H2O/5/
20.    H2O2+H=HO2+H2                      1.7E12  0.0    3755
21.    H2O2+H=OH+H2O                      1.0E13  0.0    3576
22.    H2O2+O=OH+HO2                      6.6E11  0.0    3974
23.    H2O2+OH=H2O+HO2                    7.8E12  0.0    1330
       DUP
24.    H2O2+OH=H2O+HO2                    5.8E14  0.0    9560 ! +
       DUP
  !
  ! *****************************************
  ! *    CO Subset                          *
  ! *****************************************
  !
25.    CO+O+M=CO2+M                       6.2E14  0.0    3000 ! nbs86
       H2O/5/
26.    CO+OH=CO2+H                        1.5E07  1.3    -758 ! gla86
27.    CO+O2=CO2+O                        2.5E12  0.0   47700 ! nbs86
28.    HO2+CO=CO2+OH                      5.8E13  0.0   22934 ! gla86
  !
  ! *****************************************
  ! *    CH2O/HCO Subset                    *
  ! *****************************************
  !
29.    CH2O+M=HCO+H+M                     3.3E16  0.0   81000 ! gla86
       H2O/5/
30.    CH2O+H = HCO+H2                    1.3E08  1.62   2166 ! CEC94
31.    CH2O+O=HCO+OH                      1.8E13  0.00   3080 ! nbs86
32.    CH2O+OH=HCO+H2O                    3.4E09  1.18   -447 ! nbs86
33.    CH2O+HO2 = HCO+H2O2                3.0E12  0.00  13000 ! cec92
34.    CH2O+O2 = HCO+HO2                  6.0E13  0.00  40660 ! cec92
35.    HCO+M=H+CO+M                       1.9E17 -1.0   17000 ! tim87
       H2O/5/
36.    HCO+H=CO+H2                        1.2E13  0.25      0 ! lrev (harding,21st)
37.    HCO+O=CO+OH                        3.0E13  0.000     0 ! cec92
38.    HCO+O=CO2+H                        3.0E13  0.000     0 ! cec92
39.    HCO+OH=H2O+CO                      1.0E14  0.00      0 ! cec92
40.    HCO+O2=HO2+CO                      7.6E12  0.0     400 ! tim88
  !
  ! *****************************************
  ! *    CH4/CH3/CH2/CH/C Subset            *
  ! *****************************************
  !
41.    CH2+H=CH+H2                        1.0E18 -1.56      0 ! gla86
42.    CH2+O=CO+H+H                       5.0E13  0.0       0 ! lrev
43.    CH2+O=CO+H2                        3.0E13  0.0       0 ! lrev
44.    CH2+OH=CH+H2O                      1.1E07  2.0    3000 ! m
45.    CH2+OH=CH2O+H                      2.5E13  0.0       0 ! m
46.    CH2+O2=CO+H2O                      2.2E22 -3.3    2867 ! dom92,m
47.    CH2+O2=CO2+H+H                     3.3E21 -3.3    2867 ! dom92,m
48.    CH2+O2=CH2O+O                      3.3E21 -3.3    2867 ! dom92,m
49.    CH2+O2=CO2+H2                      2.6E21 -3.3    2867 ! dom92,m
50.    CH2+O2=CO+OH+H                     1.6E21 -3.3    2867 ! dom92,m
51.    CH2+CO2=CH2O+CO                    1.1E11  0.0    1000 ! gla86
52.    CH2(S)+M=CH2+M                     1.0E13  0.0       0 ! m
       H/0/ H2O/0/ N2/0/ AR/0/
53.    CH2(S)+N2=CH2+N2                   1.3E13  0.0     430 ! Hayes, 1996
54.    CH2(S)+AR=CH2+AR                   1.5E13  0.0     884 ! Hayes, 1996
55.    CH2(S)+H=CH2+H                     2.0E14  0.0       0 ! m
56.    CH2(S)+H2O=CH2+H2O                 3.0E13  0.0       0 ! WAGNER
```

```
57.    CH2(S)+H=CH+H2                  3.0E13   0.0        0 ! nbs86
58.    CH2(S)+O=CO+H+H                 3.0E13   0.0        0 ! nbs86
59.    CH2(S)+OH=CH2O+H                3.0E13   0.0        0 ! nbs86
60.    CH2(S)+O2=CO+OH+H               7.0E13   0.0        0 ! m
61.    CH2(S)+CO2=CH2O+CO              3.0E12   0.0        0 ! nbs86
62.    CH+H=C+H2                       1.5E14   0.0        0 ! m
63.    CH+O=CO+H                       5.7E13   0.0        0 ! gla86
64.    CH+OH=HCO+H                     3.0E13   0.0        0 ! m
65.    CH+OH=C+H2O                     4.0E7    2.0     3000 ! m
66.    CH+O2=HCO+O                     3.3E13   0.0        0 ! cec92
67.    CH+H2O=CH2O+H                   5.7E12   0.0     -751 ! cec92
68.    CH+CO2=HCO+CO                   3.4E12   0.0      690 ! cec92
69.    CH+CH2=C2H2+H                   4.0E13   0.0        0 ! m
70.    CH+CH2O=CH2CO+H                 9.5E13   0.00    -515 ! cec92
71.    CH+HCCO=C2H2+CO                 5.0E13   0.00       0 ! m
72.    C+OH=CO+H                       5.0E13   0.00       0 ! m
73.    C+O2=CO+O                       2.0E13   0.00       0 ! gla86
  !
  ! *********************************************
  ! *   C2H6/C2H5/C2H4/C2H3/C2H2/C2H/C2 subset *
  ! *********************************************
  !
74.    C2H3+H(+M)=C2H4(+M)             6.1E12   0.27     280 ! GRI2.11
       LOW /0.98E30 -3.86 3320./
       TROE /0.7820 207.50 2663.00 6095.00/
       H2/2.85/ CO/2.1/ CO2/2.85/  H2O/7.14/  N2/1.43/
75.    C2H4+M=C2H2+H2+M                3.5E16   0.0    71500 ! cec92
       N2/1.5/  H2O/10/
76.    C2H4+H=C2H3+H2                  5.4E14   0.0    14900 ! cec92
77.    C2H4+O = CH2CO+H2               6.8E05   1.88     180 ! cec94
78.    C2H4+OH=C2H3+H2O                2.0E13   0.00    5940 ! cec92
79.    C2H3+H=C2H2+H2                  4.0E13   0.00       0 ! mrev
80.    C2H3+O=CH2CO+H                  3.0E13   0.000      0 ! cec92
81.    C2H3+OH=C2H2+H2O                2.0E13   0.0        0 ! m
82.    C2H3+O2 = CH2O+HCO              1.1E23  -3.29    3890 ! boz93
83.    C2H3+O2=C2H2+HO2                5.2E15  -1.26    3310 ! boz93
84.    C2H3+CH2O = C2H4+HCO            5.4E03   2.81    5860 ! nbs86
85.    C2H3+HCO = C2H4+CO              9.0E13   0.00       0 ! nbs86
86.    C2H3+C2H3 = C2H4+C2H2           1.5E13   0.00       0 ! Fahr 91
87.    C2H2+M=C2H+H+M                  9.1E30  -3.7   127138 ! nbs86
       H2/2/ CO/2/ CO2/3/  H2O/5/
88.    H2+C2H=C2H2+H                   4.1E05   2.39     864 ! gla86
89.    C2H2+O=CH2+CO                   6.1E6    2.00    1900 ! JAM,FONT,PEETERS
90.    C2H2+O=HCCO+H                   1.4E7    2.00    1900 ! JAM,FONT,PEETERS
91.    C2H2+O=C2H+OH                   3.2E15  -0.60   15000 ! gla86
92.    OH+C2H2=C2H+H2O                 3.4E7    2.0    14000 ! mil88
93.    OH+C2H2=CH2CO+H                 2.2E-4   4.5    -1000 ! mil88
94.    C2H2+O2=HCO+HCO                 2.0E08   1.5    30100 ! m,ben96
95.    C2+H2=C2H+H                     4.0E5    2.4     1000 ! m
96.    C2H+O=CH+CO                     5.0E13   0.00       0 ! gla86
97.    C2H+OH=HCCO+H                   2.0E13   0.00       0 ! m
98.    C2H+OH=C2+H2O                   4.0E7    2.0     8000 ! m
99.    C2H+O2=CO+CO+H                  2.5E13   0.0        0 ! mrev
100.   C2+O2=CO+CO                     5.0E13   0.0        0 ! m
  !
  ! ****************************************************
  ! *   CH3HCO/CH2HCO/CH3CO/CH2CO/HCCOH/HCCO/C2O subset *
  ! ****************************************************
  !
101.   CH2+CO(+M)=CH2CO(+M)            8.1E11   0.5     4510 ! GRI2.11
       LOW/ 1.88E33 -5.11 7095./
       TROE/ 0.5907 275 1226 5185/
       H2/2/ CO/2/ CO2/3/  H2O/8.58/  N2/1.43/
102.   CH2CO+H=HCCO+H2                  3.0E7    2.0    10000 ! m
103.   CH2CO+O=CO2+CH2                 1.8E12   0.0     1350 ! mrev
104.   CH2CO+O=HCCO+OH                 2.0E7    2.0    10000 ! m
105.   CH2CO+OH=HCCO+H2O               1.0E7    2.0     3000 ! m
106.   H+HCCO=CH2(S)+CO                1.0E14   0.0        0 ! mrev
```

```
107.   O+HCCO=H+CO+CO                    1.0E14  0.0       0 ! mrev
108.   HCCO+O2=CO2+CO+H                  1.4E7   1.7    1000 ! mrev
109.   HCCO+O2=CO +CO +OH                2.9E7   1.7    1000 ! mrev
110.   HCCO+HCCO=C2H2+CO+CO              1.0E13  0.00      0 ! m
  !
  ! ****************************************************
  ! *   H/N/O subset                                    *
  ! *   taken from [nh2no2] except where noted          *
  ! ****************************************************
  !
111.   H+NO+M=HNO+M                      2.7E15  0.0    -600 ! bau73
       H2O/10/  O2/1.5/ H2/2/ CO2/3/ N2/0.0/
112.   H+NO+N2=HNO+N2                    7.0E19 -1.50      0 ! see text
113.   NO+O+M=NO2+M                      7.5E19 -1.41      0 !
       N2/1.7/   O2/1.5/  H2O/10/
114.   HO2+NO=NO2+OH                     2.1E12  0.00   -479 !
115.   NO2+H=NO+OH                       8.4E13  0.0       0 !
116.   NO2+O=NO+O2                       3.9E12  0.0    -238 !
117.   NO2+NO2=NO+NO+O2                  1.6E12  0.0   26123 !
118.   HNO+H=H2+NO                       4.5E11  0.72    655 !
119.   HNO+O=NO+OH                       1.0E13  0.0       0 ! +
120.   HNO+OH=NO+H2O                     3.6E13  0.0       0 !
121.   HNO+O2=HO2+NO                     1.0E13  0.0   25000 !
122.   HNO+HNO=N2O+H2O                   9.0E08  0.0    3100 ! *
123.   HNO+NH2=NH3+NO                    3.63E6  1.63  -1252 ! lin96
124.   NH3+M = NH2+H+M                   2.2E16   0    93470 ! +
125.   NH3+H=NH2+H2                      6.4E05  2.39  10171 !
126.   NH3+O=NH2+OH                      9.4E06  1.94   6460 ! *
127.   NH3+OH=NH2+H2O                    2.0E06  2.04    566 !
128.   NH3+HO2=NH2+H2O2                  3.0E11  0.0   22000 !
129.   NH2+H=NH+H2                       4.0E13  0.00   3650 !
130.   NH2+O=HNO+H                       6.6E14 -0.50      0 !
131.   NH2+O=NH+OH                       6.8E12  0.        0 !
132.   NH2+OH=NH+H2O                     4.0E06  2.     1000 !
133.   NH2+HO2=NH3+O2                    1.0E13  0.0       0 !
134.   NH2+NO=NNH+OH                     8.9E12 -0.35      0 ! bodenstein
135.   NH2+NO=N2+H2O                     1.3E16 -1.25      0 ! bodenstein
       DUP
136.   NH2+NO=N2+H2O                    -8.9E12 -0.35      0 !
       DUP
137.   NH2+NO2=N2O+H2O                   3.2E18 -2.2       0 !
138.   NH2+NH2=N2H2+H2                   8.5E11  0.        0 !
139.   NH2+NH=N2H2+H                     5.0E13  0.        0 !
140.   NH2+N=N2+H+H                      7.2E13  0.        0 !
141.   NH+H=N+H2                         3.0E13  0.        0
142.   NH+O=NO+H                         9.2E13  0.        0
143.   NH+OH=HNO+H                       2.0E13  0.        0
144.   NH+OH=N+H2O                       5.0E11  0.50   2000
145.   NH+O2=HNO+O                       4.6E05  2.     6500 !
146.   NH+O2=NO+OH                       1.3E06  1.5     100 !
147.   NH+NO=N2O+H                       2.9E14 -0.4       0 !
       DUP
148.   NH+NO=N2O+H                      -2.2E13 -0.23      0
       DUP
149.   NH+NO=N2+OH                       2.2E13 -0.23      0
150.   NH+NO2=N2O+OH                     1.0E13  0.        0
151.   NH+NH=N2+H+H                      2.5E13  0.        0
152.   NH+N=N2+H                         3.0E13  0.        0
153.   N+OH=NO+H                         3.8E13  0.        0
154.   N+O2=NO+O                         6.4E09  1.     6280
155.   N+NO=N2+O                         3.3E12  0.30      0
156.   N2H2+M=NNH+H+M                    5.0E16  0.    50000
       H2O/15/ O2/2/ N2/2/ H2/2/
157.   N2H2+H=NNH+H2                     5.0E13  0.     1000
158.   N2H2+O=NH2+NO                     1.0E13  0.        0
159.   N2H2+O=NNH+OH                     2.0E13  0.     1000
160.   N2H2+OH=NNH+H2O                   1.0E13  0.     1000
161.   N2H2+NO=N2O+NH2                   3.0E12  0.        0
```

```
162.   N2H2+NH2=NH3+NNH                1.0E13  0.     1000
163.   N2H2+NH=NNH+NH2                 1.0E13  0.     1000
164.   NNH=N2+H                        1.0E7   0.        0 ! bodenstein
165.   NNH+H=N2+H2                     1.0E14  0.        0
166.   NNH+O=N2+OH                     8.0E13  0.        0
167.   NNH+O=N2O+H                     1.0E14  0.        0
168.   NNH+O=NH+NO                     5.0E13  0.        0
169.   NNH+OH=N2+H2O                   5.0E13  0.        0
170.   NNH+O2=N2+HO2                   2.0E14  0.        0 ! bodenstein
171.   NNH+O2=N2+O2+H                  5.0E13  0.        0 ! bodenstein
172.   NNH+NO=N2+HNO                   5.0E13  0.        0
173.   NNH+NH2=N2+NH3                  5.0E13  0.        0
174.   NNH+NH=N2+NH2                   5.0E13  0.        0
175.   N2O+M=N2+O+M                    4.0E14  0.    56100
       N2/1.7/   O2/1.4/ H2O/12/ CO/1.5/  CO2/3/
176.   N2O+H=N2+OH                     3.3E10  0.     4729
       DUP
177.   N2O+H=N2+OH                     4.4E14  0.    19254
       DUP
178.   N2O+O=NO+NO                     6.6E13  0.    26630 ! nbs91
179.   N2O+O=N2+O2                     1.0E14  0.    28000 ! nbs91
180.   N2O+OH=N2+HO2                   1.3E-2  4.72  36561 ! Mebel,Lin IJCK 1996
181.   N2O+OH=HNO+NO                   1.2E-4  4.33  25081 ! Mebel,Lin IJCK 1996
182.   N2O+NO=NO2+N2                   5.3E05  2.23  46281 ! Mebel,Lin IJCK 1996
  !
  ! ****************************************************
  ! *  cyanide subset                                  *
  ! ****************************************************
  !
183.   CN+H2=HCN+H                     3.0E05  2.45   2237 !
184.   HCN+O=NCO+H                     1.4E04  2.64   4980
185.   HCN+O=NH+CO                     3.5E03  2.64   4980
186.   HCN+O=CN+OH                     2.7E09  1.58  29200
187.   HCN+OH = CN+H2O                 3.9E06  1.83  10300 !
188.   HCN+OH=HOCN+H                   5.9E04  2.40  12500
189.   HCN+OH=HNCO+H                   2.0E-3  4.     1000
190.   HCN+OH=NH2+CO                   7.8E-4  4.     4000
191.   CN+O=CO+N                       7.7E13  0.        0 !
192.   CN+OH=NCO+H                     4.0E13  0.        0 !
193.   CN+O2=NCO+O                     7.5E12  0.     -389 !
194.   CN+CO2=NCO+CO                   3.7E06  2.16  26884 !
195.   CN+NO2=NCO+NO                   5.3E15 -0.752   344 !
196.   CN+NO2=CO+N2O                   4.9E14 -0.752   344 !
197.   CN+NO2=N2+CO2                   3.7E14 -0.752   344 !
198.   CN+HNO=HCN+NO                   1.8E13  0.00      0
199.   CN+HNCO=HCN+NCO                 1.5E13  0.        0 !
200.   HNCO+M=NH+CO                    1.1E16  0.    86000 !
201.   HNCO+H=NH2+CO                   2.2E07  1.7    3800 !
202.   HNCO+O=HNO+CO                   1.5E08  1.57  44012 !
203.   HNCO+O=NH+CO2                   9.8E7   1.41   8524 !
204.   HNCO+O=NCO+OH                   2.2E6   2.11  11425 !
205.   HNCO+OH=NCO+H2O                 6.4E05  2.     2563 !
206.   HNCO+HO2=NCO+H2O2               3.0E11  0.    22000 !
207.   HNCO+O2=HNO+CO2                 1.0E12  0.    35000 !
208.   HNCO+NH2=NH3+NCO                5.0E12  0.     6200 !
209.   HNCO+NH=NH2+NCO                 3.0E13  0.    23700 !
210.   HOCN+H=NCO+H2                   2.0E07  2.     2000 !
211.   HOCN+O=NCO+OH                   1.5E04  2.64   4000 !
212.   HOCN+OH=NCO+H2O                 6.4E05  2.     2563 !
213.   NCO+M=N+CO+M                    3.1E16 -0.50  48000 !
214.   NCO+H=NH+CO                     5.0E13  0.        0 !
215.   NCO+O=NO+CO                     4.7E13  0.        0 !
216.   NCO+OH=NO+HCO                   5.0E12  0.    15000 !
217.   NCO+O2=NO+CO2                   2.0E12  0.    20000 !
218.   NCO+H2=HNCO+H                   7.6E02  3.     4000 !
219.   NCO+HCO=HNCO+CO                 3.6E13  0.        0 !
220.   NCO+NO=N2O+CO                   6.2E17 -1.73    763 !
221.   NCO+NO=N2+CO2                   7.8E17 -1.73    763 !
```

```
222.   NCO+NO2=CO+NO+NO                  2.5E11   0.      -707 !
223.   NCO+NO2=CO2+N2O                   3.0E12   0.      -707 !
224.   NCO+HNO=HNCO+NO                   1.8E13   0.         0 !
225.   NCO+N=N2+CO                       2.0E13   0.         0 !
226.   NCO+NCO=N2+CO+CO                  1.8E13   0.         0 !
  !
  ! *****************************************************
  ! *  subset for CxHyOz+nitrogen species reactions     *
  ! *  (see paper for refs)                             *
  ! *****************************************************
  !
227.   CO+NO2 = CO2+NO                   9.0E13   0.     33779 !
228.   CO+N2O=N2+CO2                     3.2E11   0.     20237 !
229.   CO2+N=NO+CO                       1.9E11   0.      3400 !
230.   CH2O+NCO=HNCO+HCO                 6.0E12   0.         0 !
231.   HCO+NO=HNO+CO                     7.2E12   0.         0 !
232.   HCO+NO2 = H+CO2+NO                8.4E15 -0.75    1930 !
233.   HCO+HNO=CH2O+NO                   6.0E11   0.      2000 !
234.   CH2+NO=HCN+OH                     2.2E12   0.      -378 !
235.   CH2+NO2=CH2O+NO                   5.9E13   0.         0 !
236.   CH2+N=HCN+H                       5.0E13   0.         0 !
237.   CH2+N2=HCN+NH                     1.0E13   0.     74000 !
238.   CH2(S)+NO=HCN+OH                  2.0E13   0.         0 !
239.   CH2(S)+NO=CH2+NO                  1.0E14   0.         0 !
240.   CH+NO2=HCO+NO                     1.0E14   0.         0 !
241.   CH+NO = HCN+O                     4.8E13   0.00       0 !
242.   CH+NO = HCO+N                     3.4E13   0.00       0 !
243.   CH+NO = NCO+H                     1.9E13   0.00       0 !
244.   CH+N=CN+H                         1.3E13   0.         0 !
245.   CH+N2=HCN+N                       3.7E07   1.42   20723 !
246.   CH+N2O=HCN+NO                     1.9E13   0.      -511 !
247.   C+NO=CN+O                         2.0E13   0.         0 !
248.   C+NO=CO+N                         2.8E13   0.         0 !
249.   C+N2=CN+N                         6.3E13   0.     46019 !
250.   C+N2O=CN+NO                       5.1E12   0.         0 !
251.   HCCO+NO=HCN+CO2                   1.6E13   0.         0 !
!
! *** HCl Subset *** (simplified, from Roesler et al, Comb Flame 100,495,1995)
!
252.   H+CL+M = HCL+M                 7.2E21 -2.0       0 !
253.   HCL+H = CL+H2                  1.7E13  0.0    4140 !
254.   HCL+O = CL+OH                  3.4E13  2.87   3510 !
255.   HCL+OH = CL+H2O                2.7E07  1.65   -220 !
256.   CL+HO2 = HCL+O2                1.1E13  0.00   -340 !
END
NOTE:  A units: mole-cm-sec-K, E units: cal/mole
```